# Etude locale par diffusion incohérente du comportement moyen et perturbé de la région F1 de l'ionosphère et de la basse thermosphère aurorale : [thèse soutenue sur un ensemble de travaux]

Chantal Lathuillère

# THESE

PRESENTEE A

L'UNIVERSITE
SCIENTIFIQUE ET MEDICALE

L'INSTITUT
NATIONAL POLYTECHNIQUE

DE GRENOBLE

POUR OBTENIR

LE TITRE DE DOCTEUR D'ETAT ES-SCIENCES

PAR

**Chantal LATHUILLERE**

---

# Etude locale par diffusion incohérente du comportement moyen et perturbé de la région F1 de l'ionosphère et de la basse thermosphère aurorale.

---

Soutenue le 30 Janvier 1987 devant la Commission d'Examen

JURY

| | | |
|---|---|---|
| Monsieur | R. MORET | Président |
| Messieurs | P. BAUER | |
| | P. BROCHE | |
| | J.L. LACOUME | Examinateurs |
| | G. LEJEUNE | |
| | V.B. WICKWAR | |
| | D. ALCAYDE | Invité |

# INSTITUT NATIONAL POLYTECHNIQUE DE GRENOBLE

**Président :** Daniel BLOCH

**Vice-Présidents:** B. BAUDELET
R. CARRE
H. CHERADAME
J.M PIERRARD

## Professeurs des Universités

| | | |
|---|---|---|
| BARIBAUD | Michel | ENSERG |
| BARRAUD | Alain | ENSIEG |
| BAUDELET | Bernard | ENSIEG |
| BEAUFILS | Jean-Claude | ENSEEG |
| BESSON | Jean | ENSEEG |
| BLIMAN | Samuel | ENSERG |
| BLOCH | Daniel | ENSIEG |
| BOIS | Philippe | ENSHG |
| BONNETAIN | Lucien | ENSEEG |
| BONNIER | Etienne | ENSEEG |
| BOUVARD | Maurice | ENSHG |
| BRISSONNEAU | Pierre | ENSIEG |
| BRUNET | Yves | ENSIEG |
| BUYLE-BODIN | Maurice | ENSERG |
| CAILLERIE | Denis | ENSHG |
| CAVAIGNAC | Jean-François | ENSIEG |
| CHARTIER | Germain | ENSIEG |
| CHENEVIER | Pierre | ENSERG |
| CHERADAME | Hervé | UERMCPP |
| CHERUY | Arlette | ENSIEG |
| CHIAVERINA | Jean | UERMCPP |
| COHEN | Joseph | ENSERG |
| COUMES | André | ENSERG |
| DURAND | Francis | ENSEEG |
| DURAND | Jean-Louis | ENSIEG |
| FONLUPT | Jean | ENSIMAG |
| FOULARD | Claude | ENSIEG |
| GANDINI | Alessandro | UERMCPP |
| GAUBERT | Claude | ENSIEG |
| GENTIL | Pierre | ENSERG |
| GUERIN | Bernard | ENSERG |
| GUYOT | Pierre | ENSEEG |
| IVANES | Marcel | ENSIEG |
| JAUSSAUD | Pierre | ENSIEG |
| JOUBERT | Jean-Claude | ENSIEG |
| JOURDAIN | Geneviève | ENSIEG |
| LACOUME | Jean-Louis | ENSIEG |
| LESIEUR | Marcel | ENSHG |
| LESPINARD | Georges | ENSHG |
| LONGEQUEUE | Jean-Pierre | ENSIEG |
| LOUCHET | François | ENSEEG |
| MASSELOT | Christian | ENSIEG |
| MAZARE | Guy | ENSIMAG |
| MOREAU | René | ENSHG |
| MORET | Roger | ENSIEG |
| MOSSIERE | Jacques | ENSIMAG |
| OBLED | Charles | ENSHG |
| PARIAUD | Jean-Charles | ENSEEG |
| PAUTHENET | René | ENSIEG |
| PERRET | René | ENSIEG |
| PERRET | Robert | ENSIEG |
| PIAU | Jean-Michel | ENSHG |
| POLOUJADOFF | Michel | ENSIEG |
| POUPOT | Christian | ENSERG |
| RAMEAU | Jean-Jacques | ENSEEG |
| RENAUD | Maurice | UERMCPP |
| ROBERT | André | UERMCPP |
| ROBERT | François | ENSIMAG |
| SABONNADIERE | Jean-Claude | ENSIEG |
| SAUCIER | Gabrielle | ENSIMAG |
| SCHLENKER | Claire | ENSIEG |
| SCHLENKER | Michel | ENSIEG |
| SERMET | Pierre | ENSERG |
| SILVY | Jacques | UERMCPP |
| SOHM | Jean-Claude | ENSEEG |
| SOUQUET | Jean-Louis | ENSEEG |
| TROMPETTE | Philippe | ENSHG |
| VEILLON | Gérard | ENSIMAG |

## Professeurs Université des Sciences Sociales (Grenoble II)

| | |
|---|---|
| BOLLIET | Louis |
| CHATELIN | Françoise |

## Chercheurs du C.N.R.S

| | | |
|---|---|---|
| CARRE | René | Directeur de recherche |
| CAILLET | Marcel | " |
| FRUCHART | Robert | " |
| JORRAND | Philippe | " |
| LANDAU | Ioan | " |
| ALLIBERT | Colette | Maître de recherche |
| ALLIBERT | Michel | " |
| ANSARA | Ibrahim | " |
| ARMAND | Michel | " |
| BINDER | Gilbert | " |
| BONNET | Roland | " |
| BORNARD | Guy | " |
| CALMET | Jacques | " |
| DAVID | René | Maître de recherche |
| DEPORTES | Jacques | " |
| DRIOLE | Jean | " |
| EUSTATHOPOULOS | Nicolas | " |
| GIVORD | Dominique | " |
| JOUD | Jean-Charles | " |
| KAMARINOS | Georges | " |
| KLEITZ | Michel | " |
| LEJEUNE | Gérard | " |
| MERMET | Jean | " |
| MUNIER | Jacques | " |
| SENATEUR | Jean-Pierre | " |
| SUERY | Michel | " |
| WACK | Bernard | " |

**Personnalités agrées à titre permanent à diriger des travaux de recherche** (Décision du conseil scientifique)

## E.N.S.E.E.G

| | | | | | |
|---|---|---|---|---|---|
| BERNARD | Claude | FOSTER | Panayotis | RAVAINE | Denis |
| CAILLET | Marcel | GALERIE | Alain | SAINFORT | Paul |
| CHATILLON | Catherine | HAMMOU | Abdelkader | SARRAZIN | Pierre |
| CHATILLON | Christian | MALMEJAC | Yves | SIMON | Jean-Paul |
| COULON | Michel | MARTIN GARIN | Régina | TOUZAIN | Philippe |
| DIARD | Jean-Paul | NGUYEN TRUONG | Bernadette | URBAIN | Georges |

## E.N.S.E.R.G

| | | | |
|---|---|---|---|
| BOREL | Joseph | DOLMAZON | Jean-Marc |
| CHOVET | Alain | HERAULT | Jeanny |

## E.N.S.I.E.G

| | | | | | |
|---|---|---|---|---|---|
| BORNARD | Guy | KOFMAN | Walter | MAZUER | Jean |
| DESCHIZEAUX | Pierre | LEJEUNE | Gérard | PERARD | Jacques |
| GLANGEAUD | François | | | REINISCH | Raymond |

## E.N.S.H.G

| | | | | | |
|---|---|---|---|---|---|
| ALEMANY | Antoine | DARVE | Félix | ROWE | Alain |
| BOIS | Daniel | MICHEL | Jean-Marie | VAUCLIN | Michel |

## E.N.S.I.M.A.G

| | | | | | |
|---|---|---|---|---|---|
| BERT | Didier | COURTIN | Jacques | FONLUPT | Jean |
| CALMET | Jacques | COURTOIS | Bernard | SIFAKIS | Joseph |
| | | DELLA DORA | Jean | | |

## U.E.R.M.C.P.P

| | |
|---|---|
| CHARUEL | Robert |

## C.E.N.G

| | | | | | |
|---|---|---|---|---|---|
| CADET | Jean | JOUVE | Hubert | PERROUD | Paul |
| COEURE | Philippe | NICOLAU | Yvan | PEUZIN | Jean-Claude |
| DELHAYE | Jean-Marc | NIFENECKER | Hervé | TAIEB | Maurice |
| DUPUY | Michel | | | VINCENDON | Marc |

**Laboratoires extérieurs :**

## C.N.E.T

| | | | | | |
|---|---|---|---|---|---|
| DEMOULIN | Eric | GERBER | Roland | MERCKEL | Gérard |
| DEVINE | | | | PAULEAU | Yves |

**********

# ECOLE NATIONALE SUPERIEURE DES MINES DE SAINT-ETIENNE

Directeur : Monsieur M. MERMET
Directeur des Etudes et de la formation : Monsieur J. LEVASSEUR
Directeur des recherches : Monsieur J. LEVY
Secrétaire Général : Mademoiselle M. CLERGUE

## Professeurs de 1ère Catégorie

| | | |
|---|---|---|
| COINDE | Alexandre | Gestion |
| GOUX | Claude | Métallurgie |
| LEVY | Jacques | Métallurgie |
| LOWYS | Jean-Pierre | Physique |
| MATHON | Albert | Gestion |
| RIEU | Jean | Mécanique - Résistance des matériaux |
| SOUSTELLE | Michel | Chimie |
| FORMERY | Philippe | Mathématiques Appliquées |

## Professeurs de 2ème catégorie

| | | |
|---|---|---|
| HABIB | Michel | Informatique |
| PERRIN | Michel | Géologie |
| VERCHERY | Georges | Matériaux |
| TOUCHARD | Bernard | Physique Industrielle |

## Directeur de recherche

| | | |
|---|---|---|
| LESBATS | Pierre | Métallurgie |

## Maîtres de recherche

| | | |
|---|---|---|
| BISCONDI | Michel | Métallurgie |
| DAVOINE | Philippe | Géologie |
| FOURDEUX | Angeline | Métallurgie |
| KOBYLANSKI | André | Métallurgie |
| LALAUZE | René | Chimie |
| LANCELOT | Francis | Chimie |
| LE COZE | Jean | Métallurgie |
| THEVENOT | François | Chimie |
| TRAN MINH | Canh | Chimie |

## Personnalités habilitées à diriger des travaux de recherche

| | | |
|---|---|---|
| DRIVER | Julian | Métallurgie |
| GUILHOT | Bernard | Chimie |
| THOMAS | Gérard | Chimie |

## Professeur à l'UER de Sciences de Saint-Etienne

| | | |
|---|---|---|
| VERGNAUD | Jean-Maurice | Chimie des Matériaux & chimie industrielle |

**********

UNIVERSITÉ
SCIENTIFIQUE ET MÉDICALE
DE GRENOBLE

Saint-Martin-d'Hères, le

Domaine Universitaire, Bâtiment administratif Sciences
B. P. n° 68
38402 SAINT-MARTIN-D'HERES CEDEX

Président de l'Université :

M. TANCHE

## MEMBRES DU CORPS ENSEIGNANT DE SCIENCES

Ne figurent pas dans la liste les professeurs de Médecine-Pharmacie

### - PROFESSEURS DE 1ère CLASSE

| | |
|---|---|
| ARNAUD Paul | Chimie Organique |
| ARVIEU Robert | Physique Nucléaire I.S.N. |
| AUBERT Guy | Physique CNRS |
| AURIAULT Jean-Louis | Mécanique |
| AYANT Yves | Physique Approfondie |
| BARBIER Marie-Jeanne | Electrochimie |
| BARBIER Jean Claude | Physique Expérimentale CNRS |
| BARJON Robert | Physique Nucléaire I.S.N. |
| BARNOUD Fernand | Biochimie macromoléculaire végétale |

Téléphone ( 76 ) 51.46.00
Adresse télégraphique : EXACSCIENCES 38 GRENOBLE

| | |
|---|---|
| DEPORTES Charles | Chimie Minérale |
| DESRE Pierre | Electrochimie |
| DOLIQUE Jean-Michel | Physique des Plasmas |
| DOUCE Rolland | Physiologie végétale |
| DUCROS Pierre | Cristallographie |
| FONTAINE Jean-Marc | Mathématiques Pures |
| GAGNAIRE Didier | Chimie Physique |
| GERMAIN Jean-Pierre | Mécanique |
| GIRAUD Pierre | Géologie |
| IDELMAN Simon | Physiologie animale |
| JANIN Bernard | Géographie |
| JOLY Jean-René | Mathématiques Pures |
| KAHANE André, détaché | Physique |
| KAHANE Josette | Physique |
| KOSZUL Jean-Louis | Mathématiques Pures |
| KRAKOWIAK Sacha | Mathématiques Appliquées |
| KUPKA Yvon | Mathématiques Pures |
| LACAZE Albert | Physique |
| LAJZEROWICZ Jeannine | Physique |

| | |
|---|---|
| SAKAROVITCH Michel | Mathématiques Appliquées |
| SENGEL Philippe | Biologie Animale |
| SERGERAERT Françis | Mathématiques Pures |
| SOUTIF Michel | Physique |
| VAILLANT François | Zoologie |
| VALENTIN Jacques | Physique Nucléaire I.S.N. |
| VAN CUTSEN Bernard | Mathématiques Appliquées |
| VAUQUOIS Bernard | Mathématiques Appliquées |
| VIALLON Pierre | Géologie |

- PROFESSEURS DE 2ème CLASSE

| | |
|---|---|
| ADIBA Michel | Mathématiques Pures |
| ANTOINE Pierre | Géologie |
| ARMAND Gilbert | Géographie |
| BARET Paul | Chimie |
| BECKER Pierre | Physique |
| BEGUIN Claude | Chimie Organique |
| BLANCHI J. Pierre | STAPS |
| BOITET Christian | Mathématiques Appliquées |

| | |
|---|---|
| GUITTON Jacques | Chimie |
| HACQUES Gérard | Mathématiques Appliquées |
| HERBIN Jacky | Géographie |
| HICTER Pierre | Chimie |
| JOSELEAU Jean Paul | Biochimie |
| KERKOVE Claude | Géologie |
| LEBRETON Alain | Mathématiques Appliquées |
| LONGEQUEUE Nicole | Sciences Nucléaires I.S.N. |
| LUCAS Robert | Physique |
| LUNA Domingo | Mathématiques Pures |
| MANDARON Paul | Biologie |
| MARTINEZ Francis | Mathématiques Appliquées |
| MASCLE Georges | Géologie |
| NEMOZ Alain | Thermodynamique CNRS - CRTBT |
| OUDET Bruno, détaché | Mathématiques Appliquées |
| PELMONT Jean | Biochimie |
| PERRIN Claude | Sciences Nucléaires I.S.N. |
| PFISTER Jean-Claude, détaché | Physique du Solide |
| PIBOULE Michel | Géologie |
| PIERY Yvette | Biologie |

| | |
|---|---|
| CHOUTEAU Gérard | Physique IUT 1 |
| CONTE René | Physique IUT 1 |
| GOSSE Jean-Pierre | EEA IUT 1 |
| GROS Yves | Physique IUT 1 |
| KUHN Gérard | Physique IUT 1 |
| MARECHAL Jean | Mécanique IUT 1 |
| MICHOULIER Jean | Physique IUT 1 |
| MONLLOR Christian | EEA IUT 1 |
| NOUGARET Marcel | Automatique IUT 1 |
| PEFFEN René | Métallurgie IUT |
| PERARD Jacques | EEA IUT 1 |
| PERRAUD Robert | Chimie IUT 1 |
| TERRIEZ Jean Michel | Génie Mécanique IUT 1 |

# REMERCIEMENTS

J'exprime tout d'abord ma reconnaissance aux personnes qui ont bien voulu accepter de juger ce travail, à M. le Professeur Moret qui a accepté de présider le jury, ainsi qu'à M. le Professeur Broche qui a eu la gentillesse d'accepter d'en être membre; à M. le Professeur Lacoume, directeur de Centre d'Etudes des Phénomènes Aléatoires et Géophysiques, qui m'a accueillie au sein de son laboratoire.

Je remercie tout particulièrement MM. P. Bauer et D. Alcayde dont les critiques amicales et constructives ont permis d'améliorer notablement mon manuscrit.

C'est avec M. V. Wickwar, lors d'un séjour de six mois dans son laboratoire, que j'ai abordé l'étude de l'ionosphère des zones aurorales. Il m'a fait bénéficier de sa compétence et de ses conseils. Qu'il trouve ici l'expression de ma gratitude et de mon amitié.

Mr G. Lejeune a dirigé ce travail par des conseils pertinents et une aide précieuse. Je lui en suis très reconnaissante.

J'ai bénéficié d'un encouragement et d'un soutien constant de la part de M. F. Glangeaud. En particulier les études concernant les pulsations magnétiques ont abouti grâce à lui. Je l'en remercie très sincèrement.

Je suis très reconnaissante à M. W. Kofman qui a étroitement collaboré à mes recherches. Il m'a apporté sa compétence scientifique et m'a conseillé lors de la rédaction de ce mémoire.

Je remercie M. A. Brekke qui s'est interressé à mon travail sur la composition ionique et m'a fait profité de ses connaissances sur l'ionosphère aurorale.

Mme C. Latombe a très gentiment joué le rôle de candide en acceptant de relire ce manuscrit et d'en retoucher la prose. Je tiens à la remercier sincèrement.

J'adresse mes remerciements aux personnels des radars de Chatanika et d'EISCAT sans lesquels ce travail n'aurait pu être accompli, ainsi qu'aux membres de la communauté française EISCAT pour leurs soutiens scientifique et informatique.

Enfin je suis reconnaissante à tous les membres du CEPHAG pour l'atmosphère chaleureuse et détendue qu'ils savent créer dans le laboratoire. Je remercie plus particulièrement Mme B. Pibaret pour le dépouillement des données qu'elle effectue avec une constante bonne humeur. Mle Carret, Mme Morey et M. Sarrazin ont participé à l'élaboration matérielle des articles de ce mémoire; je les en remercie ainsi que M. Macintosh qui a assuré la dactylographie et la mise en page du texte de synthèse.

# SOMMAIRE

## LISTE DES ARTICLES

1 - Incoherent Scatter Measurements of Ion-neutral collision frequencies and temperatures in the lower thermosphere of the auroral region.
Lathuillere C., V.B Wickwar, W. Kofman.
J. Geophys. Res., 88, 10137 - 10144, 1983.

2 - Neutral Atmosphere studies in the altitude range 90-110 km by EISCAT.
Kofman W., C. Lathuillere, B. Pibaret.
J. Atmos. Terr. Phys., 48, 837-848, 1986.

3 - Direct Measurements of Ion composition with EISCAT in the high latitude F1 region.
Lathuillere C., G. Lejeune, W. Kofman.
Radio Sci., 19, 887-893, 1983.

4 - Incoherent scatter Measurements in F1 region.
Lathuillere C., W. Kofman, B. Pibaret.
J. Atmos. Terr. Phys., 48, 857-866, 1986.

5 - Ion Compositions in the auroral ionosphere as observed by EISCAT.
Lathuillere C., A. Brekke.
Annales Geophysicae, 3, 557-568, 1985.

6 - Elevated Electron temperatures in the Auroral E layer measured with the Chatanika Radar.
Wickwar V.B., C. Lathuillere, W. Kofman, G. Lejeune.
J. Geophys. Res., 86, 4721-4730, 1981.

7 - Ionospheric ion Heating by ULF Pc5 Magnetic Pulsations.
Lathuillere C., F. Glangeaud, Z.Y. Zhao.
J. Geophys. Res., 91, 1619-1626, 1986.

8 - EISCAT Multipulse technique and its contribution to auroral ionosphere and thermosphere description.
Kofman W., C. Lathuillere.
J. Geophys. Res., 90, 3520-3524, 1985.

## 1. INTRODUCTION

Si les premières références aux aurores boréales apparaissent dès l'ancien testament, il faut attendre le 17e siècle avec Kepler, Galiléo et Descartes pour trouver des descriptions non superstitieuses de ces phénomènes lumineux des hautes latitudes. Hypothèses, théorie et modèles sur les aurores ont alors été très nombreux, mais ce n'est qu'à la fin du 19e siècle que l'on associe aurores et perturbations du champ magnétique terrestre. En 1878, Becquerel suggère que ces deux phénomènes sont causés par des particules rapides guidées par les lignes de force du champ magnétique, puis Birkeland lors de plusieurs expéditions au début du siècle, réunit les premières données sur les aurores et les perturbations du champ magnétique, et établit les 4 premières stations de surveillance aurorales (Eather,1980).

Depuis lors, et plus particulièrement depuis les années 1960, les progrès de la physique aurorale ont été considérables grâce aux développements techniques du 20e siècle. Observations et théories ont alors montré que les aurores n'étaient que les phénomènes visibles associés aux processus très complexes du couplage entre le vent solaire, la magnétosphère et la haute atmosphère terrestre. Des quantités d'énergie importantes sont déposées dans l'atmosphère aurorale à partir de 90 Km d'altitude environ par les particules énergétiques qui précipitent le long des lignes de force du champ magnétique, et par les champs électriques d'origine magnétosphérique sous forme de chauffage Joule. Ces quantités d'énergie sont très variables dans le temps et dans l'espace. Elles peuvent atteindre plusieurs dizaines de $mW/m^2$, ce qui est nettement supérieur à l'énergie déposée dans la même gamme d'altitudes par le rayonnement EUV et UV solaire, qui, aux moyennes et basses latitudes, constitue la principale source d'énergie de la thermosphère.

Actuellement un effort important est réalisé pour modéliser empiriquement et théoriquement les entrées d'énergie particulaire et d'énergie Joule. Parrallèlement on cherche à modéliser l'ionosphère et la thermosphère aurorale et leur réponses à ces apports d'énergie; notre travail est une contribution expérimentale à ces études.

L'ionosphère, composante ionisée du gaz atmosphérique, a été décrite sous forme de couches D (60—90 Km d'altitude), E ( 90-140 Km) et F (altitudes supérieures à 140 Km) par Appleton qui reçut le prix Nobel en 1947. Mais ce sont Hulbert en 1928 et Chapman en 1931, qui ont les premiers formulé quantitativement l'action ionisante du rayonnement ultraviolet solaire sur la haute atmosphère terrestre. Actuellement

l'ionosphère des moyennes latitudes est correctement modélisée grâce en particulier à l'apport observationnel des radars à diffusion incohérente qui a depuis 1961 complété les mesures de densité électronique obtenues par les ionosondes.

L'étude de la thermosphère, région de la haute atmosphère neutre qui s'étend à partir du minimum de température vers 90 km d'altitude, s'est considérablement développée depuis le lancement du premier satellite artificiel en 1957. L'interprétation des données de freinage de satellites permet en effet la mesure de la densité de l'atmosphère . A partir de ces données et de mesure complémentaires obtenues par fusées et plus récemment par les radars à diffusion incohérente, des modèles semi-empiriques de la densité et de la température des particules neutres ont été développés. Ils reproduisent maintenant de façon satisfaisante les variations de la thermosphère des altitudes supérieures à 120 Km. La modélisation théorique des variations observées a progressé lorsque que les sources d'énergie aurorales ont été ajoutées à la principale source d'énergie que constitue le rayonnement ultraviolet solaire. Elle donne de bons résultats dans les zones de moyenne latitude.

La technique de diffusion incohérente a été intensivement utilisée pour l'étude de l'ionosphère et de la thermosphère des moyennes latitudes. L'utilisation de cette même technique en zone aurorale doit tenir compte de la grande variabilité spatiale et temporelle des paramètres mesurés ainsi que de la présence d'entrées d'énergie importantes qui peuvent dans certains cas remettre en question les hypothèses habituellement utilisées.

La première partie de ce travail s'intéresse à la théorie de la mesure par diffusion incohérente en zones aurorales pour ce qui concerne les paramètres de la basse thermosphère: température et densité neutre et le paramètre de composition ionique dans la région $F_1$ de l'ionosphère.

Dans la deuxième partie, nous commençons par décrire deux nouvelles sources d'énergie spécifiques aux zones aurorales qui se rajoutent aux énergies Joule et particulaire bien connues: le chauffage des ions par les pulsations magnétiques et le chauffage des électrons en région E par des instabilités.

Puis nous présentons des observations de la basse thermosphère obtenues avec les radars de Chatanika et d'EISCAT ainsi que des mesures de composition ionique obtenues avec EISCAT. Ces différentes observations sont discutées par rapport aux modèles, et/ou par rapport à des observations similaires obtenues à moyenne latitude. Nous

essayons en particulier de décrire la réponse de la basse thermosphère et de l'altitude de transition entre ions moléculaires et ions oxygène atomique aux apports d'énergie Joule et particulaire.

Dans la conclusion nous insistons sur la nécessité de continuer ce type d'observations afin d'obtenir une base de données de zone aurorale indispensable à la modélisation globale de l'ionosphère et de la thermosphère en périodes calmes et perturbées.

## 2. MESURE DES PARAMETRES IONOSPHERIQUES ET NEUTRES PAR DIFFUSION INCOHERENTE DANS LES REGIONS E ET F1 DE L'IONOSPHERE AURORALE

La technique de diffusion incohérente appliquée à l'étude de l'ionosphère a été introduite par Gordon (1958) et Bowles (1958); actuellement plusieurs stations radars sont exploitées à basse et moyenne latitudes: Arecibo (Puerto Rico), Millstone Hill (USA), St Santin (France) et à haute latitude: EISCAT (Scandinavie) et maintenant Sondre Stromfjord (Groenland), nouvelle implantation du radar de Chatanika (Alaska).

Une expérience de diffusion incohérente consiste à illuminer le plasma ionosphérique avec une onde incidente de fréquence très élevée (par rapport à la fréquence caractéristique du plasma) et à observer la puissance diffusée de manière incohérente par les électrons libres du milieu (diffusion de Thomson). Dans le cas où la longueur d'onde utilisée est grande devant la longueur de Debye du milieu ionosphérique, le spectre de puissance reçu traduit le comportement collectif des électrons et se compose de deux parties: le spectre ionique corespondant aux oscillations pseudo acoustiques du milieu et les raies de plasma corespondant aux oscillations de plasma. On trouvera dans Bauer (1975) une revue de la théorie de diffusion incohérente.

Nous ne nous interessons dans ce travail qu'au spectre ionique dont la forme dépend d'un certain nombre de paramètres caractéristiques du plasma: la densité électronique, les températures électroniques et ioniques, la composition ionique, la fréquence de collisions ions-neutres et la vitesse ionique dans la direction du vecteur d'onde différence entre vecteur d'onde incidente et diffusée. Ces paramètres sont obtenus par ajustement non linéaire au sens des moindres carrés entre spectre ionique observé et spectre théorique ou de manière équivalente entre fonction d'autocorrélation observée et théorique (Walteufel 1970b, Wickvar 1974, Lejeune 1978).

La technique de diffusion incohérente a été mise en oeuvre soit en appliquant la méthode classique du radar à impulsions (simple ou multiples), c'est à dire en émettant et recevant avec la même antenne (radar de Chatanika par exemple) , soit en utilisant un système à plusieurs antennes (radar de St Santin). Dans le premier cas l'altitude de la zone ionosphérique que l'on veut étudier depend de la durée entre émission et réception, et la résolution en altitude de la mesure est fonction de la durée de l'impulsion émise; dans le second cas altitude et résolution en altitude sont déterminées par le volume défini par l'intersection des lobes de l'antenne d'émission et de l'antenne de réception. Ces deux méthodes ont été associées dans la conception du radar européen EISCAT. Le tableau suivant résume les caractéristiques

des deux systèmes radar à diffusion incohérente installés en zone aurorale et avec lesquelles nous avons travaillé.

| | Coordonnées geomagnétiques | Puissance crête | Fréquences | Stations réception additionnelles | Schémas d'impulsions |
|---|---|---|---|---|---|
| Chatanika | 64.75°N 105°W | 4MW | 1290Mhz | | Impulsion simple 60µs, 320µs Impulsions multiples 3*60µs 2*160µs |
| EISCAT UHF Tromsö | 66.6°N 104.9°E | 2MW | 933.5Mhz ±3.5 | Kiruna Sodankyla | Programmable 10µs à 10ms |
| VHF | | 5MW | 224Mhz ±1.75 | | Programmable 10µs à 1ms |

Alors que le radar de Chatanika est un radar monostatique travaillant à une seule fréquence et avec un nombre limité de schémas d'impulsions, le système UHF d'EISCAT est à la fois monostatique (émission et réception à Tromso) et tristatique (émission à Tromso, réception à Kiruna et Sodankyla) permettant ainsi la mesure vectorielle de la vitesse des ions et l'obtention simultanément du profil en altitude des paramètres ionosphériques. De plus le système est multifréquences et les possibilités de schémas d'impulsions très variés grâce à l'utilisation dans chaque station d'un corrélateur programmable. Les premières expériences avec le système VHF d'EISCAT (monostatique) n'ont été réalisées que très récemment (pendant l'automne 1986) et ne seront pas discutées dans ce travail. On trouvera une description détaillée du système EISCAT dans Folkestad et al. (1983) et du radar de Chatanika dans Leadabrand et al. (1972).

## 2.1 Les différents schémas d'impulsions

Nous ne décrivons ici que les schémas d'impulsions qui ont été utilisés pour obtenir les résultats décrits dans ce travail.
Le choix du schéma d'impulsion pour une expérience de diffusion incohérente est fait en fonction de plusieurs considérations:

- la résolution en altitude de la mesure doit être adaptée à la variabilité des paramètres mesurés (voir figure 1a)

- la largeur du spectre de diffusion incohérente est fonction des différents paramètres et varie en particulier avec l'altitude (figure 1b)
- le rapport signal sur bruit instantané est proportionnel à la durée de l'impulsion émise et à la densité électronique.

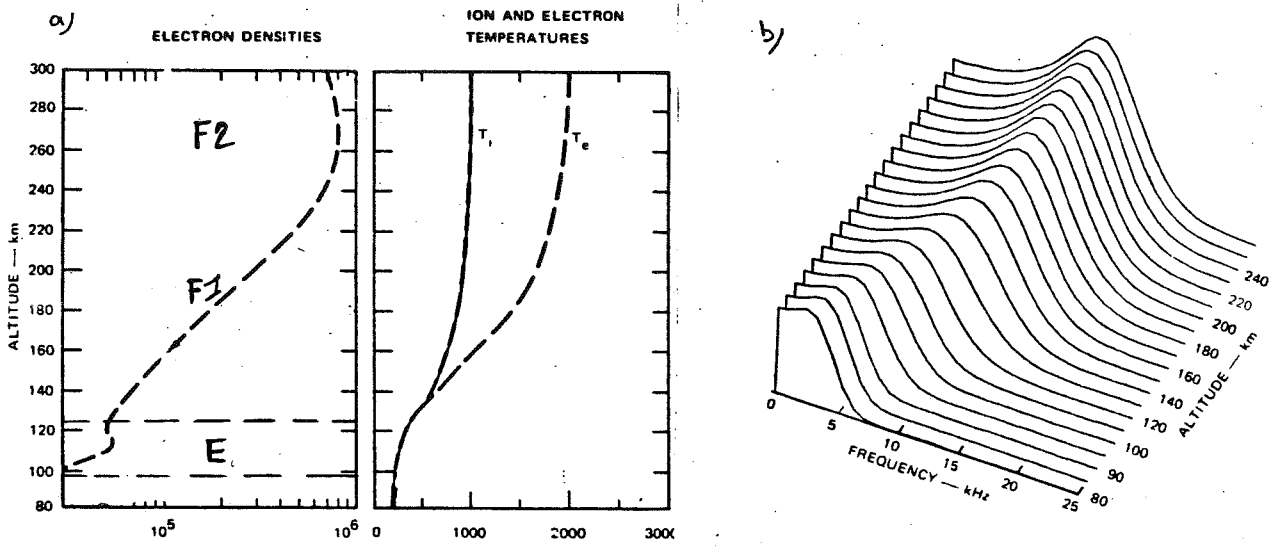


Figure 1: a) Variation des paramètres ionosphériques en fonction de l'altitude et indication des différentes régions ionosphériques E, F1 et F2 pour une ionosphère typique de jour, et b) Spectres de diffusion incohérente correspondants .

L'étude des différentes régions ionosphériques (figure 1a) est faite en utilisant deux manières de calculer la fonction d'autocorrélation du signal reçu, la première correspondant à l'émission d'une impulsion unique, la deuxième à l'émission d'une série d'impulsions. Ces deux techniques sont souvent associées pour définir une expérience.

Le mode " impulsion simple" consiste en l'émission d'une seule impulsion de durée suffisamment longue pour permettre le calcul de la fonction d'autocorrélation du signal reçu à l'intérieur d'une fenêtre temporelle de durée égale à l'impulsion émise (figure 2a). Dans la pratique, ce mode est utilisé pour la mesure à des altitudes supérieures à 150 Km. A Chatanika, on émet une impulsion de 320 µs, ce qui corespond à un volume diffusant de ± 48 Km. A Tromsö , la longueur de l'impulsion émise est variable: nous utilisons des données obtenues avec une impulsion de 360 µs ( c'est à dire un volume diffusant de ± 54 Km) dans la majorité des cas, exceptionnellement avec une impulsion de 500 µs utilisée en particulier au début du fonctionnement d'EISCAT.

Dans le mode " impulsion multiples", plusieurs impulsions très courtes sont émises successivement afin de calculer la fonction d'autocorrélation du signal reçu. Dans ce cas, le volume diffusant correspond à la durée de l'impulsion élémentaire mais le signal sur bruit de la mesure diminue: sur la figure 2b, on peut voir que seul le signal provenant de l'altitude z contribue à la mesure alors que le bruit provient de diverses altitudes. Cette technique n'est donc utilisable que lorsque la densité électronique est suffisamment grande. A Chatanika on émet une série de 3 impulsions de 60 µs ( volume diffusant ±9 Km) . A Tromso on émet une série de 5 impulsions de 15 µs ( volume diffusant ± 2.25 Km); on associe de plus la mesure à deux fréquences différentes pour augmenter la statistique des résultats.
La technique " impulsions multiples" est employée pour les mesures en région E jusque vers 140 Km d'altitude. Nous la décrivons plus précisément dans l'**article 8** ( EISCAT) et dans l'**article 6** (Chatanika).

Il apparait que la région F1 est très mal couverte par les 2 techniques présentées car le volume diffusant correspondant au mode " impulsion simple" est grand par rapport à l'échelle de hauteur des paramètres ionosphériques de cette région ,soit 20 Km environ. D'autre part, pour des altitudes supérieures à environ 130 Km, le rapport signal sur bruit obtenu avec le mode " impulsions multiples" à Chatanika est trop faible et la période d'échantillonnage utilisée à Tromsö est trop proche du temps de corrélation du milieu ionosphérique interdisant l'utilisation de la technique "impulsions multiples" en région F1 pour le moment. Dans l'avenir, avec le système VHF D'EISCAT, on pourra utiliser la technique "impulsions multiples" avec des impulsions élémentaires plus longues: la fréquence utilisé par le système VHF étant de 224 MHz au lieu de 933 MHz pour le système UHF, la largeur de la fonction d'autocorrélation est environ 4 fois plus grande, ce qui permet d'utiliser une période d'échantillonnage nettement plus grande.

En pratique donc, les paramètres ionosphériques sont obtenus au dessus de 140 Km par la technique " impulsion simple". L'influence de la technique de mesure sur les résultats géophysiques est discutée quantitativement dans l'**article 4** où l'on montre entre autres que les erreurs ainsi introduites peuvent atteindre 50% sur la température électronique et 20% sur la température ionique vers 150 Km d'altitude.

Il faut rajouter à ces deux modes, le mode appelé "puissance" dans lequel une seule impulsion relativement courte est émise et pour lequel on ne cherche à déterminer que la puissance du signal reçu qui est proportionnelle à la densité électronique ( l'information spectrale n'est pas utilisée). Le mode "puissance" à EISCAT consiste en une impulsion de 60 µs, ce qui corespond à un volume diffusant de ± 9 Km.

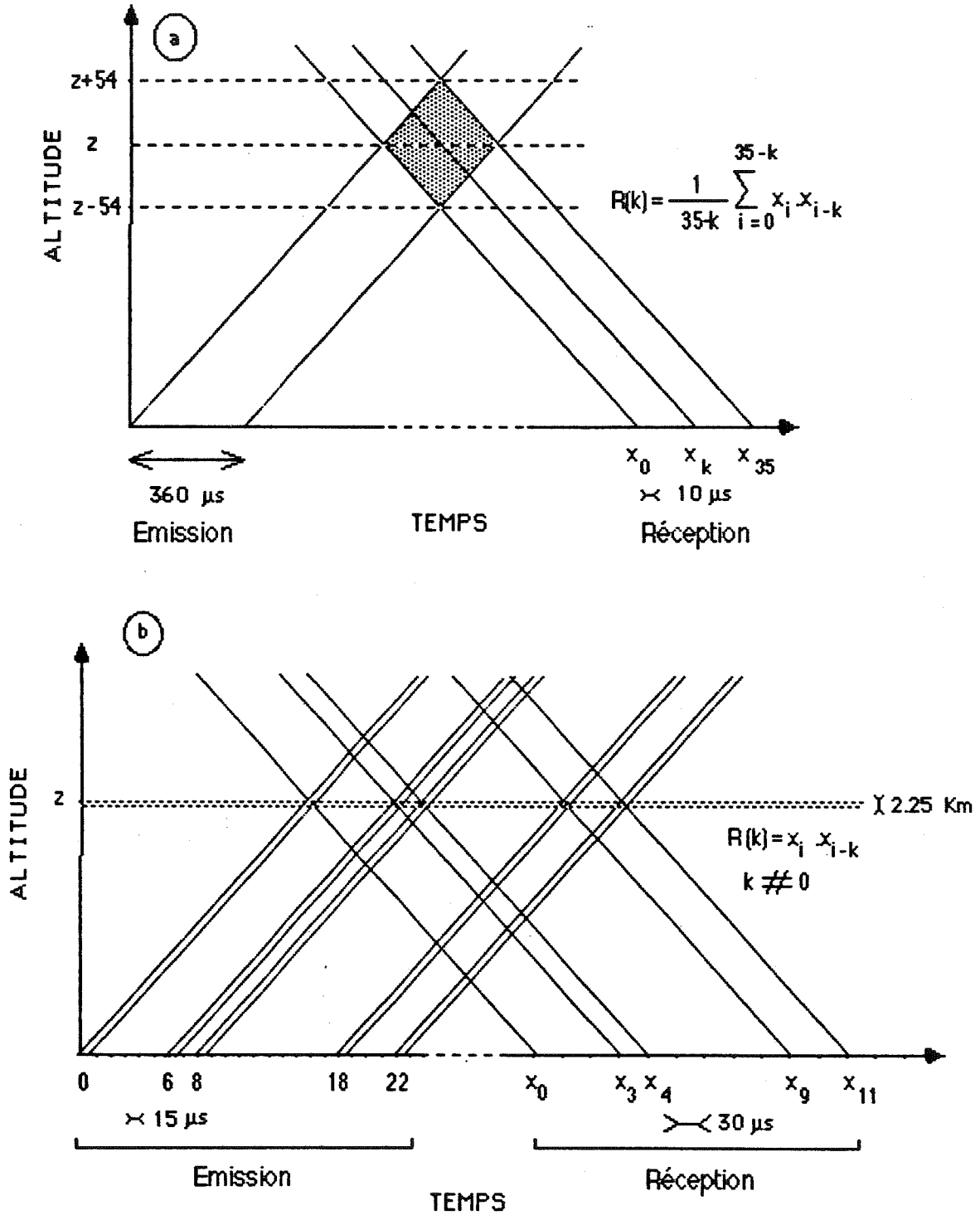


Figure 2: Schémas des modes "impulsion simple" (a), et "impulsions multiples " (b) utilisés à Tromsö. On a indiqué dans chaque cas la durée du ou des impulsions émises. R(k) représente le retard k de la fonction d'autocorrélation du signal reçu.

## 2.2 Analyse des données de diffusion incohérente en région E: Température et densité neutres

Le spectre de diffusion incohérente mesuré en région E donne accès non seulement aux températures du plasma mais aussi à la fréquence de collision ion-neutre. En effet l'augmentation des collisions entre ions et molécules neutres à basse altitude a pour effet un rétrécissement de la largeur du spectre (Dougherty et Farley 1963, Walteufel 1969). Cet effet est mesurable jusque vers 110 Km pour les radars de Chatanika et d'EISCAT (système UHF).

Dans la région E de moyenne latitude, il y a équilibre thermique entre le plasma et la population de particules neutres. La mesure de la température du plasma est donc une mesure de la température neutre et la fréquence de collisions ion-neutre peut être déterminée sans ambiguité. Cette fréquence de collisions est en première approximation proportionnelle à la densité neutre. La diffusion incohérente permet donc d'étudier la température et la densité de la basse thermosphère (90 Km à 110 Km) . Les données des différents radars de moyenne latitude ont été intensivement utilisées pour ces études (voir l'article de synthèse de Alcayde et Bernard 1982).

Dans les **articles 1 et 2** nous avons étendu ces mesures aux radars de Chatanika et d'EISCAT en tenant compte des conditions spécifiques aux zones aurorales. En effet, l'hypothèse d'équilibre thermique utilisée pour obtenir la fréquence de collisions ion-neutre n'est plus toujours vérifiée. Pendant les périodes de précipitations particulaires la température électronique peut être supérieure à la température ionique; la différence entre ces températures dépend du spectre d'énergie des précipitations et est en général négligeable aux altitudes inférieures à 110 Km où les processus de perte d'énergie des électrons sont encore très efficaces. Pendant les périodes de fort champ électrique, le chauffage Joule des ions est efficace pour les altitudes supérieures à 120 Km (Banks 1977, Wickwar et al. 1975) alors que le chauffage Joule des électrons est complètement négligeable ( Schunk et Walker 1971, Banks 1979). De plus pendant ces mêmes périodes des instabilités peuvent être à l'origine du chauffage " anormal" des électrons dans une zone d'altitude très limitée: 100 - 120 Km ( **article 6**, Schlegel et St Maurice 1981, St Maurice et al. 1981).

En zone aurorale, la mesure de la fréquence de collisions à partir du spectre de diffusion incohérente est donc possible en dessous de 100 Km en toutes circonstances mais l'est seulement en dehors des périodes de fort champ électrique au dessus de cette altitude.

Les fréquences de collisions étant proportionnelles aux densités neutres, leur profil en fonction de l'altitude permet de calculer l'échelle de hauteur de l'atmosphère neutre lorsque l'on suppose cette dernière en équilibre hydrostatique dans la région de mesure soit 90 à 110 Km (**article 1**).

Echelle de hauteur et température neutre sont calculées en utilisant la moyenne des données sur plusieurs heures de mesure après s'être assuré que l'on n'incluait aucune période de chauffage Joule (tests sur la température ionique à plus haute altitudes et/ou sur les champs électriques).

Pendant les périodes de chauffage "anormal", l'échelle de hauteur est déduite des mesures inférieures à 100 Km d'altitude. La valeur trouvée est utilisée pour calculer les fréquence de collision entre 100 Km et 110 Km, puis les spectres de diffusion incohérentes dépouillés en utilisant ces valeurs afin d'obtenir les températures electroniques et ioniques. La température ionique est alors une mesure de la température neutre. Cette analyse des données pendant les périodes de chauffage Joule mise au point sur les données d' EISCAT ( **article 2**) n'est pas utilisable pour les données de Chatanika pour lesquelles nous ne disposons au maximun que de 4 altitudes de mesure (au lieu de 8 pour les données de Tromsö).

## 2.3 Analyse des données de diffusion incohérente en région F1: la composition ionique

La composition ionique est un des paramètres géophysiques dont depend la forme du spectre de diffusion incohérente. En région E, la population ionique est constituée d'un mélange d'ions moléculaires $NO^+$ et $O_2^+$ ; puis en région F1 ces ions moléculaires sont progressivement remplacés par l'ion oxygène $O^+$. Entre 300 Km et 450 Km on considère généralement que cet ion est le seul présent alors qu'au dessus de 450 Km commencent à apparaitre des ions légers $H^+$.

La différence de masse importante entre les ions $H^+$ et $O^+$ a permis de mettre en évidence la présence d'ions légers à haute altitude à l'aide des premières données d'EISCAT (Lejeune et al. 1982) mais il faudra attendre le fonctionnement du système VHF d'EISCAT pour poursuivre cette étude.

A basse altitude, les masses des ions présents sont beaucoup trop proches pour que l'on puisse envisager de déduire leur proportions respectives des spectres de diffusion incohérente. Dans cette région on

considère qu'on se trouve en présence d'un ion fictif de masse 30.5 a.m.u. (ou 31 a.m.u.) pour déterminer les températures électroniques et ioniques et le cas échéant la fréquence de collisions ion-neutre.

C'est dans la région F1 que le problème de la détermination de la composition ionique est le plus critique. Les paramètres géophysiques sont déduits des mesures de diffusion incohérente par ajustement non linéaire au sens des moindres carrés entre fonction d'autocorrélation mesurée et fonction d'autocorrélation théorique du milieu ionosphérique. Dans la région F1, cet ajustement non linéaire ne converge pas toujours lorsqu'on lui laisse 5 degrés de liberté ( température électronique, température ionique, densité électronique, vitesse ionique et composition ionique) car les fonctions d'autocorrélation mesurées sont plus ou moins bruitées. Dans la pratique, pour les dépouillements de routine, on fixe un modèle de composition et l'ajustement n'est alors réalisé qu'avec 4 degrés de liberté.

Fixer une mauvaise valeur de composition entraîne une erreur systématique importante sur les résultats de températures électroniques et ioniques, c'est pourquoi, plusieurs méthodes ont été développées à partir des données des sondeurs de moyenne latitude pour obtenir cette composition. La plupart d'entre elles consistent à faire des hypothèses complémentaires sur les profils en altitude de la température ionique (Evans 1967, Evans et Cox 1970, Wand et Perkins 1970). Kelly et Wickwar (1981) font de plus des hypothèses de continuité temporelle des températures électroniques, afin de s'adapter aux situations particulières rencontrées en zone aurorale et particulièrement aux situations de chauffage Joule. Carru et al. (1967) et Petit (1968) recherchent, dans l'ensemble des solutions possibles pour la composition, celle qui leur permet d'obtenir une certaine continuité à la fois sur les profils de composition et sur les profils de températures; cette méthode est formalisée par Oliver (1979) qui introduit des contraintes physiques sur les profils de composition et de température ionique.

Dans toutes ces méthodes l'ajustement non linéaire réalisé n'a pour but la détermination que de 4 paramètres. Seuls Alcayde et al. (1974) et Fontanari et Alcayde (1974) ont utilisé les résultats de l'ajustement non linéaire avec 5 degrés de liberté pour les données du sondeur de St Santin, mais ils ont dû effectuer des moyennes diurnes de la composition afin de réduire les erreurs.

La méthode que nous avons développée dans l'**article 3**, à partir des données du sondeur EISCAT, consiste à forcer la convergence de l'ajustement non linéaire avec 5 degrés de liberté, en choisissant des valeurs initiales les plus proches possibles de la solution; celles ci

correspondent aux minima (il y en a en général deux) de l'écart quadratique entre la fonction d'autocorrélation mesurée et les fonctions d'autocorrélation théorique calculées avec les diverses valeurs possibles de composition.

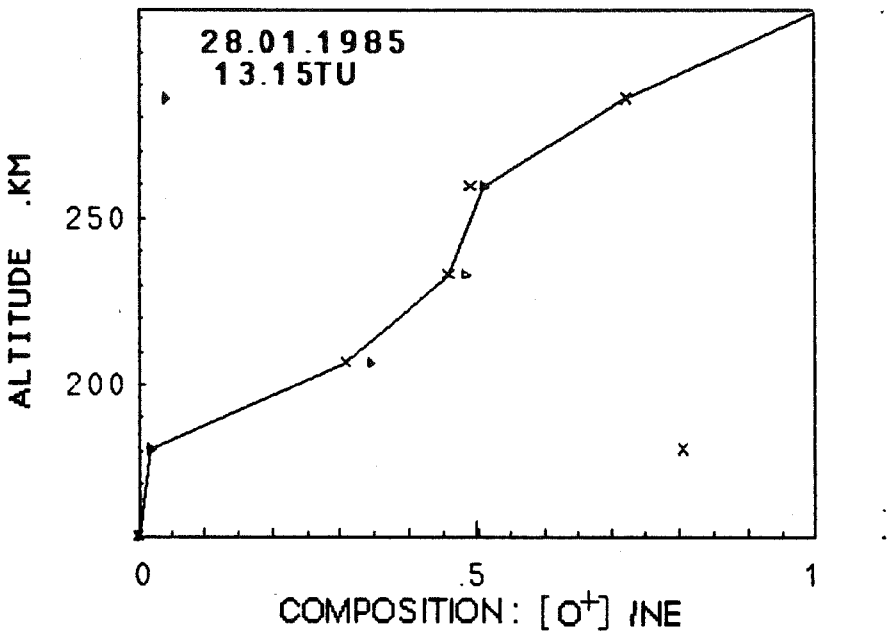


**Figure3:** Procédure de détermination du profil de composition ionique: les × et les ▷ sont les deux solutions obtenues par régression aux moindres carrés.La ligne brisée représente le résultat du choix automatique entre les deux solutions.

Un des problèmes de cette méthode est qu'il y a deux solutions correspondantes à deux valeurs de composition. Ces deux valeurs peuvent être très proches l'une de l'autre (voir figure 3) et leur écart est alors inférieur à l'erreur de mesure. Elles peuvent aussi être approximativement symétriques par rapport à une composition de 50% d'ions moléculaires, ceci veut dire que dans le cas où la solution est un ion unique, celui ci peut être au choix l'ion moléculaire ou l'ion O+. Le choix entre les deux solutions est fait a posteriori et de manière automatique afin d'obtenir un profil de composition avec l'altitude qui soit monotone (voir figure 3). Cette contrainte est très faible en comparaison des contraintes imposées aux profils de températures par les autres méthodes.

A partir de fonctions d'autocorrélation mesurées à Tromsö et intégrées pendant 5 minutes, notre méthode permet d'obtenir la composition ionique avec une erreur moyenne de l'ordre de 20%.

Le temps d'intégration choisi, 5 mn, est un compromis satisfaisant entre la nécessité d'intégrer suffisamment longtemps pour obtenir un bon rapport signal sur bruit, et le fait que, surtout en zone aurorale, les paramètres ionosphériques varient très rapidement.

Dans la suite de ce travail, nous présentons les résultats de composition ionique sous la forme d'une altitude de transition notée $Z_{40}$, altitude où le pourcentage d'ions O+ est égal à 40%. Ce choix avait été fait au vu de résultats de simulations théoriques, montrant que le biais d'estimation de la composition résultant de l'utilisation de la technique "impulsion simple" ( volume diffusant très grand) était minimal à cette altitude. Ce biais d'estmation est alors de l'ordre de 10 Km. L'étude expérimentale de l'influence du volume diffusant sur la détermination des paramètres en région F1 (**article 4**) confirme que dans la zone d'altitude où le pourcentage d'ions O+ varie entre 40% et 60%, c'est à dire entre 180 Km et 220 Km, le biais d'estimation est faible alors que en dehors de cette zone les compositions ioniques obtenues sont largement surestimées (à haute altitude) ou sousestimées (à basse altitude).

## 3. OBSERVATIONS DE L'IONOSPHERE ET DE LA BASSE THERMOSPHERE AURORALE

L'implantation du premier radar à diffusion incohérente à Chatanika en zone aurorale a permis de préciser les répartitions spatiales et temporelles de l'énergie déposée dans la thermosphère par les particules énergétiques précipitées le long du champ magnétique terrestre et par les champs électriques sous forme de chauffage Joule (Vickrey et al. 1982, Banks 1977,Wickwar et al. 1975, Ponthieu 1982). Parallèlement à l'évaluation de ces quantités d'énergie, un effort important est actuellement réalisé pour décrire la thermosphère et l'ionosphère des zones aurorales et leur réponse à ces apports d'énergie:

Des modèles numériques à trois dimensions de l'ionosphère (Schunk et Raitt 1980, Sojka et al. 1981 a b, Schunk et Sojka 1982) et de la thermosphère (Dickinson et al 1981, Fuller Rowell et Rees 1980) essayent d'évaluer de manière indépendante la réponse de l'ionosphère et de la thermosphère (altitudes supérieures à 120Km) aux apports d'énergie auroraux. L'effet du chauffage auroral sur la basse thermosphère a été examiné plus récemment par Roble et Kasting (1984) à l'aide d'un modèle à deux dimensions. Ces modèles ne traitent pas encore de manière autocohérente le couplage entre ionosphère et atmosphère neutre et la comparaison avec les résultats expérimentaux reste difficile particulièrement à basse altitude (voir par exemple Prölss 1980).

Les modèles semi-empiriques permettent de décrire l'atmosphère neutre en fonction de différents paramètres tels que position géographique du lieu étudié, heure, indices de flux solaire et indices géomagnétiques , à partir d'une limite inférieure variable entre 90Km et 120Km. Dans le modèle MSIS-83 (Hedin 1983) les conditions aux limites à l' altitude de base sont variables mais la variation des températures et densités neutres entre 90 et 120Km et à haute latitude n'est encore basée que sur quelques mesures effectuées à bord de fusées.

La technique de diffusion incohérente permet d'obtenir des données à long et court termes indispensables aux modèles empiriques et permettant une comparaison avec les modèles théoriques. Notre contribution est double: d'une part nous étudions les conditions aux limites à la base de la thermosphère: température, densité totale et masse moyenne; d'autre part nous étudions la composition ionique de la région F1 de l'ionosphère aurorale : les variations diurnes, saisonnières et la réponse aux apports d'énergie.

## 3.1 Les entrées d'énergie:

Les chauffages Joule et particulaire sont les deux principales sources d'énergie spécifiques aux zones aurorales. Ces énergies s'ajoutent à l'energie déposée par le rayonnement électromagnétique solaire dans l'atmosphère terrestre. Après avoir rappelé brièvement les effets sur l'ionosphère de ces deux sources d'énergie, nous étudions deux autres sources: la dissipation Joule de l'énergie des pulsations magnétiques (**article 7**) et le chauffage "anormal" des électrons en région E (**article 6**).

### 3.1.1 Chauffage particulaire

Un faisceau d'électrons énergétiques (0.1 à 100 Kev) ou de protons qui pénètre dans l'atmosphère terrestre perd toute son énergie au cours de réactions d'ionisation, de dissociation et d'excitation des particules neutres, produisant ainsi les aurores boréales et australes. Le chauffage particulaire dû à ces électrons précipitant le long des lignes de force du champ magnétique terrestre et dont l'énergie moyenne est de l'ordre du Kev, est très variable dans le temps et l'espace; son amplitude varie entre 0.1 $mW/m^2$ et plusieurs dizaines de $mW/m^2$.

Alors que 50% à 60% de l'énergie incidente résulte en un chauffage de l'atmosphère neutre ( Singh et Gerard 1982, Rees et al. 1983), la signature des précipitations particulaires dans l'ionosphère consiste en une augmentation de l'ionisation à une altitude dépendant de l'énergie des électrons incidents, et en un chauffage des électrons thermiques.

Dans l'**article 8** (figure 5) nous montrons un exemple de réponse de l'ionosphère à une précipitation particulaire intense: 50 $mW/m^2$ et dont le spectre en énergie est assez large. On observe une augmentation de la densité électronique très importante ( multiplication par un facteur 5 à 10) en région E principalement mais aussi jusque vers 300 Km d'altitude. Simultanément on observe une augmentation de la température électronique de 50K à 120 Km d'altitude et 60K à 300 Km d'altitude; en dessous de 110 Km le plasma ionosphérique reste en équilibre thermique.

### 3.1.2 Chauffage Joule "classique"

Le champ électrique de convection, induit par le couplage entre le vent solaire et la magnétosphère, est à l'origine dans l'ionosphère d'un transfert d'énergie ( chauffage Joule) et de quantité de mouvement (

entrainement ionique) important entre les particules ionisées et les particules neutres. L'entrainement ionique peut modifier la circulation des vents neutres particulièrement pendant les périodes magnétiquement agitées ( voir l'article de synthèse de Roble 1983). Le chauffage Joule provoque une augmentation de la température ionique dans toute l'ionosphère ( Stubbe et Chandra 1970, Schunk et Walker 1973, St maurice et Hanson 1982, Baron et Wand 1983), associée à une diminution de la densité électronique en région F ( Schunk et al. 1975, Schlegel 1984).

Le dépot d'énergie Joule qui peut atteindre 100 $mW/m^2$ domine généralement le dépot d'énergie particulaire dans le secteur soir mais la moyenne diurne de ces deux sources d'énergie est sensiblement la même ( Vickrey et al. 1982).

### 3.1.3 Dissipation Joule de l'énergie des pulsations magnétiques

Les pulsations magnétiques, oscillations du champ magnétique terrestre, avec des périodes pouvant aller de quelques secondes à plusieurs minutes, constituent un des mécanismes de transfert de l'énergie de la magnétosphère externe à l'ionosphère. A haute latitude, ces ondes électromagnétiques peuvent avoir des amplitudes importantes, en particulier pendant les périodes de forte activité magnétique.

La dissipation Joule dans l'ionosphère est un des mécanismes d'atténuation des pulsations ( Newton et al. 1978). Il a été mis en évidence indirectement à partir de mesures au sol ( Glassmeier et al. 1984) et à partir de mesures avec le radar Stare dans l'ionosphère (Greenwald et Walker 1980). Le radar EISCAT permet de mesurer dans l'ionosphère simultanément les fluctuations de la vitesse ionique associées aux pulsations magnétiques et les fluctuations de température ionique. La mesure directe du transfert d'énergie entre pulsations et plasma ionosphérique est alors possible.

Les premières études de pulsations dans l'ionosphère, utilisant la technique de diffusion incohérente et associées à des mesures sol, ont été réalisées avec le sondeur de St Santin, à moyenne latitude (Lathuillere et al. 1981), puis avec le radar EISCAT à haute latitude (Glangeaud et al. 1985). Ces études nécessitent l'acquisition des données de diffusion incohérente avec une très bonne résolution temporelle: 10 sec. pour les pulsations de type Pc3-Pc4 ( périodes de 10 à 150 sec.), 1 minute pour les Pc5 ( périodes supérieures à 150 sec ).

Deux campagnes de mesure ECSIM ( Etude du Couplage Sol-Ionosphère-Magnétosphère) ont été réalisées en Scandinavie en Novembre et Décembre 1983: la présence de pulsations de type Pc5 a été mise en évidence pendant 5 journées sur 6 ( Glangeaud et al. 1985). Dans l'**article 7** nous montrons que les fluctuations de vitesse ionique ayant des périodes supérieures à trois minutes sont parfaitement corrélées avec les fluctuations de températures ionique pour des altitudes variant entre 135 Km et 400 Km (voir figure 4). Des méthodes plus élaborées de traitement de signal ont permis d'étudier expérimentalement la relation simplifiée exprimant le chauffage Joule en région F: $T_i - T_n = R( V_i - V_n)^2$ (voir **article 7**) et de montrer que le coefficient R était comparable aux valeurs théoriques et ne dépendait pas de la période des pulsations. Ce résultat était attendu car la constante de temps des variations de température ionique en région F varie de quelques secondes à quelques dizaines de secondes. Ainsi l'augmentation de température dûe à un champ électrique continu (effet Joule "classique") ou associé aux pulsations magnétiques, est identique, pourvu que les particules neutres n'aient pas eu le temps de se mettre en mouvement par entrainement ionique, ce qui se produit dans le cas de champs électriques continus.

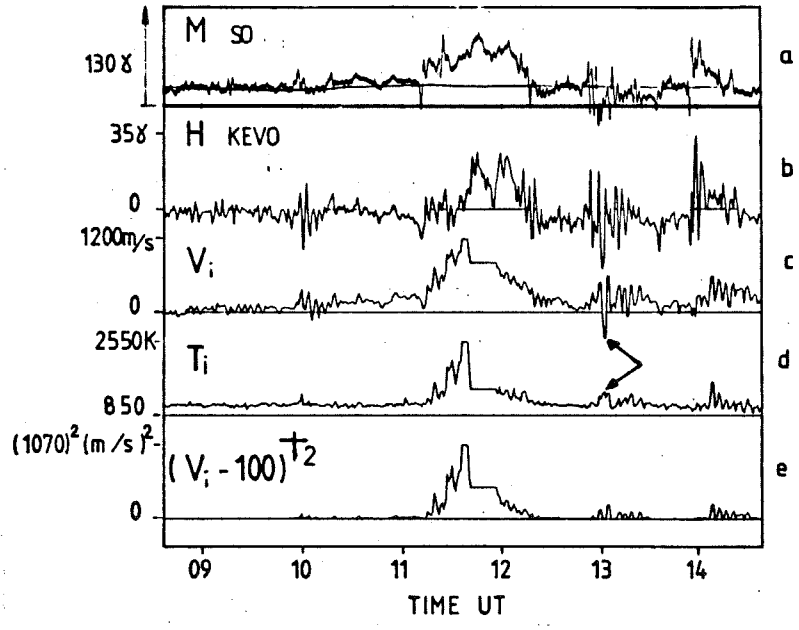


Figure 4: 11 Novembre 1983. Données brutes montrant la relation entre le champ magnétique mesuré au sol -composante H mesuré à Sodankyla (courbe a), composante H filtrée entre 0.3 et 8 mHz mesurée à Kevo (courbe b)- la vitesse ionique (courbe c et e) et la température ionique (courbe d) mesurée à Tromsö à 300Km d'altitude.

L'étude que nous avons réalisée ne porte pas sur un seul évènement d'amplitude exceptionnel (Glassmeier et al. 1984, Crowley et al. 1985), mais sur des pulsations magnétiques nombreuses et d'amplitude tout à fait habituelles en zone aurorale (amplitude maximum parmi nos observations inférieure à 40 γ). Nous prouvons ainsi que la dissipation Joule de l'énergie des pulsations magnétiques est une source d'énergie non négligeable pour le plasma ionosphérique .

Dans le cas de résonances du champ magnétique dans le mode toroïdal, on peut calculer la quantité d'énergie Joule W dissipé localement par une pulsation: $W = \Sigma_p E_0^2$ (Greenwald et Walker 1980), où $E_0$ est l'intensité efficace du champ électrique de la pulsation et $\Sigma_p$ la conductivité Pedersen intégrée de l'ionosphère.

Les données du 11 Novembre 1983, présentées sur la figure 4, entre 13.00 et 13.20 TU, nous permettent d'estimer cette quantité d'énergie Joule. En effet, pendant cette période, l'intensité de la pulsation mesurée au sol est de l'ordre de 20 γ. Dans l'ionosphère (300 Km d'altitude), elle correspond à des vitesses ioniques polarisées principalement dans la direction Est-Ouest équivalentes à un champ électrique $E_0$ de l'ordre de 26 mV/m. Les valeurs typiques de conductivité Pedersen sont, durant la journée et en zone aurorale, de 2 à 4 $\Omega^{-1}$ ( Vickrey et al. 1981). On trouve ainsi que l'énergie Joule dissipée localement par cette pulsation est de l'ordre de 1.4 à 2.8 $mW/m^2$, c'est à dire comparable à l'énergie UV solaire absorbée au dessus de 120 Km d'altitude. Ces chiffres sont une approximation par valeurs inférieures, en effet l'expérience ne permet pas la description en latitude des pulsations et l'on ne peut pas savoir où la mesure a lieu par rapport au maximum de la résonance du champ magnétique.

Greenwald et Walker (1980), utilisant des données du radar STARE, qui permet l'étude de la répartition latitudinale et longitudinale des pulsations de type Pc5, ont montré que ce taux d'énergie Joule pour une pulsation d'amplitude au maximum de la résonance 2 fois supérieure à notre exemple, représentait environ un tiers du dépot d'énergie Joule correspondant à un sous orage magnétique peu intense.

### 3.1.4 Chauffage électronique "anormal" en région E

Les données de diffusion incohérente acquises à Chatanika en Mars et Novembre 1978 ont permis de mettre en évidence une augmentation de la température électronique en région E (entre 95 et 115 Km d'altitude) pouvant atteindre plusieurs centaines de degrés (**article 6**). Nous

avons montré que ce chauffage exceptionnel des electrons avait lieu pendant les périodes de dépot d'énergie Joule.

Les travaux de Rees et Walker (1968) et Schunk et Walker (1971) montrent que le chauffage Joule des electrons est complètement négligeable. Pourtant, le chauffage Joule des ions et l'augmentation des températures électroniques étant correlées, on peut en déduire que le chauffage électronique en région E a lieu lorqu'il existe des champs électriques importants ( supérieurs à 20 mV/m), c'est à dire lorsque les électrons ont une vitesse relative par rapport aux ions et aux neutres supérieure à 400 m/s. Ces grandes vitesses relatives peuvent donner lieu à des instabilités ( Farley 1963). Ce processus est étudié par St Maurice et al. (1981) qui montrent que l'instabilité double faisceau et l'instabilité de gradients peuvent être à l'origine de nos observations et d'observations similaires obtenues par Schlegel et St Maurice (1981).

Dans l'**article 6** nous examinons différentes conséquences des déséquilibres thermiques de la région E pendant les périodes de fort champ électrique. En particulier l'interprétation des spectres de diffusion incohérente en supposant l'équilibre thermique tel qu'on le fait habituellement jusque vers 110 Km d'altitude, donne dans ce cas des valeurs de fréquences de collisions beaucoup trop faibles. L'obtention des paramères de la basse thermosphère est donc impossible pendant les périodes de fort champ électrique (comme nous l'avons souligné dans la première partie de ce travail) à cause de ce chauffage électronique.
Des températures électroniques élevées ont été également observées en région E avec le radar EISCAT avec une meilleure résolution en altitude. Des exemples sont présentés dans l'**article 2**.

### 3.2 La basse thermosphère aurorale:

Nous présentons dans l'**article 1** les mesures de température neutre et de fréquence de collisions obtenues avec le radar de Chatanika en Mars et Novembre 1978 et dans l'**article 2** des mesures similaires obtenues avec le radar EISCAT entre Décembre 1983 et Février 1985.

Les échelles de hauteur calculées à partir des profils de fréquence de collisions moyennées sur plusieurs nuits d'expérience en Mars et Novembre 1978 sont égales respectivement à 6.76 $\pm$ 0.25 Km et 7.64 $\pm$ 0.59 Km, c'est à dire légèrement supérieures à l'échelle de hauteur du modèle d'atmosphère neutre Jacchia (1971). Les profils de température correspondants entre 90 et 110 Km sont très proches du profil de

température du même modèle. Nous avons utilisé ces profils de températures pour calculer théoriquement les fréquences de collisions en utilisant l'hypothèse d'équilibre hydrostatique de l'atmosphère neutre et une masse moyenne égale à celle du modèle Jacchia (1971); les fréquences de collisions calculées sont en accord avec les mesures lorsque l'on tient compte des barres d'erreur.

Une étude plus détaillée des profils de températures entre 90 et 140 Km d'altitude pendant 4 nuits d'expérience (Mars 1978) nous a permis de mettre en évidence une augmentation systématique de la température pendant la deuxième moitié de la nuit (Figure 5). Cette augmentation semble correspondre aux caractéristiques des marées semi-diurnes (longueur d'onde verticale 40 à 60 Km et amplitude 10 à 20%), qui sont prépondérantes dans la région E de moyenne latitude (Bernard 1974, Salah et al. 1975, Wand 1976). Par contre aucune corrélation n'a pu être mise en évidence entre l'activité magnétique et les variations des paramètres de l'atmosphère neutre à partir de ces données.

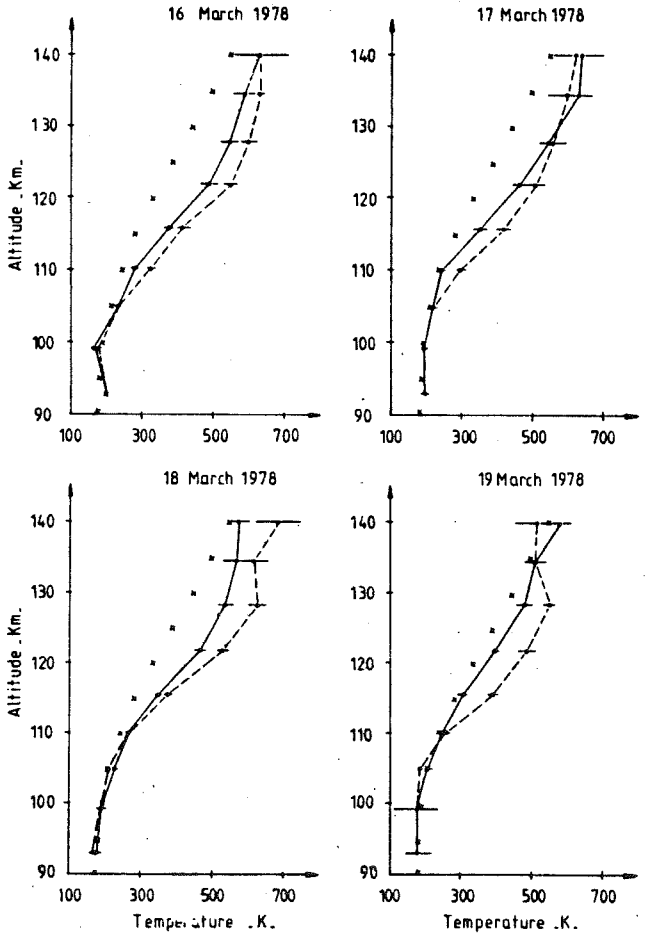


Figure 5: Profils de température neutre; les courbes continues et pointillées correspondent respectivement aux périodes avant et après 12.00 TU; les croix sont les températures du modèle Jacchia 71.

Les températures et les fréquences de collision obtenues avec le radar EISCAT ont une meilleure précision et surtout une meilleure résolution en altitude que celles obtenues avec le radar de Chatanika ( 2.25 Km au lieu de 9 Km). Sept expériences réparties sur l'année 1984 ont permis d'obtenir les profils de températures et de fréquences de collisons moyennées sur une période variant entre 3 et 10 heures.

Les profils de température ( Figure 6) sont relativement variables d'une journée à l'autre. Les cas extrêmes sont : une atmosphère relativement isotherme entre 95 et 105 Km, le 31 Janvier 1984 (T = 190 K) et un gradient de température d'environ 10 K/Km le 6 Juin 1984. Si l'on compare ces profils moyens aux profils obtenus par le modèle MSIS-83 (Hedin 1983) ( modèle dans lequel l'indice $A_p$ et le flux solaire ont été ajustés pour chaque chaque expérience), on remarque que les résultats des mesures sont, en général, inférieurs à ceux du modèle sauf le 6 Juin 1984. Par contre les différences de gradients entre les profils sont compatibles avec le modèle (différence entre le 31.01.84 et le 06.06.84 par exemple).

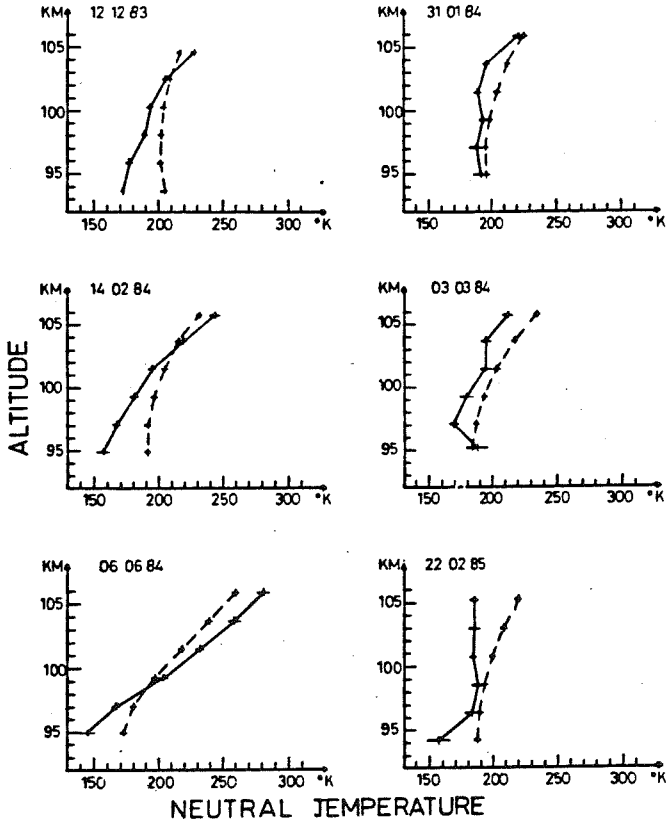


Figure 6: Profils de température neutre mesuré avec EISCAT (ligne continue) comparés au modèle MSIS-83 (ligne pointillée)

Les échelles de hauteur, calculées à partir des profils de fréquences de collisions, varient entre 5.4 Km et 6.5 Km. Echelles de hauteur et températures neutres permettent de calculer la masse moyenne de l'atmosphère à l'altitude moyenne de 100 Km. Les masses obtenues varient entre 25.6 a.m.u et 28.2 a.m.u, avec une moyenne de 26.8 a.m.u. Cette moyenne est plus proche de la masse moyenne du modèle Jacchia 71 (27.5 a.m.u) que celle du modèle MSIS-83 (28.5 a.m.u). La température moyenne à 100 Km : 187 K, est aussi très inférieure à la température moyenne de MSIS-83: 196 K (Jacchia 71: 192 K).

Les différentes causes pouvant conduire à des erreurs d'estimation des températures et fréquences de collisions ont été examinées mais aucune ne permet d'expliquer les différences entre mesures et modèles. Le fait que nous obtenions des masses inférieures à celles des modèles semblerait donc indiquer qu'il y a une plus grande proportion d'oxygène atomique dans la zone d'altitude considérée. Ce résultat est en accord avec l'étude de Audiushin et al. (1986) qui compare le rapport de la densité d' oxygène atomique à la densité d'azote moléculaire obtenu à partir de nombreux tirs fusées entre 120 et 150 Km d'altitude à ce même rapport calculé à partir de différents modèles dont MSIS-83. A haute latitude en particulier il trouve que ce rapport est sous estimé par les modèles (d'un facteur pouvant atteindre 3).

Les données obtenues à partir d'EISCAT nous ont aussi permis d'aborder le problème de la réponse de la basse thermosphère à l'activité magnétique.

Dans l'**article 8** , nous comparons deux nuits de mesure 12/13 Décembre 1983 et 3 Mars 1984, caractérisées d'une part, par des champs électriques relativement faibles (ce qui indique l'absence de dépot d'énergie Joule), d'autre part par une différence importante des taux moyens de chauffage particulaire ( 10 $mW/m^2$ et 3 $mW/m^2$ respectivement). On observe une atmosphère plus chaude et une échelle de hauteur plus grande le 12/13 Décembre, nuit où le chauffage particulaire est particulièrement intense: les différences de température sont de l'ordre de 10 à 15 K à 100 Km d'altitude et 25 K à 105 Km (Figure 6 de l'**article 8**). Ces différences ne peuvent pas être expliquées par la variation saisonnière de la basse thermosphère telle qu'elle est décrite par les modèles empiriques actuels; par exemple la température obtenue par le modèle MSIS-83 à 100 Km le 12 Décembre 1983 est supérieure de 9K à celle du 3 mars 1984, mais à 105Km elle est inférieure de 6K, ce qui ne correspond pas du tout à notre observation.

Sur la figure 7 nous avons regroupé les résultats des mesures de température neutre et échelle de hauteur à 99 Km pour les 7 expériences EISCAT présentées dans l'**article 2**. Les indices magnétiques $A_p$ et $\sum K_p$ sont aussi indiqués ainsi que le chauffage particulaire moyenné sur toute la durée de l'expérience. Le chauffage Joule est négligeable, sauf pour la nuit du 15 au 16 Novembre 1984 où il est, au contraire, très important.

Lorsque l'on ne considère que les quatres journées regroupées sur l'hiver 83/84, on retrouve la relation indiquée dans le paragraphe précédent entre le chauffage particulaire d'une part, et l'échelle de hauteur et la température neutre d'autre part. Les trois autres journées sont très différentes: le 6 Juin 1984 ne contient que des données de jour contrairement aux autres expériences, la nuit du 15/16 Novembre 1984 est particulièrement agitée (indice $A_p$ supérieur à 100) et l'expérience du 22 Février étant distante de plus d'un an des 4 premières journées considérées, le flux solaire corespondant a diminué pratiquement d'un facteur 2.

Ces résultats ne sont bien sûr pas suffisants pour affirmer qu'il existe une corrélation entre les paramètres de la basse thermosphère et le chauffage particulaire, mais ils montrent que le problème de la réponse de la basse thermosphère à l'activité magnétique peut être étudié expérimentalement en utilisant les données du sondeur EISCAT.

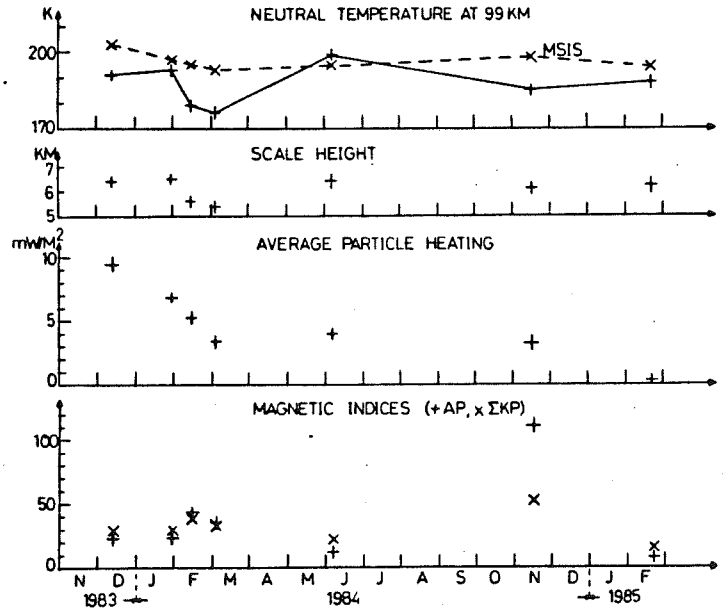


Figure 7: Comparaison des données d'atmosphère neutre et de dépot d'énergie pour les 7 expériences étudiées.

Alors que l'on commence à modéliser la réponse de la thermosphère moyenne (altitudes supérieures à 160 Km) à l'activité magnétique ,ce qui se passe aux altitudes inférieures est encore très mal connu. Aux altitudes de la région F, le système de vent thermosphérique peut être profondément modifié par l'entraînement ionique associé à la convection magnétosphérique. La température et la composition du gaz neutre dépendent alors de l'activité magnétique (voir l'article de synthèse de Roble 1983). Aux plus basses altitudes les précipitations électroniques dissipent environ 50% de leur énergie sous forme de chauffage de l'atmosphère neutre ( Singh et Gerard 1982, Rees et al. 1983), ce qui modifie à la fois la structure de l'atmosphère et de l'ionosphère (températures et compositions) et leur dynamique. Les mesures satellites et fusées montrent en effet une grande variabilité de la température et de la composition neutre pendant les périodes magnétiquement perturbées (Offerman 1981, Dickinson et al. 1985 par ex.).

Une étude systématique de l'ensemble des données disponnibles, moyennées si possible sur des temps beaucoup plus courts que ce qui a été réalisé dans cette étude, sera nécessaire pour préciser les relations entre les paramètres de la basse thermosphère et le chauffage auroral.

## 3.3 La composition ionique en région F1

### 3.3.1 Observations

A partir de six expériences EISCAT réparties entre Octobre 1981 et Décembre 1982, nous avons étudié la composition ionique dans la région F1 et plus particulièrement l'altitude de transition $Z_{40}$ entre ions moléculaires et ions O+ ( **article 5**).

Les tracés couleur du pourcentage d'ions O+ ( figure 1 et 2 de l'**article 5**), en fonction de l'altitude et du temps, font ressortir, pour toute les expériences , la variation diurne de la composition ( on a effectué une moyenne glissante d'une heure pour obtenir les résultats de composition avec une erreur de l'ordre de 10%). Pendant la nuit, on observe une prédominance des ions lourds à une altitude plus élevée que celle du jour. La variation diurne du pourcentage d'ions O+, est toutefois moins nette sur les deux expériences de Novembre 1982, pour lesquelles les données sont plus bruitées. De plus la présence de précipitations de particules, particulièrement le soir, complique le comportement diurne des compositions.

L'analyse des variations de l'altitude $Z_{40}$, pendant toutes les expériences, nous a permis d'obtenir des modèles moyens de la variation diurne de ce paramètre. Les six expériences ont été regroupées en deux catégories: été et hiver.

Nous avons représentés les valeurs de $Z_{40}$ en fonction de l'angle solaire zénithal $\chi$ par une fonction tangente hyperbolique semblable à celles obtenues par Oliver (1975) à partir de données fusées.

Pour les données d'été nous trouvons:

$$Z_{40}(\chi) = 200 + 25 \tanh ( (\chi - 85°)/10°) \quad \text{Km}$$

et pour les données d'hiver:

$$Z'_{40}(\chi) = Z_{40}(\chi) - 20 \text{ Km}$$

La différence été-hiver que nous obtenons est du même ordre de grandeur que les résultats obtenus par Kelly et Wickwar (1981) et par Oliver (1979) pour les périodes d'activité solaire faible. Une analyse harmonique de la variation saisonnière n'est pas possible car les six expériences étudiées ne constituent pas un échantillon représentatif.

Sur la figure 8, nous avons tracé l'altitude de transition $Z_{40}$ en fonction du temps pour chacune des six expériences étudiées ainsi que le modèle moyen été ou hiver. Il apparait que pendant certaines périodes l'altitude de transition est très différente du modèle: la variation de la composition ionique n'est plus alors uniquement contrôlée par le rayonnement électromagnétique solaire. Nous avons ainsi sélectionné plusieurs évènements (indiqués par une flèche sur la figure) d'une durée variable ( 1 heure à plusieurs heures) pendant lesquelles la différence entre la mesure et le modèle est au moins égale à 20 Km , c'est à dire supérieure à toute éventuelle erreur liée à la méthode de mesure .

La présence de variations de la composition ionique associées aux entrées d'énergie spécifiques aux zones aurorales, a été mise en évidence expérimentalement, avec les données du sondeur de Chatanika, par Kelly et Wickwar (1981). Ils ont montré que l'altitude de transition d'une part diminuait en période de précipitations, et d'autre part, augmentait en période de chauffage Joule.

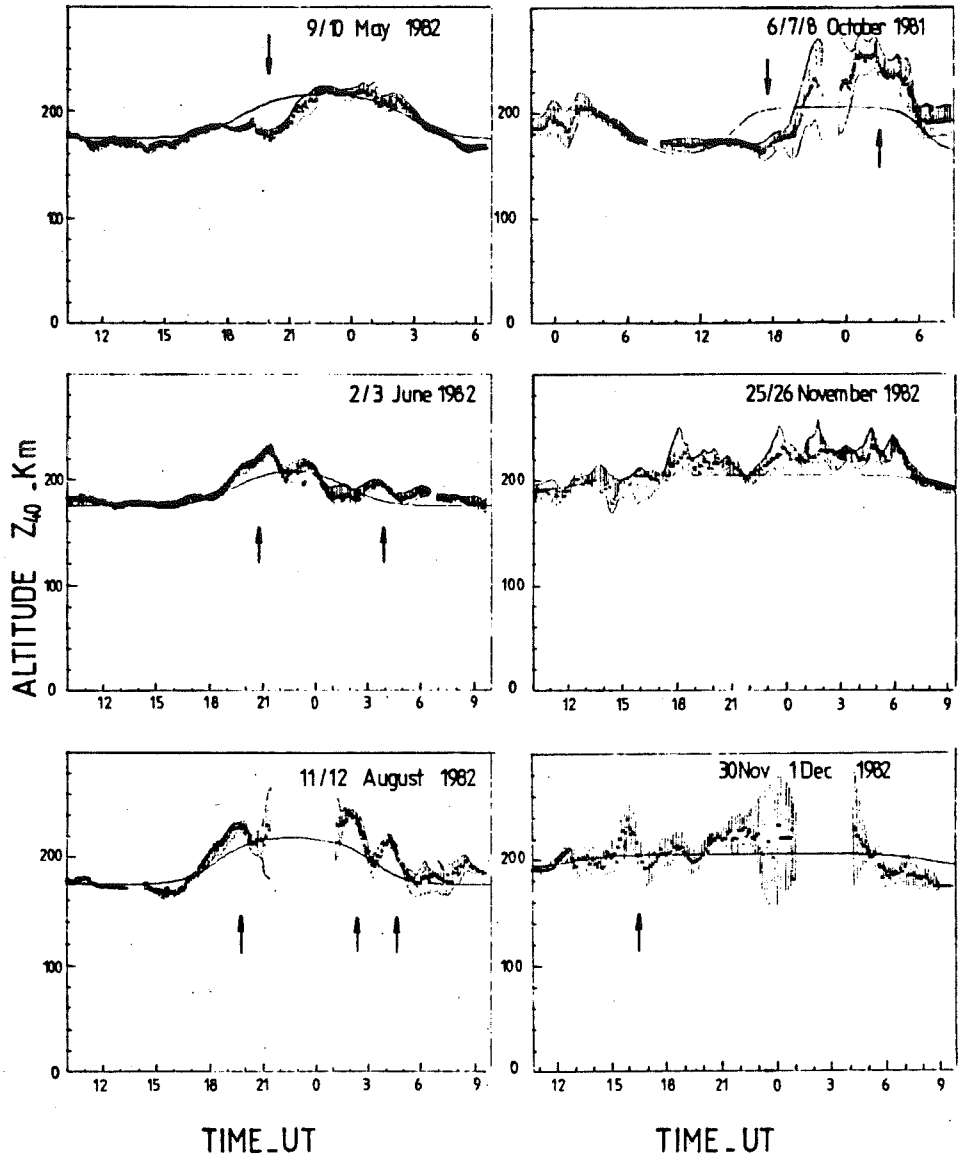


Figure 8: Variations de l'altitude de transition entre ions moléculaires et ions O+ pour chacune des expériences étudiées. La ligne continue représente le modèle décrit ci-dessus.

L'étude (réalisée dans l'**article 5**) des évènements sélectionnés, en fonction des conditions ionosphériques: champs électriques, précipitations particulaires, mouvements des ions, nous ont permis de dégager les résultats suivants:

- Les diminutions de l'altitude de transition, observées dans deux cas, ont été associées avec des précipitations de particules de faible énergie.
- Les augmentations de l'altitude de transition ont été associées, dans un cas, à une augmentation de la température ionique dûe au chauffage Joule, et dans les autres cas, à des précipitations de particules d'énergie plus grande.

Un exemple de modification du profil de composition ionique associé au chauffage Joule est présenté sur la figure 9. Les profils de composition et de températures ont dans ce cas particulier été calculés avec une résolution temporelle de deux minutes; l'augmentation très importante de la température ionique à 12.16 TU est caractéristique d'un chauffage Joule intense. On observe à ce moment là une diminution du pourcentage d'ions O+ particulièrement entre 200 et 300 Km d'altitude. Cette figure est discutée en détail dans Kofman et Lathuillere (1985). Elle met en évidence les limites du travail présenté dans l'**article 5**:
- premièrement, la seule étude de l'altitude de transition peut masquer des variations de la composition ionique ayant lieu à une altitude plus élevée
- deuxièmement, l'utilisation de données moyennées sur une heure n'est pas adaptée à l'étude quantitative instantanée des effets des chauffages auroraux sur la composition ionique. Elle permet toutefois une approche des effets intégrés.

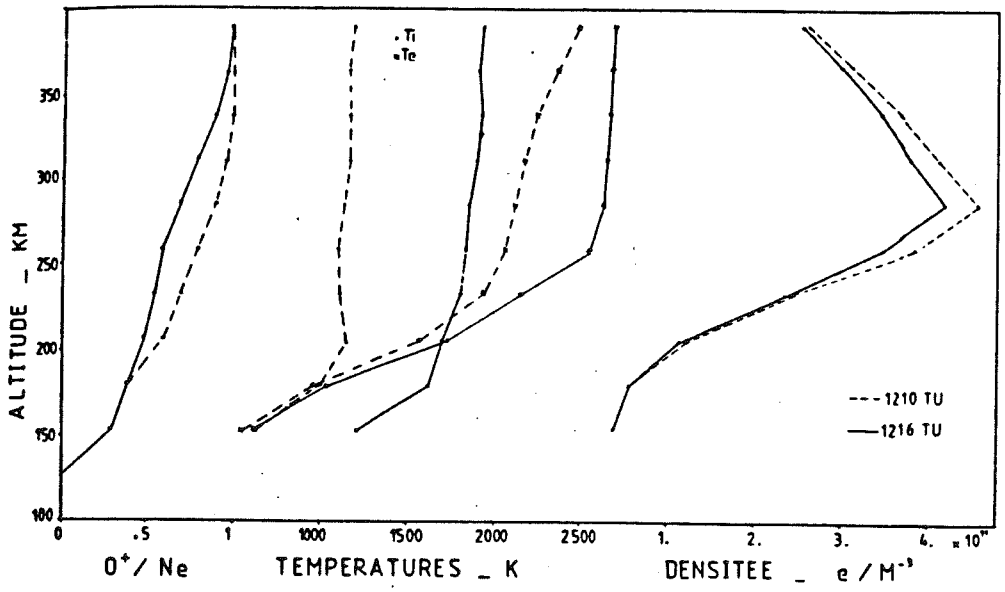


Figure 9: Composition ionique, température électronique et ionique et densité électronique mesurées le 30 Novembre 1982 avant et pendant une période de chauffage Joule (12.16 TU).

Sur la figure 10 (d'après Kofman et Lathuillere, 1985), nous comparons le profil moyen de composition calculé sur la nuit du 12/13 Décembre 1983 au modèle de composition ionique utilisé normalement dans l'analyse des données (modèle calculé à partir des résultats présentés dans l'**article 5**). La différence entre les deux profils ne peut pas être seulement attribuée à un effet saisonnier. Dans l'**article 8**, nous avons étudié cette expérience, caractérisée par un taux de chauffage particulaire intense pendant presque toute l'expérience, et trouvé que l'échelle de hauteur de l'atmosphère neutre à 100 Km était particulièrement grande (6.5 Km). Une augmentation de la densité neutre pourrait donc être dans ce cas à l'origine de l'augmentation de la proportion d'ions moléculaires dans la région F1.

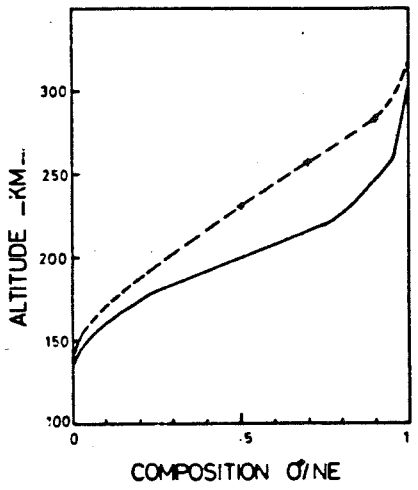


Figure 10: Composition ionique obtenue le 12 Décembre 1983 (ligne pointillée) comparée au modèle utilisé habituellement dans l'analyse des données de diffusion incohérente (ligne continue).

### 3.3.2 Tentative d'explication

La concentration de chaque espèce ionique $n_i$ est donnée par l'équation de continuité:

$$\frac{\partial n_i}{\partial t} = -\nabla(n_i \vec{V}_i) + P_i - n_i L_i$$

où dans le membre de droite le premier terme correspond au terme de transport et le deuxième et le troisième termes représentent respectivement la production et les pertes locales.

Dans la basse région E de l'ionosphère les transports sont négligeables, alors que dans la région F2 ils sont essentiels. Dans la région F1, zone de transition, on peut négliger dans une première approche ce terme de transport et ne considérer que l'équilibre chimique local.

Le diagramme de la figure 11 ( d'après Rees 1982) résume les principales réactions de production, transfert de charge et recombinaison pour les quatre ions principaux des régions E et F de l'ionosphère. Ce diagramme néglige en particulier toute la chimie de l'ion N+; il nous semble suffisant pour expliquer qualitativement ce qui se passe dans la zone de transition que nous avons étudiée expérimentalement c'est à dire vers 200 Km d'altitude.

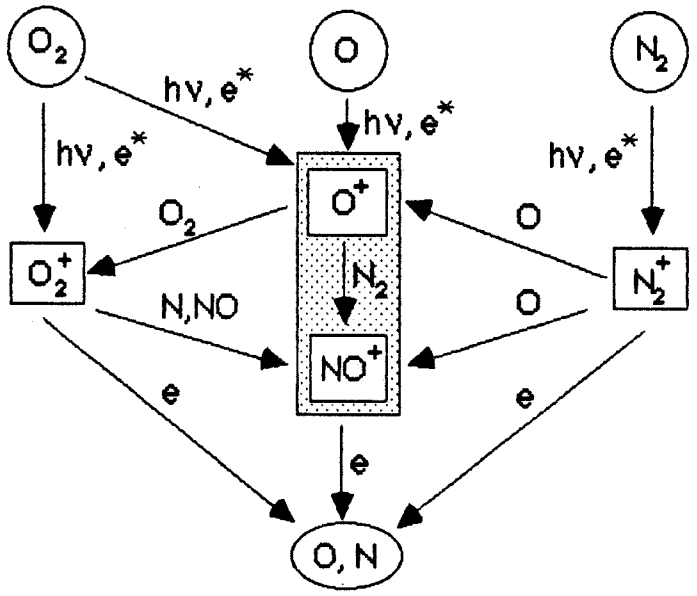


Figure 11: Diagramme des principales réactions dans l'ionosphère aurorale (voir le texte ci-dessous).

Les trois composants majoritaires de l'atmosphère neutre, azote moléculaire, oxygène atomique et oxygène moléculaire, peuvent être ionisés soit par le rayonnement EUV et UV solaire, représenté par hν sur le diagramme, soit par les électrons de haute énergie précipitant dans l'ionosphère aurorale, représentés par e*. Aux espèces ioniques directement crées $O^+$, $N_2^+$, $O_2^+$, il faut ajouter l'ion $NO^+$ dont la production résulte de réactions de transfert de charges et de réarrangement chimique, en particulier la réaction avec l'ion $O^+$ (réaction centrale du diagramme).

Au dessus de 150 Km d'altitude les deux ions majoritaires étant les ions O+ et NO+ (voir par exemple Banks et Kockarts 1973), cette réaction centrale va jouer un rôle important pour définir l'altitude de transition entre ions O+ et ions moléculaires.

La densité de l'ion O+ à l'équilibre s'écrit

$$n(O+) = \frac{I\, n(O)}{k_1 n(N_2) + k_2 n(O_2)} \qquad (1)$$

lorsque l'on ne considère que la production par photoionisation (coefficient I) ; $k_1$ et $k_2$ sont respectivement les taux des réactions $O+ + N_2 \rightarrow NO+ + N$ (2) et $O+ + O_2 \rightarrow O_2+ + O$ (3).

Nous n'écrirons pas explicitement la densité de l'ion NO+ à l'équilibre, mais nous remarquerons que ces pertes sont du type recombinaison avec les électrons thermiques (notés e sur le diagramme de la figure 11), c'est à dire proportionnelles au carré de la densité électronique.

Variations journalières:

Pendant le jour, sous l'effet du rayonnement solaire, la production de O+ et de NO+ augmente; à une altitude donnée, le temps de vie de O+ reste le même alors que le temps de vie de NO+ diminue puisque la densité électronique augmente (où encore les pertes de NO+ proportionnelles à $n_e^2$ augmentent plus rapidement que celles de O+ proportionnelles à $n_e$ ). Ceci résulte en une augmentation de la proportion d'ions O+ pendant le jour, ce qui corespond bien à la diminution de l'altitude de transition que l'on observe.

Variations saisonnières:

En hiver on observe une diminution de l'altitude de transition, ce qui correspond à une augmentation de la proportion des ions O+ à altitude fixe. Ce comportement est en accord avec la variation saisonnière de l'atmosphère neutre, c'est à dire l'augmentation de l'oxygène atomique relativement à l'azote moléculaire pendant l'hiver (Alcayde et al. 1974, Kasting et Roble 1981, Hedin 1983), car la densité de O+ est contrôlée par le rapport $n(O)/n(M_2)$ (voir équation 1) ou $M_2$ représente les composants moléculaires de l'atmosphère neutre.

Variations associées au chauffage Joule:

Pendant les périodes de chauffage Joule, le principal changement dans la photochimie de la région F1 provient de la variation de l'efficacité de la réaction entre O+ et $N_2$ ( réaction 2) ( Schunk et al. 1975, 1976, Kelly et Wickwar 1981). Le taux de cette réaction varie en effet comme le carré de la température efficace qui varie elle-même avec la vitesse différentielle ions-neutres ( voir figure 12). De plus cette réaction augmente aussi avec la quantité de $N_2$ d'une part, et la température vibrationnelle de $N_2$ d'autre part. L'équivalence entre l'action de ces troix facteurs, vitesse relative ions-neutres (exprimée en terme de champ électrique perpendiculaire équivalent), densité de $N_2$ et température vibrationnelle $T_v$, sur les compositions relatives de O+ et NO+ est indiquée dans la table suivante (d'après Schunk et al. 1975):

| $E_\perp$ mV $m^{-1}$ | $N_2$ Factor | $T_v$ K |
|---|---|---|
| 0 | 1.0 | 944 |
| 25 | 1.5 | 1.223 |
| 50 | 4.0 | 1.837 |
| 100 | 25 | 4.624 |
| 200 | 300 | 15.770 |

Pendant les périodes de chauffage Joule, la présence de champs électriques importants mais aussi une éventuelle modification de l'atmosphère neutre: augmentation de la quantité de $N_2$, diminution du rapport $n(O)/n(N_2)$ (Taeusch 1977, Prölss 1980) contribuent à l'augmentation de la proportion d'ions moléculaires à altitude fixe.

Un autre facteur pouvant contribuer à cette augmentation provient du fait que le coefficient de recombinaison des ions NO+ est inversement proportionnel à la température électronique( voir Schunk et al. 1975 par example). Pendant les périodes de chauffage Joule, la diminution de la densité électronique totale et l'augmentation de la température des électrons qui en résulte agissent dans le sens d'une diminution de la recombinaison, c'est à dire une diminution des pertes de NO+.

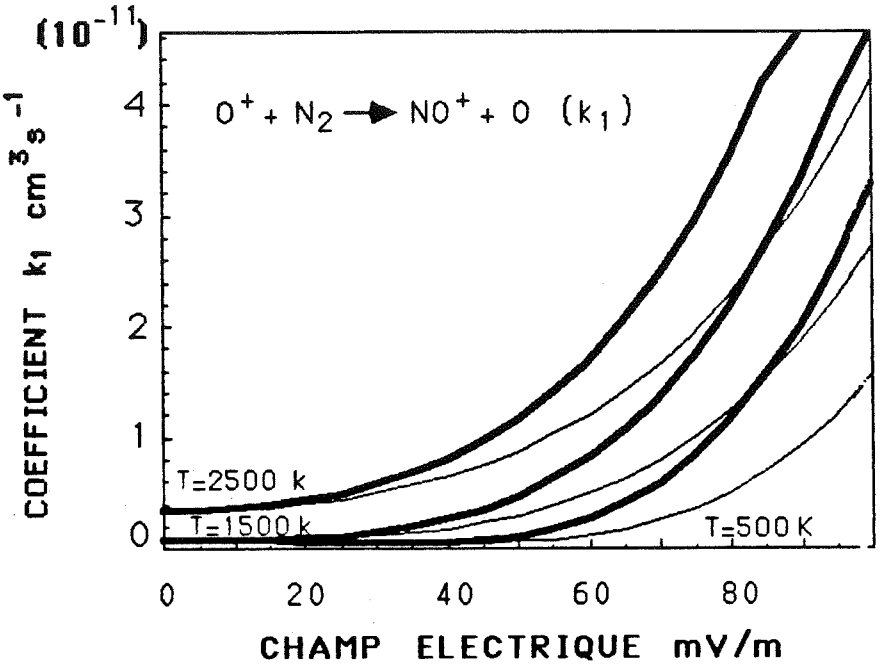


Figure 12: Variation du coefficient de la réaction entre O+ et $N_2$ en fonction du champ électrique équivalent à la vitesse relative ions-neutres. Les courbes en trait plein correspondent à une atmosphère dont le composant majoritaire est $N_2$ , celles en trait fin correspondent à une atmosphère dont le composant majoritaire est O.

Variations associées aux précipitations particulaires:

Contrairement à ce qui se passe pendant les périodes de chauffage Joule, où toutes les modifications de la chimie de la région F1 vont dans le sens d'une augmentation de la proportion d'ions lourds, les modifications engendrées par les précipitations peuvent entraîner soit une augmentation, soit une diminution de cette proportion.

Que la production directe augmente par l'effet du rayonnement solaire ou par l'impact des électrons énergétiques, le résultat est le même c'est à dire va dans le sens d'une augmentation de la proportion de O+. A cet effet, il faut opposer l'augmentation de la température vibrationnelle de $N_2$ dûe à l'impact des électrons énergétiques, qui entraine une augmentation de la réaction entre O+ et $N_2$ ( Newton et al. 1974, 1977). Kelly et Wickwar (1981) ont modélisé ces 2 effets et en ont conclu que l'augmentation de la production était prépondérante entrainant ainsi une diminution de l'altitude de transition, ce que suggéraient leurs observations.

Lorsque les précipitations particulaires sont douces, c'est à dire lorsque effectivement la production ionique augmente dans la région F1 (à partir de 150 Km d'altitude), nos observations sont en accord avec celles de Kelly et Wickwar (1981). Lorsqu'au contraire les précipitations sont dures, l'augmentation de la production se situe dans la région E, c'est à dire vers 100-110 Km d'altitude. Dans ce cas nous observons au contraire une augmentation de l'altitude de transition. Les mécanismes qui pourraient contribuer à cette augmentation sont:

- Une modification de l'atmosphère neutre: augmentation de la quantité de $N_2$ et diminution du rapport $n(O)/n(N_2)$ engendrées par les mouvements verticaux de l'atmosphère neutre (voir ci dessous).
- La diminution des pertes de NO+ due à une augmentation de la température électronique sur tout le profil en altitude provoquée par les précipitations particulaires.

Que ce soit pendant les périodes de chauffage Joule ou pendant les périodes de précipitations particulaires, une quantité importante d'énergie est déposée dans la basse thermosphère, entrainant des modifications de la dynamique et de la composition de l'atmosphère neutre: les transports horizontaux et verticaux sont en particulier importants pour déterminer la distribution des constituants de l'atmosphère neutre ( voir par example l'article de synthèse de Roble 1983) donc, par l'intermédiaire de la chimie, la distribution des composants ioniques.

De plus, en présence de champs électriques, le terme de transport dans l'équation de continuité de chaque espèce ionique ne peut plus être négligé: les transports verticaux d'ionisation dus aux champs électriques zonaux (un champ électrique vers l'ouest entrainant une vitesse ionique vers le bas et inversement) résultent en un déplacement de toute la couche F. Ils contribuent donc aussi de manière importante à déterminer l'altitude de transition entre ions moléculaires et ions O+ (Schunk et Sojka 1982). Par exemple dans l'**article 5** on montre que la diminution de l'altitude de transition observée le 9 mai 1982 est associée non seulement à des précipitations particulaires douces mais aussi à un champ électrique vers l'ouest qui peut contribuer à un transport des ions O+ vers le bas.

La modélisation des variations de l'altitude de transition dans la région F1 de l'ionosphère aurorale implique de traiter de manière autocohérente le couplage entre atmosphère neutre et ionisée, dans le cadre d'un modèle à 3 dimensions (voir Fuller-Rowell 1986). Il nous semble de plus qu'il sera indispensable de modéliser précisément l'action des précipitations particulaires en utilisant les modèles de

dégradation des fluxs d'électrons incidents (Strickland et al. 1976, Stamnes 1980, 1981).

## CONCLUSION

Le travail présenté dans ce mémoire concerne l'étude de la basse thermosphère et de la région F1 de l'ionosphère aurorale en périodes calmes et perturbées, en utilisant la technique de diffusion incohérente.

Dans la première partie de notre travail nous nous sommes interressés à la théorie de la mesure des paramètres tels que densité neutre, température neutre et composition ionique dans les zones aurorales où, à cause des entrées d'énergie spécifiques de ces zones, les hypothèses utilisées en moyenne latitude ne sont pas valables en toutes circonstances. En particulier les hypothèses concernant l'équilibre thermique entre populations électronique, ionique et neutre dans la région E et entre populations ionique et neutre dans la région F1 sont à utiliser avec précautions Nous avons ainsi mis au point une méthode qui permet d'obtenir la composition ionique en région F1 sans faire aucune hypothèse sur les températures électroniques et ioniques.

Dans la deuxième partie de ce travail, nous présentons les résultats d'observations réalisées avec les radars de Chatanika et d'EISCAT.

L'étude de l'ionosphère et de la basse thermosphère des zones aurorales en périodes perturbées nous a amené à décrire deux sources d'énergie qui s'additionnent aux sources d'énergie considérées habituellement, à savoir énergies Joule et particulaire. Ces deux nouvelles sources d'énergie sont le chauffage des ions par les pulsations magnétiques et le chauffage des électrons en région E par des instabilités double-faisceaux ou des instabilités de gradients.

Les pulsations magnétiques constituent un transfert d'énergie important entre la magnétosphère externe et l'ionosphère. Nous avons montré que, dans tous les cas d'observations de pulsations de type Pc5 dans l'ionosphère, on mesurait simultanément des variations de la température ionique parfaitement corrélées au champ électrique de la pulsation. Ce résultat confirme directement l'importance de la dissipation Joule dans l'ionosphère de l'énergie des pulsations magnétiques.

Le chauffage des électrons, en région E, par des instabilités, a lieu pendant les périodes de fort champ électrique, et est important par ses conséquences sur la détermination des paramètres de diffusion incohérente. En effet, dans cette région ionosphérique, ces paramètres

sont obtenus habituellement en faisant l'hypothèse d'équilibre thermique. Négliger ce chauffage peut entrainer une sous-estimation importante de la densité électronique et de la fréquence de collisions ion-neutre et une sur-estimation de la température ionique.

L'utilisation des mesures de diffusion incohérente dans la région E aurorale nous a permis de faire les premières comparaisons entre température et densité neutre mesurées à 100 Km d'altitude sur de longues périodes, et décrits par les modèles semi-empiriques tels que Jacchia-71 et MSIS-83. Dans le modèle Jacchia-71, les températures et densité neutres sont constantes à la base de la thermosphère; dans le modèle MSIS-83 elles dépendent de nombreux paramètres tels position géographique du lieu étudié, heure, indices de flux solaire et indices géomagnétiques mais leur variations jusqu'à 120 Km d'altitude n'est encore fondée, à haute latitude, que sur quelques mesures de fusées. Les mesures systématiques de température et densité neutre telles qu'elles peuvent être faites avec une station sol, et l'étude de leurs variations de manière statistique sont indispensables à l'obtention de modèles valables quelles que soient la latitude et les conditions d'activité géomagnétique.

L'effet des chauffages auroraux sur la basse thermosphère a tout juste été abordé dans ce travail. Nous avons montré que les températures et échelles de hauteur neutres vers 100 Km d'altitude pendant quatre journées d'expérience regroupées sur l'hiver 1983/1984 étaient plus grandes lorsque le chauffage particulaire était plus intense. L'étude de données beaucoup plus nombreuses sera nécessaire pour confirmer ce premier résultat.

Les premières mesures systématiques de la composition ionique en zone aurorale que nous avons réalisées avec le radar EISCAT ont permis dans un premier temps d'établir un modèle moyen de composition qui est maintenant utilisé pour l'obtention routinière des températures à partir des données d'EISCAT. Ce nouveau modèle, en élevant l'altitude de transition entre ions moléculaires et ions oxygène atomique ( altitude où $O^+/N_e = 40\%$) de 150 Km à 190 Km permet d'obtenir des températures beaucoup plus réalistes entre 150 et 250 Km d'altitude. L'étude des variations de cette altitude de transition en fonction du temps nous a amené à décrire le comportement de la composition ionique en région F1 comme la superposition d'une variation diurne et saisonnière controlée par le rayonnement EUV et UV solaire et la composition de l'atmosphère neutre, et de variations beaucoup plus rapides liées aux apports d'énergie tels que chauffages Joule et particulaire.

Alors qu'au chauffage Joule correspond une augmentation de la proportion d'ions moléculaires à une altitude donnée, nous avons montré que l'effet des précipitations particulaires dépendait de leur énergie: on observe en effet une diminution de la proportion d'ions moléculaires pendant les précipitations de faible énergie et au contraire une augmentation de cette même proportion lorsque les précipitations sont très dures. La modélisation de l'effet des chauffages auroraux sur la composition ionique ne rentre pas dans le cadre de ce travail mais nous avons essayé de préciser, à partir d'un schéma très simple de la chimie de la région F1, quelles étaient les réactions susceptibles d'être modifiées pendant les périodes de chauffage auroral.

L'étude simultanée des paramètres de la basse thermosphère et de la région F1 pendant les périodes perturbées devrait permettre de préciser le rôle de la composition et de la dynamique de l'atmosphère neutre dans les perturbations de la composition ionique. L'exemple du 12/13 Décembre 1983 où l'on observe simultanément une basse thermosphère particulièrement chaude, une proportion d'ions lourds lourds au dessus de 150 Km plus importante que celle obtenue par le modèle d'hiver et un chauffage particulaire important pendant toute l'expérience, montre la nécessité d'une modélisation autocohérente des perturbations de l'ionosphère et de la thermosphère des zones aurorales.

Les perspectives ouvertes par notre travail nous semblent donc être axées sur deux pôles.

Le premier est expérimental et concerne l'étude à long terme des paramètres de la basse thermosphère et de la composition ionique. Nous avons déjà souligné l'importance de réaliser une base de données de température et de densité neutres aussi complète que possible. A partir d'une étude identique de la composition ionique, il serait intéressant de réaliser un modèle expérimental incluant les variations diurnes, saisonnières et les variations avec le flux solaire, et restant suffisamment simple pour pouvoir être inclus dans le programme de dépouillement des données de diffusion incohérente. Dans cette optique, le démarrage des expériences VHF avec EISCAT devrait permettre d'obtenir des informations non seulement sur l'altitude de transition entre ions moléculaires et ions oxygène atomique mais aussi sur l'extension en altitude de la zone de transition grâce à la possibilité d'utiliser la technique "impulsions multiples" (c'est à dire d'avoir une bonne résolution en altitude) dans la région F1.

Le deuxième pôle est théorique puiqu'il concerne la modélisation de l'effet des chauffages Joule et particulaire sur la composition ionique.

Il nous semble que la modélisation de l'effet du chauffage particulaire ne pourra être entreprise que dans le cadre d'une modélisation autocohérente de l'ionosphère et de la thermosphère. La modélisation de l'effet du chauffage Joule a été abordée par Schunk et al. (1975,1976), Sojka et al. (1981) et Sojka et Schunk (1984). Leurs résultats sont qualitativement en accord avec nos observations mais une comparaison quantitative est actuellement difficile. Du point de vue expérimental il faudrait arriver à obtenir une description de la composition ionique en fonction de la latitude. Sur le plan modélisation, il serait nécessaire d'inclure dans le modèle d'une part la résolution de l'équation du bilan thermique des électrons et d'autre part une variation de la dynamique et de la composition de l'atmosphère neutre qui pourrait être en partie déduite des observations.

## REFERENCES BIBLIOGRAPHIQUES

ALCAYDE D. et R. BERNARD : Modelling of the lower thermosphere : contributions of incoherent scatter observations. J. Atmos. Terr. Phys. 44, 95-109, 1982.

ALCAYDE D., P. BAUER, and J. FONTANARI : Long-term variations of thermospheric temperature and composition, J. Geophys. Res., 79, 629-637, 1974.

AVDIUSHIN S.I., A.A. POKHUNKOV and G.F. TULINOV : An analysis of the Empirical Models and the Measurement Results of the Polar Atmospheric Composition at 120-150 km Heights. Communication présentée au 26e COSPAR- TOULOUSE - 1986.

BANKS P. : Observations of Joule and particle heating in the auroral zone, J. Atmos. Terr. Phys., 39, 179-193, 1977.

BANKS P. : Joule heating in the high-latitude mesosphere, J. Geophys. Res., 84, 11, 6709-6712, 1979.

BANKS P.M. and G. KOCKARTS : Aeronomy, part B, Academic, Orlando, Fla., 1973.

BARON M. and R.H. WAND : F region ion temperature enhancements resulting from Joule heating. J. Geophys. Res., 88, 4114-4118, 1983.

BAUER P. : Theory of waves incoherently scattered. Phil. Trans. Roy. Soc. London A 280 167-191 - 1975.

BERNARD R. : Tides in the E region observed by incoherent scatter radar over St. Santin. J. Atmos. Terr. Phys., 36, 1105-1120, 1974.

CARRU H., M. PETIT and P. WALDTEUFEL : Mesures de températures électroniques et ioniques par diffusion incohérente. J. Atmos. Terr. Phys. 29, (4), 351-366, 1967.

CROWLEY G., N. WADE, J.A. WALDOCK, T.R. ROBINSON AND T.B. JONES : High time resolution observations of periodic frictionnal heating associated with a Pc5 micropulsation, Nature 316, 528-530, 1985.

DICKINSON R.E., E.C. RIDLEY and R.G. ROBLE : A three dimensional general circulation model of the thermosphere. J. Geophys. Res. 86, 1499, 1981.

DICKINSON P.H.G. , U. VON ZAHN, K.D. BAKER and D.B. JENKINS : Lower thermosphere densities of $N_2$, 0 and Ar under high latitude winter conditions. J. Atmos. Terr. Phys. 47, 283-290, 1985.

DOUGHERTY J. and D.T. FARLEY : A theory of incoherent scattering of radio waves by plasma. J. Geophys. Res. 68, 5473-5486, 1963.

EATHER R.H. : Majestic Lights, American Geophys. Union - Washington 1980

EVANS J.V. : Electron temperature and ion composition in the F Region. J. Geophys. Res. 72 , 3343-3355, 1967.

EVANS J.V. and L.P. COX : Seasonal variation of the F region ion composition, J. Geophys. Res. 75, 159-164, 1970.

FARLEY D.T. : A plasma instability resulting in field-Aligned irregularities in the ionosphere, J. Geophys. Res., 68, 6083-6097, 1963.

FOLKESTAD K., T. HAGFORS and S. WESTERLUND : EISCAT : an updated description of technical characteristics and operational capabilities. Radio Sci., 18, 867, 1983.

FONTANARI and D. ALCAYDE : Observation of neutral temperature Tidal-Type oscillations in the $F_1$ Region. Radio Sci. 9, 275-280, 1974.

FULLER-ROWELL T.J. : Numerical investigations of thermospheric/ionospheric coupling in the polar regions. Communication présentée au 26e COSPAR - TOULOUSE 1986.

FULLER-ROWELL T.J. and D. REES : A three dimensional time dependent global model of the thermosphere. J. Atmos. Sci., 37, 2545, 1980.

GLANGEAUD F., C. LATHUILLERE, M. LAMBERT and Z.Y. ZHAO : Pc3 ULF Magnetic variations measured in the ionosphere by EISCAT. J. Geophys. Res., 90, 8319-8331, 1985.

GLASSMEIER K.H. , H. VOLPERS and W. BAUMJOHANN : Ionospheric Joule dissipation as a damping mechanism for high latitude ULF pulsations : observational evidence. PLanet Space Sci., 32, 1463-1466, 1984.

GREENWALD R.A. and A.D.M. WALKER : Energetic of long period resonant hydromagnetic waves, Geophys. Res. Lett., 7, 745, 1980.

HEDIN A.E. : A revised thermospheric model based on mass spectrometer and incoherent scatter data : MSIS 83, J. Geophys. Res. , 88, 10.170-10. 188, 1983.

JACCHIA L.G. : Revised static models of the thermosphere and exosphere with empirical temperature profiles, Smithson. Astrophys. Obs. Rep., 332, 1971.

KASTING J.F. and R.G. ROBLE : A zonally averaged chemical-dynamical model of the lower thermosphere, J. Geophys. Res. 86, 9641-9653, 1981.

KELLY J. and V.B. WICKWAR : Radar measurements of high-latitude ion composition between 140 and 300 km altitude. J. Geophys. Res. 86, 7617-7626, 1981.

KOFMAN W. and C. LATHUILLERE : Observations of the auroral ionosphere using EISCAT. AGARD Conference Proceedings n° 382. Edited by H. Soicher. New Jersey 1985.

LATHUILLERE C. , F. GLANGEAUD, J.L. LACOUME and G. LEJEUNE : Relationship between ionospheric electric fields and ground magnetic pulsations in the Pc3 domain at midlatitudes. J. Geophys. Res. 86, 7669-7678, 1981.

LEADABRAND R.L., M.J. BARON, J. PETRICEKS and H.F. BATES : Chatanika, Alaska, auroral-zone incoherent-scatter facility, Radio Sci. 7, 747-756, 1972.

LEJEUNE G. : EISCAT data analysis, Rapp. 36/78, Centre d'Etudes des Phénomènes Aléatoires et Géophysiques, St-Martin-d'Hères, France, 1978.

LEJEUNE G., C. LATHUILLERE and W. KOFMAN. On the possibility to measure the high altitude light ion concentrations with EISCAT. Ann. Geophys., 38, 467-472, 1982.

NEWTON G.P., J.C.G. WALKER, and P.H.E. MEIJER : Vibrationally excited nitrogen in stable auroral red arcs and its effect on ionospheric recombination. J. Geophys Res. 79, 3807, 1974.

NEWTON G.P., J.C.G. WALKER and G.P. MANTAS : Effects of soft electron precipitation on the distribution of vibrational energy of $N_2$, J. Geophys. Res. 82, 187-190, 1977.

NEWTON R.S., D.J. SOUTHWOOD et W.J. HUGUES : Damping of geomagnetic pulsations by the ionosphere. Planet. Space Sci., 26, 201, 1978.

OFFERMANN D , V. FRIEDRICH, P. ROSS and U. VON ZAHN : Neutral gas composition measurements between 80 and 120 km, Planet. Space Sci., 29, 747-764, 1981.

OLIVER W.L. : Models of F1 region ion composition variations. J. Atmos. Terr. Phys. 37, 1065-1076, 1975.

OLIVER W.L. : Incoherent scatter radar studies of the daytime middle thermosphere. Ann. Geophys. 35, 121-139, 1979.

PETIT M. : Mesures de températures, de densité électronique et de composion ionique dans l'ionosphère par diffusion de Thomson. Etude du déséquilibre thermodynamique dans l'ionosphère diurne. Ann. Geophys., 24, 1-37, 1968.

PONTHIEU J.J. : Les sources d'énergie de la thermosphère en région aurorale : une étude par diffusion incohérente. Thèse Paris VI. 1981.

PROLSS G.W. : Magnetic storm associated perturbations of the upper atmosphere : recent results obtained by satellite-borne gas Analyzers. Rev. Geophys. Space Phys. 18, 183-202, 1980.

REES M.H. : Auroral excitation and energy dissipation. Solar-Terrestrial Physics, edited by R.L. Carovillano and J.M. Forbes, Dordrecht, Holland, 1983.

REES M.H. and J.C.G. WALKER : Ion and electron heating by auroral electric fields, Ann. Geophys., 24, 193-199, 1968.

REES M.H., B.A. EMERY, R.G. ROBLE and K. STAMNES : Neutral and ion gas heating by auroral electron precipitation. J. Geophys. Res. 88, 6289-6300, 1983.

ROBLE R.G. : Dynamics of the earth's thermosphere. Rev. Geophys. and Space Phys. 21, 217-233, 1983.

ROBLE R.G. and J.F. KASTING : The zonally averaged circulation, temperature and compositionnal structure of the lower thermosphere and variations with geomagnetic activity. J. Geophys. Res. 89, 1711-1724, 1984.

ST-MAURICE J.P. and W.B. HANSON : Ion frictionnal heating at high latitudes and its possible use for an in situ determination of neutral thermospheric winds and temperatures. J. Geophys. Res. 87, 7580-7602, 1982.

ST-MAURICE J.P., K. SCHLEGEL and P.M. BANKS : Anomalous heating of the polar E region by unstable plasma waves, 2, Theory. J. Geophys. Res. 86, 1453-1462, 1981.

SALAH J.E., R.H. WAND and J.V. EVANS : Tidal effects in the E region from incoherent scatter radar observations. Radio Sci., 10, 347-355, 1975.

SCHLEGEL K. : A case study of a high latitude ionospheric electron density depletion. J. Atmos. Terr. Phys. 46, 517-520, 1984.

SCHLEGEL K. and J.P. ST-MAURICE : Anomalous heating of the polar E region by unstable plasma waves, 1, Observations. J. Geophys. Res., 86, 1447-1452, 1981.

SCHUNK R.W. and J.C.G. WALKER : Transport processes in the E region of the ionosphere. J. Geophys. Res. 76, 6159-6171, 1971.

SCHUNK R.W. and W.J. RAITT : Atomic nitrogen and oxygen ions in the daytime high-latitude F- region. J. Geophys. Res. 85, 1255-1272, 1980

SCHUNK, R.W. and J.J. SOJKA : Ion temperature variations in the daytime high-latitude F- region. J. Geophys. Res. 87, 5119, 1982.

SCHUNK R.W., W.J. RAITT and P.M. BANKS : Effect of electric fields on the daytime high latitude E and F regions. J. Geophys. Res. , 80, 3112-3130, 1975.

SCHUNK R.W., P.M. BANKS and W.J RAITT : Effect of electric fields and other processes upon the nighttime high-latitude F layer. J. Geophys. Res. 81, 3271-3282, 1976.

SINGH V. and J.C. GERARD : The thermospheric heating efficiency under electron precipitation conditions. Planet. Space Sci., 30, 1083-1089, 1982.

SOJKA J.J., W.J. RAITT and R.W. SCHUNK : A theoritical study of the high-latitude winter F region at solar minimum for low magnetic activity. J. Geophys. Res. 86, 609-621, 1981 a.

SOJKA J.J. , W.J. RAITT and R.W. SCHUNK : Theoretical predictions for ion composition in the high-latitude winter F-Region for solar minimum and low magnetic activity. J. Geophys. Res. 86, 2206-2216, 1981 b.

STAMMES K. : Analytic approach to electron transport and energy degradation, Planet. Space Sci. 28, 427-441, 1980.

STAMMES K. : On the two-stream approach to electron transport and thermalization, J. Geophys. Res. 86, 2405-2410, 1981.

STRICKLAND D.J., P.L. BOOK, T.P. COFFEY and J.A. FEDDER : Transport techniques for the deposition of auroral electrons, J. Geophys. Res., 81, 2755-2764, 1976.

STUBBE P. and S. CHANDRA : Ionospheric warning by neutral winds Planet. Space Sci., 19, 731, 1971.

TAEUSCH D.R. : Structure of electrodynamic and particle heating in the disturbed polar thermosphere. J. Geophys. Res. 82, 455-460, 1977.

VICKREY J.F., R.R. VONDRAK and S.J. MATTHEWS : The diurnal and latitudinal variations of auroral zone ionospheric conductivity. J. Geophys. Res., 86, 65-75, 1981.

VICKREY J.F., R.R. VONDRAK and S.J. MATTHEWS : Energy deposition by precipitating particle and joule dissipation in the auroral ionosphere. J. Geophys. Res., 87, 5184-5196, 1982.

WALDTEUFEL P. : Une étude par diffusion incohérente de la haute atmosphère neutre. Thèse, Fac. des Sci. de Paris, Paris, 1970.

WAND R.H. : Semidiurnal tides in the E region from incoherent scatter measurements at Arecibo, Radio Sci., 11, 641-652, 1976.

WAND R.H. and F.W. PERKINS : Temperature and compositon of the ionosphere : Diurnal variations and waves, J. Atmos. Terr. Phys. 32, 1921-1943, 1970.

WICKWAR V.B. : Analysis techniques for incoherent scatter data interpretation in the 100 to 300 km region. Technical report, Stanford Res. Inst., Menlo Park, Calif., 1974.

WICKWAR V.B. : Chatanika radar measurements, in Atmospheres of Earth and the Planets, 111-124, D. Reidel, Hinghan, Mass., 1975.

# ARTICLE 1

JOURNAL OF GEOPHYSICAL RESEARCH, VOL. 88, NO. A12, PAGES 10,137–10,144, DECEMBER 1, 1983

# Incoherent Scatter Measurements of Ion-Neutral Collision Frequencies and Temperatures in the Lower Thermosphere of the Auroral Region

CHANTAL LATHUILLERE

*Centre d'Etudes des Phénomènes Aléatoires et Géophysiques*

VINCENT B. WICKWAR

*SRI International*

WLODEK KOFMAN

*Centre d'Etudes des Phénomènes Aléatoires et Géophysiques*

Incoherent scatter observations performed in March and November 1978 at Chatanika have been used for studying the lower thermosphere in the auroral region. Neutral temperatures and densities have been found during periods without Joule heating. We present mean profiles of temperatures and collision frequencies (approximately proportional to neutral densities) for each month and profiles obtained during four specific nights. Between 93 km and 110 km the mean profiles of temperature are in good agreement with the Jacchia (1971) model, and the profiles of collision frequency are similar to those deduced from the model. Consistency checks between these collision frequencies and temperatures were performed, as were various simulations of the data. Neutral temperature profiles between 90 km and 140 km on the four specific nights show variations from one night to another that are not correlated to magnetic activity. However, there are systematic variations during each night that we suggest are due to atmospheric tides.

## 1. INTRODUCTION

The lower thermosphere is usually used as a limit zone for the thermospheric models: empirical models such as "Jacchia 71, 77" [*Jacchia*, 1971, 1977] or "MSIS" [*Hedin et al.*, 1977*a*, *b*] and theoretical models of auroral disturbance effects [e.g., *Mayr and Volland*, 1973]. Boundary conditions are often constant and given at an altitude of either 90 km or 120 km; however, neutral temperatures, densities, and compositions are quite variable in this region [*Offermann et al.*, 1981]. The aim of this paper is to show that the incoherent scatter technique is able to contribute to the understanding of the lower thermosphere in the auroral region by presenting first long-term results from Chatanika.

Already at middle and low latitudes, incoherent scatter radars have been extensively used for the study of the lower thermosphere: long-term variation studies [*Waldteufel*, 1970*a*; *Alcayde et al.*, 1979; *Salah et al.*, 1974; *Tepley and Mathews*, 1978] and short-term variation studies such as tides [*Bernard*, 1974; *Salah et al.*, 1975; *Wand*, 1976] and gravity waves [*Vidal-Madjar*, 1978]. At high latitudes, initial results were obtained by *Schlegel et al.* [1980].

In the second part of the paper, we recall how neutral temperatures and densities can be deduced from incoherent scatter measurements and examine the problems peculiar to the auroral zone. In the third part we present the results obtained with the Chatanika incoherent scatter radar. We describe the averaged temperature and density profiles obtained during two months of measurements: March 1978 and November 1978. We then examine the consistency of these profiles, first by assuming hydrostatic equilibrium and second by simulating the data. This latter check is performed because the altitude integration performed by the Chatanika multipulse correlator is larger than the neutral scale height. In the fourth part of this work, we present variations of collision frequency and temperature profiles observed during four specific nights. Finally, in the conclusion, we review the main results.



Paper number 3A1346.
0148-0227/83/003A-1346$05.00

## 2. DETERMINATION OF NEUTRAL ATMOSPHERE PARAMETERS WITH THE INCOHERENT SCATTER TECHNIQUE

### 2.1. *Ion-Neutral Collision Frequency*

In the $E$ region the incoherent scatter ion spectrum depends not only on the usual parameters (electron density $N_e$, electron and ion temperatures $T_e$ and $T_i$, and ion velocity $V_i$) but also on the ion-neutral collision frequency $\nu_{in}$ [*Dougherty and Farley*, 1963; *Waldteufel*, 1970*b*]. This collision effect becomes negligible above an altitude of 110 km for the radar frequency used at Chatanika.

Theoretically, it is possible to deduce simultaneously the four parameters $N_e$, $T_e$, $T_i$, and $\nu_{in}$ from the incoherent scatter spectrum or the autocorrelation function, but the presence of much noise in the measurements makes a four-parameter regression practically impossible [*Lejeune*, 1980]. In particular, it is difficult to simultaneously determine the electron-to-ion temperature ratio and the ion-neutral collision frequency. However, *Schlegel et al.* [1980] show two such fits under conditions of large electron densities. We shall attempt to determine $\nu_{in}$ during periods when there is thermal equilibrium between electrons and ions: $T_e = T_i$. At middle and low latitudes, thermal equilibrium exists in the lower $E$ region and its existence has been verified. However, at high latitude, different heating processes can disturb the thermal equilibrium. In the presence of particle precipitation, the electron temperature may be higher than the ion temperature; in the presence of electric fields the classical process of Joule heating will prefer-

entially enhance the ion temperature, and a new heating mechanism due to unstable plasma waves (modified two-stream instability) will preferentially enhance the electron temperature [*St. Maurice et al.*, 1981].

Only this latter process is able to significantly change the thermal equilibrium below the altitude of 110 km. Indeed recent results from Chatanika show electron temperatures of 1200 K between 105 km and 110 km when ion temperatures remain between 250 K and 300 K [*Wickwar et al.*, 1981; *Schlegel and St. Maurice*, 1981]. During these periods of "elevated electron temperature," which are simultaneous to periods of high electric field, it will be impossible to determine the collision frequency $\nu_{in}$.

### 2.2. *Neutral Temperature and Density*

The neutral temperature is deduced directly from the ion temperature determination, indeed the high value of the ion-neutral collision frequency below the altitude of 110 km ensures thermal equilibrium between ions and neutrals most of the time. However, during periods of very high electric field, Joule heating could raise the ion temperature above the neutral one: an electric field of approximately 40 mV/m would create a 20-K increase of $T_i$ at 110-km altitude [*Banks and Kockarts*, 1973].

One must also keep in mind a possible enhancement of the ion temperature due to the modified two-stream instability heating process. This enhancement could be of the order of 30 K to 60 K in the $E$ region [*St. Maurice et al.*, 1981]. Therefore great care must also be taken when studying neutral temperatures during periods of high electric field.

Neutral density and collision frequency are connected by

$$\bar{\nu}_{in} = 2.59 \times 10^{-9} n_n \left\{ \frac{\alpha_0}{\mu(i, n)} \right\}^{1/2} \tag{1}$$

[*Banks and Kockarts*, 1973], where $\bar{\nu}_{in}$ is the collision frequency for momentum transfer between ion species $i$ and neutral species $n$, measured in the center of mass frame; $n_n$ is the number density of neutral species $n$, $\mu(i, n)$ is the ion-neutral reduced mass (in atomic mass units), and $\alpha_0$ is the neutral gas atomic polarizability (in units of $10^{-24}$ cm$^3$).

The ion-neutral collision frequency, $\nu_{in}$, used in the calculation of the incoherent scatter spectrum is the momentum transfer collision frequency measured in the laboratory frame:

$$\nu_{in} = \frac{m_n}{m_i + m_n} \bar{\nu}_{in} \tag{2}$$

where $m_i$ and $m_n$ are the ion and neutral particle masses (in atomic mass units), respectively. Combining (1) and (2) and summing over the three principal neutral species in the $E$ region, we obtain

$$\nu_{in} = KN \tag{3}$$

for each ion species, where $N$ is the total neutral density,

$$K = 2.59 \times 10^{-11}(1/m_i)[1.76^{1/2}\mu(i, N_2)^{1/2}\%(N_2) + 1.59^{1/2}\mu(i, O_2)^{1/2}\%(O_2) + 0.79^{1/2}\mu(i, O)^{1/2}\%(O)] \tag{4}$$

and $\%(n)$ represents the percentage of neutral species $n$ in the neutral gas. Equations (3) and (4) indicate that each ion will have a different collision frequency. In addition, the incoherent scatter spectrum is a nonlinear combination of the spectra for each ion. However, the two principal ions in the $E$ region, $NO^+$ and $O_2^+$, are close enough in mass that negligible error is introduced in the total ion-neutral collision frequency by assuming one ion with an intermediate mass.

We consider an ion population composed of 75% $NO^+$ and 25% $O_2^+$, thereby obtaining

$$K = \frac{2.59 \times 10^{-11}}{30.5} [5.07\%(N_2) + 4.98\%(O_2) + 2.88\%(O)] \tag{5}$$

In the remainder of the paper we continue to use the symbol $\nu_{in}$, but it now represents the total ion-neutral collision frequency.

We can see that the factor $K$ depends on the neutral composition (thus on the altitude) and especially on the percentage of atomic oxygen. If we use the "Jacchia 71" neutral model with an exospheric temperature of 1000 K, a 7% difference is obtained between 90 km and 110 km. While this small difference with altitude could vary with the choice of model atmosphere, it would remain small. However, the magnitude of $K$ is less certain. It could vary because of atomic oxygen concentration variations as large as a factor of 4 to 5 that have been observed in this region [*Offermann et al.*, 1981]. More fundamentally, (1) is limited because it includes only a pure polarization interaction.

Because of the small variation of $K$ with altitude, we will consider it constant, especially when compared with the precision of the collision frequency measurements. We note that the value used in the "EPEC" routines, which compute Joule heating and electric fields from Chatanika data [*de la Beaujardière et al.*, 1980], is $3.75 \times 10^{-10}$. This value corresponds to more than 25% atomic oxygen. In the following sections we shall present collision frequencies instead of neutral densities so that no additional error is introduced by the use of the factor $K$.

### 2.3. *Experimental Conditions*

The data that are presented here were acquired at Chatanika during the joint American-French plasma line experiments in March and November 1978 [*Kofman and Wickwar*, 1980]. We use autocorrelation function measurements obtained with the multipulse correlator in its 60-$\mu$s pulse configuration with a 9-km altitude resolution. The time resolution was 15 min, and almost all the data were acquired at night. The radar was pointing along the magnetic field line (in a fixed position), which did not allow electric field measurements.

We have seen that in the auroral zone it is necessary to work during periods without strong electric fields in order to deduce the neutral temperature and the collision frequency. Because these high electric field periods are also characterized by strong Joule heating that enhances the ion temperature $T_i$ at altitudes above 120 km, we have used multipulse measurements immediately above 120 km (where we can indeed determine both $T_i$ and $T_e$ because collisions are no longer important) and single long-pulse measurements in the $F$ region to determine Joule heating periods, i.e., periods during which $T_i$ was enhanced above its quiet time value. These periods have been systematically eliminated prior to analysis for neutral temperature and collision frequency.

## 3. MEAN PROFILES OF COLLISION FREQUENCY AND TEMPERATURE BETWEEN 90 KM AND 110 KM

First we obtained the mean collision frequency and temperature profiles for March and for November 1978. Seventeen

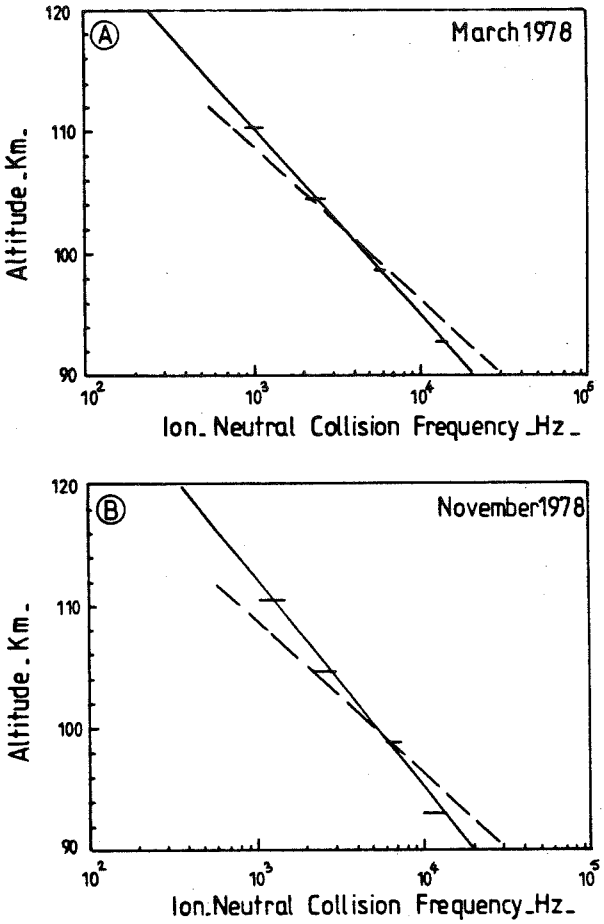


Fig. 1. Mean profiles of collision frequencies deduced from March 1978 and November 1978 measurements. The dotted line is computed from the Jacchia 71 model.

hours of nighttime data were chosen between March 13 and 20 and 8 hours were chosen between November 17 and 25. Values of $v_{in}$ and $T_n$ were derived from autocorrelation functions, which were integrated for 15 min, using the regression routine ACFIT that is described by *de la Beaujardière et al.* [1980]. Sixty-eight values of $v_{in}$ and $T_n$ were averaged to obtain the mean profiles for March and 32 values for the mean profiles for November. For the computation of the average, each value of $v_{in}$ (or $T_n$) was scaled by the inverse square of the corresponding experimental uncertainty. This uncertainty was computed in the ACFIT routine from the errors for each lag of the autocorrelation function [*Lejeune*, 1980; *Lathuillere*, 1981]. Error bars presented in the figures correspond to the standard deviation of the computed average.

### 3.1. *Collision Frequencies*

The results obtained for March and November 1978 are presented in Figures 1*a* and 1*b*, respectively; the horizontal axis is collision frequency with a logarithmic scale (bars are error bars for each $v_{in}$ value) and the vertical axis is altitude.

For each profile we have performed a least squares fit with an exponential function, $v_{in}(z) = v_{in}(z_0)\ \exp\ [(z - z_0)/H]$, in order to compute the scale height $H$ for the collision frequencies, i.e., for the neutral atmosphere. The reference altitude $z_0$ is 90 km. The results of the regression are drawn as solid lines in Figures 1*a* and 1*b*.

While the collision frequencies at the reference height are almost equal for the two months ($2.12 \times 10^4 \pm 0.11 \times 10^4$ in March and $1.94 \times 10^4 \pm 0.23 \times 10^4$ in November), the scale heights are somewhat different ($6.76 \pm 0.25$ km in March and $7.64 \pm 0.59$ km in November).

Also drawn in Figures 1*a* and 1*b* (with a dashed line) is the collision frequency profile corresponding to the Jacchia 71 neutral model. Although we have used exospheric temperatures of 800 K and 1200 K, the collision frequency values are the same because the lower boundary conditions of the model are constant. The model scale height is smaller than scale heights for the March and November profiles, but the 98-km and 104-km model values and experimental values agree quite well.

### 3.2. *Neutral Temperatures*

Neutral temperature profiles for March and November 1978 are displayed in Figures 2*a* and 2*b*, respectively. As previously, horizontal bars represent error bars for each mean temperature. The Jacchia 71 model temperatures corresponding to an exospheric temperature of 1000 K are included for comparison (dashed line). The temperatures observed in March and November are not very different from those of the model.

### 3.3. *Consistency of the Results*

The mean temperatures and collision frequencies shown above agree well with the Jacchia 71 model. Indeed, in each

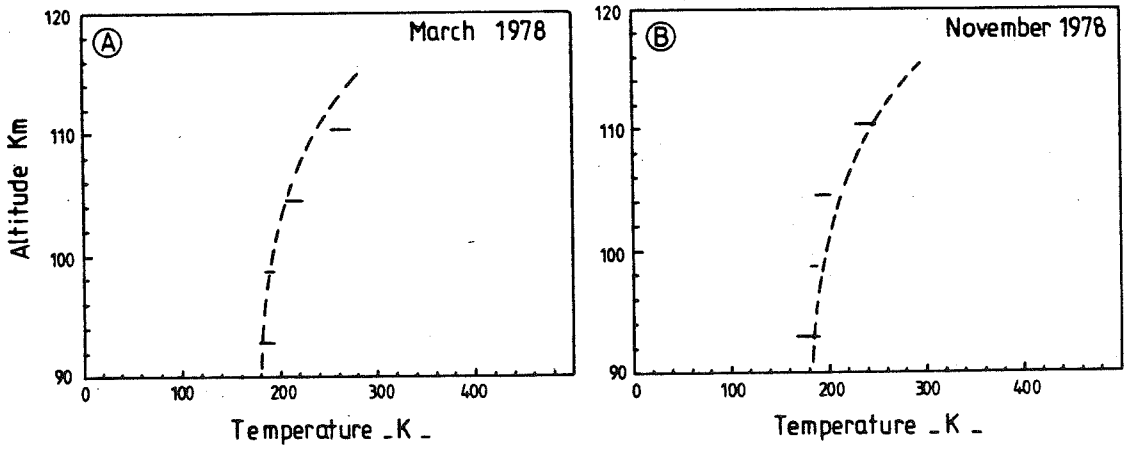


Fig. 2. Mean neutral temperatures deduced from March and November 1978 measurements. The dotted line is the temperature profile from the Jacchia 71 model for a 1000-K exospheric temperature.

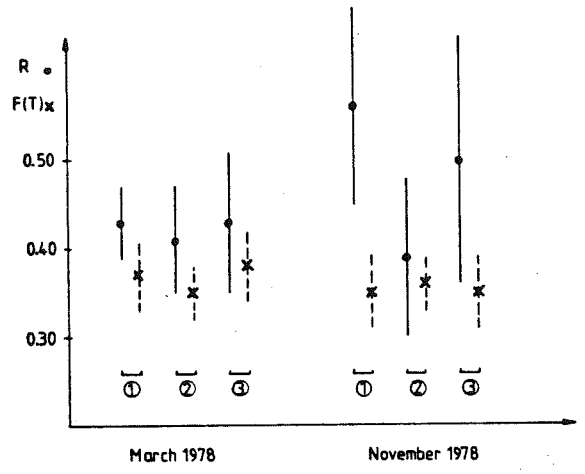


Fig. 3. Comparisons of neutral density ratios obtained from collision frequency measurements ($R$) and temperature measurements ($F(T)$). Numbers 1 to 3 correspond to the three pairs of measurement altitudes.

case half the points agree with the model. However, the scale heights computed from the collision frequency measurements are greater than the model ones. In order to examine this apparent discrepancy, or, more importantly, to examine the consistency of the temperatures and collision frequencies, we rewrite the equation for hydrostatic equilibrium of the neutral atmosphere in the following form:

$$\frac{N(z_2)}{N(z_1)} = \exp - \left[\frac{Mg}{RT}(z_2 - z_1) + \frac{T_2 - T_1}{T}\right] \qquad (6)$$

[*Waldteufel*, 1970*b*], where $T$, $M$, and $g$ are the mean values of the neutral temperature, the molecular mass, and the gravitational acceleration between the altitudes $z_2$ and $z_1$. $N(z_2)$ and $T_2$ ($N(z_1)$ and $T_1$) are the neutral density and temperature at the altitude $z_2$ ($z_1$).

For the evaluation of this equation, we take a constant mass $M$ equal to 27.64 amu, i.e., the value of the Jacchia 71 model at the mean altitude of the measurements, 100 km. The error that we introduce is negligible in comparison with the measurement uncertainty. This assumption, which is equivalent to our previous assumption of a constant $K$ parameter, allows us to consider the density ration $N(z_2)/N(z_1)$ equal to the collision frequency ratio $R = \nu_{in}(z_2)/\nu_{in}(z_1)$. The right-hand side of the equation is calculated from the measured temperatures and called $F(T)$. Figure 3 presents the results obtained for three measurement altitude pairs:

$z_1 = 92.8$ km $\quad z_1 = 98.7$ km $\quad z_1 = 104.5$ km

$z_2 = 98.7$ km $\quad z_2 = 104.5$ km $\quad z_2 = 110.4$ km

For each pair $z_1$, $z_2$ the $g$ value is the value of the mean altitude $(z_1 + z_2)/2$. The dots represent the $R$ values, and the crosses represent the corresponding $F(T)$ values. Thus Figure 3 shows consistency between the temperature and collision frequency determinations when error bars are taken into account.

Another way to check the consistency of the results is to determine whether systematic errors can be introduced by the measurement technique. The Chatanika multipulse correlator performs a 9-km altitude integration, which is larger than the scale height of the neutral atmosphere. To check this possible source of error, we simulated the measurements. Theoretical autocorrelation functions (ACF) of the ionospheric medium were computed with a 1.5-km altitude resolution using different neutral temperature profiles and the corresponding ion collision frequency profiles. These values were obtained from the analytical static model of the neutral atmosphere developed by *Alcayde* [1981]. Then the spatial average of these theoretical ACF's was computed in the same way as in the correlator. The theoretical "mean" ACF's at five altitudes close to the real measurement altitudes were analyzed to obtain the "mean" collision frequencies and temperatures.

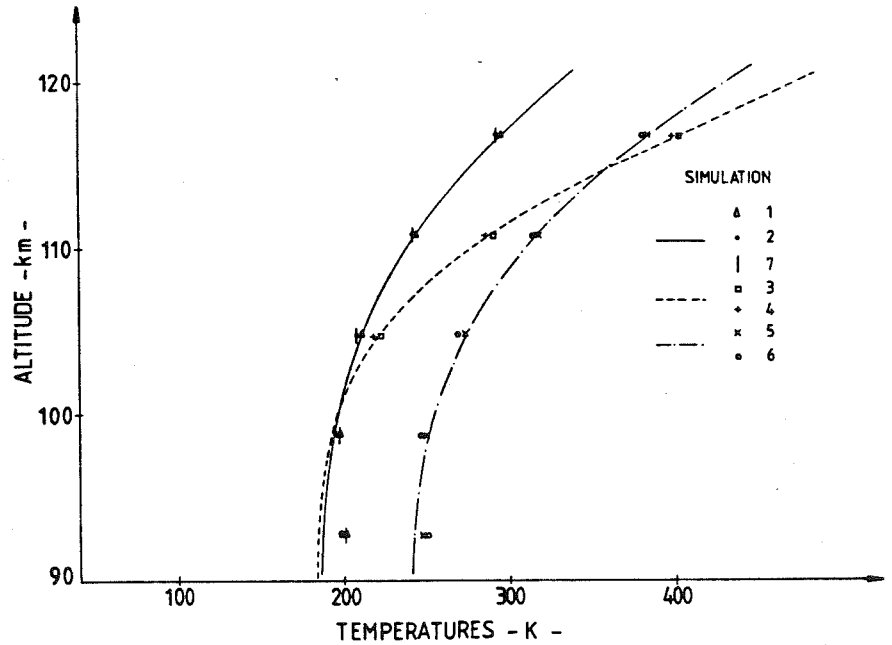


Fig. 4. Results of the altitude integration simulations: the temperature profiles used for the simulation are represented by lines, and the temperatures obtained by symbols.

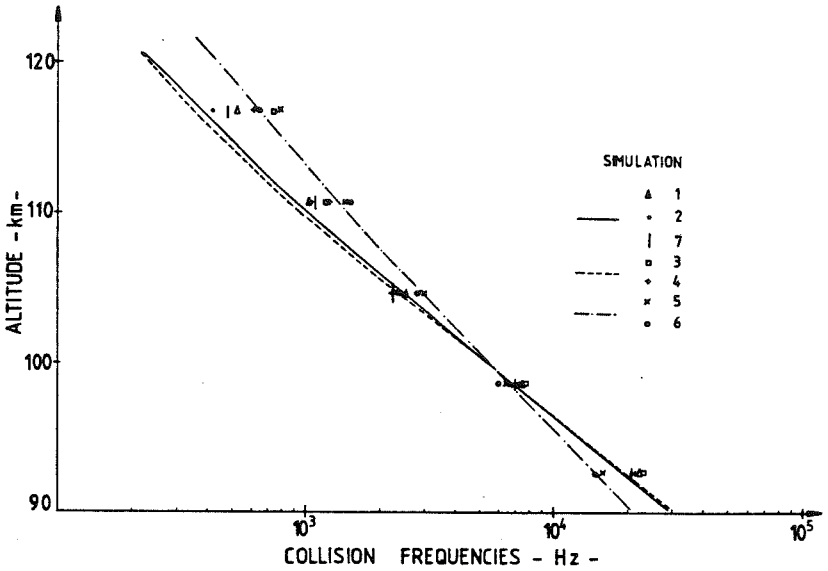


Fig. 5. Same as Figure 4, but for collision frequencies.

Results from these simulations are presented in Figures 4 and 5, which display temperature and collision frequencies, respectively. Simulations 1, 2, and 7 were made with a temperature profile equivalent to the Jacchia 71 neutral model (with an exospheric temperature of 1000 K); simulations 3 and 4, with a model corresponding to the experimental mean profile of March 1978; and simulations 5 and 6, with a model of a very warm atmosphere [*Alcayde*, 1981]. For simulations 1, 3, 5, and 7 the electron density was assumed constant throughout the *E* region. In contrast, simulations 2, 4, and 6 were made with a density profile corresponding to the average of the March 1978 data, i.e., with the *E* layer maximum at 105-km altitude. In addition, in simulation 7 we have included a nonconstant ion velocity profile (variations from 10 to 100 m/s over the 9-km altitude range) in order to evaluate the effects of strong wind shears.

Figure 4 shows that the mean temperatures obtained by the simulations (represented by symbols) are in very good agreement with the model (represented by lines); only at 93 km are they a little overestimated. The collision frequency estimates (represented by symbols in Figure 5) are more scattered, but the error is always less than 15% at the three lowest measurement altitudes. This error is small in comparison with the experimental uncertainties. Above 105 km the worst estimates come from simulations 2 and 3, where the temperature and collision frequency gradients are larger than those in the other cases. These gradients give rise to the larger errors. In contrast to the large influence of the neutral model of the $\nu_{in}$ determination, the electron density profile has very little effect. Furthermore, simulation 7 shows that strong wind shears have no noticeable effect on the mean collision frequencies and temperatures.

For these simulations we have not added noise. Therefore the "mean" values obtained represent the bias due to the altitude integration. The receiver noise would add some scatter centered on our simulated values. We have also assumed that the return signal was received through an infinite bandwidth filter. The influence of a finite bandwidth filter would lead to a greater mixing of the contribution from each altitude. Thus our simulations overestimate the errors introduced by the altitude integration.

## 4. Neutral Temperature and Collision Frequency Variation

For this study we chose four consecutive nights in March 1978: March 16, 17, 18, and 19 during which the experiment was performed from approximately 0800 UT to 1600 UT. After removing Joule heating periods (indicated by solid areas in Figure 6), each night was divided in two parts corresponding to measurements made before 1200 UT (i.e., 0200 hours local time) and after 1200 UT. The exact measurement periods are indicated in Figure 6 (crosshatched areas). Temperature and collision frequency data were then averaged to obtain two data points for each night.

In Figure 6 we used a solid line to depict the 3-hourly magnetic index *Kn*, which represents the magnetic activity over the northern auroral oval (left scale). Corresponding to the right scale, the dotted line depicts the maximum signal-to-noise ratio obtained with the multipulse correlator between the altitudes of 98 km and 110 km. This signal-to-noise ratio is proportional to the electron density and is a local measurement of the auroral particle precipitation at Chatanika.

The four nights that we chose are characterized by different behaviors. During the nights of March 16 and 17, there is an enhancement of the magnetic index and of the local precipitation. On March 18 the magnetic index and local precipitation are constant and quite great during the two measurement periods. In contrast, during the night of March 19, the magnetic index is constant when there is an important enhancement of the local precipitation.

### 4.1. *Ion-Neutral Collision Frequencies*

In order to characterize the collision frequency profiles, we have chosen the scale height estimated by a least squares fitting procedure identical to the one used for the mean profiles presented in the preceding section. On March 16 and 17, collision frequency values were not obtained at 93 km. Therefore to do the fit, we used the mean collision frequency value previously found at this altitude for this month. For each part of the night we have presented the scale heights in Figure 7. The values are all between 6 km and 8 km.

Scale height variations between the two parts of each night are within the error bars. Thus no variation greater than 15%

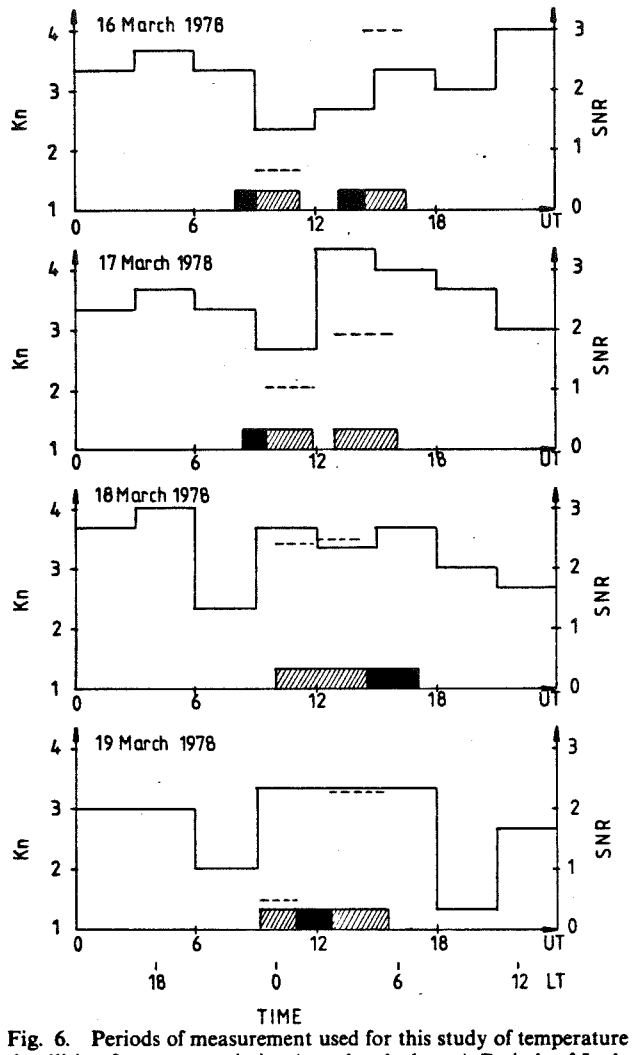


Fig. 6. Periods of measurement used for this study of temperature and collision frequency variation (crosshatched area). Periods of Joule heating, which were not used for this study, are indicated by solid areas. The solid line and the left scale give the *Kn* index; the dashed line and the right scale give the mean signal-to-noise ratio of the measurements.

is found in the scale height for the 93- to 110-km region between late evening and early morning. As a result of the fitting procedure, we also obtain the value of the collision frequency at 90-km altitude. Again, the data points are scattered around the value of the collision frequency obtained for the month of March, and the variations stay within the error bars.

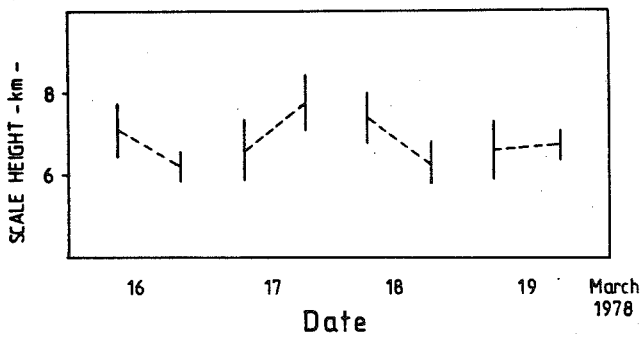


Fig. 7. Variation of neutral scale heights for four nights of measurements. The first data point of each night corresponds to the period prior to 1200 UT; the second, to the period after 1200 UT.

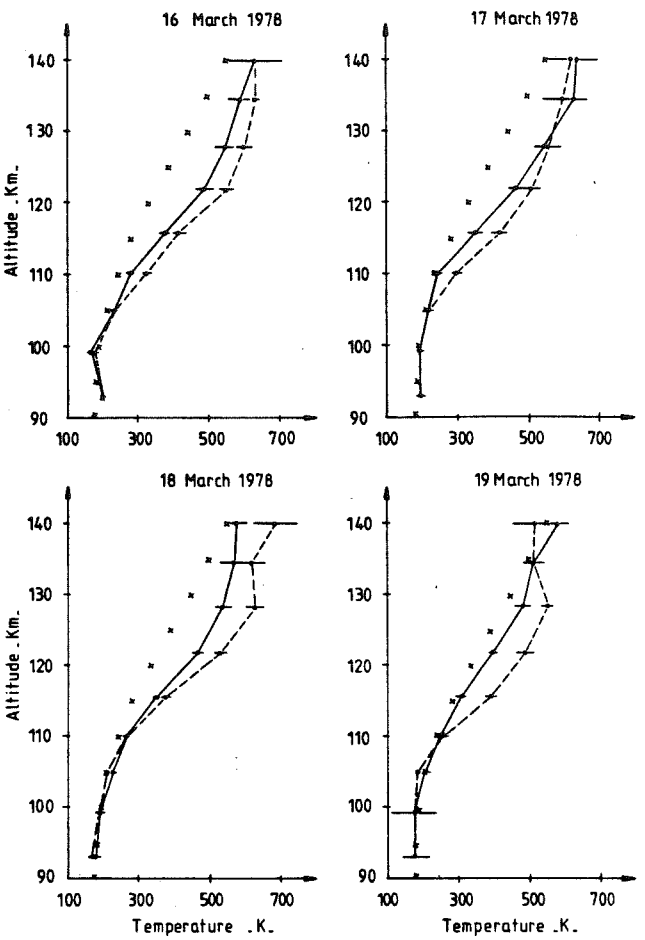


Fig. 8. Variations of neutral temperature profiles for four nights of measurements. The solid line and dashed line correspond to the periods prior to and after 1200 UT, respectively. Crosses are temperature from the Jacchia 71 model for a 1000-K exospheric temperature.

### 4.2. *Neutral Temperatures*

Ion temperature profiles measured during each night are presented in Figure 8. The solid line represents the profile corresponding to the first part of the night, and the dotted line is the profile corresponding to the second part. Crosses correspond to the Jacchia 71 neutral temperature model calculated with an exospheric temperature of 1000 K. Below 120 km the temperatures displayed correspond to the assumption of thermal equilibrium between ions and electrons. Above this altitude, we assumed a noncollisional medium, but the electron-to-ion ratio was variable. While no ambiguity exists in interpreting the ion temperature as the neutral temperature below 110 km (see section 2), there may be above this altitude because of Joule heating. Therefore, as usual, periods of Joule heating were removed from our data before averaging. Furthermore, we verified that ion temperatures were lower than electron temperatures. Only during the second part of the night of March 18 was $T_i$ 30 K higher than $T_e$ at the altitudes of 122 km and 128 km, which means that there was perhaps a small contribution of Joule heating still present.

Under these conditions, thermal equilibrium between ions and neutrals seems to us to be still justified. Thus we interpret these measured ion temperatures as the neutral temperatures in the lower thermosphere.

Several inferences then can be drawn from Figure 8:

1. There is a good agreement between both sets of experimental temperatures and the Jacchia 71 model below 110 km.

2. At and above 110 km the experimental profiles are more variable and the temperatures greater than those in the model.

3. We have not been able to make any correlation between these variations and the magnetic activity described before.

4. We found a systematic temperature increase between the first and the second part of each night. The maximum of this variation (14% to 20%) is located between the altitudes of 115 km and 125 km.

It is beyond the scope of this paper is make an exhaustive study of this nighttime temperature increase, but we suggest that it can be attributed to the tidal process at equinox. Indeed, while there are no observations of atmospheric tides at high latitude, many studies at middle and low latitudes with three incoherent scatter radars [*Bernard*, 1974; *Salah et al.*, 1975; *Wand*, 1976] support the preponderance of a semidiurnal tide in the *E* region whose main characteristics (vertical wavelength of 40 to 60 km and amplitude of 10 to 20%) correspond to our observations.

## 5. Conclusion

After reviewing how the incoherent scatter technique allows an experimental approach to the study of the lower thermosphere, we have discussed the conditions peculiar to the auroral regions. During periods of large electric fields, which produce Joule heating of the ions and low-altitude electron heating, we are unable to deduce neutral temperatures and densities from the incoherent scatter data.

Our study is the first one of collision frequencies and temperatures in the auroral *E* region based on a large set of data (more than 30 hours) where the altitude integration of the data is almost as small as the neutral scale height.

We showed that the mean collision frequencies are similar to those deduced from the "Jacchia 71" neutral model and that the temperatures are in very good agreement with this model. A consistency check of the temperature and collision frequency data, assuming hydrostatic equilibrium, and a detailed simulation of the data support the results. In addition, possible wind shears as large as 100 m/s in 9 km have no effect on the deduced parameters.

The study of neutral temperatures between 90 km and 140 km during four nights of March 1978 has shown that besides a mean profile that was variable from one night to another, there was a systematic increase during the night, which we suggest is the effect of atmospheric tides.

In the future, additional results on the high-latitude lower thermosphere should be obtainable from the EISCAT and Sondrestrom radars. They will be more sensitive than Chatanika and, by using coded pulses, will have the possibility of better altitude resolution.

*Acknowledgments.* We gratefully acknowledge many fruitful discussions with G. Lejeune. We would also like to thank the staff members at SRI International and CEPHAG who made these joint experiments and collaboration possible. In particular, we would like to thank J. Kelly, M. McCready, C. Code, and C. D. Feken for their assistance at Chatanika and C. Dawson and C. Leger for their programing work. The French portion of the experiment was supported by the Actions Thématiques Programmées of the Centre National de la Recherche Scientifique for the International Magnetospheric Study. It was supported, as well, by the Centre de Recherche en Physique de l'Environnement Terrestre et Planétaire and by the Centre National d'Etudes des Télécommunications. The American portion was supported by grants ATM7800129 and ATM8121671 from the Aeronomy Program, Division of Atmospheric Sciences, National Science Foundation. In addition, the Chatanika radar was operated by SRI International under contract DNA0001-77-C-0042 from the Defense Nuclear Agency and grant ATM72-01644-A05 from the Division of Atmospheric Science, National Science Foundation.

The Editor thanks K. Schlegel and J. P. St. Maurice for their assistance in evaluating this paper.

## References

Alcayde, D., An analytic static model of temperature and composition from 20 to 2000 km altitude, *Ann. Geophys.*, *37*, 515–528, 1981.

Alcayde, D., J. Fontanari, G. Kockarts, P. Bauer, and R. Bernard, Temperature, molecular nitrogen concentration and turbulence in the lower thermosphere inferred from incoherent scatter data, *Ann. Geophys.*, *35*, 41–51, 1979.

Banks, P. M., and G. Kockarts, *Aeronomy*, Academic, New York, 1973.

Bernard, R., Tides in the *E* region observed by incoherent scatter radar over St. Santin, *J. Atmos. Terr. Phys.*, *36*, 1105–1120, 1974.

de la Beaujardière, O., V. Wickwar, C. Leger, M. McCready, and M. Baron, The software system for the Chatanika incoherent scatter radar, SRI tech. rep., SRI Int., Menlo Park, Calif., 1980.

Dougherty, J. P., and D. T. Farley, A theory of incoherent scattering of radio waves by a plasma, *J. Geophys. Res.*, *68*, 5473–5486, 1963.

Hedin, A. E., et al., A global thermospheric model based on mass spectrometer and incoherent scatter data, 1, $N_2$ density and temperature, *J. Geophys. Res.*, *82*, 2139–2147, 1977*a*.

Hedin, A. E., C. A. Reber, G. P. Newton, N. W. Spencer, H. C. Brinton, and H. G. Mayr, A global thermospheric model based on mass spectrometer and incoherent scatter data, 2, Composition, *J. Geophys. Res.*, *82*, 2148–2156, 1977*b*.

Jacchia, L. G., Revised static models of the thermosphere and exosphere with empirical temperature profiles, *Spec. Rep. 322*, Smithson. Astrophys. Observ., Cambridge, Mass., 1971.

Jacchia, L. G., Thermospheric temperature, density and composition: New models, *Spec. Rep. 375*, Smithson. Astrophys. Observ., Cambridge, Mass., 1977.

Kofman, W., and V. B. Wickwar, Plasma line measurements at Chatanika with high-speed correlator and filter bank, *J. Geophys. Res.*, *85*, 2998–3012, 1980.

Lathuillere, C., Experimental study of the uncertainties in incoherent scatter estimation using the ACFIT routine and Chatanika data, *Rep. CEPHAG*, Grenoble, France, 1981.

Lejeune, G., Détermination des incertitudes sur. les paramètres measurés par diffusion incohérente, in *Le système EISCAT et l'Etude du Couplage Magnétosphère-Ionosphère-Atmosphère*, edited by D. Alcayde, Centre d'Etude Spatiale des Rayonnements, Toulouse, France, 1980.

Mayr, H. G., and H. Volland, Magnetic storm characteristics of the thermsophere, *J. Geophys. Res.*, *78*, 2251–2264, 1973.

Offermann, D., V. Friedrich, P. Ross, and U. Von Zahn, Neutral gas composition measurements between 80 and 120 km, *Planet. Space Sci.*, *29*, 747–764, 1981.

Salah, J. E., J. V. Evans, and R. H. Wand, Seasonal variations in the thermosphere above Millstone Hill, *Radio Sci.*, *9*, 231–238, 1974.

Salah, J. E., R. H. Wand, and J. V. Evans, Tidal effects in the *E* region from incoherent scatter radar observations, *Radio Sci.*, *10*, 347–355, 1975.

Schlegel, K., and J. P. St. Maurice, Anomalous heating of the polar *E* region by unstable plasma waves, 1, Observations, *J. Geophys. Res.*, *86*, 1447–1452, 1981.

Schlegel, K., H. Kohl, and K. Rinnert, Temperatures and collision frequency in the polar *F* region measured with the incoherent scatter technique, *J. Geophys. Res.*, *85*, 710–714, 1980.

St. Maurice, J. P., K. Schlegel, and P. M. Banks, Anomalous heating of the polar *E* region by unstable plasma waves, 2, Theory, *J. Geophys. Res.*, *86*, 1453–1462, 1981.

Tepley, C. A., and J. D. Mathews, Preliminary measurements of ion-neutral collision frequencies and the mean temperatures in the Arecibo 80- to 100-km region, *J. Geophys. Res.*, *83*, 3299–3302, 1978.

Vidal-Madjar, D., Gravity waves detection in the lower thermosphere with the French incoherent scatter facility, *J. Atmos. Terr. Phys.*, *40*, 685–689, 1978.

Waldteufel, P., A study of seasonal changes in the lower thermosphere and their implications, *Planet. Space Sci*, *18*, 741–748, 1970*a*.

Waldteufel, P., Une étude par diffusion incohérente de la haute atmosphère neutre, thesis, Fac. des Sci. de Paris, Paris, 1970*b*.

Wand, R. H., Semidiurnal tides in the *E* region from incoherent scat-

ter measurements at Arecibo, *Radio Sci.*, *11*, 641–652, 1976.
Wickwar, V. B., C. Lathuillere, W. Kofman, and G. Lejeune, Elevated electron temperatures in the auroral *E* layer measured with the Chatanika radar, *J. Geophys. Res.*, *86*, 4721–4730, 1981.

W. Kofman and C. Lathuillere, Centre d'Etudes des Phénomènes Aléatoires et Géophysiques, BP 46, 38402 Saint-Martin-d'Hères, France.

V. B. Wickwar, SRI International, 333 Ravenswood Avenue, Menlo Park, CA 94025.

(Received April 26, 1983;
revised July 18, 1983;
accepted August 10, 1983.)

# ARTICLE 2

*Journal of Atmospheric and Terrestrial Physics*, Vol. 48, Nos 9–10, pp. 837–847, 1986.
Printed in Great Britain.

0021-9169/86 $3.00 + .00
Pergamon Journals Ltd.

# Neutral atmosphere studies in the altitude range 90–110 km using EISCAT

W. KOFMAN, C. LATHUILLERE and B. PIBARET
CEPHAG, INPG/IEG, UA 346, BP46, 38402 St Martin d'Hères Cedex, France

(*Received for publication* 29 *April* 1986)

**Abstract**—In this paper we describe measurements by the incoherent scatter technique in the low thermosphere and compare the results to models. We find that the observed neutral temperature in winter at 100 km is lower by about 15K than predicted by the MSIS model and closer to the temperature predicted by the Jacchia 71 model. We also show that the neutral mass, which we inferred from the temperature and scale height, is about 26–28 a.m.u. and that this value is also lower than that used in the MSIS model. Finally, we show data for a very disturbed day, with very strong anomalous heating, for which the assumption of thermal equilibrium between electrons and ions is not correct.

## 1. INTRODUCTION

In 1983 the EISCAT facility started to use the multipulse technique to measure plasma parameters in the auroral *E*-region (KOFMAN and LATHUILLERE, 1985; FLÅ *et al.*, 1985), allowing studies of the behaviour of the low auroral thermosphere.

In the past the incoherent scatter technique has been used for the study of the low thermosphere at low and middle latitudes (WALDTEUFEL, 1970a,b; ALCAYDÉ *et al.*, 1979; TEPLEY and MATHEWS, 1978). Using the Chatanika incoherent scatter radar, this technique has also been applied in the auroral zone (SCHLEGEL *et al.*, 1980; LATHUILLERE *et al.*, 1983). In the work of Lathuillere *et al.* a large set of multipulse data has been analysed: scale heights of the low thermosphere and neutral temperatures have been calculated for two periods (March and November 1978) and compared with the Jacchia 71 neutral model (JACCHIA, 1971).

The multipulse data available from EISCAT, presented in this paper, come from seven days distributed over a whole year and allow for long term studies of the low atmosphere in the auroral zone, thus extending the results obtained with the Chatanika radar.

Furthermore, the Chatanika data were obtained with a 9 km altitude resolution, which is larger by about 50% than the scale height of the low atmosphere. In this sense, the EISCAT results, obtained with a 2.2 km altitude resolution, are much more precise.

In the first part of this paper we describe the data and their analysis. We recall the problems of determining parameters in the low thermosphere in the auroral zone. In the second part we describe the overall geophysical conditions for the days observed and compare our results with the MSIS-83 model (HEDIN, 1983). In the third part we show the data corresponding to a very disturbed day for which the assumption of thermal equilibrium does not apply. We propose a data analysis procedure for these periods. In the final section we discuss our results compared to the Chatanika results and their implications for atmosphere modelling.

## 2. METHOD AND DATA ANALYSIS

We analysed seven days of data acquired with the CP1 and special French experiment programs. The measurements were made in the *E*- and *F*-regions of the ionosphere along a magnetic field line. The CP1 experiment is very similar to the French special program.

The description of the experiment and the way the data were analysed have been described by KOFMAN and LATHUILLERE (1985). We recall here only the basic lines of the data analysis. Five minute integrated correlation functions were analysed assuming $T_e = T_i$ for altitudes below 108 km and $T_e \neq T_i$ for higher altitudes. For altitudes below 108 km we determine four parameters: electron density ($N_e$), plasma temperature ($T = T_e = T_i$), ion velocity ($V_i$) and ion–neutral collision frequency ($\nu_{in}$). For altitudes higher than 108 km the influence of collisions is negligible at the observing frequency.

The data were averaged over each night (see Table 1). Data for which errors were greater than 50% and 25%, respectively, for ion–neutral collision frequencies and temperatures were eliminated from the averaging process. Due to limited experimental sen-

Table 1

| Parameter | Time intervals over which averages taken | | | | | | | | | | | | | | | | | | | | | | | |
|---|---|---|---|---|---|---|---|---|---|---|---|---|---|---|---|---|---|---|---|---|---|---|---|---|
| | 12.12.83–13.12.83 19.00–03.00 UT | | | 31.01.84–01.02.84 23.00–06.00 UT | | | 14.02.84–15.02.84 24.00–09.00 UT | | | 03.03.84 19.00–24.00 UT | | | 06.06.84–07.06.84 01.30–12.00 UT | | | 15.11.84–16.11.84 19.00–09.00 UT | | | 22.02.85–23.02.85 22.00–01.00 UT | | | | |
| $Ap$ | 23 | | | 23 | | | 43 | | | 35 | | | 12 | | | 52 | | | 7 | | | 7 | |
| $\Sigma Kp$ | 29+ | | | 29 | | 23+ | 38 | | 2 | 34 | | | 22− | | 18 | 39 | | 52− | 15+ | | | 16− | |
| Minimum solar zenith angle | | 92 | | | 87 | | | 83.5 | | | 77.5 | | | 47 | | | 87 | | | 81 | | | | |

sitivity we were unable to measure ionospheric parameters for electron densities lower than about $10^{11}$ el $m^{-3}$. This implies that our results were obtained only during nights with periods of precipitation. This fact can lead to measurement problems and errors in derived parameters.

Indeed, during precipitation electron temperatures can be higher than ion temperatures. Differences between $T_e$ and $T_i$ depend on the flux and the energy spectrum of the precipitation.

For the most common auroral situation (not very disturbed) and for altitudes below 108 km these differences cannot be large, because of the very high electron–ion, electron–neutral and ion–neutral collision frequencies. The electron energy loss processes are very efficient at these altitudes.

If $T_e$ is larger than $T_i$, the assumption of $T_e = T_i$ in the data analysis will lead to an underestimate of the ion–neutral collision frequency and an overestimate of $T_i$. The ion temperature estimate would be approximately equal to the average of the true values of $T_e$ and $T_i$. However, even in the case of intense electron precipitation, we estimate that the error for this altitude range can reach only a few degrees.

Indeed, if one takes into account the electron losses to neutrals and ions, one needs about $1.1 \times 10^{-5}$ mW $m^{-3}$ to maintain $T_e - T_n = 10$K, whereas the total energy supplied to electrons by precipitation in order to create a density of about $3 \times 10^{11}$ el $m^{-3}$ is about $5 \times 10^{-6}$ mW $m^{-3}$. This value was calculated assuming that 5% of the energy input to the atmosphere goes into thermal electrons (WICKWAR *et al.*, 1975; SCHUNK and NAGY, 1978; REES, 1983).

Joule heating acts on ions and electrons, but this effect is negligibly small on electrons in this altitude range (SCHUNK and WALKER, 1971; BANKS, 1979). This effect can enhance $T_i$ and produce $T_i$ larger than $T_e$, but it is particularly effective for altitudes between 120 and 140 km (BANKS, 1977; WICKWAR *et al.*, 1975). For altitudes under 108 km and an electric field of about 40 mV $m^{-1}$ the ion temperature increases less than 5K (FLÅ *et al.*, 1985). The enhanced $T_i$ can be also observed in the *F*-region.

During periods of very high electric field (>45 mV $m^{-1}$) the electron temperature $T_e$ can also be enhanced through anomalous heating (SCHLEGEL and ST. MAURICE, 1981; ST. MAURICE *et al.*, 1981; WICKWAR *et al.*, 1981) in the altitude range 100–120 km. This $T_e$ enhancement can reach several hundred degrees.

Therefore, in the averaging process we removed the data corresponding to the anomalous heating periods. These periods were determined by a careful study of electric fields, ion and electron temperatures near

120 km and ion temperature at 300 km (LATHUILLERE *et al.*, 1983). We had to remove completely from our averaging process one night of data. This night had very high magnetic activity, during which anomalous heating was present most of the time (see Section 4).

This data selection procedure ensures that, for altitudes between 95 and 108 km, the electron and ion temperatures were very close for all the data presented in this paper.

For this altitude range the data analysis gives us the plasma temperature, electron density and ion–neutral collision frequency. We assume that the plasma temperature is very close to the neutral temperature, which is justified by a very high ion–neutral collision rate.

In the data analysis we assumed that the ion mass is 31 a.m.u. for the whole *E*-region. This assumption is not entirely correct, because one knows from models that near 100 km more than 50% of the ions are $O_2^+$. This leads to an underestimate of the temperature by at most 2%. This effect cannot be taken into account exactly, because the true ion composition is unknown for a given experiment. However, the possible small increase of the electron temperature during precipitation periods would probably compensate for this ion mass effect. The average behaviour of the neutral atmosphere which we determined can also depend on the semidiurnal tide, because our data were obtained during only portions of the night.

## 3. DATA

Seven days of data were analysed. Figure 1 shows the particle heating for each day. The particle energy input was calculated from the *E*-region density (WICKWAR *et al.*, 1975; BANKS, 1977), which was measured using a short 60 $\mu$s pulse. The determination of the electron density profile was done taking into account the $T_e$ and $T_i$ obtained from the long pulse measurements. We use in our calculations the peak transmitter power written on the data tape instead of the high voltage value, because we should like to compare the data taken for a long period (JOHANSSON *et al.*, 1984). This can lead to a 40–50% overestimate of the energy input, but allows us to compare different days. In fact, one can see very high variability of particle heating from hour to hour and from day to day. The energy input by precipitating electrons varied between 1 and 30 mW $m^{-2}$, except for a few isolated points when it reached values larger than 30 mW $m^{-2}$.

The days analysed differed substantially. For instance, 12 December 1983 was a day with an energetic and intense electron precipitation during a few hours producing an average particle heating of about 10 mW $m^{-2}$. The night of 22 February 1985 is an example of very low energy input of the order of 1–4 mW $m^{-2}$. Even in the case of such large difference in the energy input, the assumption of thermal equilibrium for altitudes below 108 km is approximately correct, as explained in Section 2.

In Fig. 2 we plot the measured electric field. When we do not have data from three stations we plot the ion velocity measured at Sodankylä. The ion velocity observed at Sodankylä is very sensitive to the east–west velocity: 100 m $s^{-1}$ corresponds approximately to a north–south electric field of 15 mV $m^{-1}$. We also indicate in these figures the periods for which we averaged the data. In Table 1 we indicate the time periods analysed and the magnetic indices. Table 1 and Figs. 1 and 2 show that we have studied days with very different magnetic activity: active days ($Ap \sim 20$–40), days with low activity (7–20) and one very disturbed night. The *Ap* indices were 52 and 112, respectively, for 15 and 16 November 1984 and the 3 h *Kp* index during the measurements was 8. These days were analysed with a different strategy than for other days (see Section 4).

Figure 3 shows the average collision frequencies for 6 days. The measured points were fitted by an error weighted exponential curve and the scale heights were determined. The collision frequency is proportional to neutral density (LATHUILLERE *et al.*, 1983). The fit by an exponential means that we assumed an almost isothermal atmosphere in the altitude range 95–108 km. We also used a linear variation of the scale height and fitted our measurements to a shape corresponding to the resultant theoretical profile. We find that the scale heights at about 100 km (center of the studied altitude range) obtained by this fit and by an exponential fit are almost the same. The measured scale heights are between 5.4 and 6.5 km, and the errors in their determination are between 0.2 and 0.5 km.

In Fig. 4 we show the average profiles of the plasma temperature, which are close to the neutral temperature (see Section 2), and profiles of the MSIS-83 model. One can see that when the profiles change from day to day the changes go in the same direction as those expected from the model (see for instance the differences between 31 January 1984 and 6 June 1984).

However, the measured temperatures were systematically lower than those of the model, except for 6 June 1984. For this day the measured temperatures were higher than those of the model for altitudes higher than about 100 km. Solar illumination was present for 24 h during that day.

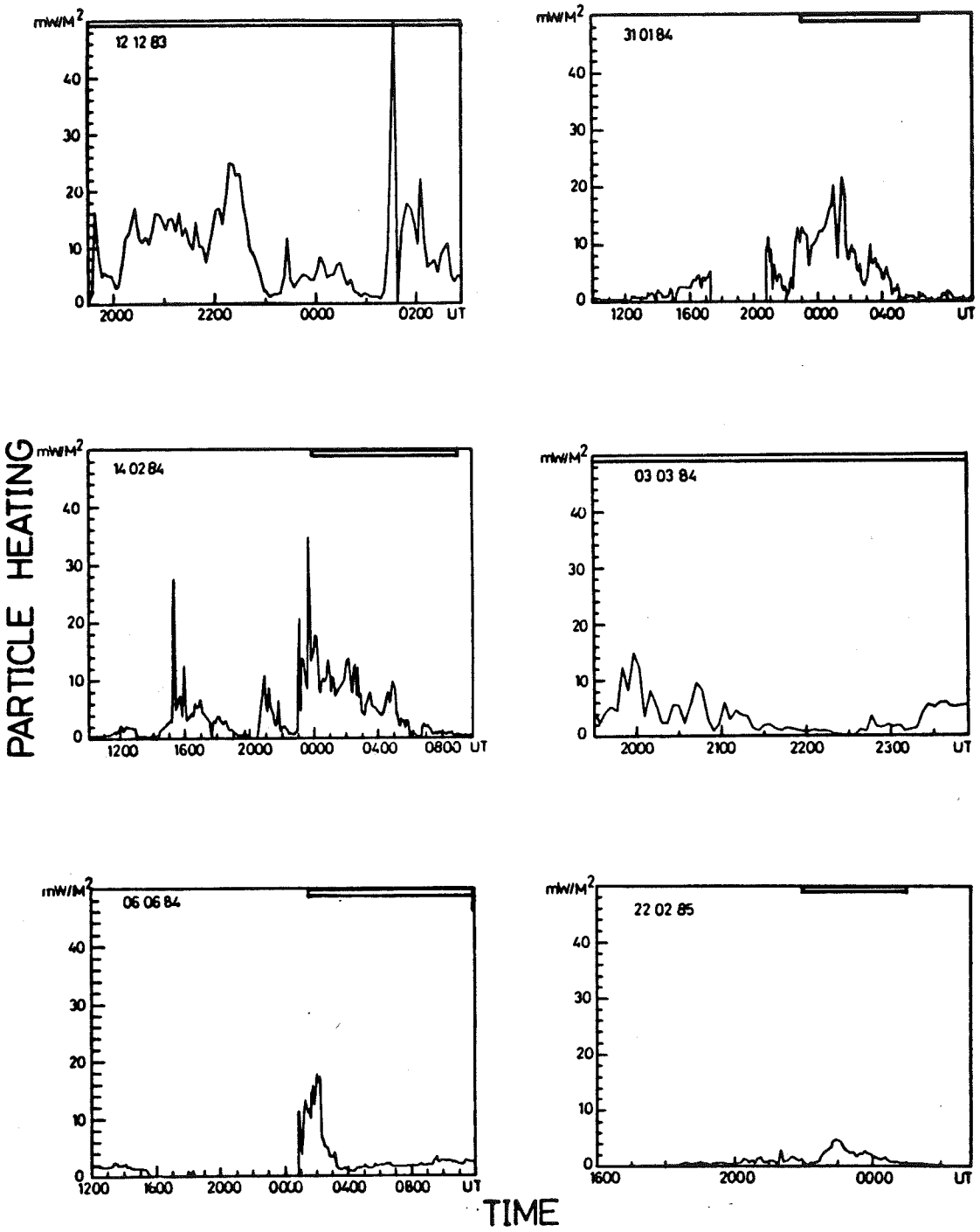


Fig. 1. Particle energy input to the atmosphere during measurements. The gap in the data means that we do not have measurements.

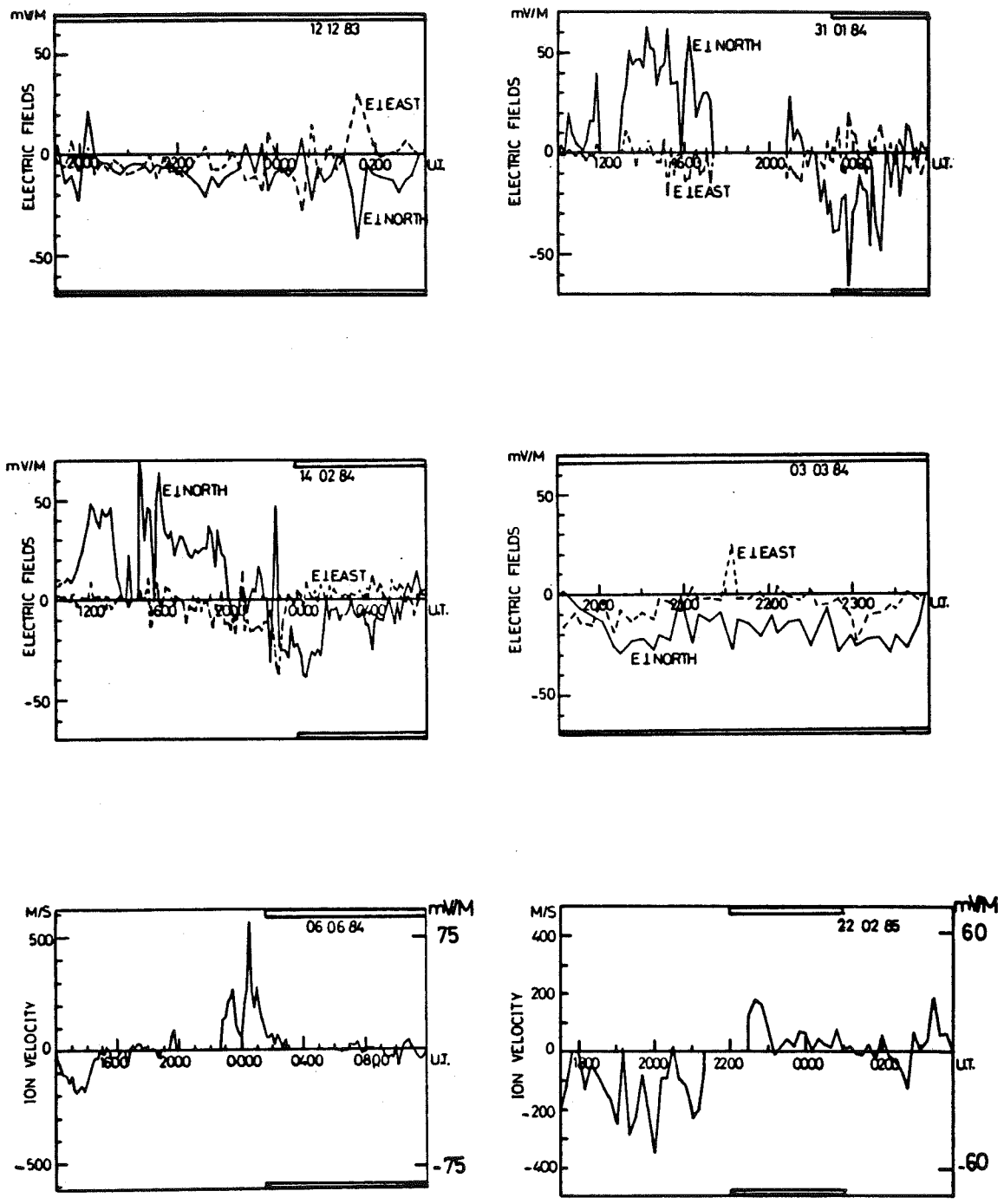


Fig. 2. Measured electric field or ion velocity at Sodankylä for each day. We indicate the periods for which the data were averaged.

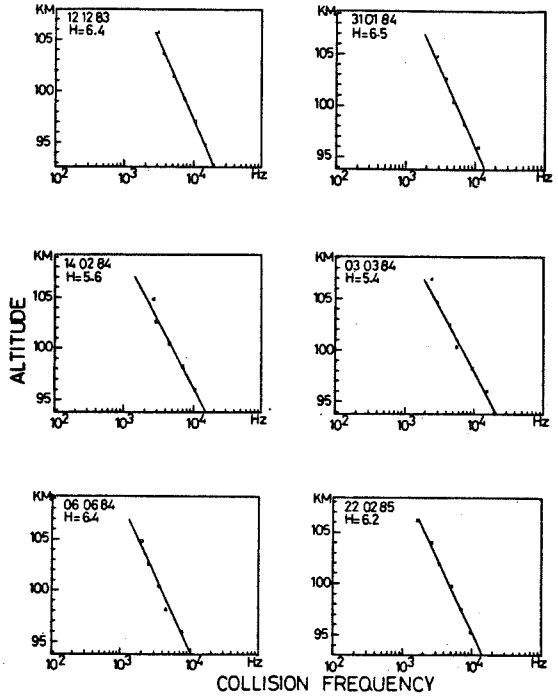


Fig. 3. The measured collision frequency and scale height.

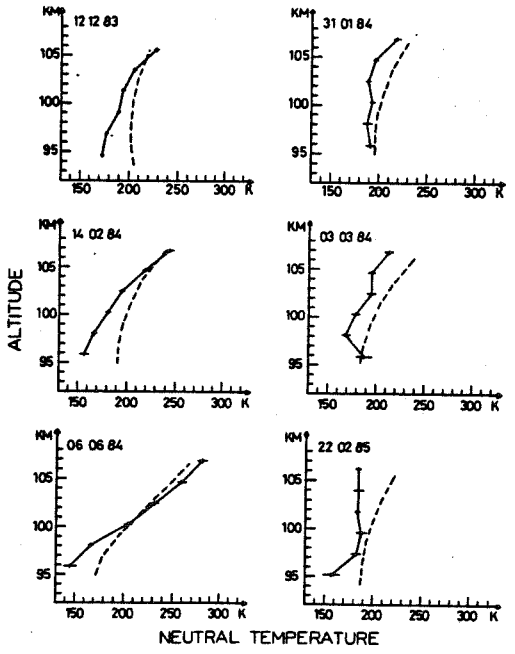


Fig. 4. The neutral temperature (continuous line) compared to MSIS-83 model (dotted line).

In Fig. 5 we summarize our results and characterize each day by its geophysical conditions. We plot in this figure the measured scale heights, average particle energy input and neutral temperature for 100 km. From the scale height ($H = kT/mg$) and temperature we derived the average neutral mass at 100 km. We compare these results to the MSIS-83 and Jacchia 71 models. The MSIS temperatures were taken at 24.00 UT for a given day.

In the same figure we add general geophysical parameters: $\Sigma Kp$ and $Ap$ indices, to describe magnetic activity, and minimum solar zenith angle, to describe solar illumination. The major part of the data was obtained during the night, except for the June day. It is clear from this figure that the measured temperature at 100 km is lower by about 15K than predicted by the model.

The values of inferred neutral mass were between 26 and 28 a.m.u., which is lower than the mass used in the MSIS model (about 28.5). The number of data points is not large enough to establish a clear correlation between particle heating and either temperature or scale height variations, even though such a correlation seems to exist for the first four days.

#### 4. 15–16 NOVEMBER 1984

We analysed these data in a different way compared to the other days. This is because it was a magnetically very disturbed day. We describe these measurements for two reasons, firstly to show the importance of the anomalous heating and in that way the importance of the careful analysis of Joule heating periods, secondly to propose a simplified method of data analysis.

In Fig. 6 we show the particle energy input, ion velocity from Sodankylä and ion and electron temperatures at 106 and 121 km. During this night the particle heating was not particularly large, but the electric field, in contrast, was very intense, as was the Joule energy input. One can see that the ions were hotter than electrons almost all night at 121 km and that, in the middle of the night, the difference reached as much as 200–400K. The very strong electric field ($>45\,\text{mV m}^{-1}$) can be accompanied by an anomalous heating effect (see Section 2). This heating by unstable plasma waves is most important for the altitudes between 100 and 120 km (ST. MAURICE and SCHLEGEL, 1981; WICKWAR *et al.*, 1981).

For this reason we analysed only the data for altitudes lower than 98 km, with the assumption of thermal equilibrium. We determined the collision frequency for these altitudes. We averaged in time all

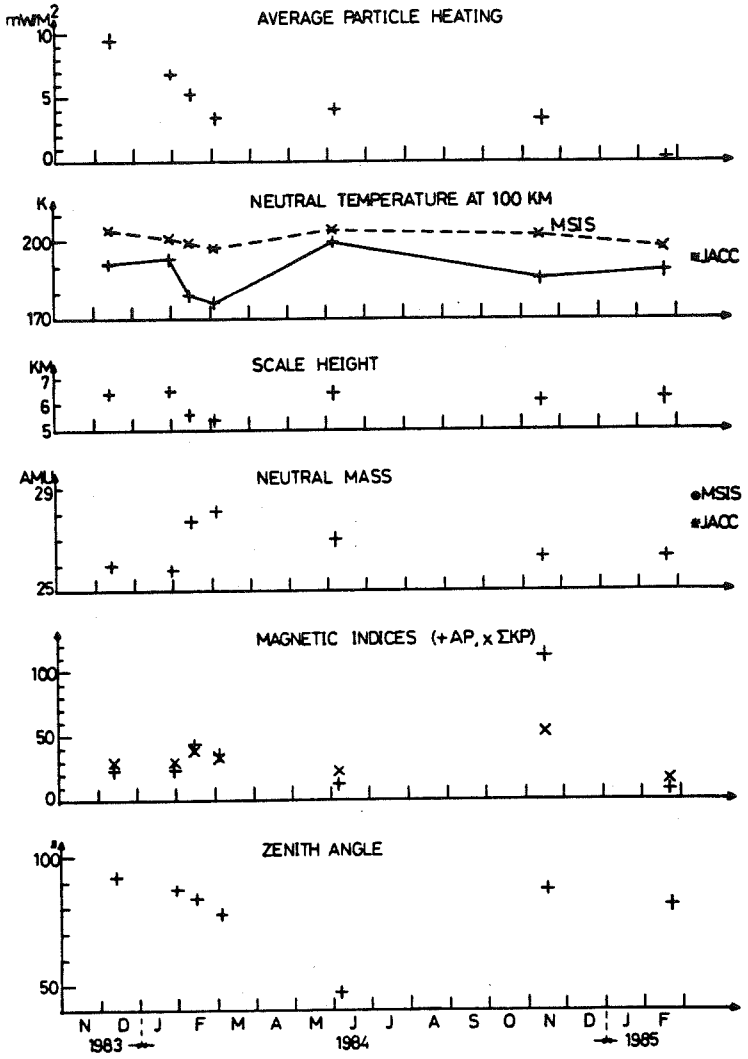


Fig. 5. The neutral temperature at 100 km, scale height, average particle energy input and average neutral mass derived for each day. Also plotted are the magnetic indices and solar zenith angles.

the data and found the ion–neutral collision profile, assuming static equilibrium. The determined scale height and the value of collision frequency at 95.3 km were, respectively, 6.1 km and $1.09 \times 10^4$ Hz. We used this profile in the data analysis, assuming $T_e \neq T_i$ for altitudes higher than 98 km. Figure 6 shows the ion and electron temperatures at 105 km. The electron temperature was higher than the ion temperature. Temperature differences exist most of the time and can reach as much as 500K or a bit more. This method is of course much less precise, due to the fact that one determines the collision frequency profile only from measurements at two or three altitudes.

In Fig. 7 we plot the measured correlation functions for three altitudes at two different times (01.43 UT corresponding to very strong heating and 02.58 UT to low heating). The most important effect is the change in the shape and zero crossing at two altitudes, 101.8 and 104 km. The change in the form of the correlation function indicates clearly that some very strong phenomenon occurred during this period. Due to the fact that this effect is accompanied by a very strong electric field, there is a very high probability of anomalous heating. Small changes in the shape of the correlation function occurred also at 97.5 km altitude at 01.43 UT, when the heating was particularly

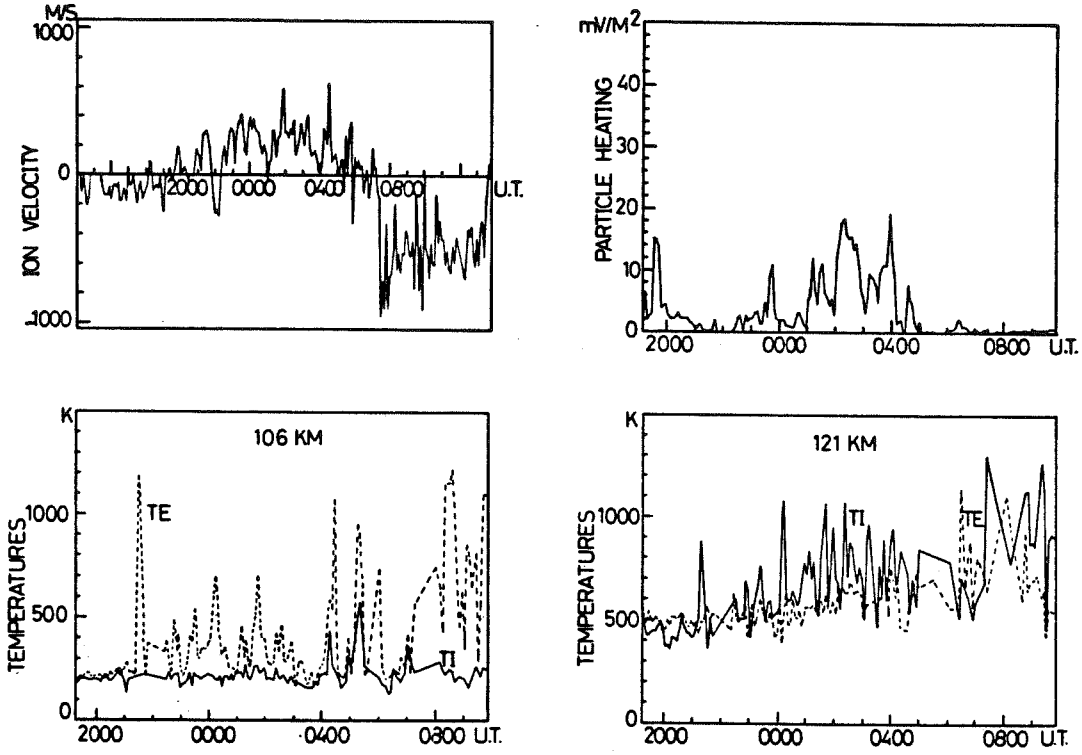


Fig. 6. Particle energy input, ion velocity at Sodankylä and ion and electron temperatures at 106 and 121 km for 15 November 1984.

intense. When one compares the correlation function for 97.5 km at 19.18 UT, when there was no heating, with the correlation function at 02.58 UT, when the heating occurred, one can see no differences.

In Fig. 8 the measured ion and electron temperature profiles are plotted. We add also the profiles at 19.18 UT. The comparison between these profiles clearly shows that at 01.43 UT there was strong heating, at 02.58 UT the heating was still present but much less intense, and at 19.18 UT this phenomenon was not present.

Another explanation could be the reduction of the average ion mass. This assumption would lead to unacceptably low ion temperatures.

Anomalous heating studies are not the goal of this paper. We should like only to emphasize the importance of careful detection of these phenomena when one studies the auroral low thermosphere.

## 5. DISCUSSION AND CONCLUSIONS

The data presented in this paper were analysed under the assumption of thermal equilibrium for altitudes below 108 km. To be sure that this assumption is correct, we eliminated from our measurements the periods of strong electric field. Due to the limited sensitivity of the radar we were able to measure only when the electron density was higher than about $1 \times 10^{11}$ el $m^{-3}$. The two major conclusions of our paper are:

(a) the observed neutral temperature is lower than the temperature predicted by the MSIS model (except for 6 June 1984);
(b) the inferred neutral mass is also lower than the mass used in the model.

For 6 June 1984 the measured temperature was higher than the temperature predicted by the model (for altitudes higher than 100 km). This was a summer day with 24 h of solar illumination. For this day the time average was done for the time period between 01.30 UT and 12.00 UT, and the influence of tides could perhaps be important. Indeed, the semidiurnal amplitude predicted by the model is about 20K.

What could lead to an underestimate of the neutral temperature in our measurements?

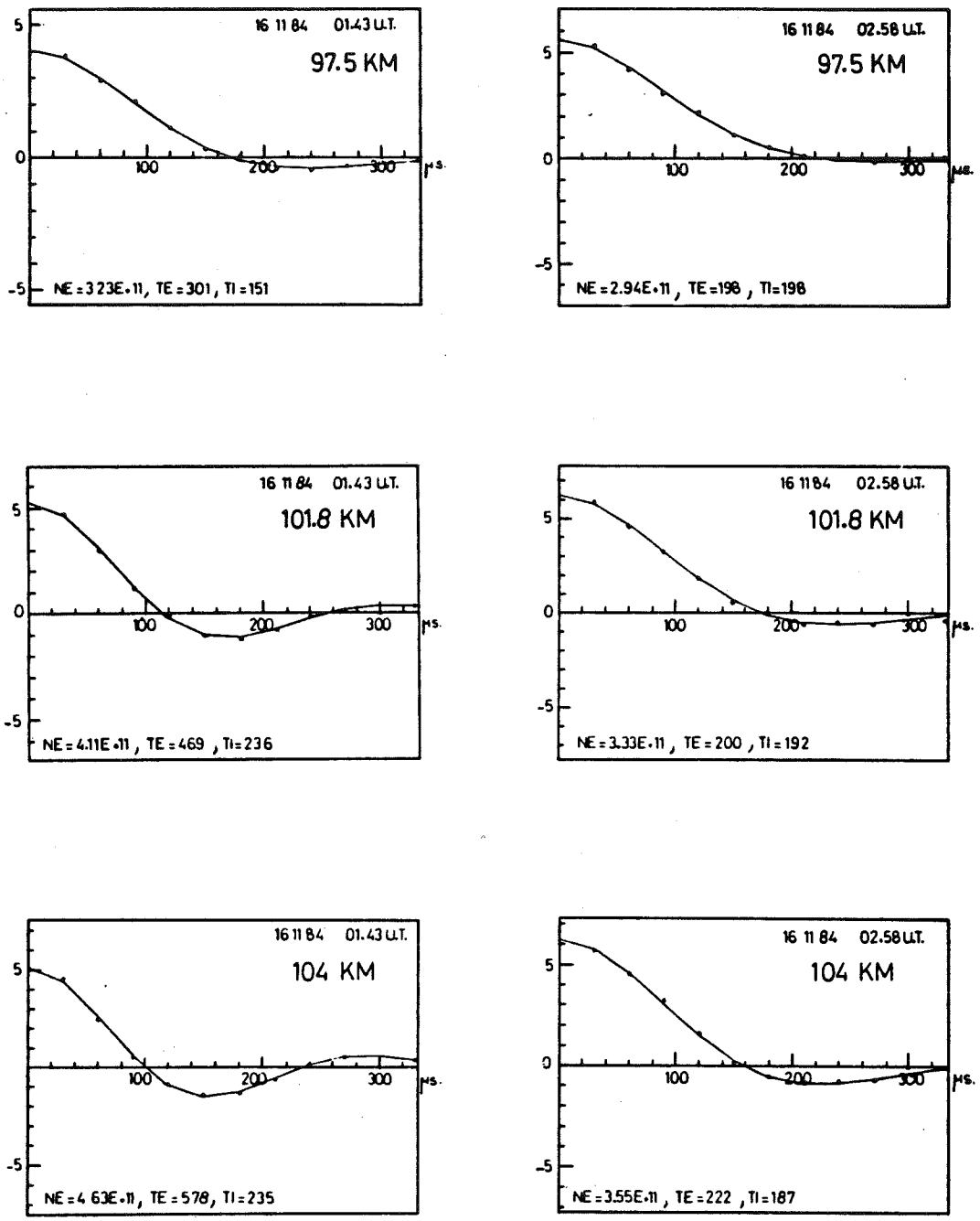


Fig. 7. The measured correlation functions for three altitudes at two different times. At 01.43 UT very strong anomalous heating was present.

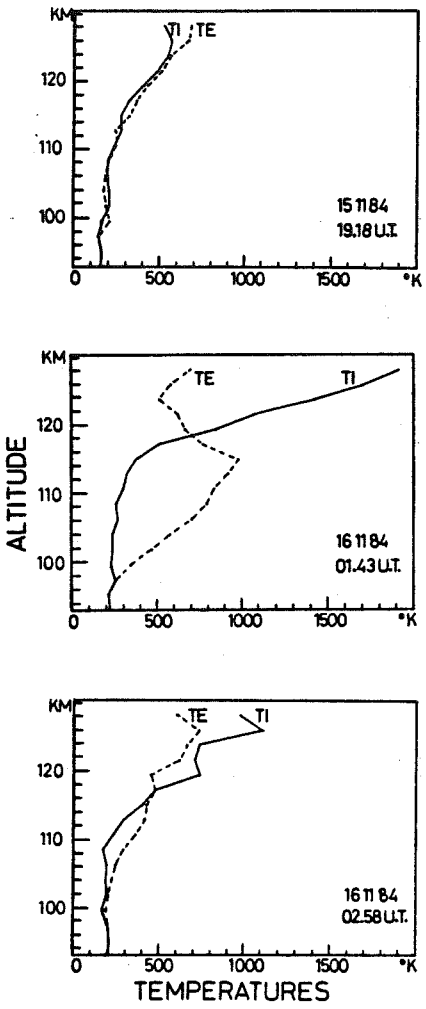


Fig. 8. Ion and electron temperature profiles for the different times. 19.18 UT, no anomalous heating; 01.43 UT, very strong anomalous heating; 02.58 UT, low anomalous heating.

Energy input by particle or Joule heating would have the opposite effect; we would estimate $T$ to be higher than it really is.

The only effect which could lead to an underestimate of neutral temperature is that the average ion mass in this altitude range was larger than 31 a.m.u., which is perhaps the case. Increasing the ion mass from 31 a.m.u. to 31.5 a.m.u. would increase the temperature by about 3K, which still maintains the observed temperature lower than the MSIS model.

The observed neutral mass is calculated from temperature and scale height. Because of the assumption of thermal equilibrium, we may underestimate the collision frequency at the highest altitudes and, in that way, underestimate the scale height (see Section 2). However, in this case the mass which we inferred from the measurements is still too large; the true mass would be lower. Therefore, we think that the scale heights are correctly determined. The fact that the mass is lower than the mass predicted by the model indicates that there is more atomic oxygen in the low thermosphere. In general, high latitude winter measurements indicate more atomic oxygen in the low thermosphere (WINNICK, 1983).

The observed temperature at 100 km and also the neutral mass are closer to Jacchia 71 model. The Chatanika radar measurements (LATHUILLERE *et al.*, 1983) also show a good agreement with this model.

In this paper we have also shown that anomalous heating can be present for a long period of time in the auroral ionosphere.

*Acknowledgements*—The EISCAT Scientific Association is supported by the Centre National de la Recherche Scientifique of France, Suomen Akatemia of Finland, Max-Planck Gesellschaft of the Federal Republic of Germany, Norges Almenvitenskapelige Forskningsråd of Norway, Natürvetenskapliga Forskningsrådet of Sweden and the Science and Engineering Research Council of the United Kingdom.

## REFERENCES


| | | |
|---|---|---|
| ALCAYDÉ D., FONTANARI J., KOCKARTS G., BAUER P. and BERNARD R. | 1979 | *Annls Géophys.* **35**, 41. |
| BANKS P. | 1979 | *J. geophys. Res.* **84**, 6709. |
| BANKS P. | 1977 | *J. atmos. terr. Phys.* **39**, 179. |
| FLÅ T., KIRKWOOD S. and SCHLEGEL K. | 1985 | *Radio Sci.* **20**, 785. |
| HEDIN A. E. | 1983 | *J. geophys. Res.* **88**, 170. |
| JACCHIA L. G. | 1971 | *Smithson. astrophys. Obs. Rep.* **332.** |
| JOHANSSON O., PERSSON K., SCHMIDT W. and TURUNEN A. L. | 1984 | EISCAT Technical Note 84/41, Kiruna, Sweden. |
| KOFMAN W. and LATHUILLERE C. | 1985 | *J. geophys. Res.* **90**, 3510. |
| LATHUILLERE C., WICKWAR V. B. and KOFMAN W. | 1983 | *J. geophys. Res.* **88**, 137. |
| REES M. H. | 1983 | *Solar Terrestrial Physics* (CAROVILLANO R. L. and FORBES J. M., Eds). D. Reidel, Dordrecht. |

| | | |
|---|---|---|
| SCHLEGEL K. and ST. MAURICE J. P. | 1981 | *J. geophys. Res.* **86,** 1447. |
| SCHLEGEL K., KOHL H. and RINNERT K. | 1980 | *J. geophys. Res.* **85,** 710. |
| ST. MAURICE J. P., SCHLEGEL K. and BANKS P. M. | 1981 | *J. geophys. Res.* **86,** 1453. |
| SCHUNK R. W. and WALKER J. C. | 1971 | *J. geophys. Res.* **76,** 6159. |
| SCHUNK R. W. and NAGY A. F. | 1978 | *Rev. Geophys. Space Phys.* **16,** 355. |
| TEPLEY C. A. and MATHEWS J. D. | 1978 | *J. geophys. Res.* **83,** 3299. |
| WALDTEUFEL P. | 1970a | *Planet. Space Sci.* **18,** 741. |
| WALDTEUFEL P. | 1970b | Thesis, Faculte des Sciences de Paris. |
| WICKWAR V. B., BARON M. J. and SEARS R. D. | 1975 | *J. geophys. Res.* **80,** 4364. |
| WICKWAR V. B., LATHUILLERE C., KOFMAN W. and LEJEUNE G. | 1981 | *J. geophys. Res.* **86,** 4721. |
| WINNICK J. R. | 1983 | *Solar Terrestrial Physics* (CAROVILLANO R. L. and FORBES J. M., Eds). D. Reidel, Dordrecht. |

# ARTICLE 3

*Radio Science*, Volume 18, Number 6, Pages 887–893, November–December 1983

# Direct measurements of ion composition with EISCAT in the high-latitude $F_1$ region

*C. Lathuillere, G. Lejeune, and W. Kofman*

*Centre d'Etudes des Phénomènes Aléatoires et Géophysiques*

(Received September 17, 1982; accepted April 18, 1983.)

We present a method for obtaining $O^+$ relative abundance directly from the autocorrelation functions measured by EISCAT; no assumption is made regarding the temperatures. Results of $O^+$ relative abundance and temperatures obtained simultaneously are shown for a 20-hour period on May 9, 1982, and the time variations of $O^+$ relative abundance are compared to previous work.

## INTRODUCTION

Recent studies of the high-latitude ionosphere have shown important variations of the relative abundance of molecular ions ($O_2^+$ and $NO^+$) and atomic oxygen ions at altitudes ranging from 150 km to 350 km. *Sojka et al.* [1981] have made theoretical predictions of ion composition in the high-latitude winter $F$ region using a plasma convection model; they found that the $O^+$ density percentage can vary from 10% to 90% at 200 km altitude over a 24-hour period.

The experimental approach of *Kelly and Wickwar* [1981] to deduce ion composition from incoherent scatter results shows large variations of the composition correlated with auroral joule heating and particle precipitation; their work is an adaptation and extension of the methods used at mid-latitudes [*Moorcroft*, 1964; *Petit*, 1968; *Evans and Cox*, 1970; *Wand and Perkins*, 1970; *Alcaydé et al.*, 1974]: assumptions are made about ion or electron temperatures in order to deduce the ion composition.

In this paper we present ion composition measurements from European Incoherent Scatter Facility (EISCAT) data, deduced directly from the incoherent scatter autocorrelation function. After the description of the method we show the $O^+$ abundance obtained during the EISCAT experiment performed May 9, 1982, and discuss the implications of a nonconstant composition for electron and ion temperatures deduced from incoherent scatter measurements. Then we show that the large variations of $O^+$ relative abundance that we measure are consistent with previous work.



Paper number 3S0611.
0048-6604/83/1112-0611$08.00

## DESCRIPTION OF THE METHOD

The incoherent scatter technique allows the determination of several ionospheric parameters: the electron density $N_e$, the ion velocity $V_L$, and the electron and ion temperature $T_e$ and $T_i$, but also the ion to neutral collision frequency $\nu_{in}$ at low altitudes and the ion composition $p$ ($p = 1 - [O^+]/N_e$) can be deduced from measurements of the autocorrelation function (ACF) of the received signal [*Salpeter*, 1960; *Rosenblut and Rostoker*, 1962; *Dougherty and Farley*, 1963].

These parameters are obtained by a nonlinear least squares fitting procedure on the measured ACF [*Waldteufel*, 1970; *Wickwar*, 1974; *Lejeune*, 1978] which minimizes the least square distance (chi square) between the theoretical ACF and the measured one. The method of analysis that we use for EISCAT measurements is described by *Lejeune* [1979, 1982] (see also *De la Beaujardière et al.* [1980]); the routine allows us to search simultaneously for all parameters which enter into the construction of the theoretical ACF. In particular, in the $F_1$ region one can ask for a fit on $T_i$, $T_e$, and $p$ in addition to the parameters $N_e$ and $V_L$. However, because the measured ACF's are noisy, the usual fitting procedure on $T_i$, $T_e$, and $p$ often fails, and one of the three parameters must be assumed: usually $p$ is fixed. But if the initial values chosen for the fit are not too far from the solution and if the data are integrated long enough (of the order of 5 min), the fit on the five parameters $N_e$, $V_L$, $T_i$, $T_e$, and $p$ can succeed.

The method that we use in order to find our initial values close enough to the solution is as follows: we make several fits on the measured ACF with fixed composition ranging from only molecular ions (ion

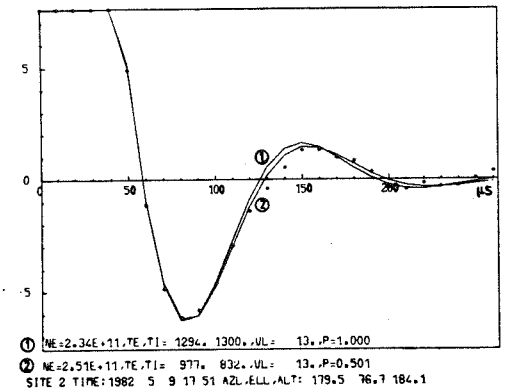


Fig. 1. Experimental autocorrelation function (ACF) measured on May 9, 1982, at 1751 UT and 184 km altitude (in diamonds) and corresponding theoretical ACF: curve 1 is the result of the fit made with a fixed composition ($p = 1.$), and curve 2 is the result of the fit on all parameters including the composition $p$.

mass = 30.5, which means a mixture of 75% $NO^+$ and 25% $O_2^+$) to only $O^+$ ions; the fit outputs for each assumed composition are the ionospheric parameters $N_e$, $V_L$, $T_i$, and $T_e$ but also the reduced chi square parameter (VAR). The parameters corresponding to the minimum value of VAR are the closest ones to the solution and are chosen as initial values.

Then a new fit is performed on all five parameters including $p$. Figure 1 shows the result of this fit compared to a fit made with a fixed composition; the measured ACF displayed with diamonds corresponds to the May 9, 1982, experiment at Tromsø, at 1751 UT and 184 km altitude. The integration time is 5 min. Curve 1 is the theoretical ACF obtained by a fit made with a fixed composition (here only molecular ions). The corresponding ionospheric parameters are given in the figure. Curve 2 corresponds to the fit made with a nonfixed composition: one obtains 50.1% of molecular ions with an uncertainty of 11%.

This figure shows clearly that curve 2 is a better fit on the measured ACF than curve 1. It is a typical example of May 9 measurements.

Now, an additional difficulty arises from the fact that there are often two minima in VAR, very close to each other, occurring for values of $p$ approximately symmetric with respect to 0.5. This is obviously true when there is only one ion which can be either $O^+$ or a heavy ion, if the thermal velocity is the same ($T_i/m_i$ = const). This proves also to be true in the case of a two-ion mixture. So when minima are found in variance, the corresponding two sets of initial values are used for the final fits, and two possible values of the composition are then obtained for each ACF. These two sets of ionospheric parameters resulting from the last two fits are kept as possible results. The choice between the two sets of data is made automatically afterward, when all the ACF's are reduced: one makes the chosen composition values, when plotted versus altitude, fit the smoothest curve between 0 and 1 among all the possibilities ($2^N$ where $N$ is the number of signal gates for which composition is determined).

The method has been used for the experiment presented below, with a postintegration time of 5 min, in order to get reasonable accuracy.

## RESULTS

In order to determine the ion composition, we have used the EISCAT common program experiment of May 9, 1982. During this experiment, which lasted for almost 21 hours, the pulse length was 360 μs, and the Tromsø antenna was in a fixed position along the magnetic field line. It was thus possible to make a postintegration of the autocorrelation function as long as one wanted. We show in Plate 1 the results of the usual data reduction performed with a time independent composition in the $F_1$ region (Figure 2 displays the model used between 110 km and 250 km altitude, i.e., the auroral ionosphere model from *Wickwar* [1974]. The integration time of the data is 1 min.

The electron density (bottom panel) and the ion temperature (top panel) are displayed as a function of time (on the $X$ axis) and altitude (on the $Y$ axis). The color scale corresponds to the magnitude of each parameter. This figure gives an overview of the experiment which shows at the same time diurnal variations and auroral phenomena.

The electron density shows clearly diurnal variations: there is a decrease of the maximum of the $F_2$ layer between 2100 UT (i.e., 2200 hours in local time) and 0200 UT. Manifestation of the auroral phenomena can be seen in the electron density and the ion temperature: at 1930 UT one can notice a strong precipitation event, and the increase of the ion temperature at all altitudes around 2200 UT is an indication of large Joule heating.

The ion composition obtained during this period is presented in Plate 2. The color scale indicates the percentage of $O^+$ ions between 130 km and 300 km altitude (black means only molecular ions and red only $O^+$ ions). The ion compositions obtained at six

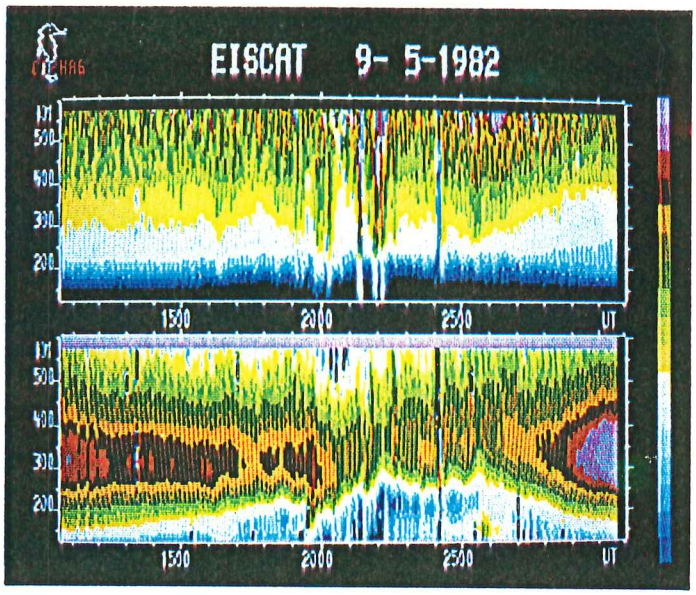


Plate 1. Electron density (bottom panel) and ion temperature (top panel) measured on May 9, 1982, as a function of time and altitude. Logarithmic color scale from $10^{11}$ el/m$^3$ to $1.6 \times 10^{12}$ el/m$^3$ for $N_e$ and linear color scale from 500 K to 2500 K for $T_i$.

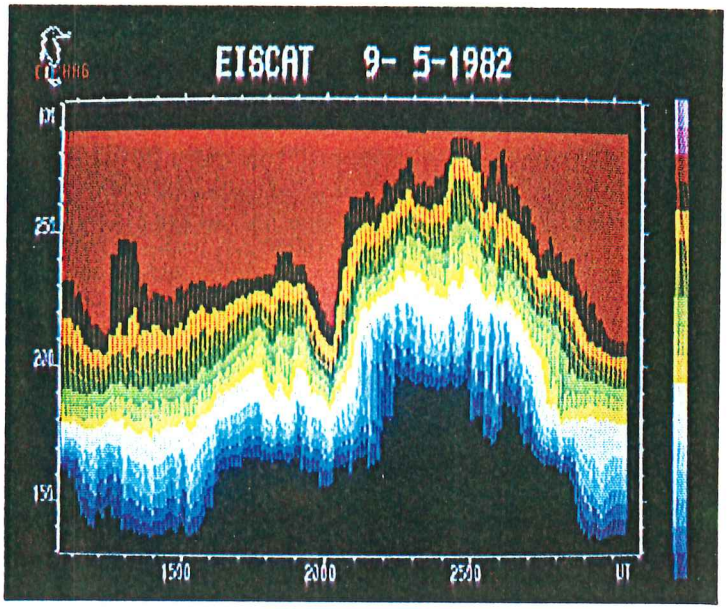


Plate 2. Measured ion composition on May 9, 1982, as a function of time and altitude. Linear color scale from 0% $O^+$ ions in black to 100% $O^+$ ions in red.

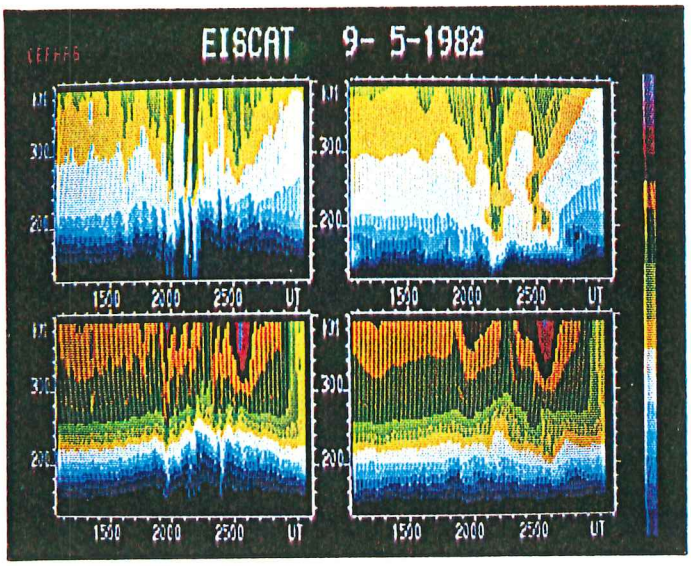


Plate 3. Electron and ion temperature (bottom and top panels, respectively) measured on May 9, 1982, as a function of time and altitude. The left panels correspond to the temperatures obtained with the composition model shown in Figure 2, and the right panels correspond to the temperatures obtained simultaneously to the composition shown in Plate 2. Linear color scale from 500 K to 2000 K for $T_i$ and 500 K to 3000 K for $T_e$.

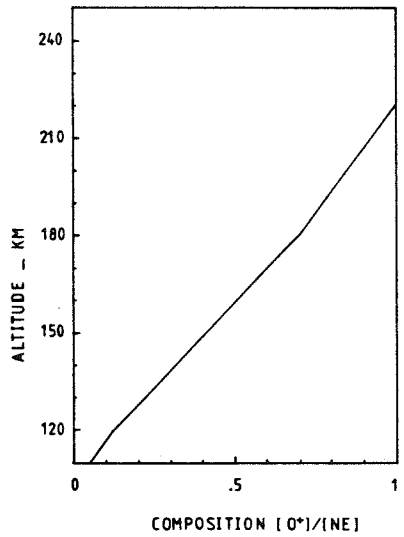


Fig. 2. Ion composition model used in the usual EISCAT data analysis.

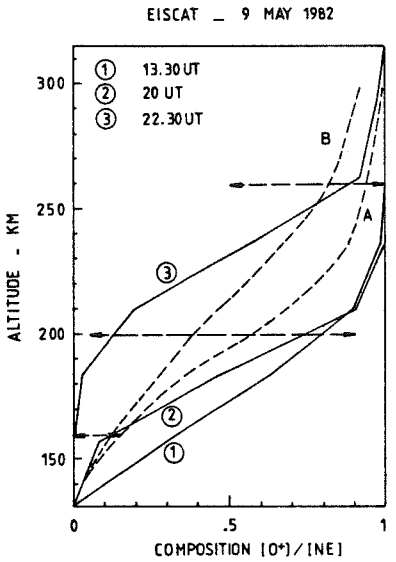


Fig. 3. Curves 1, 2, and 3 are typical ion composition profiles obtained on May 9, 1982. Curves A and B correspond to the profiles of *Kelly and Wickwar* [1981], and the horizontal dashed lines show the variations of $O^+$ composition obtained by *Sojka et al.* [1981].

altitudes have been averaged over 1 hour. The mean standard deviation of the 5-min integrated data lies between 15% and 20% depending on the altitude.

This figure shows an important time variation of the composition. Between 2200 and 0100 UT, when the electron density is low, there are almost no $O^+$ ions below 190 km. On the contrary, in the middle of the day, around 1200 UT, there are already 70% of $O^+$ ions at the same altitude. Between 1930 UT and 2030 UT one can see an increase of the percentage of $O^+$ ions above 180 km; this occurs at the time of the strong precipitation event. Moreover, the sharp increase of molecular ions below 200 km altitude at 2200 UT occurs at the time of joule heating.

Plate 3 shows the temperatures obtained the same day still as a function of time and altitude. On the left side are displayed the electron and ion temperatures (bottom and top panels, respectively) corresponding to the composition model displayed in Figure 2, and on the right side, the temperatures obtained simultaneously to the composition presented in Plate 2. The temperatures displayed on the right side have been averaged over 1 hour like the composition. The effect of this averaging can be seen above 300 km altitude where in both cases the composition is only $O^+$ ions.

This plate shows clearly the effect of the composition on temperatures deduced from incoherent scatter measurements; at low altitudes, particularly below 220 km, the temperatures obtained with a nonfixed composition (right panels) are less variable than the temperature obtained with a fixed composition, and slightly larger. For example, the increase of $T_i$ between 1930 UT and 2000 UT (which is the time of the precipitation event) almost disappears at low altitudes when one allows the composition to vary; but the increase of $T_i$ around 2200 UT is still important and corresponds to real joule heating.

## DISCUSSION AND CONCLUSION

For obtaining the composition from Chatanika data, *Kelly and Wickwar* [1981] assume a continuous and smooth time evolution of temperatures, particularly of $T_e$ before and after joule heating events. The same temperature behavior is obtained directly by our data analysis.

In order to make a more detailed comparison with other work we present in Figure 3 three typical ion composition profiles obtained during the 20-hour period shown above.

Profile 1 corresponds to 1330 UT, profile 2 is the profile at 2000 UT (corresponding to the increase of $O^+$ ions during the precipitation event), and profile 3 is that at 2230 UT in the night (just after Joule heating). These three profiles give an idea of the maximum variations of the composition over the period of measurements.

The model composition profiles from *Kelly and*

*Wickwar* [1981] showing the effect of diurnal variations and auroral phenomena on the $O^+$ composition are shown by dashed curves in Figure 3. Profile A corresponds to a quiet day or enhanced precipitation period, and profile B to a quiet night or Joule heating period.

These two curves are very close to each other below the altitude of 180 km. On the contrary our profiles can be very different even at low altitudes.

However, the difference between profiles 3, and 1 and 2 are in the same direction as the differences between the B and A profiles: at a given altitude there are more molecular ions during night or Joule heating than during the day or precipitations.

The three horizontal dashed lines in Figure 3 show the variations of the $O^+$ composition obtained by *Sojka et al.* [1981]. These variations are theoretical predictions of the composition over the site of EISCAT during a 24-hour period in winter. At low altitude the variations that we measure are larger than those obtained by Sojka et al., but at higher altitude they are quite similar.

A reason for the disagreement at lowest heights could possibly be found in our large integration volume: the pulse length used for these data is 360 s, corresponding to an altitude integration of 54 km. This large integration volume could lead to systematic errors in the composition, particularly at the lowest altitudes, where $O^+$ variations could be overestimated.

One must notice also that the different curves presented in Figure 3 correspond to different diurnal and seasonal conditions, leading to different behaviors of the ion composition, especially at low altitude.

We have presented the variations of ion composition measured by EISCAT over a 20-hour period. These variations are very important: at 200 km the ion composition can change from a majority of molecular ions (85%) to a majority of atomic oxygen ions (90%). However, we have shown that these large variations are not unexpected and that they are in the same direction as the variations observed over Chatanika by *Kelly and Wickwar* [1981].

The aim of this work was to prove the feasibility of direct measurements of ion composition in the $F_1$ region from EISCAT measurements, and we believe that our results are significant enough for this purpose.

However, there are still some questions that arise from our data and that we hope to be able to answer in the future when more EISCAT data will be available. In particular, we would like to make a clear distinction between the effects of diurnal variations and the effects of auroral heating on the ion composition. For that purpose it will be necessary to obtain ion composition with a time resolution much less than 1 hour; indeed, the long averaging used probably underestimates the effects of precipitation and Joule heating on ion composition.

Direct measurements of ion composition in the $F_1$ region by incoherent scatter radars means also reliable temperature measurements in this region; this is new and quite important for the study of the thermal structure of the high-latitude ionosphere and lower thermosphere.

*Acknowledgments.* The authors thank the EISCAT staff members for their help in making the EISCAT system operational and for their considerable effort leading to the first EISCAT observations. The EISCAT is supported by Centre National de la Recherche Scientifique (France), Suomen Akatemia (Finland), Max-Planck Gesellschaft (West Germany), Norges Almenvitenskapelige Forskningsrad (Norway), Naturevetenskapliga Forskingsradet (Sweden), and Science Research Council (United Kingdom).

## REFERENCES

Alcaydé, D., P. Bauer, and J. Fontanari, Long-term variations of thermospheric temperature and composition, *J. Geophys. Res.*, *79*, 629–637, 1974.

De la Beaujardière, O., V. Wickwar, C. Leger, M. McCready, and M. Baron, The software system for the Chatanika incoherent scatter radar, technical report, SRI International, Menlo Park, Calif., 1980.

Dougherty, J. P., and D. T. Farley, Jr., A theory of incoherent scattering of radio waves by a plasma, 3, Scattering in a partly ionized gas, *J. Geophys. Res.*, *68*, 5473–5486, 1963.

Evans, J. V., and L. P. Cox, Seasonal variation of the $F_1$ region ion composition, *J. Geophys. Res.*, *75*, 159–164, 1970.

Kelly, J., and V. B. Wickwar Radar measurements of high-latitude ion composition between 140 and 300 km altitude, *J. Geophys. Res.*, *86*, 7617–7626, 1981.

Lejeune, G., EISCAT data analysis, *Rapp. 36/78*, Centre d'Etud. des Phénomènes Aléatoires et Géophys., St-Martin-d'Hères, France, 1978.

Lejeune, G., A program library for incoherent scatter calculation, *Tech. Note 79/18*, EISCAT, Kiruna, Sweden, 1979.

Lejeune, G., EISCAT data analysis package, EISCAT technical note, Eur. Incoherent Scatter Assoc., Kiruna, Sweden, 1982.

Moorcroft, D. R., On the determination of temperature and ionic composition by electron backscattering from the ionosphere and magnetosphere, *J. Geophys. Res.*, *69*, 955–970, 1964.

Petit, M., Mesures de températures, de densité électronique et de composition ionique dans l'ionosphère par diffusion de Thomson. Etude du déséquilibre thermodynamique dans l'ionosphère diurne, *Ann. Geophys.*, *24*, 1–37, 1968.

Rosenblut, M. N., and N. Rostoker, Scattering of electromagnetic waves by a non equilibrium plasma, *Phys. Fluids*, *5*, 776, 1962.

Salpeter, E. E., Electron density fluctuations in a plasma, *Phys. Rev., 120*, 1528, 1960.

Sojka, J. J., W. J. Raitt, and R. W. Schunk, Theoretical predictions for ion composition in the high-latitude winter *F* region for solar minimum and low magnetic activity, *J. Geophys. Res., 86*, 2206–2216, 1981.

Waldteufel, P., Une étude par diffusion incohérente de la haute atmosphère neutre, thèse de doctorat d'état, Fac. des Sci., Univ. de Paris, 1970.

Wand, R. H., and F. W. Perkins, Temperature and composition of the ionosphere: Diurnal variations and waves, *J. Atmos. Terr. Phys., 32*, 1921–1943, 1970.

Wickwar, V. B., Analysis techniques for incoherent scatter data interpretation in the 100 to 300 km region, technical report, Stanford Res. Inst., Menlo Park, Calif., 1974.

C. Lathuillere, G. Lejeune, and W. Kofman, Centre d'Etudes des Phénomènes Aléatoires et Géophysiques, BP 46, 38402 Saint-Martin-d'Hères, France.

# ARTICLE 4

*Journal of Atmospheric and Terrestrial Physics*, Vol. 48, Nos 9–10, pp. 857–866, 1986.
Printed in Great Britain.

0021–9169/86 $3.00 + .00
Pergamon Journals Ltd.

# Incoherent scatter measurements in the *F*1-region

C. LATHUILLERE, W. KOFMAN and B. PIBARET
CEPHAG, INPG/IEG, UA 346, BP46, 38402 St Martin d'Hères Cedex, France

(*Received for publication* 21 *April* 1986)

**Abstract**—In the *F*1-region, temperature and ion composition measurements at EISCAT are usually obtained with a transmitted pulse of 360 $\mu$s, corresponding to a diffusive volume much larger than the ionospheric scale height. A special correlator program has been used in order to estimate the errors due to the smearing effect of the diffusive volume. We show that these errors can be as large as 50% in electron temperature and 20% in ion temperature and that they depend on electron density gradients in the diffusive volume. From ion composition results, we deduce that the transition altitude between molecular ions and oxygen ions is correctly estimated when using a 360 $\mu$s pulse, and that a diffusive volume of the order of $\pm$25 km would be good for obtaining correct composition values above 200 km altitude.

## 1. INTRODUCTION

A special French program has been run on the EISCAT facility (FOLKESTAD *et al.*, 1983) three times in 1985 in order to make a quantitative estimation of the error introduced in ionospheric parameters in the *F*1-region due to the diffusive volume.

Indeed, in this region measurements are usually made with the normal correlator program (FARLEY, 1969) working with a 360 $\mu$s pulse. The corresponding range integration is $\pm$54 km, counted from the altitude of the center of the diffusive (scattering) volume, which is much larger than the scale height of the ionospheric parameters in the *F*1-region where, among other things, the composition changes from only molecular ions in the *E*-region to oxygen ions in the *F*2-region.

The multipulse technique used in the special French experiments and common programs provides a very small range integration ($\pm$3 km or $\pm$2.25 km), but does not allow measurements higher than 135 km (KOFMAN and LATHUILLERE, 1985). In order to provide good measurements in the *F*1-region, it is thus necessary to find a new type of experimental scheme (including correlator program) providing a range integration of the order of 10–20 km.

The aim of our experiments was not to test a new experimental scheme, but only to give quantitative information concerning the validity of the measurements obtained with the normal programs. We have used a correlator program which computes from the same signal two kinds of autocorrelation functions (ACF): the 'normal' ones corresponding to the range integration of $\pm$54 km and the 'special' ones whose range integration was only $\pm$27 km. This correlator program will be presented in the first part of the paper.

Comparisons between ionospheric parameters deduced from the normal ACF and the special ones are then presented. Large differences of electron and ion temperatures at altitudes up to 250 km are outlined. It is shown that these differences depend on the state of the ionosphere (presence or not of the *E*-region) and can be as large as 200K in $T_e$ and 50K in $T_i$.

The results on ion composition obtained during the three experimental days show that only the transition altitude between molecular ions and oxygen ions is correctly estimated when using the normal ACF.

We also add a comparison of Tromsø composition measurements obtained on 15 July 1985 and results obtained at the Kiruna receiving station from different altitudes ranging from 200 to 320 km.

## 2. MEASUREMENT TECHNIQUE: THE CORRELATOR PROGRAM

The emission scheme of the experiment is composed of two pulses: one of 60 $\mu$s to measure the power profile and one of 360 $\mu$s to measure the autocorrelation functions.

The received signal corresponding to the frequency of the 360 $\mu$s pulse is sampled at the usual rate of 10 $\mu$s and the correlator program performs two kinds of ACF computations.

If one calls $x_1, x_2 \ldots x_{36}$ the samples corresponding to the signal scattered from altitudes centered around $z_0$ (see Fig. 1), the lag $k$ of the 'normal' ACF is calculated [in 'the usual' way] as (FARLEY, 1969)

$$\sum_{i=1}^{36-k} x_i \cdot x_{i+k}, \quad k = 0, 1, 2, \ldots, 35.$$

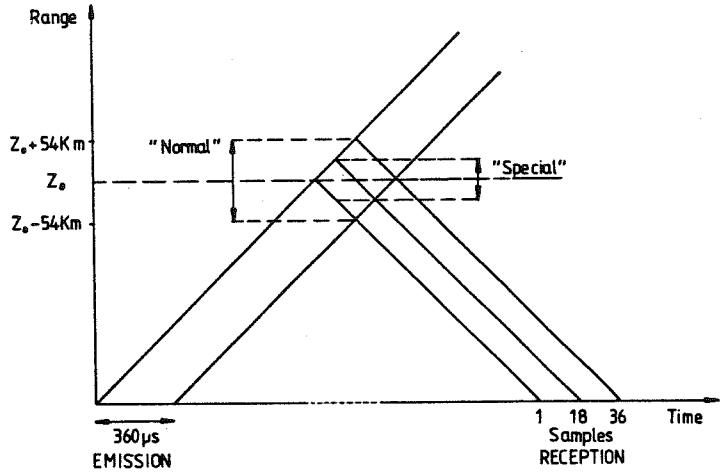


Fig. 1. Experimental scheme indicating the diffusive volume corresponding to the normal ACF calculation and the special ACF calculation.

For the 'special' ACF computation no summation is done and each lag corresponds to only one product. The lags of the ACF centered at the same altitude $z_0$ are obtained by

$$x_{18-k/2}^{*}x_{18+k/2}, \quad k=0,2,4,6\ldots$$

and

$$x_{18-(k-1)/2}^{*}x_{18+(k+1)/2}, \quad k=1,3,5\ldots$$

One can see in Fig. 1 that the special ACF computation leads to a range integration which is half of the range integration corresponding to the normal ACF.

ACFs are calculated with a first gate centered at 106 km and a gate interval of 27 km, which means an overlapping of the diffusive volumes corresponding to two successive gates. It is evident from the computation of the two kinds of ACF that the measurement error of the special ones is much larger than on the normal ones (roughly $\sqrt{36-k}$ times larger, for the lag $k$). This implies that if one wants to obtain the same accuracy of the ionospheric parameters, it will be necessary to post-integrate the special ACF much longer than the normal ACF.

However, we have preferred to use the same post-integration time of 5 min for both sets of ACF in order to obtain comparable ionospheric parameters.

### 3. EXPERIMENTAL CONDITIONS

Three EISCAT experiments of the special program have been analysed up to now: 15–16 February 1985, from 14.00 UT to 02.00 UT, 17–18 April 1985, from 16.00 UT to 01.00 UT and 15 July 1985, from 08.00 UT to 19.30 UT. For each experiment the two kinds of autocorrelation functions have been integrated during 5 min, leading to much more noisy results when deduced from the 'special' ACF. The ACF are, in a first step, analysed with a fixed composition model deduced from LATHUILLERE and BREKKE (1985) (shown in Fig. 8), in order to compare the ion and electron temperatures. Then one tries to fit also for ion composition, using the method described in LATHUILLERE *et al.* (1983).

In order to have an overall view of the experiment, we show the electron density deduced from the power profile (and temperature corrections obtained from the 'normal' ACF). These densities are presented in Fig. 2 with a logarithmic grey scale, as a function of universal time and altitude. The February and April days show the same behaviour in the *E*-region, with an *F*2-region present at the beginning of the experiment but vanishing later, and some strong precipitation leading to a sharp *E*-region in the middle of the night. The July day is a quiet summer day with high electron density. The maximum of the *F*2-region is around 260 km and one can see some structures which look like gravity waves (BERTIN *et al.*, 1983).

Because the densities are higher on the April day than on the February day, we have chosen to present ion and electron temperatures only for the April day, in addition to the July day, which is very different. Ion composition results will be shown for the three days.

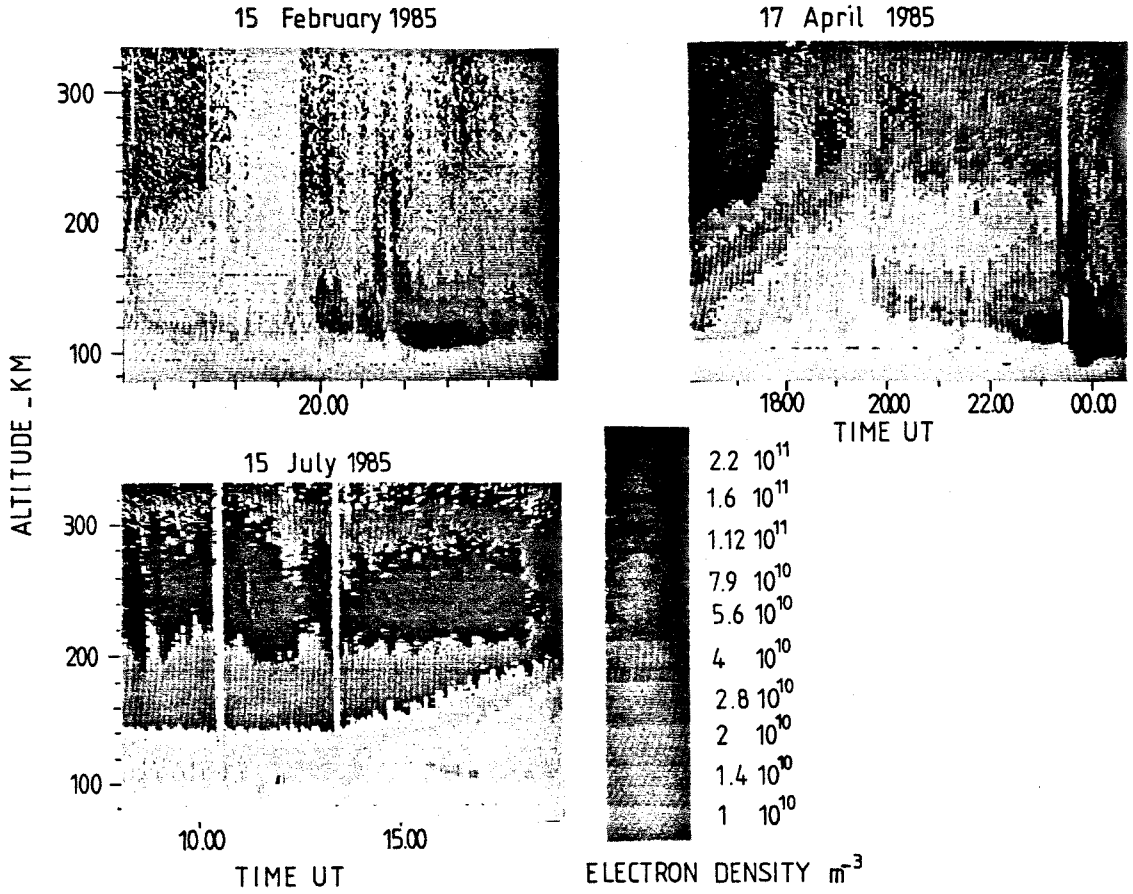


Fig. 2. Electron density on the three experimental days, as a function of time and altitude.

## 4. ION AND ELECTRON TEMPERATURE COMPARISONS

Examples of ion and electron temperatures measurements at different altitudes are presented for two experimental days in Fig. 3–6. 17 April 1985 is an example of night data with important variations of both $T_e$ and $T_i$ (Figs. 3 and 4, respectively). The left part of each figure shows the measurements obtained from the normal ACF (line) and from the special ones (crosses), as a function of time, and on the right part of each figure we show the corresponding relative difference between the two sets of data.

In Fig. 3 one sees that the normal ACFs underestimate the electron temperature (by comparison with the special ones) at the two lowest altitudes presented: 133 km and 159 km. This underestimate can be as large as 50%, as at 133 km after 0.00 UT. This

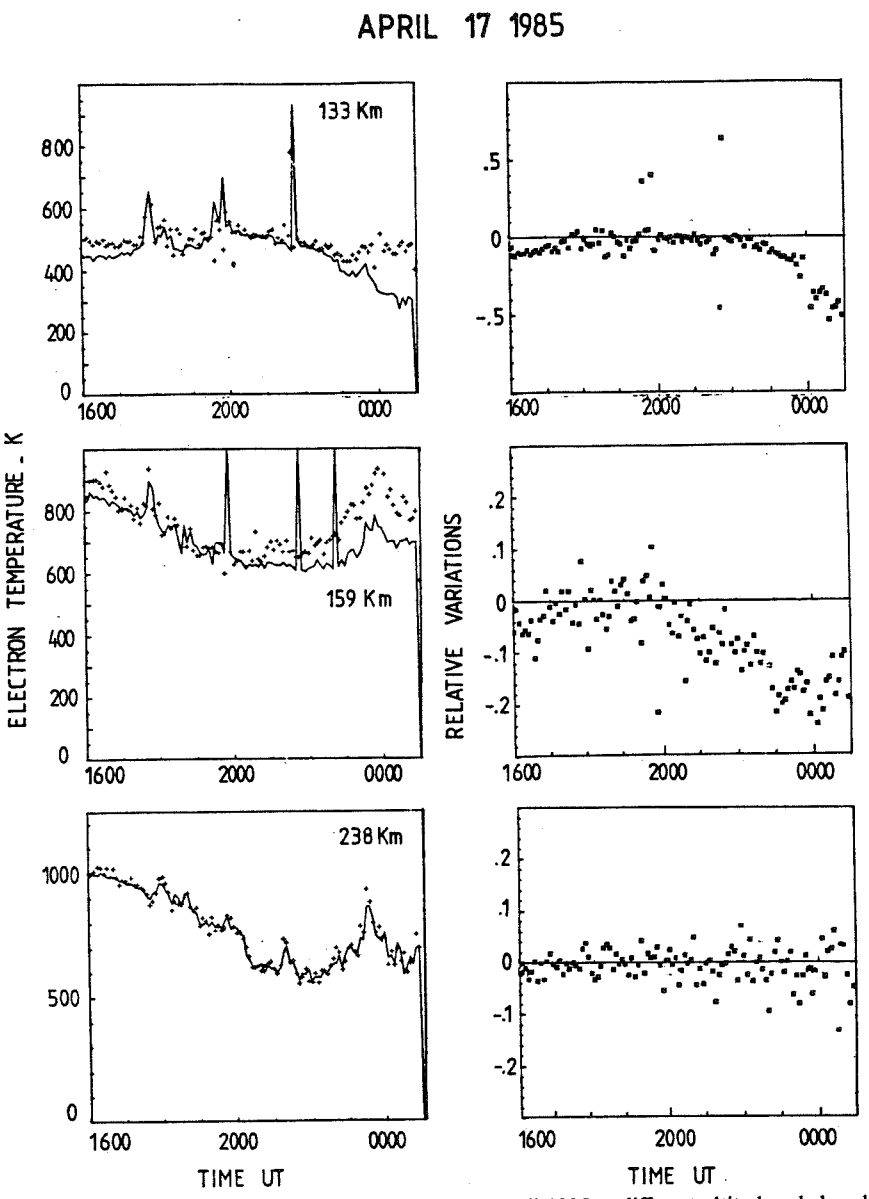


Fig. 3. Electron temperature as a function of time on 17 April 1985 at different altitudes, deduced from normal ACF (plain line) and special ACF (+), and the corresponding relative variations (a positive value means that results from normal ACF are larger than from special ACF).

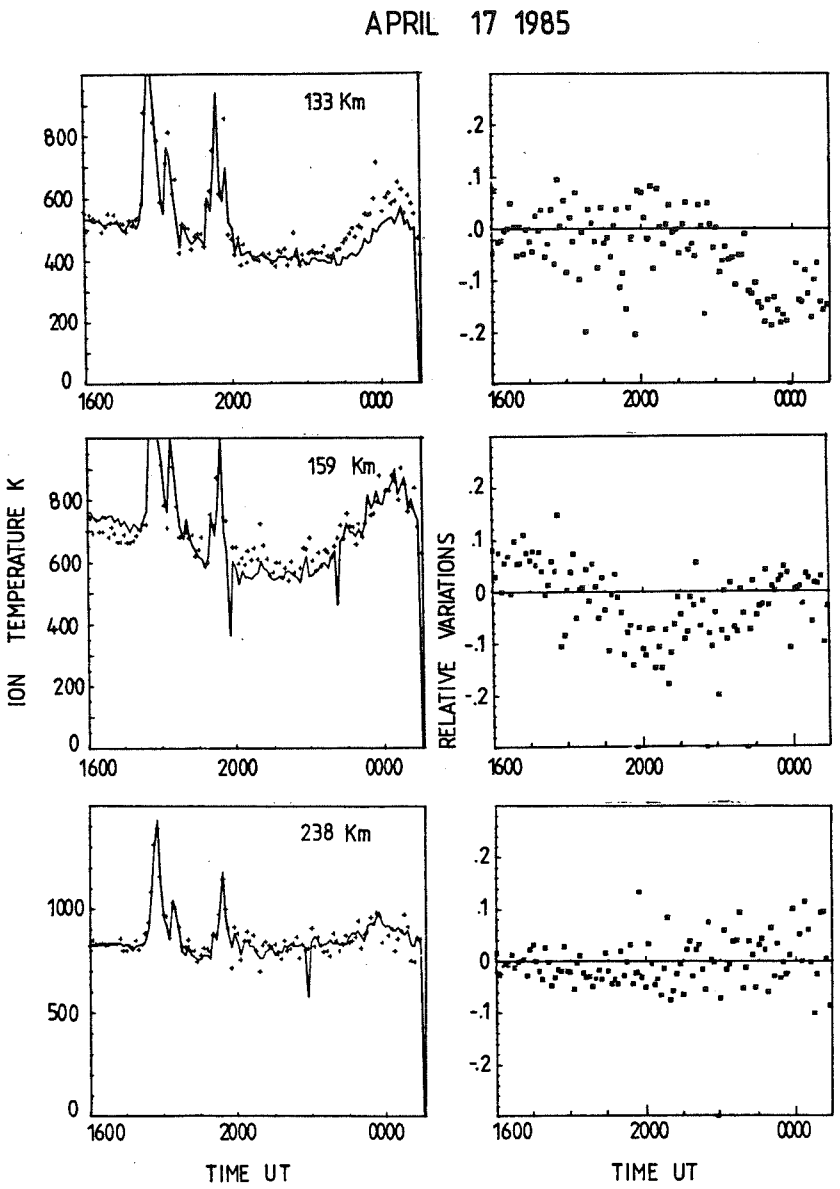


Fig. 4. As Fig. 3, but for ion temperature on 17 April 1985.

depends on the electron density profile: at this time, there is a large precipitation event leading to a sharp *E*-region (see Fig. 2). In the evening, around 20.00 UT, the ionosphere is quieter and both kinds of ACF give the same electron temperature results.

At 16.00 UT, when the maximum of electron density occurs in the *F*-region, $T_e$ is also underestimated, but only by about 10% at 133 km and 5% at 159 km. At 238 km and above the two kinds of ACF lead to the same electron temperature values, on average, meaning that the smearing effect due to the diffusive volume is not very large.

In Fig. 4, which presents ion temperature results at the same three altitudes, the differences between normal and special ACF results are smaller. They never exceed 20%. The other important feature is the direction of the difference: underestimate of $T_i$ measured by the normal ACF around 0.00 UT at 133 km, but overestimate around 16.00 UT at 159 km. Even at the same altitude, $T_i$ can be overestimated or

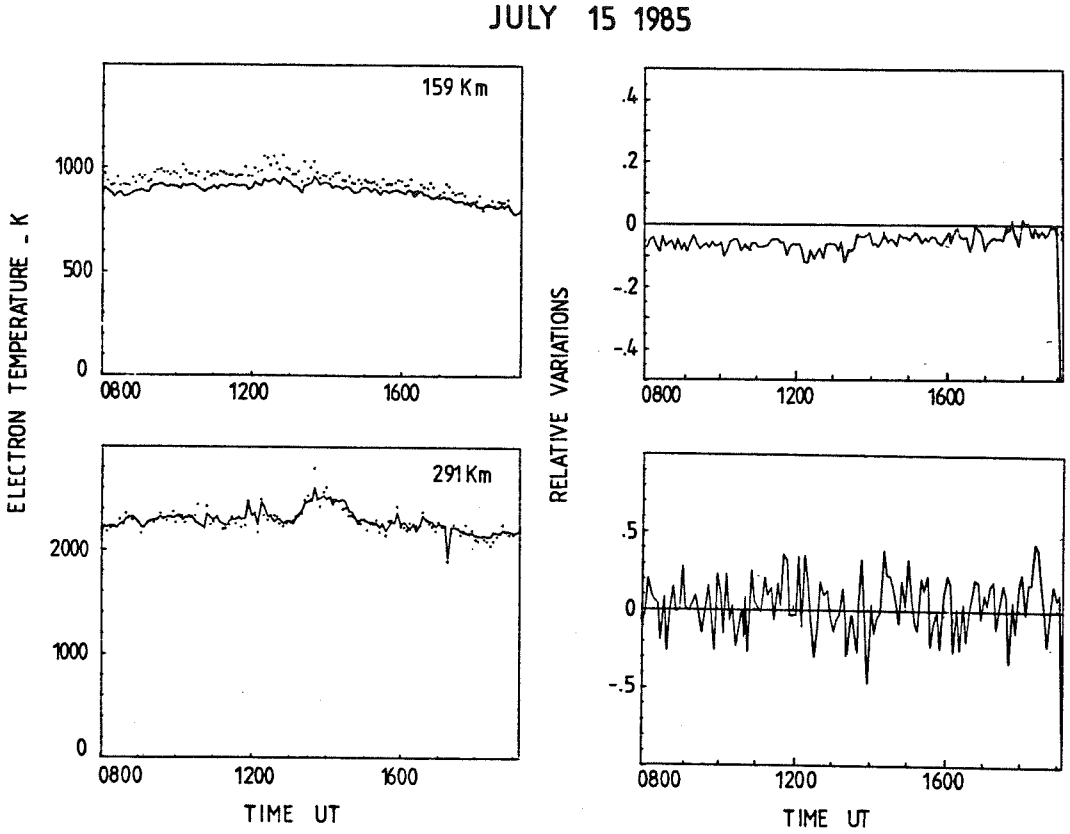


Fig. 5. As Fig. 3, but for electron temperature on 15 July 1985.

underestimated, depending on the electron density profile (+10% at 16.00 UT and −10% around 20.00 UT, at 159 km altitude).

At 238 km, as for $T_e$, no difference exists between the two sets of data, on average.

15 July 1985 is a quiet summer day with small ion and electron temperature variations throughout the experiment, and differences between the two kinds of measurements are almost constant during the day (Figs. 5 and 6). At 159 km altitude $T_e$ from normal ACF is underestimated by less than 10% and $T_i$ is overestimated by about 5%. Above 238 km for $T_i$, but only above 291 km for $T_e$, both kinds of ACF give the same results.

Electron and ion temperature profiles are displayed in Figs. 7 and 8, respectively. Two typical profiles have been chosen for the April day: around 24.00 UT, when a sharp *E*-region is present, and between 16.00 and 17.00 UT, when the density of the *F*2-region is important. Because we have seen that the electron and ion temperatures on 15 July have only small variations and that the differences between results from the normal and special ACF are constant during the day, we have chosen to present the averaged temperature profiles over the whole July experiment.

On the three temperature profiles one sees that the electron temperature is underestimated when deduced from the normal ACFs. This underestimate is more important in the case of a strong *E*-region (200K at 160 km). In all cases electron temperatures are, however, correctly estimated at altitudes above 250 km.

The situation is less dramatic for ion temperature. One can see that the error of estimation never exceeds 50K (except for the altitude of 106 km) and that above 200 km the measurements are correct. However, it is difficult to know *a priori* if one overestimates or underestimates the ion temperature. One has to know where the maximum of electron density is. On our data one sees that if this maximum is above the altitude of measurement (*F*2-region) the ion temperature is overestimated, but if it is under the altitude of measurement (*E*-region) the ion temperature is underestimated. This behaviour seems to be a general

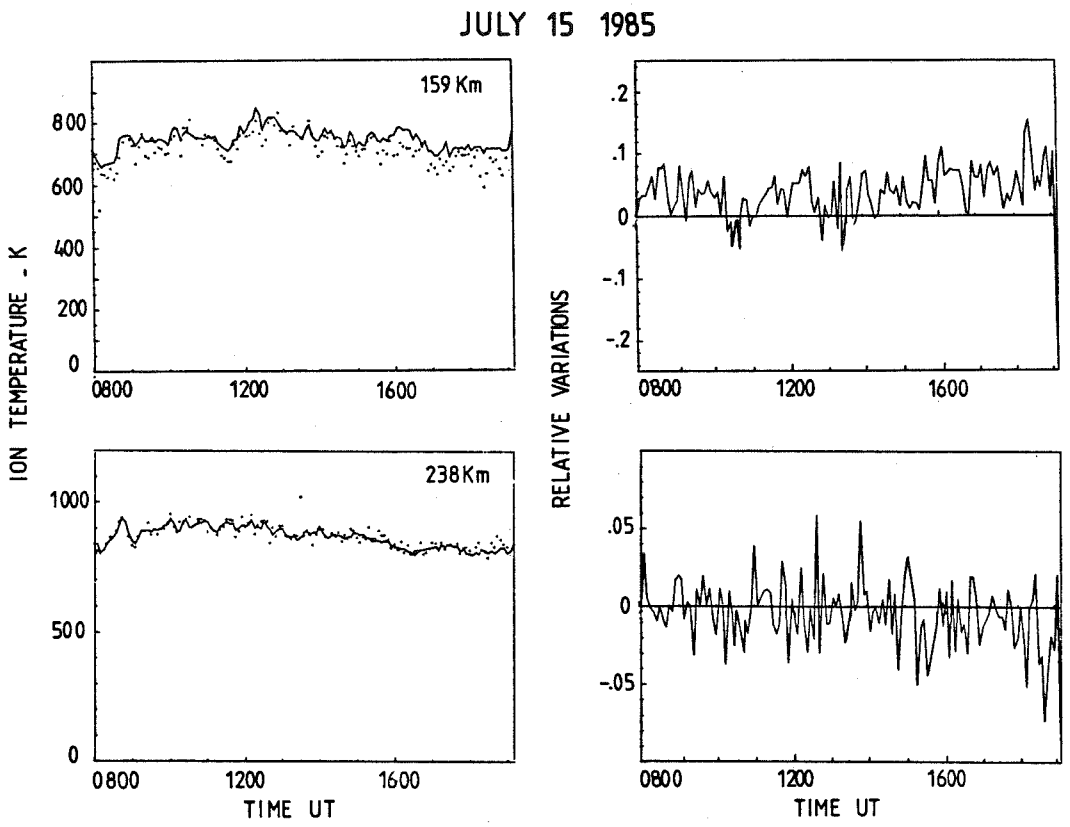


Fig. 6. As Fig. 3, but for ion temperature on 15 July 1985.

feature, and in all cases the temperature at 106 km is overestimated.

## 5. ION COMPOSITION RESULTS

We show in Fig. 9 ion composition profiles for the three experimental days. Ion composition obtained at the different measurement altitudes, every 5 min, have been averaged throughout the experiment in order to obtain these profiles.

This procedure is correct for the July day: we have seen that temperatures and densities show very small variations and, furthermore, for ion compositions deduced from the normal ACF, we have verified that the altitude where $[O^+]/N_e$ was equal to 40% was very stable during the whole experiment (see LATHUILLERE and BREKKE, 1985). This verification was not possible for ion compositions deduced from the special ACF because the data were much more noisy and it was necessary to average the data over a long time.

For the February and April days the averaged profile is certainly much less significant: it is likely that the ion composition changes quite a lot between the beginning of the experiment and the middle of the night. However, we have made an automatic average in time excluding all bad data, leading to ion composition profiles which can be compared, even if they are not physically significant.

The comparison of profiles of the three days, presented in Fig. 9, leads to the same characteristics. One obtains a higher ion composition with the normal ACF than with the special ones at high altitude (above 220 km), and a smaller ion composition at low altitude (under 180 km). Between 180 and 220 km, however, the discrepancies between normal and special profiles are very small.

In particular, the altitude transition where the ion composition $[O^+]/N_e$ is equal to 40% (LATHUILLERE and BREKKE, 1985) is almost the same for normal and special profiles in the three cases.

On the July profiles we have added results from the Kiruna receiving station (little circles). The Kiruna antenna was moved during the experiment from 312 km altitude at the beginning to 212 km at the end. Thus the composition results correspond to different periods of the day, but one has seen that the transition

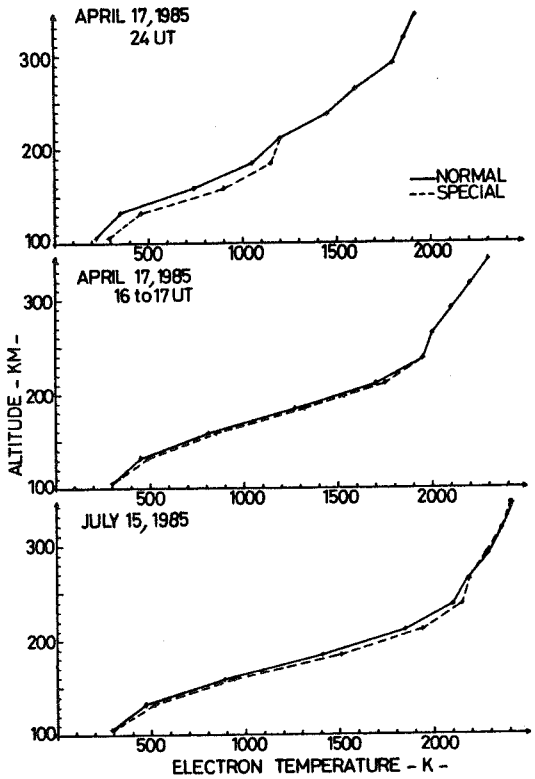


Fig. 7. Electron temperature profiles deduced from normal ACF (plain line) and special ACF (dashed line) for three time periods: 17 April 1985, around 24 UT, 17 April 1985, 16–17 UT and 15 July 1985, average profile over the whole experimental period.

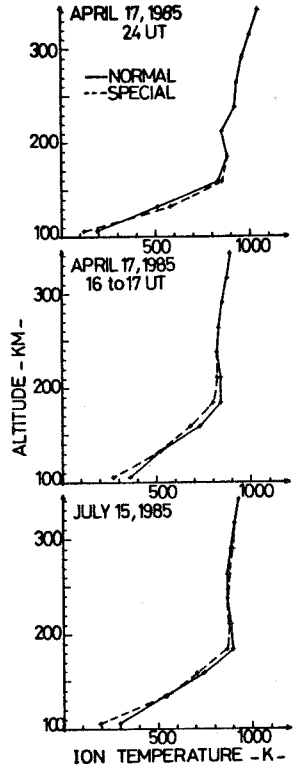


Fig. 8. As Fig. 7, but for ion temperature profiles.

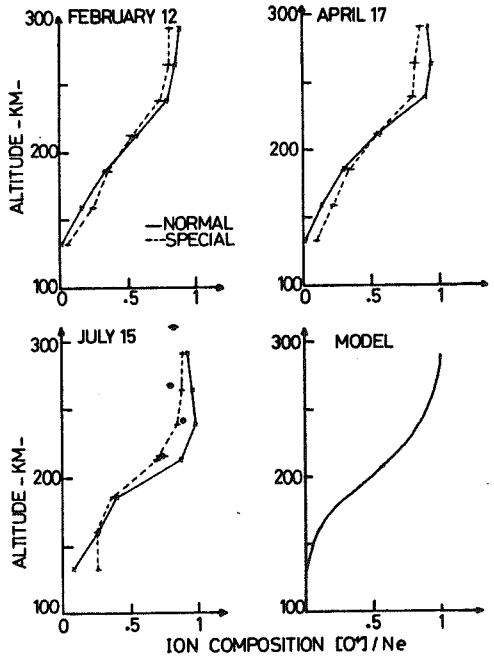


Fig. 9. Ion composition profiles deduced from normal ACF (dashed line). Each panel corresponds to the mean profiles of the whole experimental period. To the 15 July profiles has been added ion composition deduced from Kiruna data (open circles). The composition model used for temperature determination is also shown for comparison.

altitude for this day was very stable during the whole experiment. It allows us to compare the short time averaged data of Kiruna (4 h to 1 h depending on the altitude) to the mean Tromsø profile. It is evident that the Kiruna results agree much better with the special profile than the normal one.

The diffusive volume for the Kiruna data corresponds to the intersection of the two antenna lobes and is very small, even compared with the diffusive volume corresponding to the special ACF. Thus, the comparison of the Kiruna and Tromsø data means that the range integration obtained with the special ACF (27 km) is sufficiently small for obtaining good composition profiles (above 200 km altitude).

## 6. CONCLUSION

In conclusion, we résumé the main results of this work and outline some geophysical consequences.

The smearing effect due to the diffusive volume introduces some large errors into temperature measurements, principally in electron temperatures, where these errors can be as large as 50% at 133 km altitude. In ion temperatures, these errors never exceed 20%. These numbers are given assuming that the special ACF lead to correct electron and ion temperature estimates. However, the smearing effect also exists for the special ACF, which means that the errors due to the diffusive volume are underestimated. Another important feature is that the amplitude of the error of estimation depends on the electron density profile: it is larger in the case of large gradients of electron density in the diffusive volume.

Ion composition results have shown that the transition region was correctly estimated when using the normal ACF, and that a diffusive volume of the order of $\pm 27$ km was sufficiently small to obtain good ion composition estimation above 200 km. Furthermore, an important geophysical consequence is that the altitude region where the molecular ions give place to oxygen ions is certainly very large (of the order of 200 km or more), with a significant abundance of heavy ions above 300 km altitude.

The special ACF lead to an altitude integration on ionospheric parameters which seems good enough for ion composition measurements. However, the corresponding diminution of the number of samples used in ACF estimation does not allow the use of our special correlator program for routine ion composition measurements, unless one can use all the multifrequency capabilities of the EISCAT system, as is proposed presently in the GEN programs (TURUNEN, 1985). One can also think of a deconvolution procedure which would permit the use of the normal ACF technique to determine ionospheric parameters in the *F*1-region (see LEJEUNE and LATHUILLERE, 1986).

*Acknowledgments*—The EISCAT Scientific Association is supported by the Centre National de la Recherche Scientifique of France, Suomen Akatemia of Finland, Max-Planck-Gesellschaft of the Federal Republic of Germany, Norges Almenvitenskapelige Forskningsråd of Norway, Naturvetenskapliga Forskningsrådet of Sweden and the Science and Engineering Research Council of the United Kingdom.

## REFERENCES


| | | |
|---|---|---|
| BERTIN F., KOFMAN W. and LEJEUNE G. | 1983 | *Radio Sci.* **18,** 1059. |
| FARLEY D. T. | 1969 | *Radio Sci.* **4,** 935. |
| FOLKESTAD K., HAGFORS T. and WESTERLUND S. | 1983 | *Radio Sci.* **18,** 867. |
| KOFMAN W. and LATHUILLERE C. | 1985 | *J. geophys. Res.* **90,** 3520. |
| LATHUILLERE C. and BREKKE Å. | 1985 | *Annls Géophys.* **3,** 557. |
| LATHUILLERE C., LEJEUNE G. and KOFMAN W. | 1983 | *Radio Sci.* **18,** 887. |
| LEJEUNE G. and LATHUILLERE C. | 1986 | *J. atmos. terr. Phys.* 849. |
| TURUNEN T. | 1985 | EISCAT Technical Note 85/44. |

# ARTICLE 5

# Ion compositions in the auroral ionosphere as observed by EISCAT

Chantal LATHUILLERE (*) and Asgeir BREKKE (**)

(*) *CEPHAG, BP* 46, 38402 *St. Martin d'Hères Cedex France*

(**) *Air Force Geophysics Laboratory Hanscom Air Force Base, Bedford, MA* 01731, *U.S.A.*

Received 27/09/84, accepted 21/02/85.

ABSTRACT. The method to extract information of the ion composition directly from incoherently scattered spectra measured in the ionospheric transition region between atomic and molecular dominated ions as described previously by Lathuillere *et al.* (1983) has been employed on measurements performed by EISCAT in the auroral zone. It is found that the hourly mean daily variation of the height ($Z_{40}$) where the atomic $O^+$ ion contributes 40 % to the total ion density varies by the solar zenith angle in a similar manner as found by Oliver (1975) for the transition height $Z_{50}$ where $O^+$ contributes by half the ion density. The $Z_{40}$ parameter is found to decrease on the average by 20 km from summer days to winter days also in qualitative agreement with the works by Oliver (1975) and Kelly and Wickwar (1981). These results indicate that on an hourly mean basis the bottom side *F*-region auroral ionosphere is in photochemical equilibrium. Incidences are, however, found where auroral disturbances introduce larger variations in $Z_{40}$ within an hour or so than are else observed between seasons, indicating that severe disturbances occur in the ion composition at *F*-region heights during such events.

It is evident for several of these outstanding features that the ionosphere deviates from the photochemical equilibrium model. These discrepancies are discussed with reference to variations in other ionospheric parameters measured such as electric fields, particle precipitation and temperature. A new result concerns the effect of particle precipitation which can act either to lower or to increase the percentage of atomic ions, depending on the altitude of penetration.

*Key words* : ion composition, auroral ionosphere, *F*-region, incoherent scatter measurements.

*Annales Geophysicae*, 1985, **3**, 5, 557-568.

## 1. INTRODUCTION

In a previous paper (Lathuillere *et al.*, 1983) it has been shown that the incoherent scatter technique can provide direct measurements of ion composition between 140 and 320 km altitude. In this region, the molecular ions ($NO^+$ and $O_2^+$) dominating the lowest ionosphere yield progressively place to atomic ions ($O^+$). This transition is relatively well-known at midlatitude (Oliver, 1975) where the ionization is mainly governed by daily and seasonal variations in the solar radiation. At high latitudes, however, the ionization produced by particle precipitation, strong ion heating induced by large electric fields, vertical and horizontal transport, will lead to variations of the ion composition which will add in complexity to the diurnal and seasonal midlatitude behaviour.

Effects of such high altitude disturbances on the *F*-region composition have been treated theoretically by Schunk *et al.* (1975, 1976), Schunk and Raitt (1980) and Sojka *et al.* (1981). In particular, Schunk *et al.* (1975) have shown that owing to the rapid increase of the reaction

$$O^+ + N_2 \rightarrow NO^+ + N$$

with ion energy, high-latitude electric fields and consequently $\mathbf{E} \times \mathbf{B}$ drifts deplete $O^+$ in favour of $NO^+$, at *F*-region heights.

In their comprehensive study, Schunk *et al.* (1976) have compared the effects of a multitude of factors on the *E*- and *F*-region ion composition, especially they focused their attention on the effects of various values of the electric field. While a strong meridional electric field for instance can increase the abundance of $NO^+$ at all heights, a westward electric field will enhance the number of $NO^+$ ions below the *F*-region peak, and consequently combined electric field components can lead to strong $NO^+$ enhancements both above and below the *F*-region peak. An eastward component of the electric field however, will probably lead to a depletion of $NO^+$ ions below the *F*-region peak.

(**) On leave of absence from The Auroral Observatory, University of Tromsø, P.O. Box 953, N-9001 Tromsø, Norway.

Furthermore, in the work by Schunk and Raitt (1980) it has been shown that the effects of enhanced electric fields are much more diversified than originally indicated by Schunk *et al.* (1975; 1976). While the primary effect of a meridional electric field is to heat the plasma through frictional interaction with the neutral atmosphere, such that the resulting elevated ion temperature acts to alter the ion chemical reaction rates, the net result may be either an increase or a decrease in the $O^+$ density depending on the ionospheric conditions. For the same meridional electric field strength, for instance, the results obtained by Baron and Wand (1983) make it likely that the composition effects may differ whether the electric field enhancement occurs in the evening or in the morning side auroral oval. This is because the heating effect on the morning side appears to be relatively stronger for the same magnitude electric field in the *F*-region than on the evening side, a fact that is probably due to a relatively larger ion-neutral velocity after midnight in the *F*-region than before.

The high latitude convection system also makes the *F*-region plasma sweep through regions of vastly different ionospheric conditions in the course of a 24 hours period, which adds a new factor of complexity to the variation in ionospheric composition as, for instance, measured in the *F*-region by a ground-based facility as EISCAT. This has been pointed out by Sojka *et al.* (1981) who have derived diurnal variations in the relative $O^+$ abundance at several *F*-region heights for the three high latitude incoherent scatter radar sites Chatanika, EISCAT and Søndre Strømfjord. They have shown that at EISCAT and Chatanika, in spite of being situated approximately at the same geomagnetic latitude, larger differences in the diurnal behaviour are expected. The main reason for this difference is according to Sojka *et al.* (1981) the offset between the geographic and geomagnetic poles.

So far, the effects on the ion composition due to particle precipitation have only vaguely been discussed by Schunk *et al.* (1976). It appears to be a rather complicated problem to attack because of the great variability both in the precipitating energy spectrum and in the conditions of the local ionosphere at the time of precipitation. Kelly and Wickwar (1981) have observed variations in the $[NO^+]/[O^+]$ ratio between 150 and 300 km altitude during particle precipitation events and concluded that the transition altitude where $O^+$ starts to dominate $NO^+$ is lowered by as much as 20 km during such events.

The reason for this, they believe, is due to enhanced ion production in the *F*-region both of $O^+$ and $NO^+$ ions. The $O^+$ ions, however, having a longer lifetime than the $NO^+$ ions, will tend to dominate to lower altitudes and thereby resulting in the observed effects. Kelly and Wickwar (1981) exclude the effects of vibrational excitation of the $N_2$ molecules as being of importance to the ion composition at the *F*-region heights during precipitation events. In contrast to the theoretical studies by Schunk *et al.* (1976) where much emphasis was centered on the effects of different components of the electric field, Kelly and Wickwar (1981) did not study these effects separately. They instead investigated effects of the electric field in a general sense through the Joule heating and found that the transition height increased substantially during events of such heating.

Another important factor to the ion composition is motion in the neutral atmosphere. The neutral wind will bring the neutral gas across the polar cap to the auroral latitudes and during this process variations in the neutral gas may occur which in turn will change the conditions for chemical reactions. More important, however, are vertical transport processes which may be present in the neutral gas during auroral disturbances. Such transport can lift the heavy molecules such as $O_2$, NO and $N_2$ to higher altitudes or bring O and N atoms down to lower altitudes. Both effects can lead to variations in the chemical reactions prevailing at certain altitude regions.

Transport effects of the neutral gas in relation to the ion composition in the auroral ionosphere has so far not been treated in a consistent manner in the literature, probably due to the great complexity of the problem.

We have analyzed in terms of ion composition EISCAT experiments performed during the years 1981 and 1982, when the Tromsø antenna was in a fixed position up along the field line at Tromsø (CP0 or Common Program Zero experiments). In the first part of this paper, we will show that a diurnal variation is present in all data with an increase, at a given altitude, of the relative abundance of molecular ions during the night. Our set of data is not sufficient for an harmonic analysis or a study of seasonal variations, but still, we can see differences between summer and winter which are similar to midlatitude variations.

In addition to these diurnal and seasonal variations we have studied in a second part of this paper the remaining significant variations which we make probable can mostly be related to auroral phenomena such as Joule heating, soft or hard particle precipitations, and variations in the electric field and the general convection pattern.

As the data show a great variability from one day to the other, it is difficult to identify a common characteristic of the data. Thus, these results tend to support a general impression that there appears to be no single cause at high altitudes of the observed variations in the relative $[NO^+]/[O^+]$ abundance ratio, but that different processes act together to create enhancements and depletions of the different ion species in different areas at different times. An experimental study from one site like EISCAT can only be tentative at best. In order to obtain a broader scope on these phenomena, a much more extensive observational coverage would be needed.

## 2. DIURNAL AND SEASONAL VARIATIONS OF $O^+$ ABUNDANCE

### 2.1. Experimental conditions

Between May and December 1982, five 24 hours runs of the CP0 experiment have been performed. This program is one of the simplest used by EISCAT as the Tromsø antenna looks in a fixed position along the magnetic field line. In addition the remote antennas

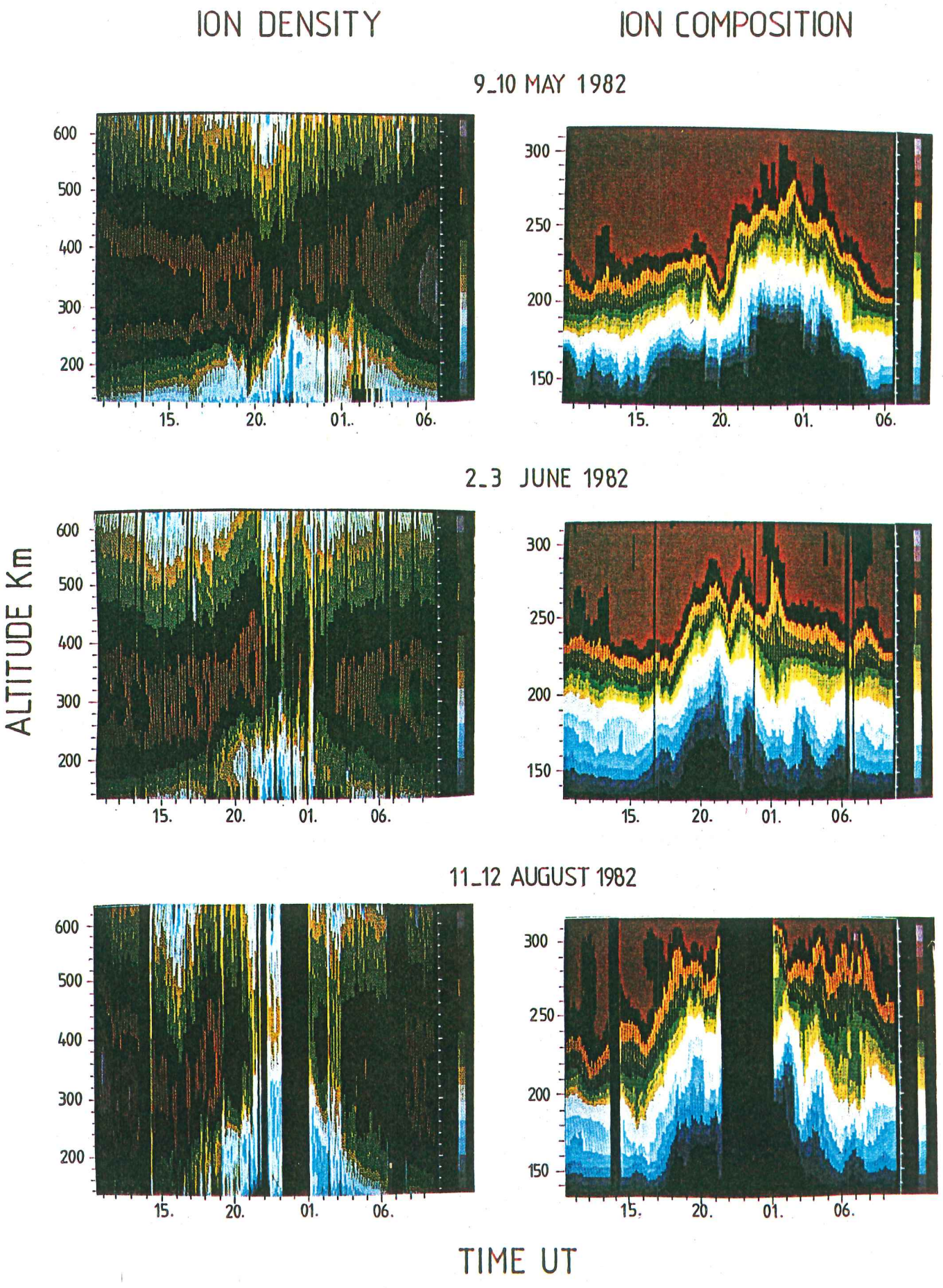


**Figure 1**

Left Row : *Ion densities* versus *height and Universal Time for 3 summer days of* 1982 *as observed by* EISCAT. *The colour scale is given on the right edge running from* $3 \cdot 10^{10}$ $m^{-3}$ *for the black to* $10^{12}$ $m^{-3}$ *for the purple.*
Right Row : *Ion composition plots* versus *height and Universal Time. The colour scale runs from zero percentage* $O^+$ (*black colour*) *to* 100 *percentage* $O^+$ (*red colour*) *in steps of* 6 %.

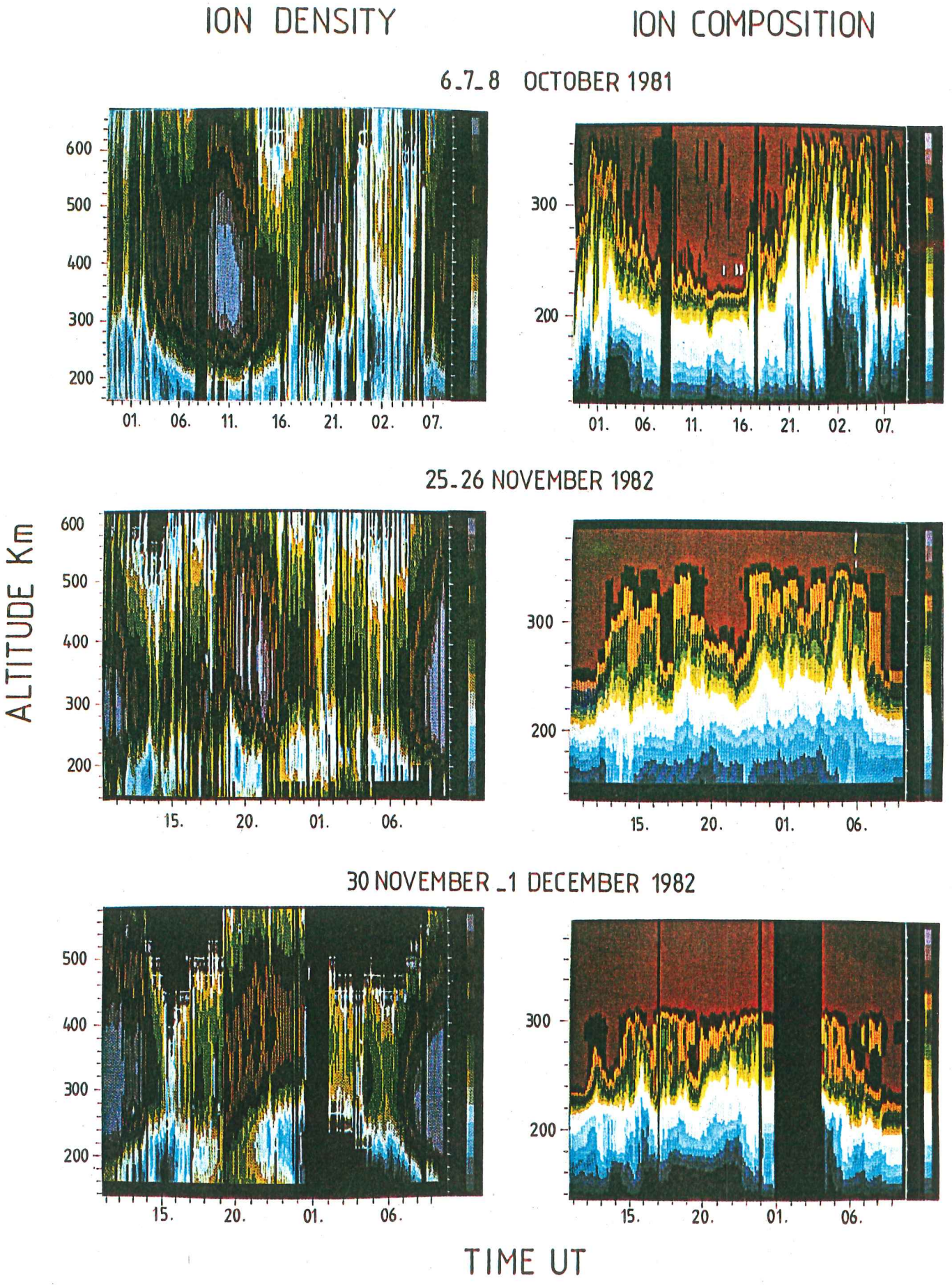


**Figure 2**

*Same as figure 1 except for 3 winter days. The ion densities colour scale for the November days runs from* $10^{10}$ $m^{-3}$ *to* $3 \cdot 10^{11}$ $m^{-3}$.

(at Kiruna and Sodankylä reception stations) are pointed to intersect the Tromsø beam at 300 km altitude allowing measurements of three independent components of the ion velocity vector within a common volume. This kind of experiment is particularly suitable for ion composition analysis, as it is possible to post-integrate the measured autocorrelation function as long as needed. In practice, we have used a five minute integration time which has shown sufficient to obtain direct measurements of the ion composition. The method used, which is described in detail by Lathuillere *et al.* (1983) does not involve any assumptions on ion and electron temperatures; indeed, it allows a simultaneous determination of electron density, electron and ion temperatures, and ion composition from each integrated autocorrelation function.

In addition to the 1982 experiments, we present data from a 30 hours run of October 6, 7 and 8, 1981; during this experiment, a 500 μs pulse was used instead of the 360 μs pulse used for 1982 data, and autocorrelation functions have been post-integrated over 3 min. As the Kiruna and Sodankylä antennas were scanning the Tromsø beam, the data obtained from these two remote sites are very poor and thus no reliable measurement of the corresponding ion velocity components are available for these days.

### 2.2. Ion composition results

The six experiments have been separated into summer days and winter days and the results are presented in figures 1 and 2. For each day, we show the electron density $N_e$ with a logarithmic colour scale and the $O^+$ relative abundance ($[O^+]/N_e$) with a linear colour scale, as a function of universal time and altitude.

$N_e$ and $[O^+]/N_e$ are deduced from the 5 min (or 3 min) integrated autocorrelation functions; a running average of one hour is then performed in order to achieve enough accuracy on $[O^+]/N_e$ (i.e., $< 0.10$).

Plots of the electron density profiles between 130 and 600 km (fig. 1 and 2) show the general behaviour of the ionosphere during each day with the typical density enhancement during the sunlight hours and depletion during nighttime, particularly at lower altitudes. An elevation in the evening hours and a descent in the morning hours of the electron density maximum is in particular evident for the summer days, in the winter days, however, events of particle precipitation are dominant in the evening hours which makes the diurnal behaviour more complicated.

The ion composition plots have been limited to the lower part of the ionosphere, i.e., below 400 km for the winter days and below 300 km for the summer days. The general trend appears to be an enhanced contribution of molecular ions at greater heights at night for the summer days. For the winter days the contribution of molecular ions also increases at greater heights at night, but in addition the content of molecular ions is also enhanced at greater heights in daytime especially for the late November days.

In all days, however, the $O^+$ ions dominate to lower heights at local midday (1100 UT) than at local midnight (2300 UT). These results appear to be in conflict with the prediction made by Sojka *et al.* (1981). There it was shown that for winter days of solar minimum and low magnetic activity the $O^+$ ions would tend to dominate to lower heights in the morning and evening hours than at midday. Although the days presented here are not chosen on the basis of the criteria used by Sojka *et al.* (1981), the November 30 to December 1, 1982 experiment is made during a period of low magnetic (see fig. 5) and relative low solar activity in good accordance with the ionospheric situation described in the work of Sojka *et al.* (1981). It is, however, also shown in the work by Sojka *et al.* (1981) that the $O^+$ dominance occurs in a very narrow auroral belt. Therefore it is impossible to perform a fair comparison between the EISCAT measurements and the model predictions, when no information is available as to the relative position between the volume probed by EISCAT and this belt.

In addition to this general long time variation, one can see variations with much shorter time scale. Some of them are significant (for instance, the increase of $O^+$ ions at lower heights around 2000 UT on the 9th of May). Others are due to experimental errors, particularly for the two November days, when the signal-to-noise ratio was lower than for the other days.

In order to compress the information contained in the ion composition profiles, we have chosen to study the altitude where $[O^+]/N_e = 40\,\%$. This choice was made by looking at results of simulations, taking into account the smearing of data due to the large integration volume : ± 54 km for a 360 μs pulse (see Lejeune and Lathuillere, 1983). At low and high altitudes corresponding to $[O^+]/N_e$ respectively smaller than 40 % or larger than 60 %, the simulations show that the bias due to the altitude integration are large and scattered, depending on the state of the ionosphere (temperatures and density gradients). The bias obtained on ion compositions between 40 and 60 % are much smaller. At the altitude where $[O^+]/N_e$ equals 40 %, this bias was less than 10 km and is therefore chosen as the reference height in this work. In the following sections, this altitude will be called $Z_{40}$.

### 2.3. Variations of $Z_{40}$ with solar zenith angle

For each day, we have plotted in figure 3 the altitude $Z_{40}$ as a function of the solar zenith angle. Only independent determinations of $Z_{40}$ are plotted, i.e., one point every hour (as we have used a running average of one hour). We have tried to fit the $Z_{40}$ data to a hyperbolic tangent function similar to the one derived by Oliver (1975). For the summer days (marked +, × and * in the graph) the best fit is obtained by the solid line in figure 3 given by the function :

$$Z_{40}(\chi) = 200 + 25 \cdot \tanh\left(\frac{\chi - 85^o}{10^o}\right) [\text{km}] \qquad (1)$$

where $\chi$ is the zenith angle measured in degrees. The diurnal variation of $Z_{40}$ for the summer days is quite evident and the difference between night and day is as large as 50 km. This difference corresponds well with the daily variation observed from rocket data by

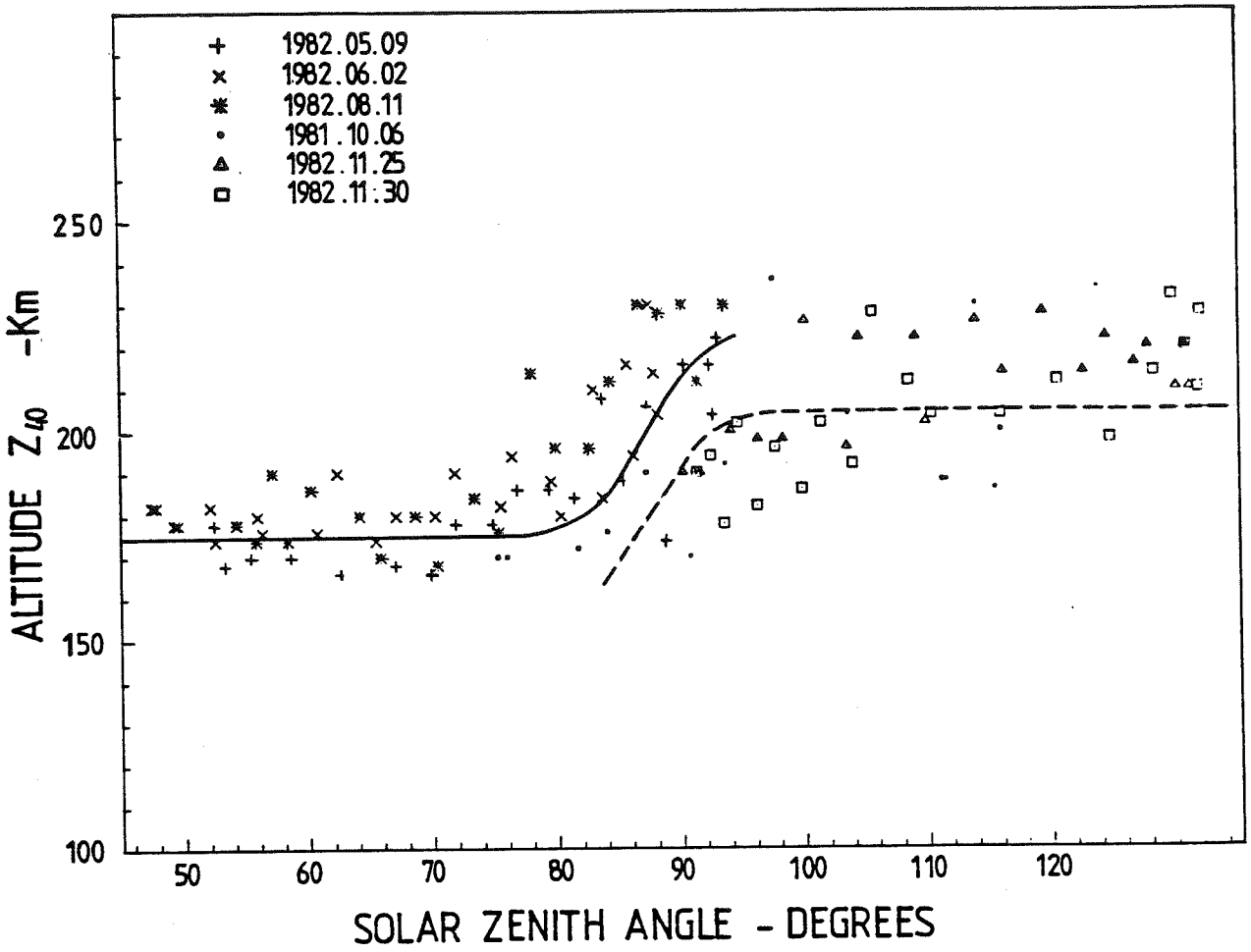


Figure 3
*The height of* 40 percentage $O^+$ *as function of zenith angle,* +, × *and* * *represents the summer days while* □, △ *and* ● *represent the winter days. The full drawn curve is a fit to a model equivalent to the work by Oliver* (1975) *based on photochemical equilibrium and no nighttime ionization sources. The dashed curve is a similar fit to the winter days obtained by shifting the extrapolated summer day curve down by* 20 km.

Oliver (1975) though it is larger than the diurnal variation observed by Kelly and Wickwar (1981) from the Chatanika incoherent scatter measurements. In the latter work the ion composition was derived through an indirect method which requires modelling of the neutral temperature profiles in contrast to the more direct observations obtained in this work.

For the winter days (marked ●, △ and □ on fig. 3) the data points appear to agree better with the curve represented by the dashed line which has the same shape as the solid line except that it is shifted downward in altitude by 20 km. Such a seasonal difference in the height of $Z_{40}$ is also consistent with the results obtained by Oliver (1975) and Kelly and Wickwar (1981) except that the former finds a difference in $Z_{50}$ closer to 45 km. The increase in $Z_{40}$ from winter to summer is explained by a decrease in the abundance of O relative to $N_2$ in the summertime *F*-region and thereby an increase in the $O^+$ loss rate at these heights.

The formula given by equation (1) for $Z_{40}$ does, however, indicate that photochemical equilibrium is present at *F*-region heights, as it inherently neglects nighttime ionization sources such as auroral particle precipitation, this may explain some of the scatter of the data points in figure 3 especially for the winter days.

The relatively good fit to equation (1) particularly for the summer days in figure 3 are, however, surprising when the work by Schunk *et al.* (1975), Schunk and Raitt (1980) and Sojka *et al.* (1981) are taken into consideration, as these clearly do indicate that the ion composition measured by a ground-based technique such as EISCAT will be highly variable depending on the general situation in the ionosphere, and in particular on the strength and direction of the electric field.

To investigate further any effects of auroral disturbances such as enhanced electric fields might have on the ion composition, we have presented the observed $Z_{40}$ parameter as function of Universal Time for all the 6 days separately in figure 4. For each day the theoretical $Z_{40}$ as derived from equation (1) is also indicated by a solid line. Superimposed on the individual measurements indicated by crosses are the r.m.s. variation hatched in grey. The r.m.s. deviation is more pronounced for the winter days partly because these data are observed under conditions with lower electron densities, i.e., lower signal-to-noise ratios.

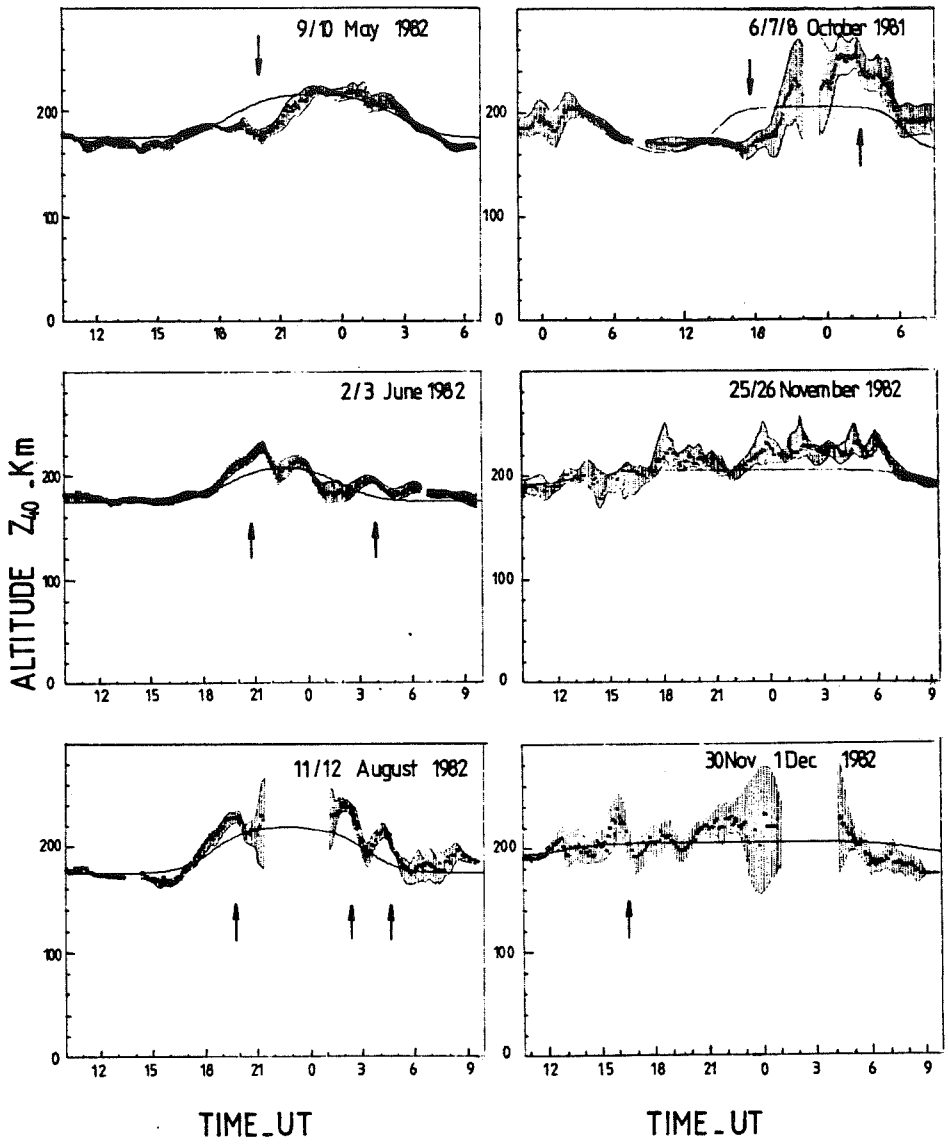


Figure 4
*The variation in height of* 40 *percentage* $O^+$ *abundance* ($Z_{40}$) *as function of Universal Time for all six days studied. The full drawn curves are the model calculation as described by Oliver* (1975) *and applied for the* EISCAT *latitude.*

In contrast to the work by Oliver (1975) it is not possible to study the thickness of the transition region where the $O^+$ ion content increases from 0 % to 100 % as the long pulses used do integrate over too broad a region in altitude. This smearing in height will most likely lead to erroneous results at the lower and upper edges of the transition region.

It is clear from this presentation (fig. 4) that large and irregular variations are superimposed on the diurnal and seasonal variations previously described. Because of the existence of a non-constant bias due to the altitude integration in our data (see above) these other variations are significant only when we take into account the r.m.s. deviations, that have at least an amplitude of 20 km. We have indicated with arrows in figure 4 the variations that we in this sense believe are the most significant.

## 3. VARIATIONS OF $O^+$ ABUNDANCE ASSOCIATED WITH AURORAL PHENOMENA

As already mentioned, there are several effects present in the high altitude ionosphere which can have an influence on the ion composition and therefore also the altitude where the ratio $[O^+]/N_e$ is 40 %. Such effects are particle precipitation, frictional or Joule heating due to large electric fields and variations in vertical and horizontal transport processes. In this section, we will therefore investigate closer those large and irregular variations demonstrated in figure 4 in an effort to try to relate them to some of these characteristical effects in the high latitude ionosphere.

According to figure 5, where the 3 hours *Kp* indices are plotted for each day, May 9 to 10, 1982 as globally the most quiet day together with November 30 to December 1, 1982, and June 2 to 3, 1982. In particular the derived $Z_{40}$ curves for the two summer days follow the theoretical $Z_{40}$ curves very closely with relatively little scatter in the data points (see fig. 4).

There are however, three marked deviations from the theoretical curves which we will return to later. On November 30 to December 1, 1982, the error bars on each data point are very large, giving the impression of a less successful fit to the theoretical curve (fig. 4). On the other winter day November 25 to 26, 1982, there are relatively small error bars on the measured points but the derived values appear to be systematically offset

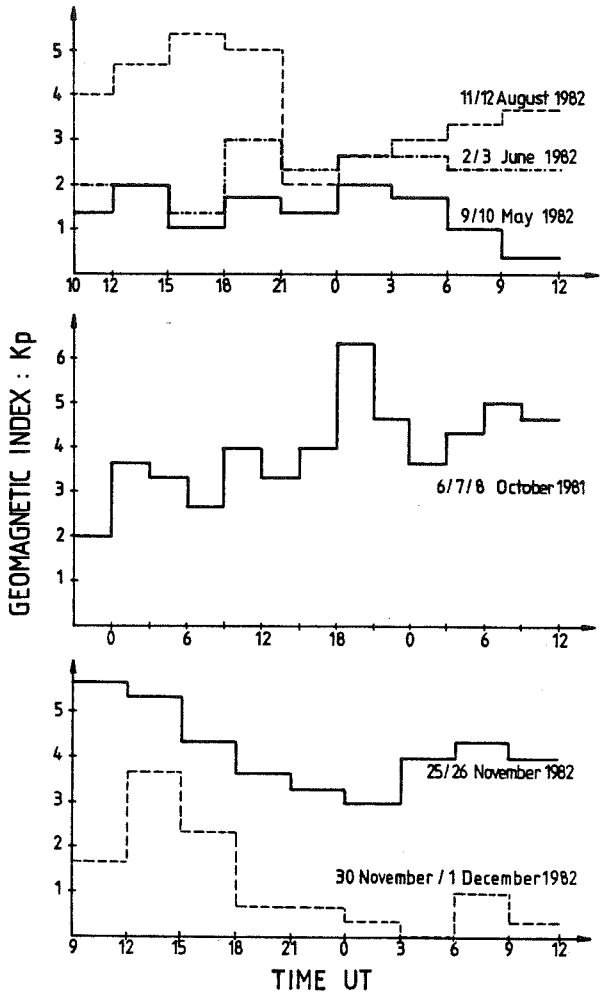


Figure 5
*3-hour Kp indices for the 6 different days of measurement.*

to a large height in particular between 2200 UT on November 25 and 0700 UT November 26. This, however, was a strongly disturbed day according to the *Kp* values shown in figure 5, and also to the local magnetogram at Tromsø.

For the autumn days, August 11-12, 1982 and October 06-08, 1981 which are globally both very disturbed

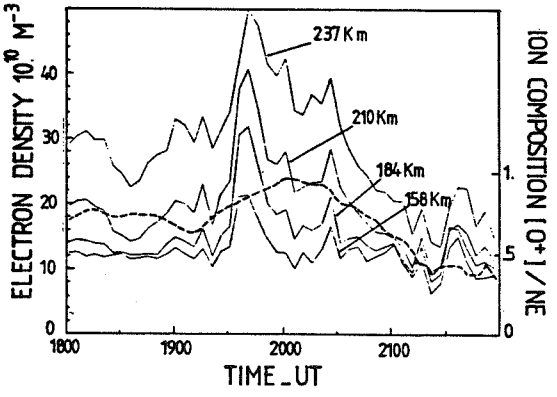


Figure 6
*Variations by Universal Time of the electron density at* 158, 184, 210 *and* 237 km *altitudes for May* 3, 1982 *between* 1800 *and* 2200 UT. *The dashed line shows the variation in the relative abundance of* $O^+$ *at* 184 km *altitude in the same period.*

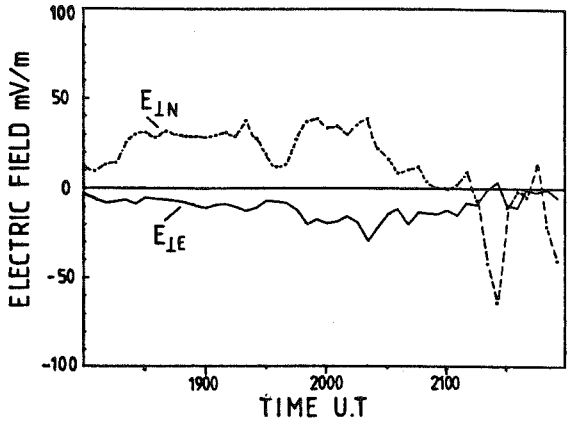


Figure 7
*The electric field components perpendicular to the earth magnetic field as measured by* EISCAT *on May* 3, 1982. $E_{\perp N}$ *and* $E_{\perp E}$ *represents the geomagnetic northward and eastward components respectively.*

(see fig. 5) the discrepancies between derived $Z_{40}$ values and the theoretical curves are the largest (fig. 4).

Although the two summer days (May 9-10, 1982 and June 2-3, 1982) are both geomagnetically quiet days on a global scale (fig. 5) some outstanding deviations from the theoretical quiet day behaviour of $Z_{40}$ are, as already noticed, seen for these days in figure 4. In particular on May 9, 1982 a strong descent in the measured $Z_{40}$ height is found to occur between 1900 and 2000 UT. This event appears to be associated with a soft energy particle precipitation as seen from figure 6 where the electron densities at 4 altitudes 158, 184, 210 and 237 km respectively, are shown in the period between 1800 and 2400 UT. Also shown in figure 6 is the $[O^+]/N_e$ ratio at 184 km which is increasing between 1900 and 2000 UT. An increase of the relative amount of $O^+$ ions during events of soft particle precipitation has also been observed by Kelly and Wickwar (1981) and is explained by them as due to enhanced ion production caused by the particle precipitation. As the $O^+$ ions have a longer lifetime than the $NO^+$ ions the former ions will dominate to lower heights during such events and the $Z_{40}$ height will decrease accordingly. One also notices that the electric field perpendicular to the geomagnetic field has a persistent westward component of 20 mV/m ($E_{\perp E}$) during this event (fig. 7). This component will be associated with a downward directed ion motion that can contribute to an enhanced $O^+$ abundance below 200 km. The northward component of the electric field ($E_{\perp N}$) is fairly large ($\sim$ 30 mV/m) between 1830 and 2030 UT except for the event discussed when it decreased to about 10 mV/m. As there is no apparent increase in the ion temperature as due to frictional heating caused by this electric field no change in the ion composition is expected to be due to the northward component $E_{\perp N}$.

After 2100 UT an increase is observed in $T_i$ to be associated with the spike in the southward component of the electric field ($E_{\perp N} \cong -70$ mV/m). Because of the running average of 1 hour performed on the data to obtain $Z_{40}$, however, no change is observed in the composition.

June 2-3, 1982 is magnetically less quiet than May 9-10, 1982 as judged from the *Kp* values shown in figure 5 and also from the local magnetograms at Tromsø. A relatively modest geomagnetic activity appears to take place from 1800 UT until 0400 UT and then followed by relatively strong pulsations for the rest of the experiment. In this period, it is seen from figure 4 that $Z_{40}$ increases above the theoretical values between 1900 and 2200 UT and between 0230 and 0500 UT. For both these events the electric field is very weak ($< 10$ mV/m). In association with these events, however, two strong and prolonged electric precipitation events take place, one between 1800 and 2200 UT and the other between 0200 and 0400 UT. This can be seen from figure 8 which shows the height integrated particle heating calculated from the power profiles measured in Tromsø.

It is then conceivable that for this day, considerable heat is released in the *E*-region due to particle precipitation, resulting in an increase of the heavy ion content at *F*-region heights which forces the $Z_{40}$ to increase.

August 11-12, 1982 and October 06-07-08, 1981 are all globally relatively disturbed days according to figure 5. As mentioned earlier, no reliable measurements from the remote sites are available for October 06-07-08, 1981 and therefore no comparison can be made between the variations in the composition and the electric field. Nevertheless, there is a precipitation event taking place between 1600 and 2200 UT on October 07, which appears to be related to the lowering of $Z_{40}$. The precipitation can be observed in the colour plot of figure 2 to occur above about 200 km. It is therefore possible that this represents a similar example to the ones reported by Kelly and Wickwar (1981) and to the one found for May 9, 1981.

According to figure 5, the night between October 07 and 08 is very active. The local magnetogram in Tromsø shows three large negative excursions of the *H* component (300 $\gamma$) suggesting the presence of large electric fields. This may indicate that heating is taking place below 200 km and that an upwelling of the atmosphere is present thereby increasing the heavy ion content at higher levels and resulting in the increase of $Z_{40}$ between 2000 and 0600 UT at the end of the experiment.

August 11-12, 1982 is more strongly disturbed locally in Tromsø than for the preceding day. This is in particular true for the period between 1300 and 2100 UT on August 11 when a strong ($\sim 500\ \gamma$) positive bay is observed. The last part of this bay is associated with an increase in $Z_{40}$ compared to the quiet mean value. We also notice from figure 9 an increase in the height integrated particle heating between 1600 and 2100 UT corresponding to the increase in $Z_{40}$. We have here probably an example similar to the two events found on June 2-3.

For the other two events seen in $Z_{40}$ in figure 4 at about 0200 UT and 0400 UT on August 12, 1982, it is very difficult to find any relationship with similar variations in other parameters.

November 25-26, 1982 was a rather disturbed day while November 30-December 1, 1982 was very quiet as seen from the *Kp* values in figure 5, and also as revealed by

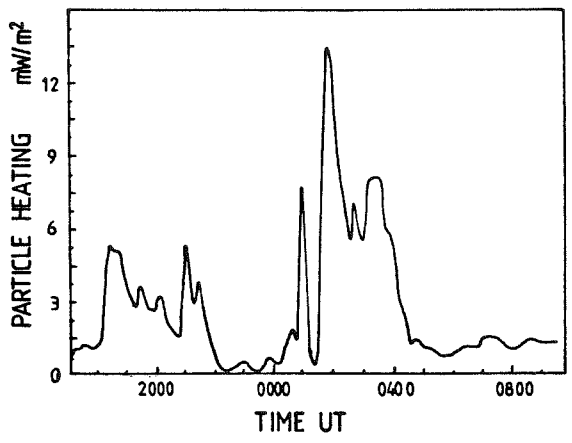


Figure 8
*The height integrated particle heating in* mW/m² *for June* 2-3, 1982 *between* 1700 *and* 1000 UT *showing two outstanding heating events referred to in the text.*

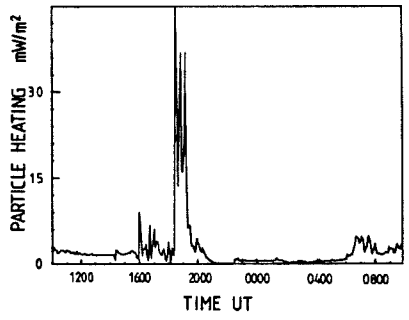


Figure 9
*Height integrated particle heating in* mW/m² *between* 1000 *and* 1000 UT *for August* 11-12, 1982, *showing an outstanding heating event referred to in the text between* 1800 *and* 2000 UT.

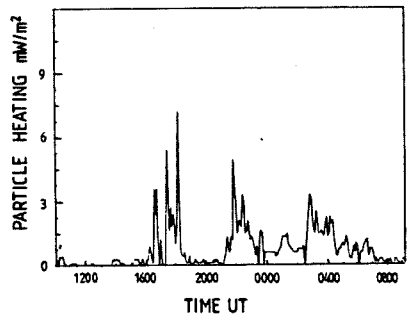


Figure 10
*Height integrated particle heating in* mW/m² *between* 1000 *and* 0900 UT *on November* 25-26, 1982 *showing a prolonged heating event from* 2100 *to* 0700 UT *as referred to in the text.*

the local magnetograms at Tromsø. Some of the EISCAT data for these days have already been presented by Perraut *et al.* (1984) where the effects of enhanced electric fields and Joule heating on the *F*-region ion temperature were discussed. In spite of the rather strong disturbances as revealed by an enhanced electric field ($\sim 50$ mV/m) between 1300 and 1700 UT on November 25, no outstanding discrepancies can be found between the observed and modelled $Z_{40}$ curves

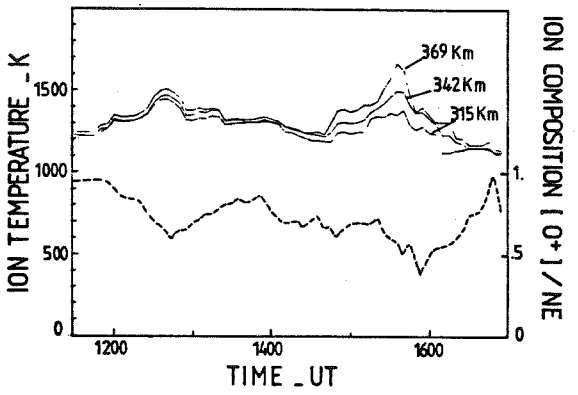


Figure 11
*Variations of the ion temperature ($T_i$) at 315, 342 and 369 km as function of Universal Time between 1145 and 1630 UT on November 30, 1982. The dashed line represents the relative abundance $[O^+]/[N_e]$ at 237 km altitude as function of time in the same period.*

in figure 4. On the contrary the observed $Z_{40}$ curve seems to be systematically higher than the one modelled in a period of moderate but relatively stable particle heating (2300-0600 UT) (fig. 10). By examining the colour plot on figure 2, however, it appears that an abrupt enhancement of molecular ions relative to the abundance of the $O^+$ ions sets in at about 1200 UT and lasts until about 1600 UT. The signal-to-noise ratio is however very low on this day, therefore no conclusive statement can be made.

On November 30, a rather small geomagnetic disturbance took place between 1200 and 1800 UT according to the *Kp* values plotted in figure 5 and also the local magnetogram in Tromsø. In spite of these small disturbances, however, the *F*-region ion temperature is enhanced at two occasions (see fig. 11); firstly between 1200 and 1300 UT and then between 1430 and 1630 UT. In both periods the $[O^+]/N_e$ ratio at 237 km altitude as shown in figure 11 is found to decrease quite dramatically, indicating that the molecular ions are getting more abundant at higher altitudes during these events. These ion temperature enhancements are related to a relatively strong oscillating electric field which is displayed on figure 12 (see also Perraut *et al.* 1984). In agreement with the theoretical work by Schunk *et al.* (1975) such *F*-region ion temperature enhancements will lead to increased abundance of molecular ions at higher altitudes as observed here in figure 11.

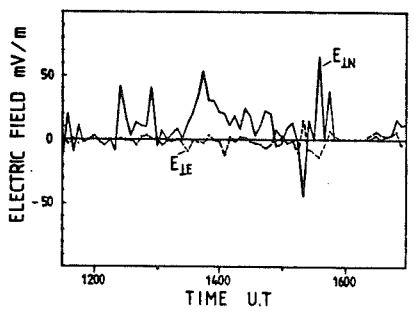


Figure 12
*Same as for figure 7 except the data is Nov. 30, 1982.*

## 4. CONCLUSIONS

By using the newly developed method of deriving the ion composition directly from incoherent radar spectra as presented by Lathuillere *et al.* (1983), we have been able to deduce from six EISCAT CP0 experiments, diurnal variations of the percentage of $O^+$ ions in the high latitude *F*-region. The variation with solar zenith angle of the level where $[O^+]/N_e = 40\,\%$ can be approximated by :

$$Z_{40} = 200 + 25 \cdot \tanh\left(\frac{\chi - 85^o}{10^o}\right) \text{ [km]}$$

for summer data, and :

$$Z'_{40} = Z_{40} - 20 \text{ km}$$

for winter data.

These diurnal and seasonal variations are consistent with results obtained from rocket measurements (Oliver, 1975) and from similar incoherent scatter data obtained by the Chatanika radar (Kelly and Wickwar, 1981). Our set of data do not at present allow for an analysis in further detail of the diurnal and seasonal variations of the ion composition. In particular, one cannot study the variations of the thickness of the transition region because the altitude integration performed in our measurements (54 and 75 km) will lead to erroneous results of the ion composition, particularly at the lowest and highest altitudes of the measurements.

The general good agreement between the observed $Z_{40}$ data points and the values for $Z_{40}$ derived from the formulas indicates that the *F*-region ion production at auroral latitudes is mainly controlled by solar radiation and that the *F*-region ionosphere below say 300 km is in chemical equilibrium. It, therefore, appears that the auroral disturbances such as auroral particle precipitation and enhanced electric fields and Joule heating only introduces second order effects to the ion composition at *F*-region heights in the auroral region, which is somewhat in contrast to the strong importance that has been related to such disturbances in recent theoretical works by Schunk *et al.* (1977) and Sojka *et al.* (1981).

In spite of the good agreement found between the measured one hour average diurnal variation of $Z_{40}$ and the model based on photochemical equilibrium there are some outstanding features observed on a finer time scale which deviates quite strongly from this model. In some cases the discrepancies observed appear to be related to events of enhanced particle precipitation and electric fields. In particular there are two events on May 9, 1982 between 1900 and 2100 UT and on October 7, 1981 between 1600 and 2000 UT, where particle precipitation appears to enhance the $O^+$ abundance at lower altitudes. During the first event, however, a westward electric field is present which may create a downward transport of $O^+$ ions below the *F*-region peak, and thereby contribute to the enhanced $O^+$ abundance at lower levels.

At two events on June 2-3, 1982 between 1800 and 2200 UT and 0200 and 0430 UT respectively, the $Z_{40}$

parameter is found to increase in response to a stronger dominance of molecular ions at greater heights which again may be caused by strong heating in the lower ionosphere due to particle precipitation. Finally, on November 30, 1982 between 1200 and 1330 UT and between 1430 and 1630 UT the $Z_{40}$ parameter appears to increase as considerable Joule heating is released due to oscillating electric fields of about 50 mV/m. This Joule heating is found by Perraut *et al.* (1984) to enhance the *F*-region ion temperature during these periods which then will lead to a depletion of the $O^+$ ions at greater heights according to the work by Schunk *et al.* (1975).

The one hour integration time used here in order to improve the signal-to-noise ratio is comparable to the characteristic times for auroral disturbances such as enhanced electric fields and particle precipitation. Therefore, it is possible that the effect of auroral disturbances has been attenuated in this work and it is even possible that some outstanding disturbances from the quiet daily pattern have been averaged out. The variation observed so far, however, has given enough evidence that changes in the ion composition do take place under enhanced electric fields and particle precipitation.

**Acknowledgement**

The authors are indebted to the French EISCAT group who offered us its electrodynamic program which has been used extensively throughout this work. This work was partly supported by Grant No. AFOSR 84-0074 from the United States Air Force when A. Brekke was a visiting scientist at AFGL. The EISCAT Scientific Association is supported by the Centre National de la Recherche Scientifique of France, Suomen Akatemia of Finland, Max-Planck Gesellschaft of West Germany, Norges Almenvitenskapelige Forskningsråd of Norway, Naturvetenskapliga Forskningsrådet of Sweden and the Science and Engineering Research Council of the United Kingdom.

*REFERENCES*

**Baron M. J., Wand R. H.,** 1983. *F*-region ion temperature enhancements resulting from joule heating. *J. Geophys. Res,* **88,** 4114-4118.

**Kelly J. D., Wickwar V. B.,** 1981. Radar measurements of high latitude ion composition between 140 and 300 km altitude. *J. Geophys. Res.*, **86,** 7617-7626.

**Lathuillere C., Lejeune G., Kofman W.,** 1983. Direct measurements of ion composition with EISCAT in the high latitude *F*1 region. *Radio Sci.*, **18,** 887-893.

**Lejeune G., Lathuillere, C.,** 1983. On the measurement of ionosphere parameters from EISCAT single pulse data in the *F*1 region and the problems due to correlation of ACF's by the diffusive volume. Presented at EISCAT Workshop, Aussois, France, Sept. 1983.

**Oliver W. L.,** 1975. Models of *F*1 region ion composition variations. *J. Atmos. Terr. Phys.*, **37,** 1065-1076.

**Perraut S., Brekke A., Baron M., Hubert D.,** 1984. EISCAT measurements of ion temperatures which indicate non-Maxwellian ion velocity distributions. *J. Atmos. Terr. Phys.*, **46,** 531-544.

**Schunk R. W., Raitt W. J., Banks P. M.,** 1975. Effect of electric fields on the daytime high latitude *E* and *F* regions. *J. Geophys. Res.*, **80,** 3112-3130.

**Schunk R. W., Banks P. M., Raitt W. J.,** 1976. Effect of electric fields and other processes upon the nighttime high-latitude *F* layer. *J. Geophys. Res.*, **81,** 3271-3282.

**Schunk R. W., Raitt W. J.,** 1980. Atomic nitrogen and oxygen ions in the daytime high-latitude *F*-region. *J. Geophys. Res.*, **85,** 1255-1272.

**Sojka J. J., Raitt W. J., Schunk R. W.,** 1981. Theoretical predictions for ion composition in the high-latitude winter *F*-region for solar minimum and low magnetic activity. *J. Geophys. Res.*, **86,** 2206-2216.

# ARTICLE 6

JOURNAL OF GEOPHYSICAL RESEARCH, VOL. 86, NO. A6, PAGES 4721–4730, JUNE 1, 1981

# Elevated Electron Temperatures in the Auroral *E* Layer Measured With the Chatanika Radar

VINCENT B. WICKWAR[1] AND CHANTAL LATHUILLERE[2]

*Radio Physics Laboratory, SRI International, Menlo Park, California 94025*

WLODEK KOFMAN AND GERARD LEJEUNE

*Centre d'Etude des Phénomènes Aléatoires et Géophysiques, BP 46, 38402 St. Martin d'Hères, France*

An extensive series of spectral measurements has been made in the auroral *E* region with the Chatanika incoherent scatter radar. Becasue of the small scale length for variations of electron density, temperatures, and ion-neutral collisions we used the operating mode with the best possible range resolution—9 km. About 5% of the time the data exhibited an unusual spectral shape that was most pronounced at 105 and 110 km. Instead of being almost Gaussian with only a small hint of two peaks, the spectra are much wider, with two well-developed peaks. After carefully considering the validity of the measurements and their interpretation, we conclude that the unusual spectra are due to greatly enhanced electron temperatures. At 110 km, the electron temperature may increase from 250 K to 800 K, while the ion temperature remains near 250 K. This enhancement of the electron temperature extends from 99 km to at least 116 km. We show that the temperature increase is too large to be accounted for by auroral particle precipitation, though it coincides in time with ion temperature enhancements at altitudes above 125 km. Because these latter enhancements are believed to be due to joule heating, we deduce that electric fields of 24–40 mV/m are present and that the electrons are moving through the ions and neutrals at speeds of 500–800 m/s. Despite these velocities, we find that joule heating of the electrons also cannot account for the elevated electron temperatures. Several consequences of the elevated electron temperatures are discussed. One is that the rate constants for molecular recombination are reduced. Another is that during periods of significant joule heating, the deduced electron density profile, when fully corrected for temperatures, has a significantly lower peak altitude and greater density than that deduced under the usual assumption of equal electron and ion temperatures. Since conductivities, currents, ionization rates, and differential energy spectra are dependent upon the density profile, care must be taken to account properly for the temperature effects when deriving these quantities.

## INTRODUCTION

The interpretation of a large portion of the data acquired with the Chatanika incoherent scatter radar has involved the use of the electron density that comes from the total power in the return signal and the ion velocity that comes from the Doppler shift of the return signal. In this paper we examine the details of the shape of the power spectrum of this returned signal. The spectral shape is the result of the combined effects of electron and ion temperatures, ion mass, and ion-neutral collisions [e.g., *Evans*, 1969]. Because the temperatures and the neutral densities are changing rapidly with altitude in the auroral *E* layer, the data have to be acquired with as good an altitude resolution as possible. A large body of such spectral data was acquired with the multipulse autocorrelator (MAC) [*Rino et al.*, 1974] with a 9-km altitude resolution during the joint American-French plasma line experiments in 1978 [*Kofman and Wickwar*, 1980].

Here we report on an unusual feature of the incoherent scatter spectrum that we observed between 99 and 116 km in a small portion of the data. These unusual spectra are due to greatly increased electron temperatures. This finding was quite unexpected according to a large body of theoretical work [e.g., *Rees and Walker*, 1968; *Walker and Rees*, 1968; *Rees et al.*, 1971]. We, too, cannot account for these elevated electron temperatures by either particle precipitation or joule heating. Nonetheless, the electron temperature enhancements occur simultaneously with strong joule heating of the ions at higher altitudes. Because of the unexpected nature of these temperatures, we have made a considerable effort to ensure that the measurements are good and that the temperature interpretation is correct.

In the next section, we describe the measurements. Then we present the analysis that leads us to believe that these observations are of elevated electron temperatures. We further describe the phenomenon and the conditions under which it occurs. In the final section we discuss these findings and their implications and give our conclusions.

## OBSERVATIONS

The observations were made at Chatanika, Alaska, with the incoherent scatter radar [*Leadabrand et al.*, 1972] pointing along the magnetic field line. *E* region spectral measurements were made simultaneously with *F* region spectral meaurements and plasma line measurements [*Kofman and Wickwar*, 1980]. The *E* region measurements themselves were obtained with a variant of the multipulse technique described by *Rino et al.* [1974]. In this technique a single 60-$\mu$s pulse is transmitted, followed one interpulse period later by a burst of three 60-$\mu$s pulses that begin at 0, 100, and 340 $\mu$s. Samples of the IF acquired at 10-$\mu$s intervals from the first pulse and the multipulse burst enable a 320-$\mu$s autocorrelation function (ACF) to be obtained containing alternate samples of the real and imaginary parts.

[1]Present address is Division of Atmospheric Sciences, National Science Foundation, Washington, D. C. 20550.

[2]Permanent address is Centre d'Etude des Phénomènes Aléatoires et Géophysiques, BP 46, 38402 St. Martin d'Hères, France.



Paper number 1A0077.
0148-0227/81/001A-0077$01.00

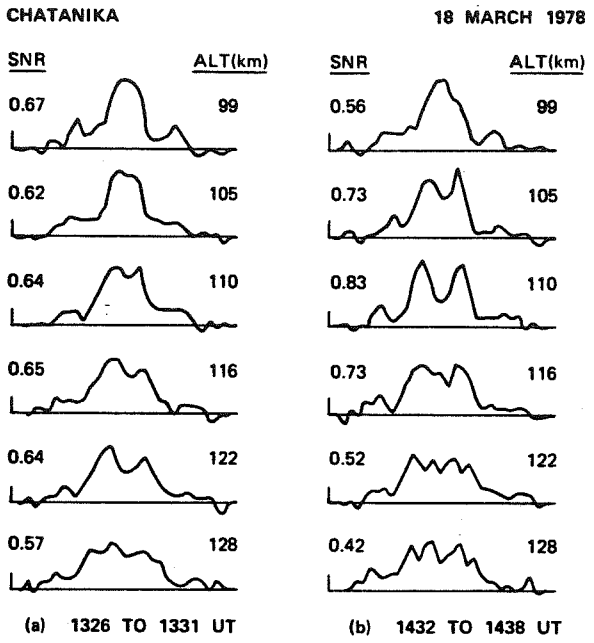


Fig. 1. *E* region spectra from March 18, 1978, obtained with the multipulse autocorrelator using a 60-$\mu$s unipulse followed one interpulse period later by a burst of three 60-$\mu$s pulses that started at 0, 100, and 340 $\mu$s. The spectral window is 50 kHz wide. The two time periods were selected, in part, because of similar signal-to-noise ratios. (*a*) Typical spectra measured between 1326 and 1331 UT. (*b*) Unusual spectra measured between 1432 and 1438 UT. In particular, they are unusual at 105 and 110 km, though at 116 km the spectrum is still considerably wider than that in the earlier time period.

In presenting the observations, we can consider either the ACF or its equivalent Fourier transform, the power spectrum. As an aid to discussion, we present the spectra. In Figure 1*a*, we show typical spectra from a medium-sized auroral layer (i.e., peak density of $2 \times 10^5$ cm$^{-3}$) from 99 to 128 km. They were obtained between 1326 and 1331 UT on March 18, 1978. (Note that 1130 UT is 0130 Alaska Standard Time and is approximately magnetic midnight.) At the two lowest altitudes, the spectra are almost Gaussian. At the next three higher altitudes, they increasingly take on a two-humped shape characteristic of most incoherent scatter spectra. (The bumps in the wings are an artifact of the multipulse technique [*Rino et al.*, 1974].)

In Figure 1*b* we show a similar series of spectra obtained an hour later, between 1432 and 1438 UT on March 18, 1978. They are typical of the unusual spectra that we found. At the four lowest altitudes the spectra are considerably wider than those shown in Figure 1*a*. Much more dramatic, however, is the two-humped nature of the spectra at 105 and 110 km and the very pronounced valley in the center of the spectrum at 110 km. By 128 km the spectra in Figures 1*a* and 1*b* are very similar.

## Analysis and Interpretation

The unknown ionospheric parameters of interest are determined from the measured data by using the ACFIT program [*Lejeune*, 1978, 1979; *de la Beaujardiere et al.*, 1980]. This program performs a nonlinear least squares fit of calculated ACF's to the observed ACF. The procedure is iterative, each calculated ACF being the Fourier transform of the incoherent scatter spectrum calculated for a set of fixed and a set of unknown ionospheric parameters. The unknown variables are incremented after each fit until a convergence criterion is achieved. This procedure produces the best estimate of the unknown ionospheric parameters and their uncertainties. The iterative procedure is a modified steepest descent method [*Bevington*, 1969; *Hagfors*, 1978].

Because some aspects of the analysis of the multipulse data in this mode are different from the analyses described in the literature, we show some of the pertinent steps in the appendix.

The theory incorporated into the program for the calculation of the incoherent scatter spectra includes most known

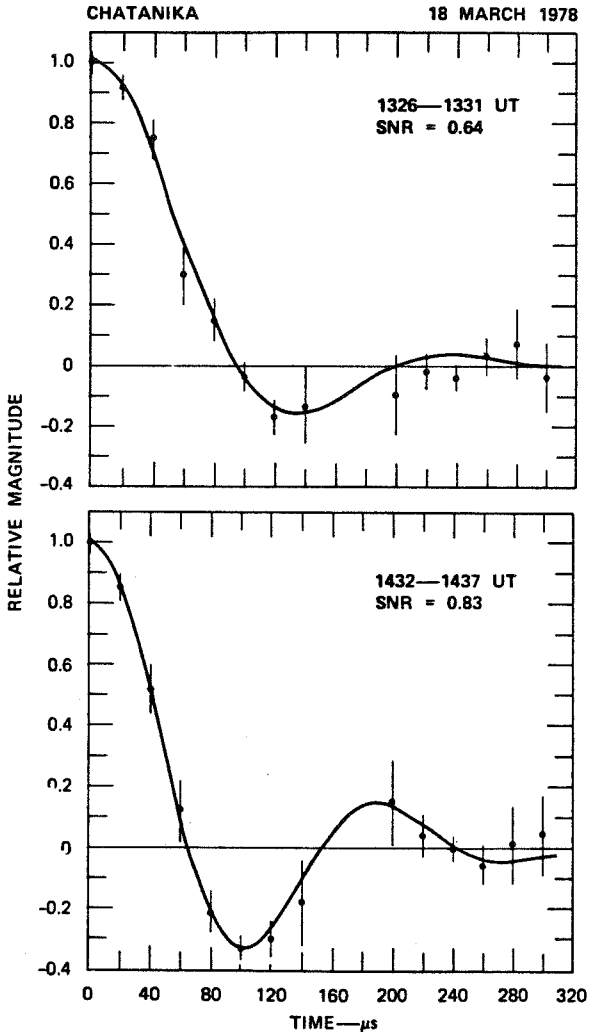


Fig. 2. Fitted and measured normalized autocorrelation functions for 110 km on March 18, 1978. The lines show the real part of the calculated best fit ACF's, Re $\rho_{TH}(t)$, from (A6). The solid circles show the real part of the observed ACF's fully corrected for the complex weighting function, Re $R_{OBS}(t)e^{-i\phi t}$, from (A4) and (A5). The error bars are calculated according to (A8*a*)–(A8*c*) and are scaled by $[S(t)S^*(t)]^{-1}$. The points at 160 and 180 $\mu$s have exceedingly large uncertainties because the magnitude of $S(t)$ is nearly zero. Consequently, they have been omitted. (*a*) Observed and fitted ACF's for the typical period 1326–1331 UT. The values of $N_e$, $T_e$, $T_i$, and $\nu_{in}$ are $2.0 \pm 0.3 \times 10^5$ cm$^{-3}$, 270 ± 30 K, 280 ± 70 K, and 1300 s$^{-1}$ and the fit parameter $\sqrt{\chi_R^2}$ (A7) is 0.72. (*b*) Observed and fitted ACF's for the unusual spectrum observed in the period 1432–1438 UT. The values of $N_e$, $T_e$, $T_i$, $\nu_{in}$, and $\sqrt{\chi_R^2}$ are $2.7 \pm 0.3 \times 10^5$ cm$^{-3}$, 670 ± 50 K, 280 ± 30 K, 1300 s$^{-1}$, and 0.50, respectively. The major difference is the elevated $T_e$.

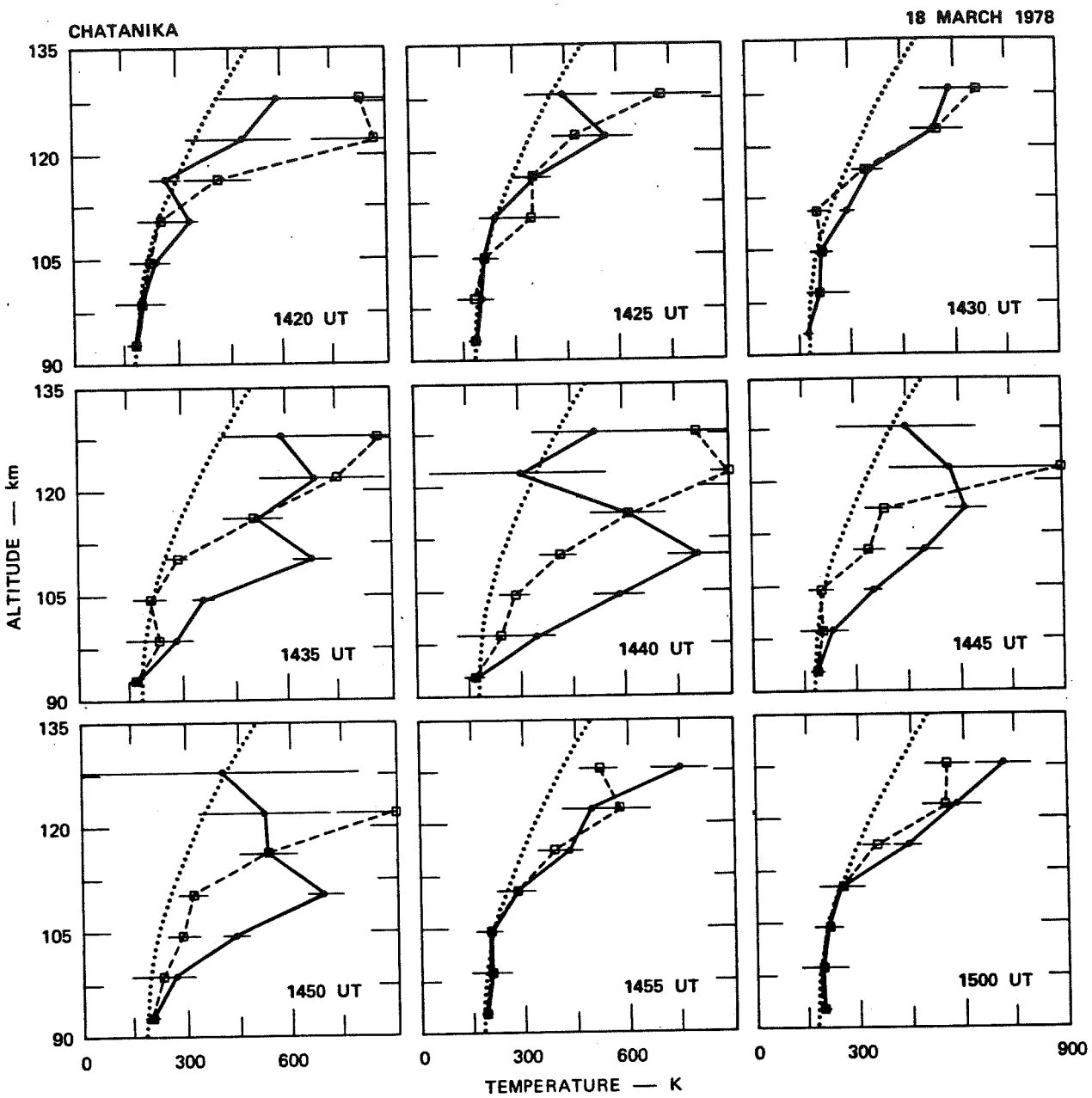


Fig. 3. Sequence of *E* region temperature profiles for March 18, 1978. The dotted curve in each is the temperature profile from the *Jacchia* [1971] model for a 1000 K exospheric temperature. It is an indication of the neutral temperature, but above all it is a convenient reference. The points connected by solid line segments are the electron temperatures. The points connected by dashed line segments are the ion temperatures.

plasma effects that would affect the shape of the spectrum. As a consequence, with ACFIT it is possible, in principle, to determine as many as ten parameters; however, the data are never precise enough to do so. Indeed, the challenge in applying ACFIT is to reduce the number of unknown parameters enough so that the uncertainties in the results are small, while simultaneously retaining enough parameters to adequately describe the physical situation. The most important parameters in the auroral *E* region are the ion velocity, the electron density, the electron and ion temperatures, and the ion-neutral collision frequency. While the ion velocity has little impact on deriving the other parameters, the effects on the spectrum of the last three parameters are strongly coupled. In order to find these parameters, we have had to perform a series of fits so as to determine some of the parameters sequentially rather than simultaneously.

Our procedure has taken advantage of the fact that the ion-neutral collision frequency $\nu_{in}$ is the most stable variable. Its mean profile was found from seven nights in March 1978 by selecting periods when we could assume that the electron and ion temperatures were equal between 93 and 116 km—i.e., periods when there was no joule heating and little precipitation. The resultant profile is similar to that obtained from the *Jacchia* [1971] model of the neutral atmosphere, for a 1000 K exospheric temperature, and with the collision frequencies for momentum transfer in the rest frame of the ions [*Schunk and*

*Walker*, 1973]. Given these $\nu_{in}$, we were then able to refit the data, this time allowing the electron temperatures $T_e$ to differ from the ion temperatures $T_i$.

In Figure 2*a* we show the quality of the fit for the "typical" data corresponding to the spectrum in Figure 1*a* for 110 km. The solid circles and error bars are derived from the real part of the measured ACF, and the solid line represents the theoretical ACF (see appendix). In Figure 2*b* we show the fit to the unusual data corresponding to the spectrum in Figure 1*b* for 110 km. The quality of the fit is just as good as it is for the "typical" data. However, to obtain the fit to the unusual spectrum, a much higher $T_e$ is required: 675 K for Figure 2*b* versus 260 K for Figure 2*a*. There is very little change in $T_i$.

Thus a straightforward fit to the data yields an elevated electron temperature. Because such incresaes are unexpected, an important question is whether this interpretation is unique. We have calculated many theoretical spectra and have experimented with the fits to examine this question. The initial values of $T_e$ and $T_i$ used for the first iteration have no effect on the results for most of the fits. Also, at the altitude of the greatest temperature effect (110 km), and because the radar frequency is high (1290 MHz), the ion-neutral collision frequency has very little effect on the deduced electron temperature. A 25% variation in $\nu_{in}$, which is large compared to what has been seen at lower latitudes, has less than a 3% effect on $T_e$. If the ion and electron temperatures are forced to be more equal, $\nu_{in}$ is reduced by an unacceptable amount. Indeed, if they are kept equal, the ACFIT program attempts to make the $\nu_{in}$ negative (which is how we found the phenomenon). If there were meteoric ions present, for example, $Mg^+$ and $Fe^+$, the spectrum would be narrower and the ACF wider, with the effect that the deduced electron temperature, which assumes a 30.5-amu ion, would be decreased instead of increased. An ion with considerably less mass would be required to deduce an elevated electron temperature, but then the ion temperature would be reduced to unacceptable values because the deduced temperature ratio is not a strong function of ion mass. Thus for the known dependence of the incoherent scatter spectrum upon the variables tested, we conclude that $T_e$ is much greater than $T_i$.

By examining the analyzed data we can learn more about the reasonableness of the deduced electron temperatures and the possible presence of spurious artifacts that would affect the analysis. In Figure 3 we present the electron and ion temperature profiles around and during an isolated electron heating event on March 18, 1978, as well as the *Jacchia* [1971] temperature profile for a 1000 K exospheric temperature. In Figure 4 we present similar data from a selected period on November 19, 1978, encompassing another electron heating event. During this second period the temporal behavior is more complex. (We believe that the decrease in $T_e$ and $T_i$ in going from 93 to 99 km in November is due to our use of a $\nu_{in}$ profile optimized for March.) On both days we have periods of minimum $T_e$ (and $T_i$): 1425, 1430, 1455, and 1500 UT in March and 1305, 1308, 1337, and 1342 UT in November. The other profiles show the phenomenon of interest, the elevated $T_e$ in the vicinity of 105 and 110 km. There are particularly large enhancements at 1440 and 1450 UT in March and at 1217, 1237, and 1327 UT in November. The ion temperatures, as mentioned previously, appear practically unchanged at these altitudes when the large $T_e$ are found. This behavior supports the idea that the fitting procedure has correctly identified $T_e$ as the cause for the unusual spectra and ACF's.

The largest $T_e$ increases are always at 110 km, although substantial increases often occur at 105 km. In most of the largest events listed above, there is an indication of elevated $T_e$ at both 99 and 116 km. Unfortunately, the measurements at 99 km are not individually precise enough to ensure that $T_e$ is elevated, but collectively they do suggest that there is an enhancement. The situation at 116 km is complicated, because $T_e$ enhancements can occur at 116 km and higher due to the loss of energy from auroral primaries and secondaries [*Rees and Walker*, 1968]. However, a comparison of the data at 1237 and 1305 UT in November shows that another heat source in addition to energetic and secondary electrons is needed to account for $T_e$ at 1237 UT. While there is more energetic electron precipitation depositing energy at 116 km at 1305 UT than at 1237 UT, the electron temperature is higher at 1237 UT.

If we go low enough in altitude, to 93 km, we find very little variation in the electron temperature. This is particularly true for the data from March, which have a more appropriate $\nu_{in}$ model and a better signal-to-noise ratio (SNR). The constancy of the spectra (and ACF's) at this altitude provides a good indication that the whole radar system is working properly throughout the observing period. While this is perhaps the best such measure, another one is that our goodness of fit parameter, $\sqrt{\chi_R^2}$ (see appendix), stays at its unusual value, close to 1, on both sides and during the elevated $T_e$ events.

When we go up in altitude, above the region of $T_e$ increase, we see other differences in the behavior of the temperature profiles during the period of the $T_e$ increase. The major effect is that the ion temperature increases greatly at 122 and 128 km (to the point that it is greater than the arbitrary 900 K temperature maximum used in Figures 3 and 4). It may even incresae at 116 km. There also appears to be a reduction in the electron temperature. These effects can be better examined by reference to Figures 5 and 6 for March 18, 1978, and November 19, 1978, respectively. The bottom curve in these figures shows the temporal variation of $T_e$ at 110 km. The middle curve shows the temporal variation of $T_i$ at 163 km. The top two curves show the variation of the electron density at 110 km and at either 99 km or 105 km. The most striking feature of these figures is the correlation between the $T_e$ at 110 and the $T_i$ at higher altitude.

In a brief aside, we need to mention that the ion temperatures at 163 km were found using another correlator and a single long pulse, 320 $\mu$s. The ion composition was assumed to be 29% $O^+$ and 71% of our fictitious molecular ion of mass 30.5. This composition is reasonable under many conditions but most likely underestimates the proportion of molecular ions during joule heating events [*Kelly and Wickwar*, 1981]. Regardless of the exact ion composition, there is a strong correlation between $T_e$ and $T_i$. The choice of 163 km was somewhat arbitrary. The temporal variation at 213 km is practically identical. At higher altitudes the same structures remain, but there are other underlying trends in the data.

From other work where temperatures could be determined simultaneously with ion velocities perpendicular to the magnetic field [*Wickwar*, 1975; *de la Beaujardiere et al.*, 1981; *Kelly and Wickwar*, 1981], we know that the elevated ion temperatures are the result of joule heating. Therefore, this comparison tells us that the elevated electron temperatures near 110 km occur during particular ionospheric conditions, namely, joule heating situations.

We can estimate the ion velocity and the electric field from

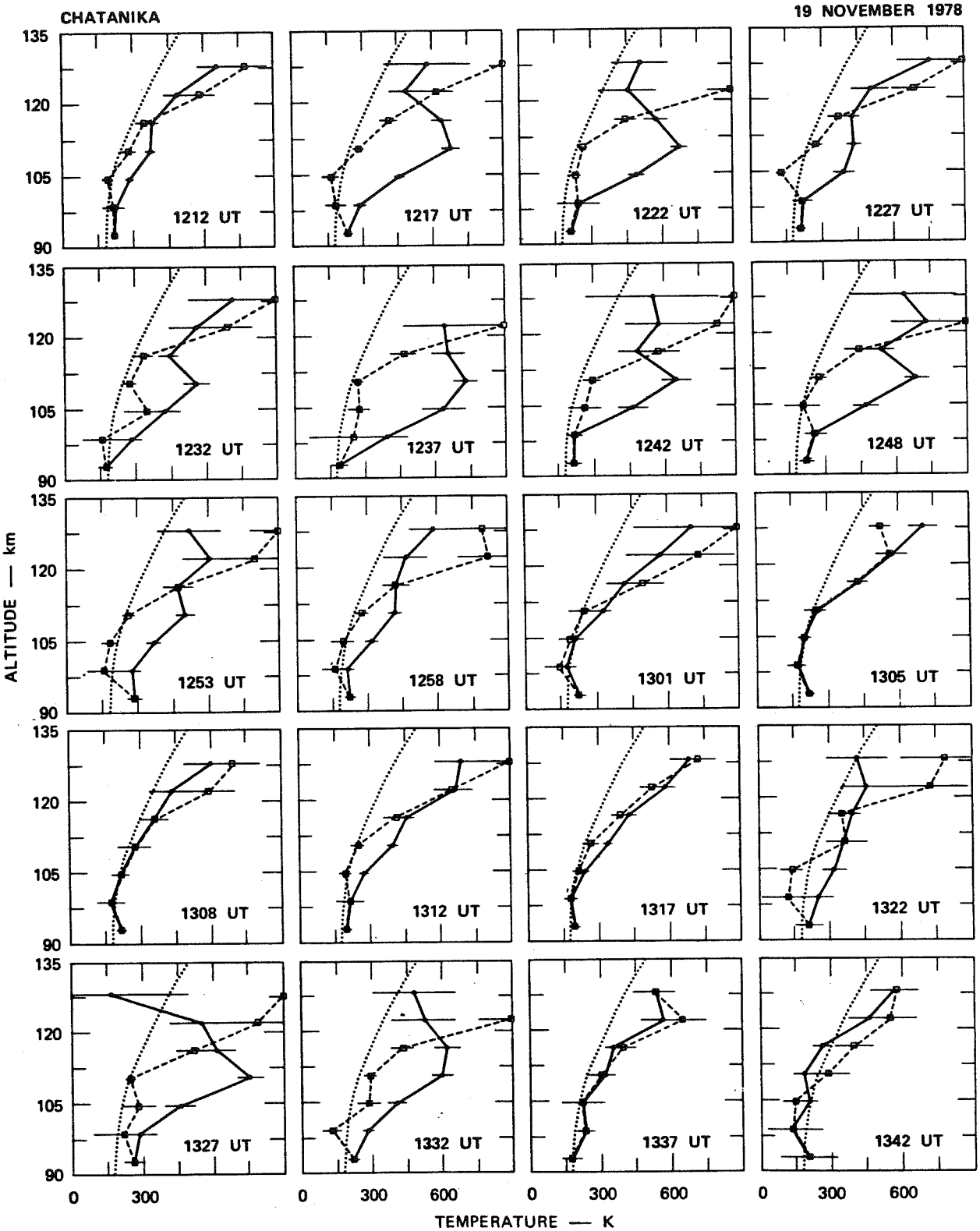


Fig. 4. Sequence of *E* region temperature profiles for November 19, 1978. The dotted curve in each is the temperature profile from the *Jacchia* [1971] model for a 1000 K exospheric temperature. It is an indication of the neutral temperature, but above all it is a convenient reference. The points connected by solid line segments are the electron temperatures. The points connected by dashed line segments are the ion temperatures.

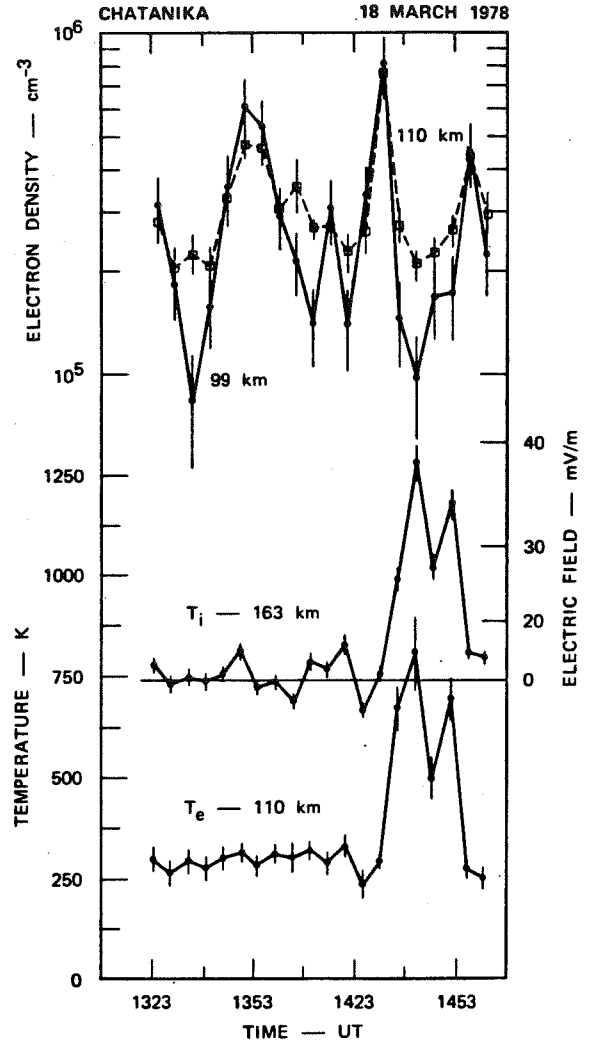


Fig. 5. Time variation of electron and ion temperatures and electron density on March 18, 1978. The bottom two curves show the covariation of $T_e$ at 110 km and $T_i$ at higher altitudes. The electric field scale is based on joule heating of the ions with stationary neutrals. The top two curves show the electron density variation at 99 and 110 km.

the ion temperature increase. Under steady state conditions and when heating by electrons can be omitted (as it can at 163 km), the difference between the ion and neutral temperatures for joule heating is given by [*Schunk*, 1975]

$$T_i - T_n = c_i(\mathbf{v} - \mathbf{u})^2 \quad (1)$$

where $\mathbf{v}$ is the ion velocity, $\mathbf{u}$ is the neutral velocity, and $c_i$ for each ion depends on the relative distribution of neutral constituents. At 163 (for the data in Figures 5 and 6), $c_i$ is approximately $8.5 \times 10^{-4}$ K s$^2$/m$^2$ for $O^+$ and $9.3 \times 10^{-4}$ K s$^2$/m$^2$ for $NO^+$ and $O_2^+$. For our purposes we can neglect the differential ion heating and use a value of $9 \times 10^{-4}$ K s$^2$/m$^2$. We will further assume that the neutrals are stationary. Then

$$T_i - T_n \simeq 9 \times 10^{-4} v^2 \quad (2)$$

enables us to estimate the ion velocity. Furthermore, above about 150 km the ion equation of motion is

$$\mathbf{v} = -\mathbf{E} \times \mathbf{B} \quad (3)$$

enabling us to estimate the electric field. Assuming that the field lines are equipotentials and noting that (3) is also the electron equation of motion above about 80 km, then (2) applied to ions near 165 km also gives a good estimate of the electron velocity above 85 km.

In Figures 5 and 6 we have drawn lines near the lowest ion temperatures to indicate the estimated $T_n$. We have then marked an electric field along the right axis according to (2) and (3). The velocities in meters per second are numerically 20 times the electric field in millivolts per meter. There are clear cases of elevated electron temperatures for electric fields of 25–40 mV/m or electron velocities of 500–800 m/s. These are large electric fields and velocities.

It would be practically impossible to find a problem in the radar system or in the analysis that could at the same time cause a $T_e$ increase in one altitude region and a $T_i$ increase in another. Thus the fact that we can correlate the occurrence of this low-altitude electron heating to another physical phenom-

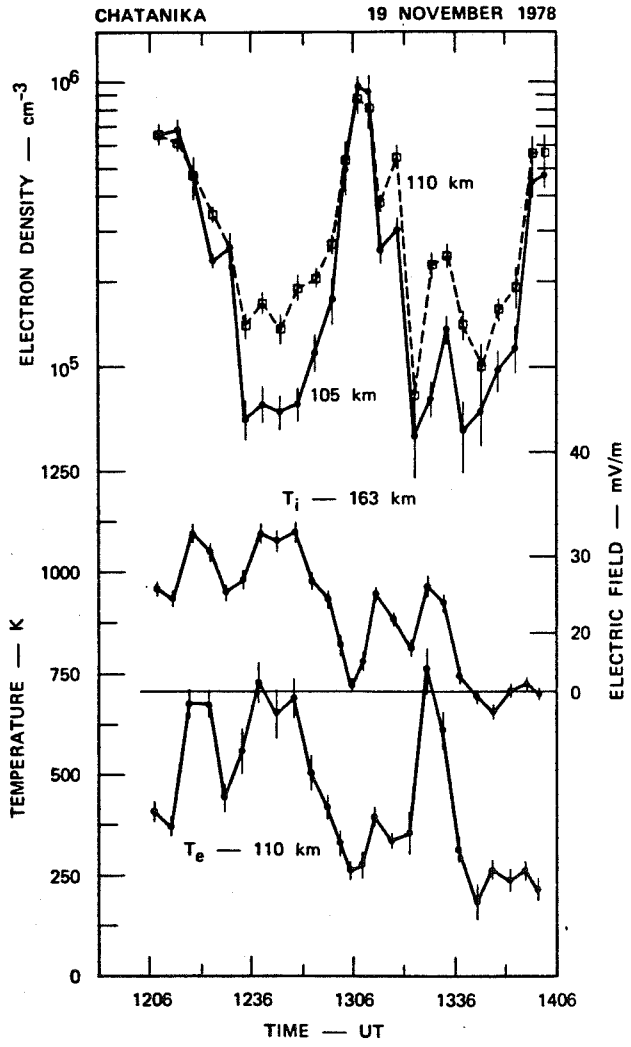


Fig. 6. Time variation of electron and ion temperatures and electron density on November 19, 1978. The bottom two curves show the covariation of $T_e$ at 110 km and $T_i$ at higher altitudes. The electric field scale is based on joule heating of the ions with stationary neutrals. The top two curves show the electron density variation at 105 and 110 km.

enon, the occurrence of joule heating, should remove any lingering doubt about the reality of the $T_e$ measurements.

The electron density curves, one at 110 km and one at a lower altitude where there is still substantial ionization, show no correlation with the elevated electron temperatures near 110 km. Between 1323 and 1425 UT in March there is practically no variation in $T_e$ despite large variations in electron density that lead us to infer an approximate factor-of-six variation in the energy input from energetic electrons [*Wickwar et al.*, 1975]. Indeed the elevated electron temperatures occur at a time when the electron density is nearly a minimum. In November the situation is similar. The highest densities, at the two ends and in the middle of the time period, coincide with some of the lowest electron temperatures. The high electron temperatures between 1237 and 1253 and between 1327 and 1332 UT occur in periods of low, though not the lowest, electron densities, while the high temperatures between 1217 and 1222 occur during a period of decreasing electron density. This lack of correlation between electron density and elevated electron temperature is the principal evidence that the elevated temperatures are not due to particle precipitation.

The electron densities, however, do suggest something about the situations under which joule heating occurs. Joule heating is not collocated with auroral arcs (where the densities approach $10^6$ cm$^{-3}$) but rather occurs in regions of reduced ionization, often adjacent to an arc.

## DISCUSSION AND CONCLUSIONS

Because of the unexpected magnitude of the elevated electron temperatures, we have gone to considerable length in the previous section to establish the reality of the observations and to establish their interpretation as elevated electron temperatures. Such temperatures may have been seen previously with in situ rocket measurements [*Ulwick et al.*, 1968]. They appear in the data presented by *Schlegel et al.* [1980] and are discussed in a parallel effort to this one by *Schlegel and St.-Maurice* [1981].

Given these temperatures, one of the immediate questions is that of the energy source. From the lack of correlation between the electron densities and the electron temperatures as discussed in the previous section, it is apparent that the energy source is not the incident flux of primary electrons. Instead, the correlation with higher-altitude ion temperatures indicates a relationship with joule heating. Yet the works by *Rees and Walker* [1968] and *Schunk and Walker* [1971] show that joule heating of the electrons is negligibly small. Our calculations, which show energy loss rates due to the rotational excitation of $N_2$ and $O_2$ to be much greater than those due to electron joule heating, confirm these theoretical results for our particular situation. Nonetheless, the electron heating and joule heating are very closely related in that we see the heating when there are 25- to 40-mV/m electric fields or, equivalently, when

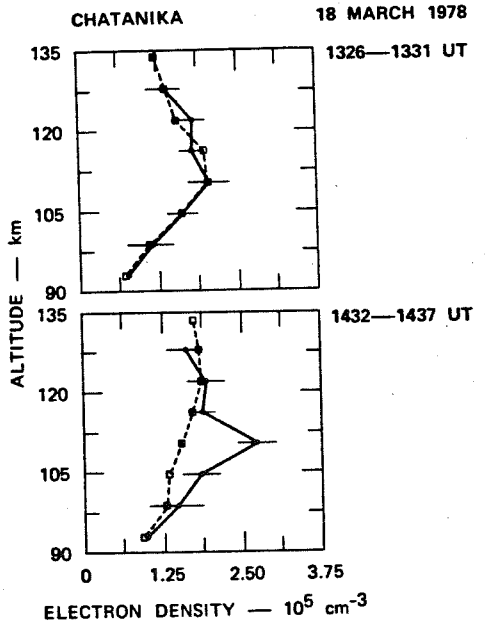


Fig. 7. Raw and corrected electron density profiles for March 18, 1978. The squares connected by dashed lines show the raw density measurements. The circles connected by solid lines show the fully corrected density measurements. (*a*) Profiles from the typical period, 1326–1331 UT, are indistinguishable. (*b*) The fully corrected profile from the unusual period, 1432–1437 UT, has its peak density at a significantly lower altitude, and the value is twice as great.

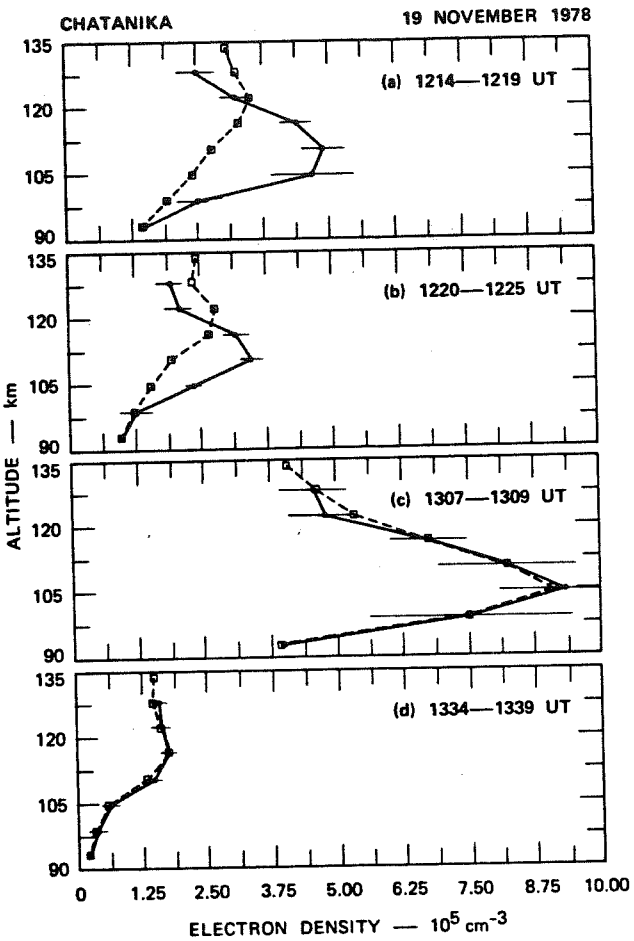


Fig. 8. Raw and corrected electron density profiles for November 19, 1978. The squares connected by dashed lines show the raw density measurements. The circles connected by solid lines show the fully corrected density measurements. For the two later time periods, the two profiles are indistinguishable. For the two earlier time periods, there are large differences. Near 110 km, the much larger densities are due primarily to the elevated electron temperatures. Above 120 km, the lower densities are due primarily to the elevated ion temperatures.

the electrons have a velocity relative to the ions and neutrals of 500–800 m/s. These large differential velocities might give rise to an instability [*Farley*, 1963]. This possibility is being explored by *Schlegel and St.-Maurice* [1981] and *St.-Maurice et al.* [1981].

Recently, it has been proposed that there is a plasma instability effective in producing pulsating auroras [*Stenbaek-Nielsen and Hallinan*, 1979]. It would have to be a different instability than the one required here. In the case of those auroras, the emitting layer was less than 2 km in extent. In our case, as previously discussed, our altitude resolution enables us to be sure that the electron heating extends over an altitude region of at least 15 km. Furthermore, pulsating auroras are not associated with joule heating events.

Another important question to consider is the implication that elevated electron temperatures have for *E* region aeronomy. The electron temperature affects the recombination rates of molecular ions and hence calculations of the energy input or ion production rate due to auroral primary and secondary electrons [*Wickwar et al.*, 1975; *Vondrak and Baron*, 1976; *Oran et al.*, 1981]. The recombination rates drop by about 25% for an electron temperature increase from 250 to 750 K [*Oran et al.*, 1981].

There is an indirect way in which these temperatures can affect the interpretation of incoherent scatter auroral *E* region data. To date, most *E* region density data determined with the Chatanika radar have assumed that the electron-to-ion temperature ratio was unity. When the temperature ratio is not unity, there can be large corrections that affect both the magnitude of the *E* region peak density and the altitude of the maximum. In Figures 7 and 8, for March 18, 1978, and November 19, 1978, respectively, we show examples of electron density profiles. In Figure 7 at 1325 UT there is good agreement between the raw and the fully corrected densities. Similarly, in Figure 8 at 1308 and 1337 UT there is good agreement. But at 1435 UT in Figure 7 and 1217 and 1222 UT in Figure 8 there is a very great difference between the raw and the fully corrected profiles.

Thus during periods of joule heating there can be significant errors in the derivation of many ionospheric parameters unless the temperatures are measured and the appropriate corrections made. To emphasize this point we give several examples. Since the conductivities are proportional to $N_e$, the conductivities near 110 km could double. Because of different conductivity altitude profiles, the ratio of integrated Hall to Pedersen conductivities would increase. Similarly, the deduced currents near 110 km could double. Since the ion production rate is proportional to the electron density squared, the deduced production rate or energy input from energetic particles would increase near 110 km by a factor of 3. (It is not a factor of 4 because the recombination rate is reduced about 25%.) As a consequence, the total energy input would increase substantially, and the deduced spectrum of auroral primary electrons would be shifted considerably toward higher energies.

In conclusion, we have on occasion measured unusual spectra near 110 km that are of ionospheric origin and that can be interpreted only as enhanced electron temperatures. These large temperatures below 116 km cannot be accounted for by either particle precipitation or joule heating; yet they occur simultaneously with large joule heating events. Enhanced electron temperatures will have effects on the *E* region aeronomy, such as causing reduced recombination rates. They must also be taken into account for the interpretation of the incoherent scatter data during periods of joule heating.

## APPENDIX: SIGNAL PROCESSING AND THE LEAST SQUARES FIT

In performing the nonlinear least squares fit, we have to allow for the fact that the ACF of the scattering medium $\rho_{TH}(t)$ is distorted by the pulse sequence and the effective filter passband. Ignoring noise and assuming appropriate normalization, the observed ACF is

$$\rho_{OBS}(t) = \int \rho_{TH}(\tau) W(\tau) R_H(t-\tau)\, d\tau \tag{A1}$$

where $W(t)$ is the ACF of the transmitted pulse pattern and $R_H(t)$ is the ACF of the filter impulse response [*Farley*, 1969; *Zamlutti and Farley*, 1975; *Rino*, 1978].

For the low-altitude *E* region measurements, $\rho_{TH}(t)$ varies slowly compared to $R_H(t)$. Therefore $R_H(t)$ can be considered as a $\delta$ function compared to $\rho_{TH}(t)$, enabling us to approximate (A1) by

$$\rho_{OBS}(t) = \rho_{TH}(t) \int W(\tau) R_H(t-\tau)\, d\tau \tag{A2}$$

Let us define a complex weighting function

$$S(t) = \int W(\tau) R_H(t-\tau)\, d\tau \tag{A3}$$

which includes the instrumental effects and can be determined to great precision.

Instead of correcting the theoretical ACF of the scattering medium for $S(t)$ on each iteration in the least squares fit, we scale the observed ACF by the modulus of $S(t)$,

$$R_{OBS}(t) = \rho_{OBS}(t)/[S(t)S^*(t)]^{1/2} \tag{A4}$$

Since the theoretical ACF is initially calculated with the assumption of no Doppler shift, we do have to correct each term for the ion velocity. At that time, we also correct $\rho_{TH}(t)$ for the phase,

$$\varphi = \tan^{-1}\left[\frac{\text{Im } S(t)}{\text{Re } S(t)}\right] \tag{A5}$$

introduced by $S(t)$. Thus, ignoring the ion velocity, we create

$$R_{TH}(t) = \rho_{TH}(t) e^{i\varphi} \tag{A6}$$

In the least squares fitting procedure we then vary the fitting parameters determining $\rho_{TH}(t)$, hence $R_{TH}(t)$, so as to obtain the best match between $R_{OBS}(t)$ and $R_{TH}(t)$. The fit minimizes the reduced chi square,

$$\chi_R^2 = \sum_{i=0}^{31} \left\{ \frac{[R_{OBS}(i) - R_{TH}(i)]^2}{\sigma^2(i)/[S(i)S^*(i)]} \right\} \Big/ (32 - N) \tag{A7}$$

where $N$ is the number of parameters being fitted and $\sigma^2(i)$ is the estimate of the variance of $\rho_{OBS}$, which will be given below. Because of the direct IF sampling, only the real parts of $R_{OBS}$ and $R_{TH}$ will be compared for $i$ even and only the imaginary parts for $i$ odd. So long as $\chi_R^2$ is reduced by each iteration, the iterations continue until the calculated increment for every fitting parameter is less than 25% of the uncertainty of that parameter. A maximum of six good iterations is performed.

The variance for each lag $\sigma^2(i)$ is estimated from the real part of the observed ACF. The real part is interpolated to obtain its value at the time when only the imaginary component is observed. The variance is given by

$$\sigma^2(0) = \frac{2}{N_{\text{pulse}}}\left\{1 + \frac{2}{\text{SNR}} + \frac{2}{(\text{SNR})^2}\right\} \quad \text{(A8a)}$$

for the zero lag,

$$\sigma^2(i) = \frac{1}{N_{\text{pulse}}}\left\{\rho_{\text{OBS}}{}^2(i) + 1 + \frac{2}{\text{SNR}} + \frac{2}{(\text{SNR})^2}\right\} \quad \text{(A8b)}$$

for the other unipulse lags ($1 \le i \le 5$), and

$$\sigma^2(i) = \frac{1}{N_{\text{pulse}}}\left\{\rho_{\text{OBS}}{}^2(i) + 9 + \frac{6}{\text{SNR}} + \frac{2}{(\text{SNR})^2}\right\} \quad \text{(A8c)}$$

for the remaining lags, where $N_{\text{pulse}}$ is the number of transmitted pulses and SNR is the signal-to-noise ratio.

As we go above about 120 km under 'normal' $E$ region conditions or when we have the elevated electron temperatures, we can no longer assume that $\rho_{\text{TH}}(t)$ varies more slowly than $R_H(t)$. The approximation enabling us to obtain (A2), then, breaks down. Instead, we use the Fourier transform of (A1):

$$s_{\text{OBS}}(f) = H(f)\int w(f - f')s_{\text{TH}}(f')\,df' \quad \text{(A9)}$$

where $H(f)$ is the filter spectrum and $w(f)$ is the spectrum of the transmitted pulse. We now inverse-filter the observed spectrum,

$$s'(f) = s_{\text{OBS}}(f)/H(f) \quad \text{(A10)}$$

and Fourier transform back to the time domain,

$$\rho'(t) = W(t)\rho_{\text{TH}}(t) \quad \text{(A11)}$$

For the least squares fit we define

$$R_{\text{OBS}}(t) = \rho'(t)/W(t) \quad \text{(A12)}$$

Ignoring ion velocity, it is this $R_{\text{OBS}}$ that is compared to the theoretical ACF in the least squares fitting procedure as previously described.

This simpler procedure, based on (A9), is not applicable at the lower altitudes because the longer correlation time of the medium leads to nonzero values for the last lags. In the transition zone above 120 km, where we pass from the applicability of the method involving the complex weighting function to the method involving inverse filtering, the difference between the answers is not great. The electron and ion temperatures near 110 km are about 10% greater with the complex weighting function method. The electron density is virtually unchanged. All the data presented here were found using the complex weighting function method. However, for the large electron temperatures, the correlation time is decreased enough that the inverse filtering method would be more appropriate. At most, the electron temperatures are overestimated due to this effect by about 5%.

*Acknowledgments.* We would like to thank the staff members at SRI International and CEPHAG who made these joint experiments and collaboration possible. In particular, we would like to thank J. Kelly, M. McCready, C. Code, and C. D. Feken for their assistance at Chatanika and C. Dawson and C. Leger for programming. The French portion of the experiment was supported by the Actions Thematiques Programmees of the Centre National de la Recherche Scientifique for the International Magnetospheric Study. It was supported, as well, by the Centre de Recherches en Physique de l'Environnement Terrestre et Planetaire and by the Centre National d'Etudes des Telecommunications. The American portion was supported by grants ATM78-00129 and ATM78-23658 from the Aeronomy Program, Division of Atmospheric Sciences, National Science Foundation. In addition, the Chatanika radar was operated by SRI International under contract DNA001-77-C-0042 from the Defense Nuclear Agency and grant ATM72-01644-A05 from the Division of Atmospheric Sciences, National Science Foundation.

The Editor thanks J. V. Evans and E. Fontheim for their assistance in evaluating this paper.

## REFERENCES

Bevington, P. R., *Data Reduction and Error Analysis for the Physical Sciences,* McGraw-Hill, New York, 1969.

de la Beaujardiere, O., V. B. Wickwar, C. A. Leger, M. McCready, and M. J. Baron, The software system for the Chatanika incoherent scatter radar, technical report, 117 pp., SRI Int., Menlo Park, Calif., 1980.

de la Beaujardiere, O., R. R. Vondrak, R. A. Heelis, W. B. Hanson, and R. Hoffman, Auroral arc electrodynamic parameters measured by AE-C and the Chatanika radar, *J. Geophys. Res., 86,* in press, 1981.

Evans, J. V., Theory and practice of ionosphere study by Thomson scatter radar, *Proc. IEEE, 57,* 469–530, 1969.

Farley, D. T., A plasma instability resulting in field-aligned irregularities in the ionosphere, *J. Geophys. Res., 68,* 6083–6097, 1963.

Farley, D. T., Incoherent scatter correlation function measurements, *Radio Sci., 4,* 935–953, 1969.

Hagfors, T., Least mean square fitting of data to physical models, *EISCAT Tech. Note 78/2,* Kiruna, Sweden, 1978.

Jacchia, L. G., Revised static models of the thermosphere and exosphere with empirical temperature profiles, *Spec. Rep. 332,* Smithson. Astrophys. Observ., Cambridge, Mass., 1971.

Kelly, J. D., and V. B. Wickwar, Radar measurements of high-latitude ion composition between 140 and 300 km, submitted to *J. Geophys. Res.,* 1981.

Kofman, W., and V. B. Wickwar, Plasma line measurements at Chatanika with high-speed correlator and filter bank, *J. Geophys. Res., 85,* 2998–3012, 1980.

Leadabrand, R. L., M. J. Baron, J. Petriceks, and H. F. Bates, Chatanika, Alaska, auroral-zone incoherent-scatter facility, *Radio Sci., 7,* 747–756, 1972.

Lejeune, G., EISCAT data analysis, *Rep. 36/78,* Centre d'Etude des Phénomènes Aléatoires et Géophys., St. Martin d'Hères, France, 1978.

Lejeune, G., A program library for incoherent scatter calculation, *EISCAT Tech. Note 79/18,* Kiruna, Sweden, 1979.

Oran, E. S., V. B. Wickwar, W. Kofman, and A. Newman, Auroral plasma lines: A first comparison of theory and experiment, *J. Geophys. Res., 86,* 199–205, 1981.

Rees, M. H., and J. C. G. Walker, Ion and electron heating by auroral electric fields, *Ann. Geophys., 24,* 193–199, 1968.

Rees, M. H., R. A. Jones, and J. C. G. Walker, The influence of field-aligned currents on auroral electron temperatures, *Planet. Space Sci., 19,* 313–325, 1971.

Rino, C. L., Incoherent scatter radar signal processing techniques, technical memo, SRI Int., Menlo Park, Calif., 1978.

Rino, C. L., M. J. Baron, G. H. Burch, and O. de la Beaujardiere, A multipulse correlator design for incoherent scatter radar, *Radio Sci., 9,* 1117–1127, 1974.

Schlegel, K., and J. P. St.-Maurice, Anomalous heating of the polar $E$ region by unstable plasma waves, I, Observations, *J. Geophys. Res., 86,* 1447–1452, 1981.

Schlegel, K., H. Kohl, and K. Rinnert, Temperatures and collision frequency in the polar $E$ region measured with the incoherent scatter technique, *J. Geophys. Res., 85,* 710–714, 1980.

Schunk, R. W., Transport equations for aeronomy, *Planet. Space Sci., 23,* 437–485, 1975.

Schunk, R. W., and J. C. G. Walker, Transport processes in the $E$ region of the ionosphere, *J. Geophys. Res., 76,* 6159–6171, 1971.

Schunk, R. W., and J. C. G. Walker, Theoretical ion densities in the lower atmosphere, *Planet. Space Sci., 21,* 1875–1896, 1973.

Stenbaek-Nielsen, H. C., and T. J. Hallinan, Pulsating auroras: Evi-

dence for noncollisional thermalization of precipitating electrons, *J. Geophys. Res., 84,* 3257–3271, 1979.
St.-Maurice, J. P., and K. Schlegel, Anomalous heating of the polar *E* region by unstable plasma waves, II, Theory, *J. Geophys. Res., 86,* 1453–1462, 1981.
Ulwick, J. C., W. Pfister, and K. D. Baker, Rocket measurements of Bremsstrahlung x-rays and related parameters during auroral absorption events, *Space Res., 8,* 171–177, 1968.
Vondrak, R. R., and M. J. Baron, Radar measurements of the latitudinal variations of auroral ionization, *Radio Sci., 11,* 939–946, 1976.
Walker, J. C. G., and M. H. Rees, Ionospheric electron densities and temperatures in aurora, *Planet. Space Sci., 16,* 459–475, 1968.
Wickwar, V. B., Chatanika radar measurements, in *Atmospheres of Earth and the Planets,* pp. 111–124, D. Reidel, Hingham, Mass., 1975.
Wickwar, V. B., M. J. Baron, and R. D. Sears, Auroral energy input from energetic electrons and joule heating at Chatanika, *J. Geophys. Res., 80,* 4364–4367, 1975.
Zamlutti, C. J., and D. T. Farley, Incoherent scatter multiple-pulse measurements at Arecibo, *Radio Sci., 10,* 573–580, 1975.

(Received July 1, 1980;
revised December 16, 1980;
accepted December 17, 1980.)

# ARTICLE 7

JOURNAL OF GEOPHYSICAL RESEARCH, VOL. 91, NO. A2, PAGES 1619–1626, FEBRUARY 1, 1986

# Ionospheric Ion Heating by ULF Pc 5 Magnetic Pulsations

C. LATHUILLERE, F. GLANGEAUD, AND Z. Y. ZHAO[1]

*Centre d'Etudes des Phénomènes Aléatoires et Géophysiques, Saint-Martin-d'Hères, France*

Frictional heating of the ions resulting from dc ionospheric electric fields is experimentally and theoretically well known. We extend these results to ion heating due to ULF magnetic pulsations of periods as low as 3 min. Ion temperature fluctuations as measured by the European incoherent scatter facility are very well correlated to magnetic Pc 5 pulsations. We present a method which estimates these ion temperature enhancements from ion velocity measurements.

## 1. INTRODUCTION

Damping sources of geomagnetic pulsations include ionospheric Joule dissipation [*Newton et al.*, 1978]. Observational evidence of this damping mechanism was reported by *Greenwald and Walker* [1980] and more recently by *Glassmeier et al.* [1984] who deduce from the damping constant of the pulsation, the ionospheric Pedersen conductivity. We shall present in this paper direct measurements of the ionospheric ion heating due to ULF pulsations.

It is well known that dc electric fields in the ionosphere drive the ions through the neutral gas, resulting in frictional heating of the ions [*Stubbe and Chandra*, 1971]. In the *F* region, the ion energy equation can be simplified as

$$T_i - T_n = \frac{m_n}{3k_b}(\mathbf{V}_i - \mathbf{V}_n)^2 + \left(\frac{m_i + m_n}{m_i}\right)\frac{\nu_{ie}}{\nu_{in}}(T_e - T_i) \qquad (1)$$

(see *St.-Maurice and Hanson* [1982] for theoretical justification).

In this equation $T_i$, $T_n$ and $T_e$ are, respectively, the ion, neutral and electron temperatures, $m_i$ and $m_n$ are the ion and neutral mass, $\nu_{ie}$ and $\nu_{in}$ are the ion-electron and ion-neutral momentum transfer collision frequencies, $k_B$ is the Bolzman constant and $\mathbf{V}_i$ and $\mathbf{V}_n$ are the ion and neutral velocities. The first term of the right-hand side of equation (1) represents the frictional heating, and the second term is the electron heat exchange term which is usually neglected in the *F* region [*Baron and Wand*, 1983; *Perraut et al.*, 1984]. As the time constant for temperature changes in the *F* region is of the order of seconds to a few tens of seconds, Pc 5 magnetic pulsations (periods greater than 150 s) will also result in ion temperature variations.

Using measurements from the European incoherent scatter (EISCAT) facility [*Folkestad et al.*, 1983], we will show such ion temperature variations due to Pc 5 pulsations of periods as low as 3 min, recorded during 4 different days of experiments.

Observations of ion velocity and ion temperature fluctuations related to magnetic pulsations are presented in the first part of the paper. Then the Wiener filter method, that we used for correlation studies between two signals, is described by showing an example of the study of east-west extension of the pulsations in the ionosphere.

The same method is applied to velocity and temperature measurements in order to estimate the ion temperature enhancements related to the velocity fluctuations: theoretical justifications are given in section 4. Results are presented for the 4 days of measurements, and a comparison is made between the theoretical expression of the heating process (equation (1)) and the experimental relation.

## 2. OBSERVATIONS

Figure 1 describes the EISCAT configuration used for ionospheric pulsation studies. The Tromsö antenna beam looks in a fixed position toward east, with an inclination of 45°, allowing measurements of ion temperatures and velocities with an altitude, or equivalently a longitude sampling interval of 27.5 km. Kiruna and Sodankyla reception stations are pointed to intersect the Tromsö beam at 312 km altitude, allowing the measurement of the ion velocity vector at this altitude.

Dc magnetic field records in permanent stations like Sodankyla are used to appreciate the magnetic activity. Magnetic pulsations are also observed on these records, but because of their small amplitude compared with dc variations, only the largest Pc 3 to Pc 5 pulsations are detected. In addition, a variometer instrument was used in Kevo, which is situated close to the vertical of the radar beam intersection. The gain of the variometer increases with frequency in order to get a good signal-to-noise ratio on the digital records of the three magnetic components (*H*, *D* and *Z*).

We have studied 4 days with Pc 5 activity from the campaigns of measurements performed in November and December 1983. We have found that the dominant organized pulsations on the ground is on the *H* component: because of the dissymmetry of the dipole field, east-west properties are more stationary in time and in longitudinal extent than north-south ones. For the 4 days studied in the paper, the ratio *H* to *D* was 1.4–3–1.8–2, and only on November 30 there was a good coherency between *H* and *D* ($C = 0.9$). The *D* component was usually more noisy than the *H* one, and the *Z* component was usually much smaller than *H* (3 times) and correlated with *H*.

The magnetic pulsation polarization on the ground is function of the external signal and the induced signal in the ground. This induced part may be more important on *Z* and *D* components than on *H* component.

These different reasons explain that the *H* component is the most intensively used in the literature. In the present study, we have found a good relation between *H* and the pulsations recorded in the ionosphere ($C = 0.8$) and no significant relation between ionospheric signals and *D* ($C = 0.5$).

We have also found that the ionospheric ion velocity measured at Tromsö (corresponding to the *H* ground pulsations in a first approximation) are coherent over the whole longitudinal extent of our observations (see an example in the next paragraph).

In Figure 2 one displays the raw data for November 11,

[1]Now at Wuhan University, Houbei, China.



Paper number 5A8562.
0148-0227/86/005A-8562$05.00

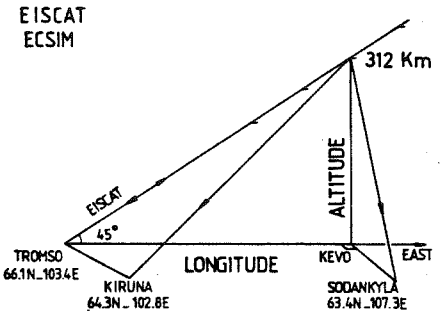


Fig. 1. Geometry of the EISCAT facility in a geophysical frame: transmission is at Tromsö, reception is from 312 km at the three stations (Tromsö, Kiruna and Sodankyla) and from several longitudes at Tromsö. Ground magnetic field is recorded at Kevo. Geomagnetic coordinates of EISCAT reception stations are indicated.

1983, which is a typical example of the obvious correlation between temperature enhancements and velocity oscillations.

The large increase of $H$ (curve a) seen from the Sodankyla magnetogram between 1115 and 1230 UT is due to large electric fields in the ionosphere: it is detected on the ion velocity measured from Tromsö at 299 km altitude (curve c), which corresponds, in a first approximation, to north-south electric fields. Curve b shows the $H$ magnetic component recorded at Kevo in the bandwidth 0.3 to 8 mHz (1 hour, 2 min). Several bursts of pulsations with an amplitude of 10 to 30 $\gamma$ occur during the day. At 1130 UT, some of them are superimposed to the very low frequency $H$ enhancement. The same behavior is seen on the ion velocity presented by the curve c but also on ion velocity $V_i$ obtained at the other altitudes of measurement or recorded in Kiruna and Sodankyla reception stations. Curve d of Figure 2 displays the ion temperature measurements from Tromsö at 299 km altitude. One can see the very good correlation occurring between enhancements of $T_i$ (up to 1200 K) and the variations of $V_i$. These curves show that the ion temperature reacts in the same way to dc electric fields and to magnetic pulsations.

However, direct observations are not sufficient to make a quantitative estimation between $T_i$ and $V_i$ fluctuations. We have used a signal processing method (described in the next section) to reject the part of $T_i$ not related to $V_i$.

## 3. Wiener Filter Method

General multicomponent estimation of pulsations has been already mentioned in *Glangeaud et al.* [1985]. The method used in this paper is applied for a two-component signal in the case where one of the components has a good signal-to-noise ratio.

Let us call $x(t)$ and $y(t)$ the two recorded components:

$$x(t) = s_1(t) \qquad y(t) = s_2(t) + n(t)$$

where $s_1(t)$ and $s_2(t)$ are the coherent parts, and $n(t)$ is the nonrelated part of $y(t)$.

We want to find the linear stationary relation between $s_1$ and $s_2$ and use it to estimate $s_2(t)$. This relation can be represented by a filter $F(f)$ (where $f$ means frequency). The $s_2$ estimation problem will therefore correspond to find the filter $F(f)$, so that $y(t) - F[x(t)]$ is not related to $x(t)$.

The filter can be expressed in function of the coherency coefficient $C(f)$ between $x$ and $y$.

$$F(f) = \left(\frac{\gamma_{xx}(f)}{\gamma_{yy}(f)}\right)^{1/2} C(f)$$

where $\gamma_{xx}(f)$ and $\gamma_{yy}(f)$ are, respectively, the spectral densities of $x(t)$ and $y(t)$ estimated with the periodogram method in this paper.

$F(f) \cdot x(f)$ is the best estimation of $s_2(f)$, i.e., of the part of $y(f)$ related to $x(f)$. In the time domain, it will be represented by $\tilde{y}(t)$.

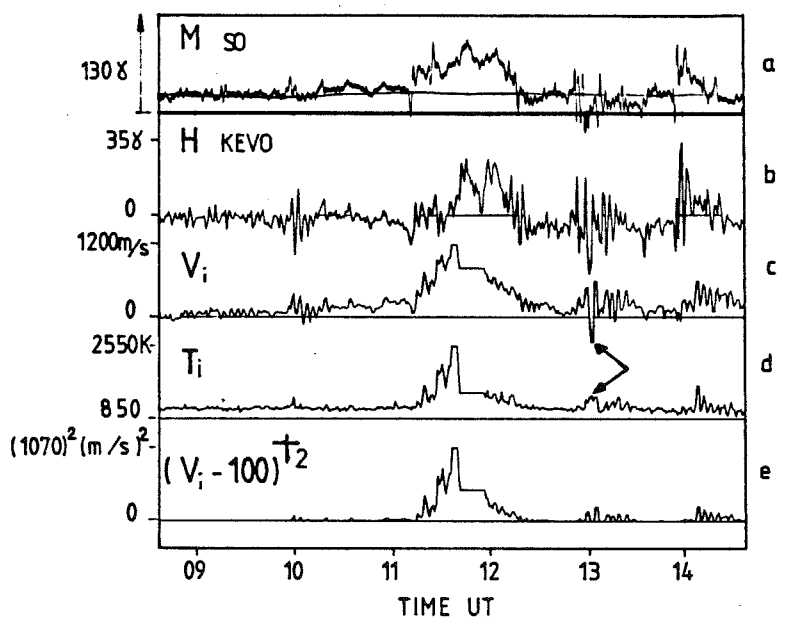


Fig. 2. November 11, 1983. Raw data showing the relation between ground magnetic components ($H$ magnetogram in Sodankyla (curve a) and $H$ magnetic component at Kevo in the bandwidth 0.3 to 8 mHz (curve b)), ion velocity (curve c) and ion temperature (curve d) measured at Tromsö from 300 km altitude. Curve e represents the function of ionospheric velocity leading to ion temperature increases. Ionospheric data are missing between 11.39 and 11.57 UT. The dagger symbol and the arrow signification are explained in text.

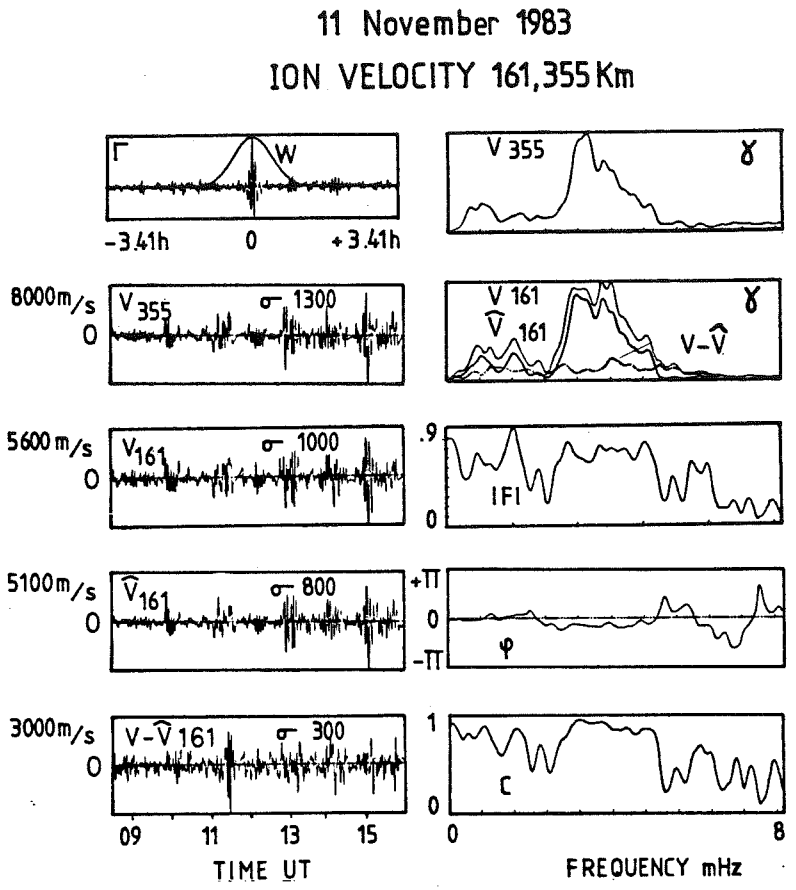


Fig. 3. The study of the relation between ionospheric velocities measured at 161 and 355 km from Tromsö, in terms of cross-correlation function Γ, spectral densities γ, Wiener filter (modulus $|F|$ and phase $\varphi$) coherency coefficient $C$ and wave forms in the bandwidth 0.8 to 8 mHz. The predicted wave form at 161 km is $\hat{V}_{161}$ and the error of prediction is $V - \hat{V}_{161}$; $\sigma$ indicates the variance of each wave form.

The precision of the estimation of the filter $F(f)$ is given by

$$\frac{\Delta|F(f)|}{|F(f)|} = \frac{1}{BD}\left[\frac{1}{C(f)^2} - 1\right]^{1/2}$$

[*Comon and Lacoume*, 1985], where $B$ is the bandwidth of the window used for coherency coefficient and spectral density calculations and $D$ is the signal duration (usually $BD = 10$ in this paper).

The coherency coefficient is also a tool to estimate the degree of relation between $x$ and $y$. It may be used to estimate the noise. It is also used to find the best representation of $x$ in order to have a linear relation.

The study of the east-west extension of the pulsations in the ionosphere is a good example of the use of the Wiener filter method and is presented in Figure 3 for November 11, 1983, data.

Ionospheric ion velocity records at 355 km and 161 km (noted $V_{355}$ and $V_{161}$) are compared in time and frequency domain (respectively, left part and right part of Figure 3). Their wave forms filtered in the bandpass 0.3 to 8 mHz are presented on the second and third panels. The two spectra (two upper panels) are somewhat different: the peak at 3.2 mHz is common, but the one at 3.8 mHz is negligible on $V_{355}$. The estimations of the spectra are made by Fourier transform of the weighted correlation functions. The cross correlation (Γ) between $V_{161}$ and $V_{355}$ is presented in the upper left panel together with the weighting function, which is a Hanning window $W$ ($BD = 10$).

By using the $V_{355}$ component as a reference, the Wiener filter method has been calculated. Its modulus $|F|$ indicates that the pulsations at 3.2 and 3.7 mHz are attenuated between 355 km and 161 km by a factor 0.65 and 0.7, respectively. The phase $\varphi$ is only significant in the bandwidth where the coherency coefficient $C$ is higher than 0.8 (2.7 to 4.9 mHz). It is constant so that we estimate that there is no delay between the two components: a delay corresponds to a slope of the phase and is related to group velocity (see *Glangeaud et al.* [1980] for more details). The phase difference is the same for the two frequency peaks: 30°. It corresponds to a phase velocity, usually expressed as the $m$ number of the pulsation ($m = 5.6$). The estimation of the part of ion velocity at 161 km perfectly coherent with the 355 km component ($V_{161}$) is presented in both time and frequency domains. In time domain, the wave form is much like the $V_{355}$ wave form. In frequency domain, the peaks observed on spectral density may be due to the statistical fluctuations or significant resonances. Because the second peak at 3.7 mHz is observed on both original data $V_{161}$ and predicted data $\hat{V}_{161}$, we can say that it is not a statistical fluctuation. It is one of the advantage of the Wiener filter method. The estimation of the noise ($V_{161} - \hat{V}_{161}$) in frequency domain is a white noise, which means that one has not detected any pulsations only present on the $V_{161}$ component. In the time domain, the noise is still important and has large fluctuations: it is not stationary. Its variance is 300 $ms^{-1}$, which gives an estimation of the signal-to-noise ratio of $V_{161}$: 800/300.

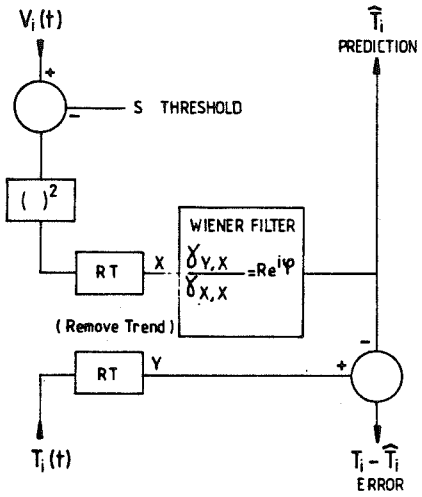


Fig. 4. Description of the Wiener filter method used for ion temperature predictions. The threshold function replace $V_i(t)$ by $V_i(t) - S$ when this value is positive, and by zero when it is negative. The result is named $(V_i - S)\dagger$. Slow variations (trends) of the functions $(V_i - S)\dagger^2$ and $T_i$ are subtracted before the Wiener filter computation. The results $\hat{T}_i$ and $T_i - \hat{T}_i$ are obtained in the bandwidth 0.8 to 8 mHz.

This example on November 11, 1983, is significant of our data for Pc 5 pulsations which are very coherent in longitude over more than 150 km. That was not the case for Pc 3 pulsations [*Glangeaud et al.*, 1985]. This result allows us to choose the altitude of comparison between ion velocities and temperatures in function of the quality of temperature data: temperature data are much more noisy than velocity data.

## 4. Estimation of Ion Heating

Let us rewrite the ion energy equation (equation (1)) as

$$T_i[1 + \alpha] = R(V_i - V_n)^2 + T_n + \alpha T_e \qquad (2)$$

where

$$\alpha = \frac{m_i + m_n}{m_i}\frac{\nu_{ie}}{\nu_{in}} \qquad R = \frac{m_n}{3k_B} \qquad (2)$$

In the $F$ region and for the ionospheric conditions encountered during the 4 days of experiments we have looked at, the $\alpha$ term varies between 4% and 9%, which is comparable with the experimental errors on $T_i$. Therefore it can be neglected in the left-hand side of equation (2).

The neutral temperature term $T_n$, which varies very slowly with time, is not in the Pc 5 pulsation bandwidth. The term proportional to electron temperature $\alpha T_e$ can vary much more quickly with time. It may be included in the Pc 5 bandwidth, but we may assume that it is independent of the magnetic pulsations.

The velocity term in equation (2) is a vectorial term: in order to be able to compare equation (2) with our data, we will restrict ourselves to pulsations polarized on the ground in the $H$ direction (see section 2 for justification), which means that they correspond in the ionosphere to the fluctuations of the east-west ion velocity. In that case, we can rewrite equation (2) as

$$T_i = R(V_E - U_E)^2 + T_n + \alpha T_e + V_0^2 \qquad (3)$$

$V_E$ and $U_E$ are the ion and neutral velocity in the east-west direction, and $V_0^2$ includes contributions to the ion energy equation of velocity terms nonrelated to $H$ magnetic pulsations.

The observed values of velocity depend on the direction of measurements, i.e., of the reception station used (see Figure 1). If we use the velocity measured in Tromsö (respectively, Kiruna and Sodankyla), which is related to the east-west velocity by the relation $V_i = (1/A_T)V_E$ (respectively, $(1/A_K)V_E$ and $(1/A_S)V_E$), then the coefficient $R$ of equation (3) becomes $R_T = A_T^2 R$ (respectively, $R_K = A_K^2 R$ and $R_S = A_S^2 R$).

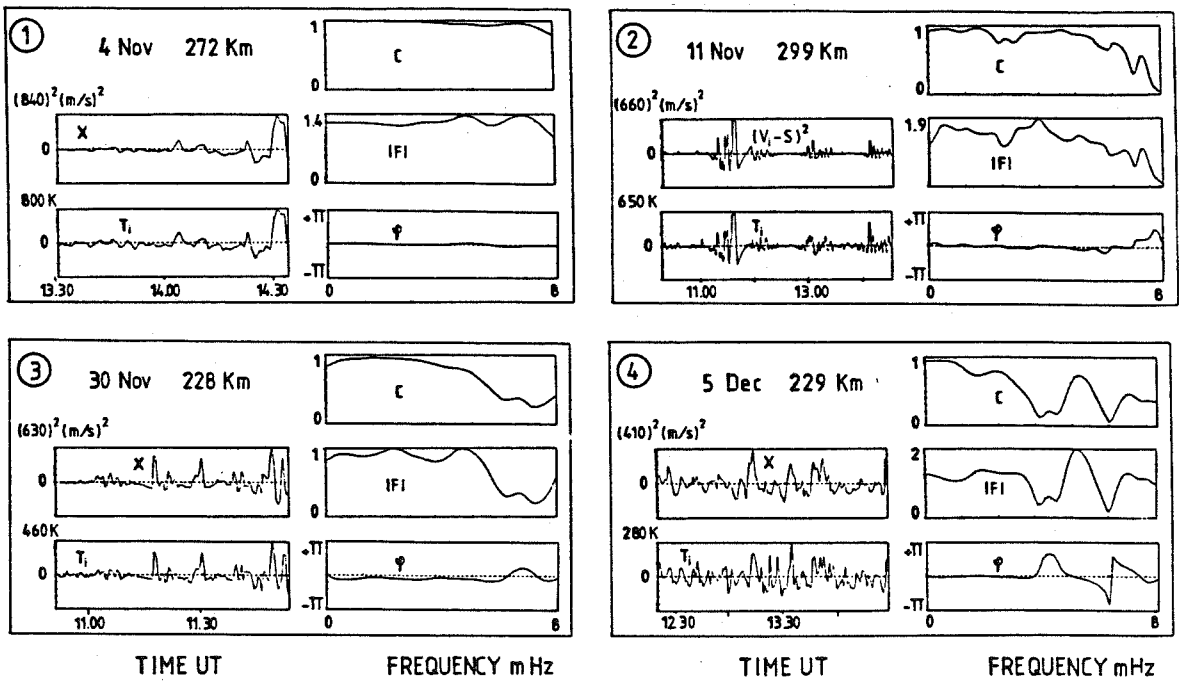


Fig. 5. Wave forms of ion velocity squared $(V_i - S)\dagger^2 = X$ and ion temperature $T_i$ are filtered in the bandwidth 0.8 to 8 mHz. Coherency coefficients $C$ between $X$ and $T_i$, and Wiener filter (modulus $|F|$ and phase $\varphi$), are plotted versus frequency. The scale of $|F|$ indicated is in $10^{-3}$ unit.

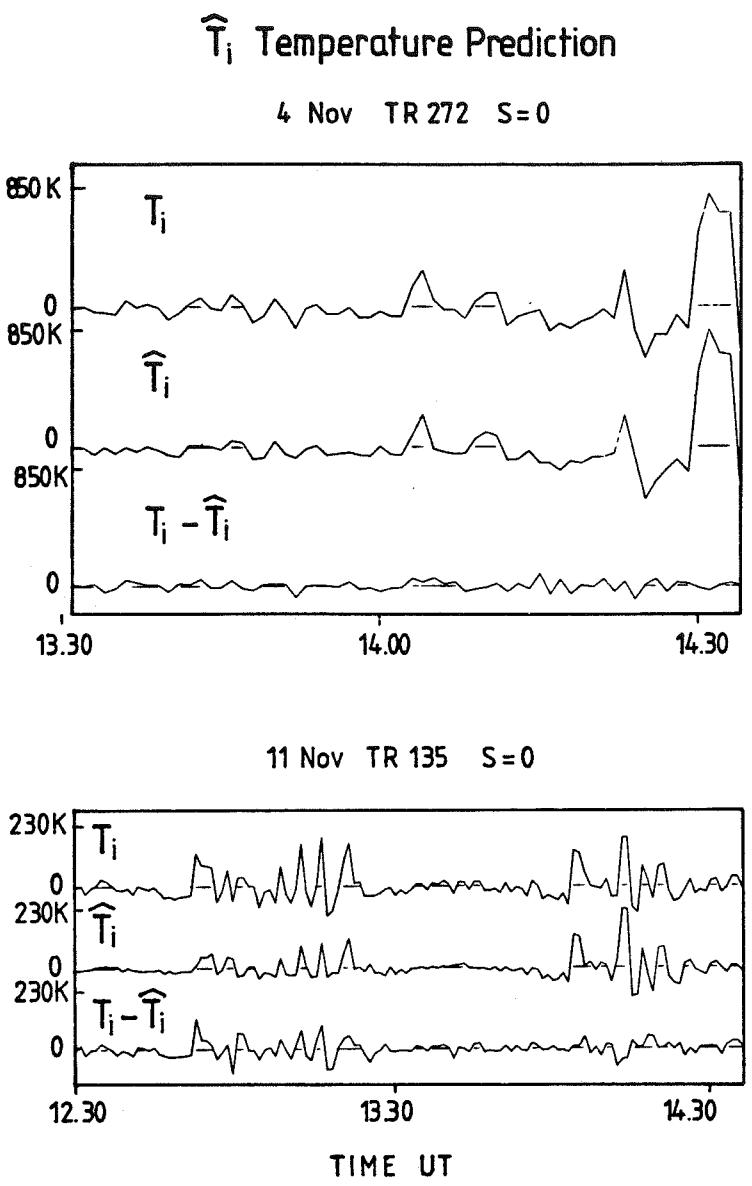


Fig. 6. Comparison between measured ion temperature $T_i$ and predicted ion temperature $\hat{T}_i$ in the bandwidth 0.8 to 8 mHz for November 4, 1983 (Tromsö data from 272 km altitude), and November 11, 1983 (Tromsö data from 135 km altitude).

Let us come back to our measurements and the evident relation that we have seen in Figure 2 between ion temperatures $T_i$ and ion velocities $V_i$ in the ULF bandwidth. We have compared, by use of coherency coefficients, $T_i$ with various functions of $V_i$: (1) $V_i$; (2) $V_i^2$; (3) $(V_i - S)^2$, $S$ being an estimation of $U_E$; (4) $(V_i - S)\dagger^2$ where $S$ is a threshold and the dagger means that negative values of $V_i - S$ are set to zero values. The coherency is always better for case 2 than for case 1. In most of the cases that we have studied, the introduction of $S$ (case 3) has increased the coherency: it is our method of estimation of $S$.

Furthermore, for the data we have looked at, there was no case of large negative $V_i - S$, except on November 11, at 1300 UT. We have not observed an increase in $T_i$ corresponding to the small negative $V_i - S$ values on the wave forms because small values of $T_i$ are noisy. For the November 11 case, it may be possible that the negative arch of $V_i$ (arrow on curve c of Figure 2) corresponds to a positive arch in $T_i$ (arrow on curve d of Figure 2). That is why the negative values of $V_i - S$ have been put to zero, resulting in an increase of the coherency coefficient between $T_i$ and $(V_i - S)\dagger^2$ (case 4).

Because the coherency is good, we can use the Wiener filter method to obtain first an estimation of the part of the temperature related to $H$ magnetic pulsations $\hat{T}_i$, second a measurement of the coefficient $R_T$ (or $R_K$, or $R_S$):

$$\hat{T}_i = R_T(V_i - S)\dagger^2$$

(for Tromsö measurements). In frequency domain, one has

$$\hat{T}_i(f) = F(f) \cdot (V_i - S)\dagger^2(f)$$

If $F(f)$ is constant over the bandwidth on which it is valid (see section 2), $R_T = |F(f)|$.

This method of estimation rejects parts of $T_i$ nonrelated to $V_i$ such as the $V_0^2$ and $\alpha T_e$ terms of equation (3). The term $T_n$ is neither taken into account because it is outside the Pc 5 bandwidth.

The experimental use of the Wiener filter method for ion heating estimations is described in Figure 4.

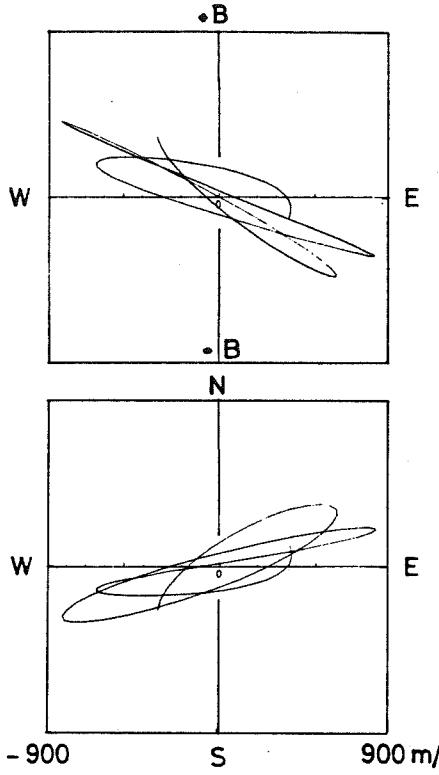


Fig. 7. Polarization plots between ionospheric ion velocity components ($V_E$, $V_{\|}$ and $V_N$) in a geomagnetic frame, for November 11, 1983, from 13.00 to 13.20 UT (in the bandwidth 0.8 to 8 mHz).

It is obvious that the coherency coefficient $C(f)$, or the Wiener filter $F(f)$, and $\hat{T}_i$ will depend on the value of the threshold chosen $S$; in particular, the coherency coefficient will be good only if the hypothesis of constant $S$ is verified. $S$ has been chosen from coherency coefficient computations: it corresponds to the highest coherency coefficient between $T_i$ and $(V_i - S)^2$ (see Figure 4).

When $C(f)$ is not sensitive enough to $S$ (data very noisy or fluctuations of great amplitude), one has chosen the value which minimizes the standard deviation of the residual wave form $T_i - \hat{T}_i$. When $S$ is correctly estimated, and with our assumption of $H$ pulsations, it gives the value of the east-west neutral wind projection on the direction of measurements: $U_T$ and the Wiener filter modulus give the value of the coefficient $R_T$ (for Tromsö measurements). The error on $R_T$ is therefore given by the error on the modulus of $F(f)$.

## 5. Results

Figure 5 displays for the 4-day experiments the wave forms of $(V_i - S)\dagger^2$ and of $T_i$ (Tromsö measurements) in the bandwidth 0.8 to 8 mHz, the coherency coefficient $C(f)$ and the Wiener filter $F(f)$ (modulus and phase).

In panel 1, one shows Tromsö data from November 4, 1983, measured at 272 km altitude. The threshold is 0. There is a very good identity between the two wave forms, which is specified by the coherency coefficient almost equal to 1 for the entire bandwidth. The Wiener filter modulus does not vary with the frequency; it means that the ion heating process does not depend on the frequency of the velocity fluctuations. The constant phase equal to zero means that the ion heating is instantaneous (no slope and no phase shift).

Panel 2 displays results for Tromsö data presented in Figure 2: November 11, 1983, but only from 1016 to 1436 UT. $S$ is equal to 100 m/s. On the two wave forms, one recognizes the pulsation bursts and at 1130 UT the oscillating part which was superimposed to the large low frequency enhancement (see $T_i$ curve $d$ and $(V_i - 100)\dagger^2$ curve e in Figure 3 where the trends have not been removed). The coherency coefficient is equal to 0.9 up to 6 mHz. The fact that $C(f)$ is very good for this time interval (equal to 3 hours) proves that the $S$ constant hypothesis was good.

November 30, 1983 (panel 3), is an example of a 1-hour period for velocity and temperatures data measured at a lower altitude: 228 km. $S$ is equal to 80 m/s; $C(f)$ is higher that 0.9 for frequencies smaller than 4 mHz and $F(f)$ modulus is relatively constant in this frequency bandwidth.

December 5, 1983 (panel 4), is the worst example of our set of data. $S$ has been chosen equal to zero, but its determination was very difficult. The amplitudes of the two wave forms are much smaller than for the 3 preceding days, and it is difficult to identify visually what is noise and what is heating on the $T_i$ curve. However, $C(f)$ is higher that 0.8 for frequencies lower than 3 mHz and $F(f)$ modulus and phase are constant in this frequency bandwidth.

In Figure 6, one shows the comparison between ion temperature measurements $T_i$ and ion temperature estimation by Wiener filter method $\hat{T}_i$ for two examples: the best one and an example of nonstationarity. In addition, the residual wave forms $T_i - \hat{T}_i$ are also shown.

Panel 1 is for November 4, 1983, data. The estimation of ion temperature is very good. The residual wave form $T_i - \hat{T}_i$ represents the noise on $T_i$ measurements. Its mean standard deviation 35 K corresponds to the statistical error due to the reception system of incoherent scatter signal.

On panel 2, one displays a case where the Wiener filter method is not good: on November 11, 1983, from 1230 to 1430 UT, $T_i$ is correctly estimated for the second burst of pulsations but not for the first one; from 1230 to 1330 UT, the residual wave form $T_i - \hat{T}_i$ has an amplitude equal to the estimated wave form amplitude. It means that the Wiener filter calculated is good only for the second burst; it is nonconstant on the chosen time interval, which could be due to a

TABLE 1. November 11, 1983, Results of Wiener Filter Method for Ion Velocity and Ion Temperature Data From the Three EISCAT Receiving Stations

| | $S$, ms$^{-1}$ | $U_E$, ms$^{-1}$ | $\|F(f)\|$ | $R$, K/m$^2$ s$^{-2}$ |
|---|---|---|---|---|
| Kiruna, 311 km altitude | $U_K = 100 \pm 10$ | 150 | $R_K = 1.6 \times 10^{-3}$ | $7.1 \times 10^{-4} \pm 20\%$ |
| Sodankyla, 311 km altitude | $U_S = 60 \pm 10$ | 150 | $R_S = 5 \times 10^{-3}$ | $8.2 \times 10^{-4} \pm 20\%$ |
| Tromsö, 299 km altitude | $U_T = 100 \pm 10$ | 150 | $R_T = 1.55 \times 10^{-3}$ | $6.9 \times 10^{-4} \pm 10\%$ |

$S$ is the velocity threshold, $U_E$ is the deduced east-west neutral wind, $|F(f)|$ is the Wiener filter modulus, and $R$ is the deduced coefficient of the ion heating equation (see Figure 4).

TABLE 2. November 11, 1983, Results of Wiener Filter Method for Tromsö Data From Different Altitudes

| Tromsö Data Altitude | $C(f)$ | $\hat{T}_i/T_i$ | $S$, ms$^{-1}$ | $R_T$ | $R$, K/m$^2$ s$^{-2}$ | $R$ From Model Thermopause = 1000 K |
|---|---|---|---|---|---|---|
| 135 km | 0.9 | 0.92 | $0 \pm 10$ | $3.65 \times 10^{-3} \pm 30\%$ | | |
| 217 km | 0.85 | 0.88 | $0 \pm 10$ | $7.8 \times 10^{-4} \pm 45\%$ | $3.5 \times 10^{-4}$ | $8.5 \times 10^{-4}$ |
| 299 km | 0.95 | 0.98 | $100 \pm 20$ | $1.46 \times 10^{-3} \pm 15\%$ | $6.5 \times 10^{-4}$ | $7.4 \times 10^{-4}$ |
| 383 km | 0.95 | 0.91 | $50 \pm 50$ | $1.4 \times 10^{-4} \pm 25\%$ | $6.2 \times 10^{-4}$ | $6.8 \times 10^{-4}$. |

Coherency coefficient, $C(f)$; ratio of estimated ion temperature to measured one, $\hat{T}_i/T_i$; velocity threshold $S$; coefficients of the ion heating equation $R_T$ and $R$.

nonconstant threshold $S$, or to a contribution to heating from other nonrelated velocity components. Furthermore, the altitude of comparison for this case is 135 km, which is not in $F$ region: some of the simplifications of the ion energy equation that we have done are not valid in the $E$ region.

## 6. Discussion and Conclusion

### 6.1. *Three Ionospheric Component Study*

The radar geometry chosen for this experiment (Figure 1) has a good sensitivity to east-west direction (the geographic one and the geomagnetic one are almost identical), but other directional components are not so well measured. Very small time shifts (due to the radar reception system) between the three measured components (Tromsö, Kiruna, Sodankyla) could introduce large errors on the ionospheric polarization pattern. However, we show in Figure 7 such a polarization pattern in a geomagnetic frame for November 11, 1983. We can conclude that the pulsations are mainly east-west but that the other components are not zero.

For the 3 other days, the ionospheric polarization study was not possible. However, the ground study of magnetic pulsations (see section 2) has shown that an hypothesis of $H$ magnetic pulsations was a good approximation.

November 11, 1983, has consequently been chosen for comparison of the ground values for the threshold $S$ and the constant $R$ obtained from the analysis of the measurements from the three reception stations. The results are resumed in Table 1 for the period from 1016 to 1252 UT.

Because the interval is long, the estimation of the threshold is quite precise. One obtains the same east-west neutral wind estimation $U_E = 150$ m/s from the three independent pairs of ion temperature, ion velocity data. The values found for $R$ agree within the error bars. They can be compared with the value calculated from the *Banks and Kockarts* [1973] thermospheric model. At 300 km altitude for a thermopause of 1000 K corresponding to our data, we found $R = 7.4 \times 10^{-4}$ K s$^2$/m$^2$, which is in good agreement with our results.

### 6.2. *Spatial Extent*

We have already pointed out in section 3 that the ionospheric ion velocities are coherent on a large extent including longitude and altitude variations. The relation between the ion temperature and the velocity is expected to be mainly a function of altitude as it depends on the neutral atmosphere. We shall therefore interpret our measurements in that way.

In Table 2, we compare results obtained from Tromsö at different altitudes for the time interval from 1037 to 1141 UT, on November 11, 1983. This short time interval has been chosen because the coherency coefficients between temperatures and velocities are particularly good. The best estimation of $T_i$ is obtained at 299 km altitude, where the results for $S$ and $R_T$ are the same as those calculated over the long time interval of Table 1.

At the two lowest altitudes, one found that the threshold $S$ or the east-west neutral velocity is close to zero. At the highest altitude, the estimation of $S$ was very unprecise. For discussion of the $R$ values, one has added in Table 2 the values calculated from the *Banks and Kockarts* [1973] thermospheric model with a thermopause of 1000 K. At the lowest altitude, one cannot discuss the value found because the equation (1) on which our method is based is valid only in the $F$ region. Furthermore, ion temperature data, at this altitude, from EISCAT single pulse measurements are always overestimated. From 299 to 383 km altitude, one observes a decrease of $R$ which is consistent with a decrease of the mean neutral mass; however, the error bars are too large for further comparisons.

At 217 km altitude, the $R$ value is more than twice as small as the model one, but the error is very large due to the relatively small coherency coefficient. Furthermore, the ion composition model used to obtain ion temperature from incoherent scatter spectra could lead at this altitude to an underestimation of $R$ up to 20% (see *Lathuillere et al.* [1983] for details).

### 6.3. *Conclusion*

The study with EISCAT facility of the relationship between ion velocity and ion temperature in the ULF bandwidth (0.8 to 8 mHz) has showed that the temperatures fluctuations are coherent with Pc 5 magnetic pulsations on a large spatial extent. As it was expected in theory, we have found that heating by pulsations is instantaneous, so that the temperatures fluctuations follow very well the velocity fluctuations. We have experimentally verified the simplified equation of the frictional heating in the ULF bandwidth: $T_i = R(V_i - S)^2$ between the coherent parts of $T_i$ and $V_i$. Tentative estimations of $S$ have been made, and experimental values of $R$ are in good agreement with the theoretical ones.

Our results show that the classical relation between ion heating in the ionosphere and dc electric fields is still applicable to magnetic pulsations of periods down to 3 min. In the auroral zone, these pulsations occur very often and are large enough to generate fluctuations of ion temperature of 200 K rms during several hours. This energy source to the ionospheric plasma is not negligible. This study has also provided a better knowledge of the interpretation of the $H$ ground magnetic pulsations, but the interpretation of $D$ has not been made and would necessitate another configuration of the EISCAT facility.

*Acknowledgments.* We would like to thank P. Aikio, T. Bosinger, E. Kataja, J. Kangas, M. Lambert and M. Sulkinoja for Kevo experiments, M. C. Prevost for computer assistance, G. Lejeune and W. Kofman for participating to the EISCAT measurements, and D. Hubert for helpful discussion. The EISCAT Scientific Association is

supported by the Centre National de la Recherche Scientifique of France, Suomen Akatemia of Finland, Max-Planck Gesellschaft of West Germany, Norges Almenvitenskapelige Forskningsrad of Norway, Natürvetenskapliga Forskningsradet of Sweden and the Science and Engineering Research Council of the United Kingdom.

The Editor thanks K. H. Glassmeier, P. Stubbe, and another referee for their assistance in evaluating this paper.

## REFERENCES

Banks, P. M., and G. Kockarts, *Aeronomy*, part B, Academic, Orlando, Fla., 1973.

Baron, M., and R. H. Wand, *F* region ion temperature enhancements resulting from Joule heating, *J. Geophys. Res.*, *88*, 4114–4118, 1983.

Comon, P., and J. L. Lacoume, Noise reduction for an estimated filter using noise reference, *IEEE Trans. Inform. Theory*, in press, 1985.

Folkestad, K., T. Hagfors, and S. Westerlund, EISCAT: An updated description of technical characteristics and operational capabilities, *Radio Sci.*, *18*, 867, 1983.

Glangeaud, F., J. L. Lacoume, H. Fargetton, R. Gendrin, S. Perraut, and V. Troitskaya, Cross-spectrum analysis of Pc 1 emissions recorded at different stations, *J. Geophys. Res.*, *85*, 4115, 1980.

Glangeaud, F., C. Lathuillere, M. Lambert, and Z. Y. Zhao, Pc 3–4 ULF magnetic variations measured in the ionosphere by EISCAT, *J. Geophys. Res.*, *90*, 8319, 1985.

Glassmeier, K. H., H. Volpers, and W. Baumjohann, Ionospheric Joule dissipation as a damping mechanism for high latitude ULF pulsations: Observational evidence, *Planet. Space Sci.*, *32*, 1463–1466, 1984.

Greenwald, R. A., and A. D. M. Walker, Energetics of long-period resonant hydromagnetic waves, *Geophys. Res. Lett.*, *7*, 745, 1980.

Lathuillere, C., G. Lejeune, and W. Kofman, Direct measurements of ion composition with EISCAT in the high-latitude $F_1$ region, *Radio Sci.*, *18*, 887–893, 1983.

Newton, R. S., D. J. Southwood, and W. J. Hughes, Damping of geomagnetic pulsations by the ionosphere, *Planet. Space Sci.*, *26*, 201, 1978.

Perraut, S., J. Bjoerna, A. Brekke, M. Baron, W. Kofman, C. Lathuillere, and G. Lejeune. Experimental evidence on nonisotropic temperature distribution of ions observed by EISCAT in the auroral *F* region, *Geophys. Res. Lett.*, *11*, 519–522, 1984.

St.-Maurice, J.-P., and W. B. Hanson, Ion frictional heating at high latitudes and its possible use of an in situ determination of neutral thermospheric winds and temperatures, *J. Geophys. Res.*, *87*, 7580–7602, 1982.

Stubbe, P., and S. Chandra, Ionospheric warning by neutral winds, *Planet. Space Sci.*, *19*, 731, 1971.

F. Glangeaud, C. Lathuillere, and Z. Y. Zhao, Centre d'Etudes des Phénomènes Aléatoires et Géophysiques, LA 346, BP46, 38402 Saint-Martin-d'Hères, France.

(Received March 13, 1985;
revised August 19, 1985;
accepted September 24, 1985.)

# ARTICLE 8

JOURNAL OF GEOPHYSICAL RESEARCH, VOL. 90, NO. A4, PAGES 3520-3524, APRIL 1, 1985

# EISCAT MULTIPULSE TECHNIQUE AND ITS CONTRIBUTION TO AURORAL IONOSPHERE AND THERMOSPHERE DESCRIPTION

Wlodek Kofman and Chantal Lathuillere

Centre d'Etude des Phénomènes Aléatoires et Géophysiques (Laboratoire Associé au CNRS)
Saint-Martin-d'Hères, France

Abstract. In this paper, we describe European Incoherent Scatter Scientific Association (EISCAT) capabilities to measure ionospheric parameters in the E and F regions simultaneously. We discuss especially the multipulse technique which we used for E region study. We show the behavior of the auroral ionosphere during a period with low energy input and its response to precipitation of electrons with wide energy spectrum. Finally, we show neutral density measurements in the lower thermosphere for two different days with different energy input.

## Introduction

In the auroral zone, in addition to solar energy input to the atmosphere, energy is deposited on occasion by particle precipitation, electric fields (Joule heating), and waves. These energy inputs, often very large [Banks, 1977; Wickwar et al., 1975], modify the circulation and composition of the neutral atmosphere and ionosphere. For these reasons, it is important to study the E and F regions simultaneously with good temporal and altitude resolution.

In the winter of 1983, the European Incoherent Scatter Scientific Association (EISCAT) facility was used for the first time to measure the whole set of ionospheric parameters (electron density, ion and electron temperatures, ion-neutral collision frequency, ion velocity) in the E and F regions simultaneously. These measurements could be made with good precision because of the multifrequency capabilities of the transmitter and receiver [Folkestad et al., 1983]. The E and F region ionospheric parameters were measured by the multipulse and single-pulse techniques, respectively [Farley, 1969, 1972; Rino et al., 1974, 1977; Brekke and Rino, 1978]. In addition, the electron density was measured with good alti-tude resolution between 90 and 350 km using a short pulse.

These simultaneous measurements in the E and F regions, with very good altitude and time resolution, give the possibility of studying the variability of the ionosphere and, especially, of examining the nature of the energy inputs to the ionosphere and atmosphere.

In this paper, we describe the measurement technique, its capabilities and limitations, as well as the quality of the data for selected examples.

We show the behavior of the ionospheric plasma (E and F regions) in response to electron precipitation. We calculate the energy input to the atmosphere and ambient electrons.

The multipulse technique for the altitude range between 90 and 110 km permits us to determine the ion-neutral collision frequency and plasma temperature. In the auroral zone, these parameters have been observed using the Chatanika radar [Lathuillere et al., 1983]. The new results, obtained with the EISCAT facility, have better time and altitude resolution. The neutral atmosphere varies depending on the energy input. The experimental study of this behavior, in the future, can answer the question of how fast the neutral atmosphere reacts to large energy inputs.



Paper number 4A8394.
0148-0227/85/004A-8394$02.00

## Measurement Technique and Data Analysis

In this experiment, we used the tristatic capabilities of the EISCAT system [Folkestad et al., 1983]. The Tromsö antenna beam was directed along the magnetic field line. The Kiruna and Sodankyla antenna beams intersected the Tromsö beam at 110 and 300 km altitude, enabling the determination of the ion velocity vector at these two altitudes.

The transmitted pulse (Figure 1) was composed of three different pulse patterns. The two identical multipulse frames contain five subpulses. The duration of each subpulse was 15 μs, which determines a range resolution of 2.25 km. These five pulses are displaced in time in order to measure 10 lags (1-11) of the correlation function. The zero lag was measured, but due to the range ambiguity problem [Farley, 1972], it was used only for normalization purposes. The tenth lag was not measured because the particular multipulse scheme did not include it. The separation between lags was 30 μs, which gives a total length of 330 μs to the correlation function. This separation between lags and the total length of the autocorrelation function determine the altitude range of the observations. For altitudes below about 90 km the measured correlation function is too short compared with the correlation function of the medium, and even the first zero crossing is not reached.

For altitudes above about 135 km, the first measured lag is too close to the zero crossing (the zero crossing occurs near the second lag). This implies that the sampling rate of the medium is too close (to the Nyquist rate) to the correlation time of the medium. These two limitations make data analysis very difficult for altitudes outside the range 90-135 km.

The statistical errors for the estimated correlation function depend on the signal-to-noise ratio (snr), integration time, and number of subpulses. The snr is proportional to electron density, pulse length, and transmitted power and inversely proportional to receiver bandwidth and square of the range. In principle, for a stationary medium the estimation error can be reduced by postintegration, but in the auroral zone where there is great time variability of the ionosphere, long postintegration does not necessarily amelio-

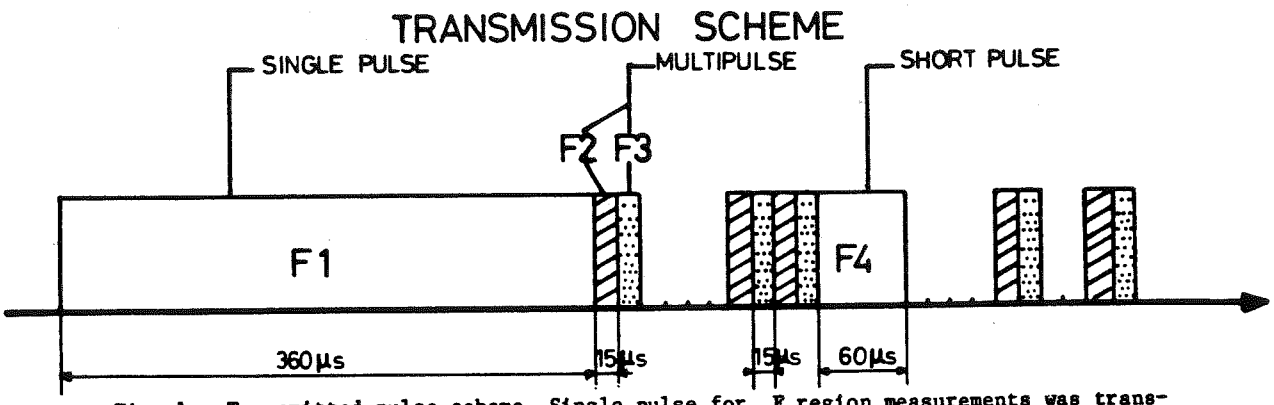


Fig. 1. Transmitted pulse scheme. Single pulse for F region measurements was transmitted on frequency F1, two multipulses on F2 and F3 for E region measurements, and short pulse for electron density measurements on F4.

rate the data quality. This variability implies that to best examine the auroral atmosphere, short integration times are necessary. To obtain good quality data with high time and altitude resolution, one needs to increase the transmitted power and use the diversity of frequencies of which the EISCAT system is capable. In our experiment we transmitted the multipulse on two frequencies and summed the two measured correlation functions before the analysis. We obtained good quality data with 2- to 4-min integration time for the following conditions: $2 \times 10^{11}$ el/m$^3$ electron density, 1-MW transmitted power, 100-kHz receiver bandwidth, 110° noise level, and 8- to 10-ms repetition rate.

In Figure 2, we show the measured correlation function from the multipulse for three altitudes and from the single pulse for one altitude. The zero lag was obtained for the multipulse with a parabolic extrapolation. We use this lag only for the first normalization in the data analysis. In the analysis, the weights, which are normally equal to the inverse of the square of the corre-

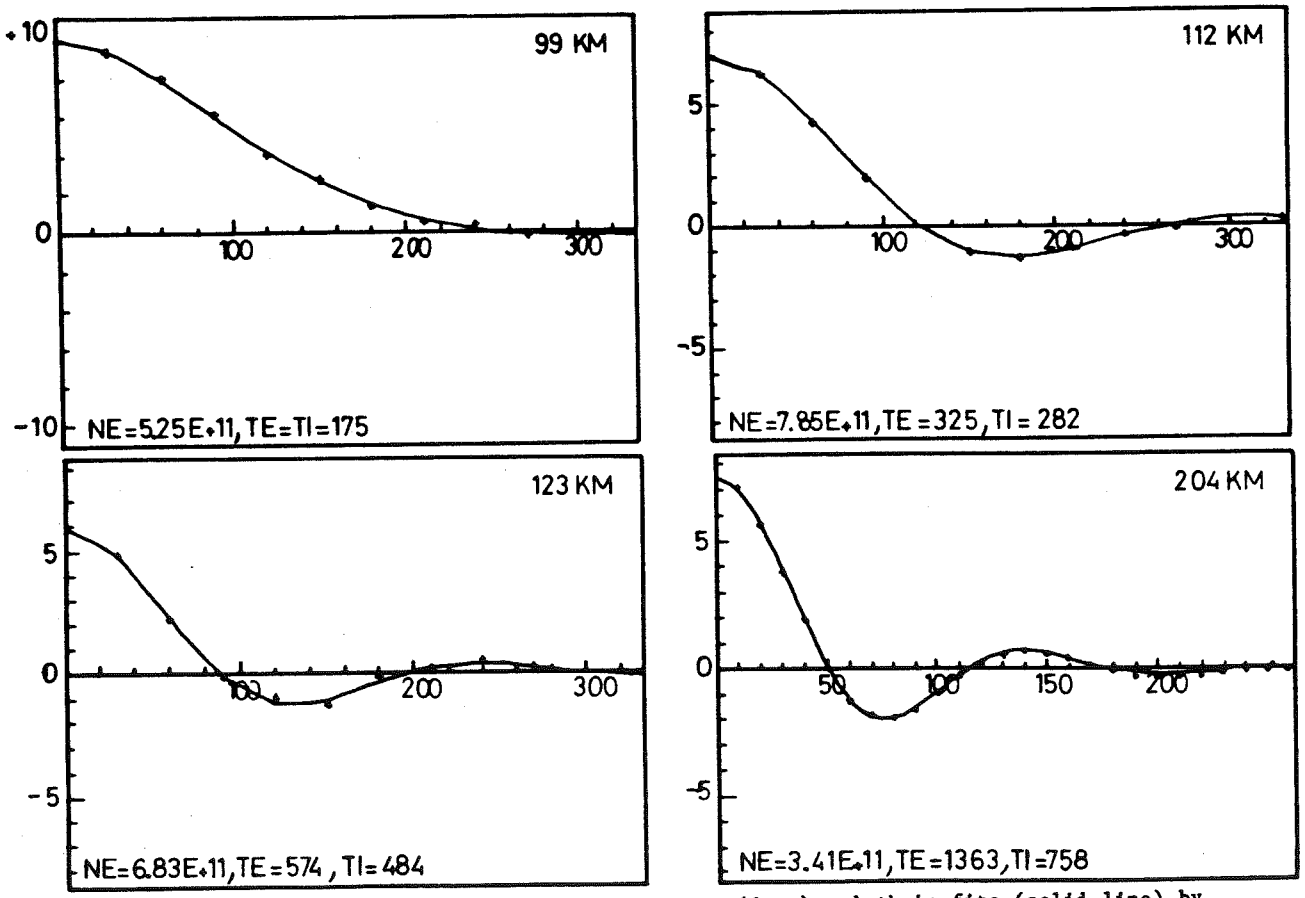


Fig. 2. Autocorrelation function measurements (dots) and their fits (solid line) by multipulse in E region and single pulse in F region.

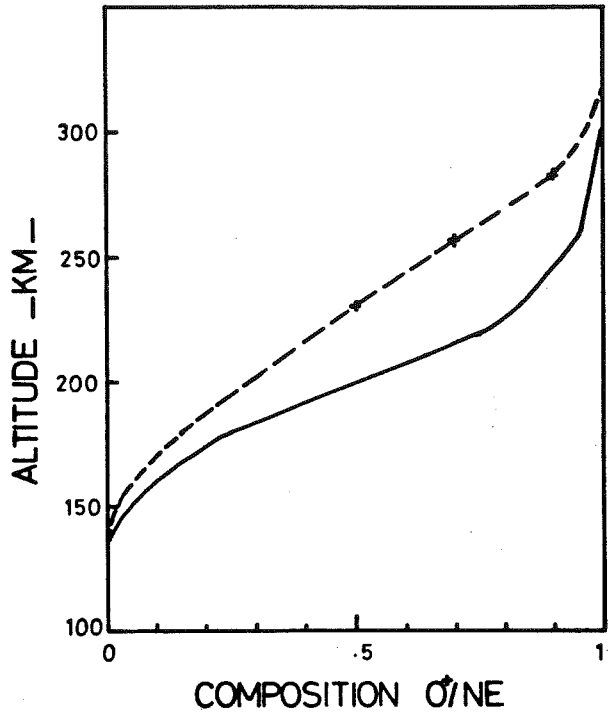


Fig. 3. Composition model (solid line) used usually in data analysis and measured composition for December 12, 1983. Plus signs correspond to measured values, and dashed line corresponds to the model used in this work for temperature determinations.

lation function error estimates, are zero for zero and tenth lags.

In Figure 2, the good quality of data and the good fit obtained in data analysis are evident. The plasma parameters in the F region were measured with a 360-μs pulse, giving 54 km range resolution. They were obtained between 150 and 600 km with a 27-km range step. The short-pulse measurements, combined with temperatures obtained from the single long pulse, provide electron densities from 80 km to 350 km with 9-km range resolution and a 1.5-km range step.

The data that we show in this paper were analyzed by a program [Lejeune, 1979] in which we can choose different analysis strategies depending on the altitude range.

In the data analysis program we implemented a new model for the ion composition (Figure 3), which was compiled from incoherent scatter measurements in the auroral zone [Lathuillere and Brekke, 1984]. This model differs from a previous one used in EISCAT data analysis. This change was necessary to better determine $T_i$ and $T_e$ in the altitude range 140-270 km. Even with the new composition model, which is a mean model, it is possible that the temperature determinations are biased on occasion.

This could occur because the ion composition can vary very rapidly in the auroral zone as a result of changes in the energy input to the atmosphere [Sojka et al., 1981]. The clear implication is that in this variable environment it is really necessary (when the snr permits) to fit the ion composition as well as the other parameters between 140 and 270 km altitude. Outside this range, the influence on the derived temperatures of departures in composition from the model is usually negligible.

## Case Study

We analyzed two nights of data. They clearly show the typical response of the auroral ionosphere to the input of energy to the atmosphere by electron precipitation. On December 12, 1983, we started the experiment in the evening at 1930 UT. The conditions were active until 2300 UT.

The E region electron density was relatively elevated, about $5 \times 10^{11}$ el/m$^3$. The energy input from the electron precipitation, calculated from the electron density profile [Wickwar et al., 1975], was about 15 mW/m$^2$ (see Figure 4). These characteristics correspond typically to active auroral conditions. The F layer plasma parameters allowed us to calculate the energy input to the thermal electrons. These calculations take into account the electron-ion and electron-neutral losses [Kofman and Wickwar, 1984]. The energy input was low (about $10^{-2}$ mW/m$^2$) (except for the period at about 1930 UT), which indicates essentially the absence of low-energy electrons in the precipitated flux.

Between 2300 UT and 0130 UT there was low intensity of precipitation with the lowest values of energy input to the E and F regions occurring at about 0100 UT. The electric field during this whole period was about 10 mV/m, which indicates that Joule heating is absent or very low.

In Figure 5, we show the electron density, ion temperature, and electron temperature profiles for this time. The multipulse measurements being scattered because of the low snr, we analyzed the data with the assumption $T_e = T_i$ up to 135 km. This assumption is justified due to the low energy input (particles and Joule heating) at this time.

In reducing the single-pulse data between 150 and 300 km, we fit the ion composition. The obtained results were relatively scattered, and we averaged the ion composition for 5 hours of data. We obtained an average model for this day, which we show in Figure 3. One can see that the transition region (50% of $NO^+$) is shifted up by about

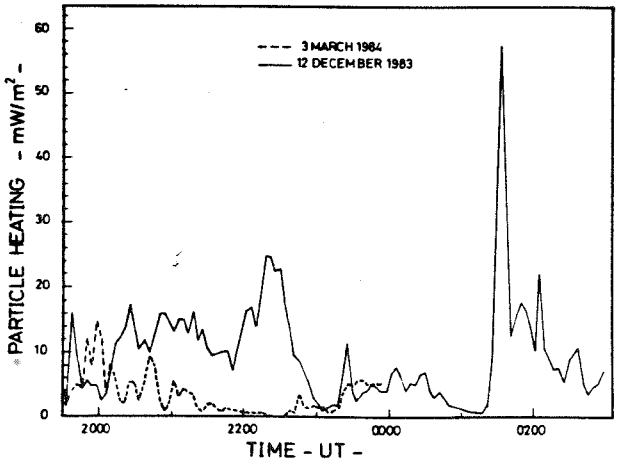


Fig. 4. Particle heating for December 12, 1983 (solid line), and March 3, 1984 (dashed line), calculated from E region electron densities.

25 km in comparison to the model. This behavior is consistent with observations made by Lathuillere and Brekke [1984], since particle heating for this night was particularly high (Figure 4). This new model was then used to obtain the temperatures presented here.

The temperatures increased monotonically from about 200 K at 100 km to 600 K at about 140 km. The long pulse measurements are much less scattered due to better snr. The ion and electron temperatures were respectively about 1000 K and 1800 K at 300 km. The electron density at the peaks of both the E and F layers was about $2 \times 10^{11}$ el/m$^3$.

Around 0130 UT a new injection of energetic electrons occurred. The behavior of the ionospheric plasma parameters is shown in Figure 5. A strong increase, relative to the data at 0110 UT, by a factor of 5 to 10 in the electron density over the whole ionospheric E and F layers (up to 300 km) indicates that electrons with a wide spectrum of energies were precipitated. Moreover, the rapid and large increase in electron temperature, 50 K at 120 km and 600 K at 300 km, confirms that high-energy (> 1 keV) and low-energy electrons (< 300 ev), respectively were precipitated. The ion temperature was almost unchanged, indicating the absence of Joule heating.

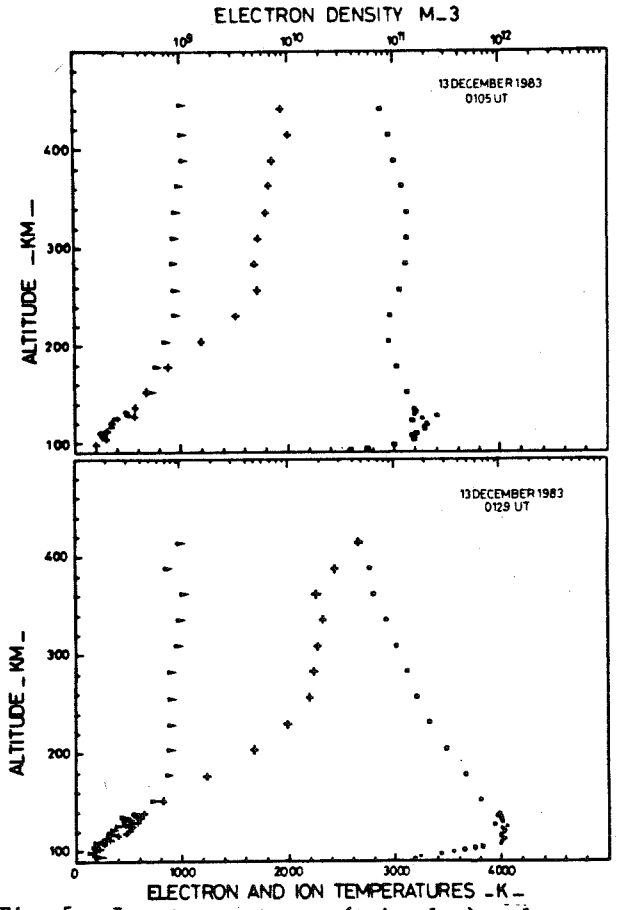


Fig. 5. Ion temperatures (triangles), electron temperature (plus signs), and electron density (squares), for December 13, 1983, at 0105 UT and 0129 UT. At 0105 UT the multipulse data were analyzed with the assumption $T_e = T_i$; the electron density corresponds to the limit of sensitivity of our experiment.

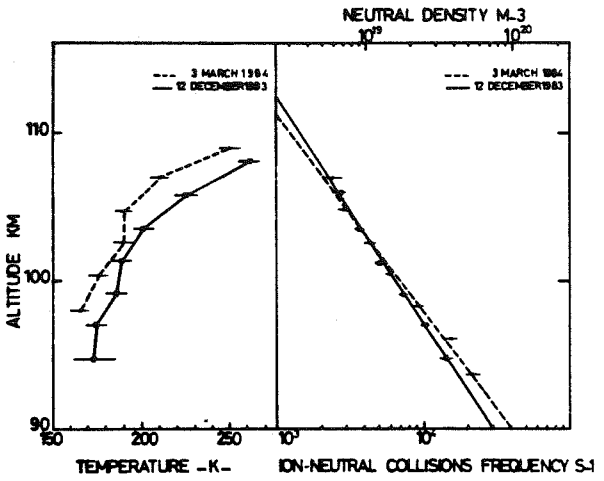


Fig. 6. Neutral temperatures and densities obtained for December 12, 1983 (solid line) and March 3, 1984 (dashed line).

From the measurements of electron density with good altitude resolution, we calculated the total energy deposed in the E layer by precipitating electrons to be about 50 mW/m$^2$. The energy input to ambient electrons in the F layer was about $6 \times 10^{-2}$ mW/m$^2$. If one assumes that this energy represents about 20% to 50% of the total energy input to the F region atmosphere, the total energy input is expected to be 0.12 to 0.3 mW/m$^2$.

## Study of the Lower Thermosphere

The multipulse capabilities provide a unique possibility of studying the low thermosphere by enabling neutral densities and temperatures to be determined. In the auroral situation, the neutral atmosphere is very greatly affected by the variability of energy deposited by precipitation and Joule heating. The possibility of observing these variations allows the quantitative study of these effects. We show the data from two days of measurements: December 12, 1983, and March 3, 1984.

The data analysis was performed for altitudes below 110 km with the assumption $T_e = T_i$. We chose periods without Joule heating to be sure that this assumption was correct. The integration time was 4 min. While the electron density and temperature uncertainties were usually less than 25%, the uncertainty in the ion-neutral collision frequency was relatively high, of the order of 50%. For this reason, we averaged in time, for the duration of the whole experiment, the temperature and ion-neutral collision frequency, for altitudes lower than 110 km. The data taken in this calculation have errors less than 25% and 50%, for temperature and collisions respectively. This procedure assumes that there were no major variations of the neutral atmosphere in that range of altitudes and at that time, which is approximately correct because of the very large heat capacity of the neutral atmosphere.

In the analysis, we determined the plasma temperature ($T_e = T_i$). In the absence of Joule heating one can assume that the plasma temperature is equal to the neutral temperature because of the very large ion-neutral collision frequency.

In Figure 6, we show the temperature and collision frequency profiles for these two days. We also scaled the collision frequency in neutral density units, assuming that ion-neutral collisions were essentially due to polarization potential [Banks and Kockarts, 1973; Lathuillere et al., 1983].

The neutral density results were fitted to an exponential curve. The neutral temperatures on March 3, 1984, were lower than those measured on December 12, 1983. This temperature observation is consistent with the slope of the neutral density profiles, which depends on the scale height (kT/mg). The slope of the December 12 profile is larger (6.5 km) than that of March 3 (5.7 km).

This different behavior on the two days is correlated with the particle energy deposition in the E region. On December 12, the energy deposited, which heated neutrals, was much larger than for March 3 (see Figure 4). Normally, the neutral atmosphere in the E region is hotter in March than in December because of the longer solar illumination and hence energy input. However, data show the opposite, as reflected in the neutral temperatures, which clearly indicates that under auroral conditions the neutral atmosphere in the 95 to 110 km range reacts strongly to "local" energy deposition.

## Conclusions

The observations reported here show that it is possible to study the variability of the ionosphere with a good temporal resolution (few minutes) and altitude resolution (2 km in E layer).

This resolution is necessary to study quantitatively the effects of auroral energy inputs on the atmosphere. We show that in a few minutes the whole auroral ionosphere can change, with a very strong increase of the ionization and electron temperature in the E and F regions. These data permit us to estimate the energy input both in the E region and in the F region. From the analysis of low-altitude E region data we determine the ion-neutral collision frequency for two different nights and show the possible correlation between the scale height of collision frequency and the energy input in the atmosphere. This kind of experimental study will permit us in the near future to estimate the response of the neutral atmosphere to energy deposition on a time scale of the order of tens of minutes.

Acknowledgments. We are grateful to G. Lejeune for fruitful discussions and for helping in data analysis programming, and we thank V. B. Wickwar for helpful comments. The EISCAT Scientific Association is supported by the Centre National de la Recherche Scientifique of France, Suomen Akatemia of Finland, Max-Planck Gesellschaft of West Germany, Norges Almenvitenskapelige Forskningsrad of Norway, Naturvetenskapliga Forskningsradet of Sweden and the Science and Engineering Research Council of the United Kingdom.

The Editor thanks T. Hagfors and C. Rino for their assistance in evaluating this paper.

## References

Banks, P. M., Observations of Joule and particle heating in the auroral zone, J. Atmos. Terr. Phys., Vol. 39, 179-193, 1977.

Banks, P. M., and G. Kockarts, Aeronomy, Academic, New York, 1973.

Brekke, A. and C. L.Rino, High-resolution altitude profiles of the auroral zone energy dissipation due to ionospheric currents, J. Geophys. Res., 83, 2517-2524, 1978.

Farley, D. T., Incoherent scatter correlation function measurements, Radio Sci., 4, 935-953, 1969.

Farley, D. T., Multiple pulse incoherent scatter correlation function measurements, Radio Sci., 7, 661-666, 1972.

Folkestad, K., T. Hagfors, and S. Westerlund, Eiscat : An updated description of technical characteristics and operational capabilities, Radio Sci., 18, 867-880, 1983.

Kofman, W., and V. B. Wickwar "Very high electron temperatures in the daytime F region at Sondrestrom, Geophys. Res. Lett., 11, 919-927, 1984.

Lathuillere, C., and A. Brekke, Ion composition in the auroral ionosphere as observed by EISCAT, Ann. Geophys., Gauthier-Villars, in press, 1985.

Lathuillere, C., V. B. Wickwar, and W. Kofman, Incoherent scatter measurements of ion neutral collision frequencies and temperatures in the lower thermosphere of the auroral region, J. Geophys. Res., 88, 10,137-10,144, 1983.

Lejeune, G., A program library for incoherent scatter calculation, Tech. Note 79/18, EISCAT, Ramfjordmoen, Norway, 1979.

Rino, C. L., M. J. Baron, C. H. Burch, and O. De La Beaujardière, A multipulse correlator design for incoherent scatter radar, Radio Sci., 9, 1117-1127, 1974.

Rino, C. L., A. Brekke, and M. J. Baron "High resolution auroral zone E region neutral wind and current measurements by incoherent scatter radar, J. Geophys. Res., 82, 2295-2304, 1977.

Sojka, J. J., W. J. Rait, and W. R. Schunk, Theoretical predictions for ion composition in the high latitude winter E region for solar minimum and low magnetic activity, J. Geophys. Res., 86, 2206-2216, 1981.

Wickwar V. B., M. J. Baron, and R. D. Sears, Auroral energy input from energetic electrons and Joule heating at Chatanika, J. Geophys. Res., 80, 4364-4367, 1975.

W. Kofman and C. Lathuillere, Centre d'Etudes des Phénomènes Aléatoires et Géophysiques, Laboratoire Associé au CNRS (LA 346), BP 46, 38402 Saint-Martin-d'Hères Cédex, France.

(Received October 24, 1984;
revised November 29, 1984;
accepted November 30, 1984.)

# AUTORISATION de SOUTENANCE

VU les dispositions de l'article 5 de l'arrêté du 16 avril 1974

VU les rapports de présentation de Messieurs

. G. LEJEUNE
. D. ALCAYDE
. V.B WICKWAR

**Madame LATHUILLERE Chantal**

est autorisée à présenter une thèse en soutenance en vue de l'obtention du grade de DOCTEUR D'ETAT ES SCIENCES.

Fait à Grenoble, le 13 janvier 1987

Le Président de l'USTM-G

Le Président
M. TANCHE

Le Président de l'I.N.P.-G

D. BLOCH
Président
de l'Institut National Polytechnique
de Grenoble

*P.O. le Vice-Président,*

**Résumé**

Dans les zones aurorales, d'importantes quantités d'énergie sont déposées dans la haute atmosphère terrestre par les particules énergétiques et par les champs électriques d'origine magnétosphérique. Ces entrées d'énergie, très variables dans le temps et l'espace, s'ajoutent à l'énergie déposée par le rayonnement EUV et UV solaire, principale source d'énergie de la thermosphère des moyennes latitudes. Elles peuvent modifier la composition et la circulation de l'atmosphère neutre et ionisée au dessus de 90 Km d'altitude environ.
La technique de diffusion incohérente, avec les radars de Chatanika en Alaska et EISCAT en Scandinavie, est utilisée pour étudier la température et la densité neutre à la base de la thermosphère et la composition ionique de la région F1 en zone aurorale, pendant les périodes calmes et perturbées.

**Mots-clés**

Basse thermosphère aurorale
Ionosphère aurorale
Composition ionique
Diffusion incohérente